UNIVERSITÉ DE LORRAINE

École doctorale IAEM Lorraine

Shape Optimisation Problems Around the Geometry of Branchiopod Eggs

THÈSE

présentée et soutenue publiquement le 29 Octobre 2020

pour l'obtention du

Doctorat de l'Université de Lorraine

(mention mathématiques)

par

Alexandre Delyon

Composition du jury

Rapporteurs :	Maria Hernandez Cifre, Professeur des universités, University of Murcia Jimmy Lamboley, Professeur des universités, Sorbonne Universités
Examinateurs :	Matthieu Fradelizi, Maitre de conférence, Université Gustave Eiffel Antoine Lemenant, Professeur des universités, Université de Lorraine Nicolas Rabet, Maitre de conférence, Sorbonne universités
Encadrants :	Antoine Henrot, Professeur des universités, Université de Lorraine Yannick Privat, Professeur des universités, Université de Strasbourg

Institut Élie Cartan Lorraine

Mis en page avec la classe thesul.

Résumé

Dans cette thèse nous nous intéressons à un problème de mathématiques appliquées à la biologie. Le but est d'expliquer la forme des oeufs d'*Eulimnadia*, un petit animal appartenant à la classe des *Branchiopodes*, et plus précisément les *Limnadiides*. En effet, d'après la théorie de l'évolution il est raisonnable de penser que la forme des êtres vivants où des objets issus d'êtres vivants est optimisée pour garantir la survie et l'expansion de l'espèce en question.

Pour ce faire nous avons opté pour la méthode de modélisation inverse. Cette dernière consiste à proposer une explication biologique à la forme des œufs, puis de la modéliser sous forme d'un problème de mathématique, et plus précisément d'optimisation de forme, que l'on cherche à résoudre pour enfin comparer la forme obtenue à la forme réelle des oeufs. Nous avons étudié deux modélisations, l'une amenant à des problèmes de géométrie et de packing, l'autre à des problèmes d'optimisation de forme en élasticité linéaire.

Durant la résolution du premier problème issue de la modélisation, une autre question mathématique s'est naturellement posée à nous, et nous sommes parvenus à la résoudre, donnant lieu à l'obtention du diagramme de Blaschke Santalo (A,D,r) complet. En d'autre mots nous pouvons répondre à la question suivante: étant donné trois nombres A,D, et r positifs, est il possible de trouver un ensemble convexe du plan dont l'aire est égale à A, le diamètre égal à D, et le rayon du cercle inscrit égal à r?

Mots-clés: Biologie, Eulimnadia, Optimisation de forme, Géométrie convexe, Analyse convexe, Analyse fonctionnelle, Calcul des Variations, Elasticité Linéaire

Abstract

In this thesis we are interested in a problem of mathematics applied to biology. The aim is to explain the shape of the eggs of *Eulimnadia*, a small animal belonging to the class *Branchiopods*, and more precisely the *Limnadiidae*. Indeed, according to the theory of evolution it is reasonable to think that the shape of living beings or objects derived from living beings is optimized to ensure the survival and expansion of the species in question.

To do this we have opted for the inverse modeling method. The latter consists in proposing a biological explanation for the shape of the eggs, then modeling it in the form of a mathematical problem, and more precisely a shape optimisation problem which we try to solve and finally compare the shape obtained to the real one. We have studied two models, one leading to geometry and packing problems, the other to shape optimisation problems in linear elasticity.

After the resolution of the first modeling problem, another mathematical question naturally arose to us, and we managed to solve it, resulting in the complete Blaschke-Santaló (A,D,r) diagram. In other words we can answer the following question: given three positive numbers A,D, and r, and it is possible to find a convex set of the plane whose area is equal to A, diameter equal to D, and radius of the inscribed circle equal to r.

Keywords: Biology, Eulimnadia, Shape optimisation, Convex geometry, Convex analysis, Functional analysis, Calculus of variations, Linear Elasticity

Long Résumé en Français

Introduction

Cette thèse est issue d'une discussion avec Nicolas Rabet, biologiste, maitre de conférence au muséum d'histoire naturelle de Paris. Travaillant sur de petits crustacés de la classe des *Branchiopodes*: *Eulimnadia*, son but est de retracer l'histoire évolutive de l'espèce en construisant l'arbre phylogénétique. Pour ce faire, il semble inévitable de passer par la compréhension de la forme si particulières de leurs oeufs (voir Figure 1).

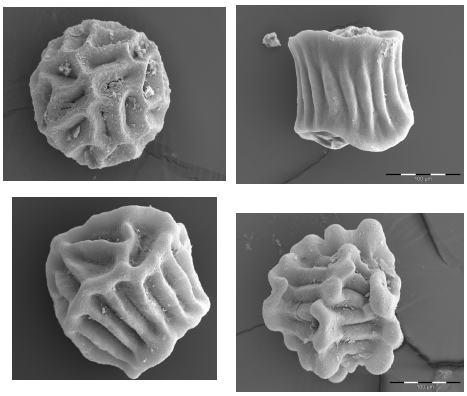

Figure 1: Différentes formes d' oeufs d'*Eulimnadia*

La méthode que l'on utilise est la modélisation inverse en adoptant le point de l'optimisation de forme. L'optimisation de forme dans un sens trés général consiste à chercher la forme que l'on doit donner à des objets pour qu'ils soient le plus adaptés possibles à la tache qui leur incombe. Mathématiquement cela s'écrit sous la forme:

$$\inf_{\Omega \in \Omega_{\text{adm}}} J(\Omega), \tag{1}$$

où Ω_{adm} est un ensemble de formes admissibles de $\mathbb{R}^n$, c'est à dire des parties de $\mathbb{R}^N$ satisfaisant certaines contraintes géométriques (volume prescrit, ou encore diamètre...) ou topologiques (connexité, domaine ouvert, compact, borné...), permettant de cibler le problème. $J : \Omega_{\text{adm}} \mapsto \mathbb{R}$ est la fonctionnelle de forme, ou critère, que l'on cherche à minimiser. Il s'agit souvent d'une énergie dont on souhaiterait par exemple minimiser la dissipation.

Il existe de nombreux domaines de l'ingénieurie où cette discipline gagne en importance, comme par exemple la construction ou l'impression 3D. En effet, dans ces secteurs nous souhaitons

avoir les structures les plus solides possibles, mais en même temps légères ou économes en matériau. Cette approche peut aussi se révéler très utile en biologie si l'on considère qu'au fil de l'évolution, certains objets de la nature adoptent une forme qui leur garantissent les chances maximales de survie, et donc que la forme est optimisée pour un certain critère que l'on cherche à découvrir.
Dans le cas de l'ingénieurie, nous avons une forme a optimiser suivant un certain critère, tandis qu'en biologie nous disposons déjà de la forme que nous supposons optimale, et nous cherchons le critère pour lequel elle est optimale.
La modélisation inverse s'inscrit dans cette dernière approche. Nous disposons donc des oeufs, dont nous supposons la forme optimale, et nous cherchons quelle critère est optimisé. Pour cela nous avons longuement discuté avec Nicolas Rabet pour dégager des hypothèse biologique plausibles, que nous traduisons mathématiquement sous la forme d'un problème d'optimisation de forme que l'on cherche à résoudre. Une fois résolu, nous comparons alors la solution obtenue avec la forme réelle des œufs. Si les formes coincident, alors à défaut de complètement valider l'hypothèse, nous pouvons dire qu'elle est plausible vis à vis des résultats.

Dans cette thèse nous avons donc retenu deux hypothèses biologiques.

- La première consiste à dire que la forme de l'oeuf permet à l'animal de stocker le maximum d'oeufs dans son utérus, lui permettant ainsi d'avoir le maximum de descendants. Cette hypothèse sera modélisée par un problème de packing
- La deuxième est issue de l'observation que les oeufs flottent à la surface, ce qui suggère qu'ils sont assez léger pour cela, et donc que la coque est perforée de petit trou. Le problème est que cela fragilise la structure. Nous supposons donc que la forme des oeufs permet de rendre la coque la plus résistante possible malgré les nombreux trous. Cette hypothèse sera modélisée par un problème de minimisation de compliance dans le cadre de l'élasticité linéaire.

La thèse se présente donc sous la forme suivante:

Chapitre d'outils

Nous présentons d'abord un premier chapitre dans lequel nous présentons plus en détails l'aspect biologique de la thèse, et nous introduisons les outils mathématiques principaux que nous utilisons, à savoir l'optimisation de forme, la fonction support, le packing et le problème d'élasticité linéaire.

Première partie: l'arrangement des œufs comme un packing optimal

Dans cette partie nous discutons du premier critère biologique. où l'on considère que les oeufs sont arrangés de telle sorte que l'animal peut en stocker le plus grand nombre dans son utérus. Le bon outil mathématique pour cette étude est le packing, dont les grandes questions sont d'une part de savoir comment les objets s'arrangent dans l'espace, et d'autre part quels sont les objets qui s'arrangent le mieux. La notion principale est celle de densité, qui permet de calculer la proportion de l'espace qui est occupée par une collection d'objet. Après un travail de modélisation et plusieurs hypothèses simplificatrices, nous sommes amenés à optimiser la combinaison convexe de la densité d'un corps convexe K: $d(K)$, et de son diamètre $D(K)$ parmi l'ensemble admissible $\mathcal{A}_{r_0,A}$ des corps convexes du plan de rayon de cercle inscrit supérieur ou égal à r_0 et d'aire A:

$$\boxed{\sup_{K\in\mathcal{A}_{r_0,A}} td(K)+(1-t)\frac{\pi}{2\sqrt{A}}D(K)} \qquad (\mathcal{P}_1)$$

Deuxième partie: Petit détour par la géométrie convexe

Cette partie n'a pas de lien direct avec la biologie, mais provient directement d'une question qui s'est posée suite à la réalisation du premier problème. Il s'agit de la complétion du diagramme de Blaschke-Santaló (A, D, r). Un diagramme de Blaschke-Santaló est une sorte de carte qui indique quelles sont les valeurs possible que peuvent prendre un certain triplet, ici l'aire, le diamètre et le rayon du cercle, pour un corps convexe donné. Cette complétion passe par la résolution du problème suivant:

$$\boxed{\sup_{K\in\mathcal{K}^2_{r,D}} |K|} \qquad (\mathcal{P}_2)$$

où $\mathcal{K}^2_{r,D}$ est l'ensemble des corps convexes du plan de diamètre égal à D et de rayon de cercle inscrit égal à r.

Troisième partie: Un critère mettant en jeu l'élasticité linéaire

Dans cette dernière partie nous étudions le second critère biologique, où nous étudions le problème suivant:

$$\boxed{\inf_{\Omega\in\Omega_{adm}} C(\Omega)} \qquad (\mathcal{P}_3)$$

où $C(\Omega)$ est la compliance de Ω. Cela correspond au travail des forces qui s'appliquent sur un structure. Ω_{adm} est l'ensemble des formes admissibles, cette fois ci des ouverts de rayon de cercle inscrit supérieur ou égal à 1, et dont l'aire et la densité massique sont aussi fixées.

1 Première partie: l'arrangement des œufs comme un packing optimal.

Dans cette partie, on suppose que la forme des oeufs est telle qu' *Eulimnadia* peut en stocker le plus grand nombre possible, et donc qu'en un sens les oeufs occupent bien l'espace. Il nous reste à donner un sens à cette notion. La bonne notion est celle de packing. Dans toute cette partie on travaille sur les corps convexes du plan, c'est à dire les ensembles convexes du plan qui sont compacts et d'intérieur non vide. On note cet ensemble $\mathcal{K}_2$. Notons que l'on se restreint à deux dimensions pour des raisons de simplicité. Une fois les résultats acquis pour cette dimension nous pouvons ensuite réfléchir à la dimension supérieure.

Considérons à présent un corps convexe $K \in \mathcal{K}_2$. Un packing de motif K est un sous ensemble de $\mathbb{R}^2$ composé de copies disjointes de K. Si un tel packing occupe tout le plan, on dit que c'est un pavage, et que K est un pavé. La densité d'un tel packing est alors la portion du plan qui est occupé par cet ensemble. Etant donné le caractère infini de $\mathbb{R}^2$, nous construisons ce nombre asymptotiquement. Nous pouvons alors définir la densité de K comme la densité du meilleur packing. Autrement dit, la densité de K est la portion maximale du plan qu'il peut occuper. Ainsi un pavé a pour densité 1. C'est ce dernier nombre que l'on souhaite manipuler.

Cependant il est difficile de travailler avec cette définition. C'est pourquoi nous avons introduit une définition proche et plus pratique:

$$d(K) = \frac{|K|}{|K^T|},$$

où K^T est le plus petit pavé qui contient K. Nous cherchons à maximiser ce nombre

A cette notion de densité, nous introduisons un autre critère qui mesure la "non dispersion" d'un packing. Nous montrons qu'un tel critère peut s'écrire de la manière suivante:

$$D_\infty(K) = \frac{2}{\sqrt{\pi}} \frac{\sqrt{|A|}}{D(K)}$$

où $D(K)$ est le diamètre de K. Nous cherchons à minimiser ce nombre, donc à maximiser son inverse.

Finalement la fonctionnelle que nous considérons est une combinaison convexe de ces deux critères:

$$\max t\ d(K) + (1-t)\frac{\sqrt{\pi}}{2\sqrt{|K|}} D(K).$$

L'ensemble admissible que l'on considère prend en compte quelques contraintes biologiques.

- La première contrainte est que l'oeuf doit contenir l'embryon, modélisé par un disque. Nous avons donc la contrainte que le rayon du cercle inscrit doit être supérieur à un nombre r_0.
- La deuxième contrainte prend en compte le fait que le matériau de construction à un cout. Donc nous voulons controller la quantité de matériau nécessaire à la fabrication d'un oeuf. Cela se traduit par une contrainte sur l'aire: $|K| = A$.

Finalement l'ensemble admissible est l'ensemble $\mathcal{A}_{r_0,A}$ des corps convexes du plan de rayon de cercle inscrit supérieur ou égal à r_0 et d'aire A.

Le problème d'optimisation est alors:

$$\boxed{\sup_{K \in \mathcal{A}_{r_0,A}} td(K) + (1-t)\frac{\pi}{2\sqrt{A}} D(K)} \qquad (\mathcal{P}_1)$$

Le théorème suivant résout en grande partie le problème:

Theorem 1. *Supposons A assez grand. Il existe $t^\star \in (0,1)$ tel que*

- *si $t \leqslant t^\star$ alors la solution est donné par un ensemble que l'on appelle "two cap body", défini comme l'enveloppe convexe d'un disque et de deux points à distance D dont le milieu est le centre du disque.*
- *si $t \geqslant t^\star$ alors la solution est donné par un certain hexagone qui pave le plan (c'est même le plus petit pavé qui contient le 2cap body).*

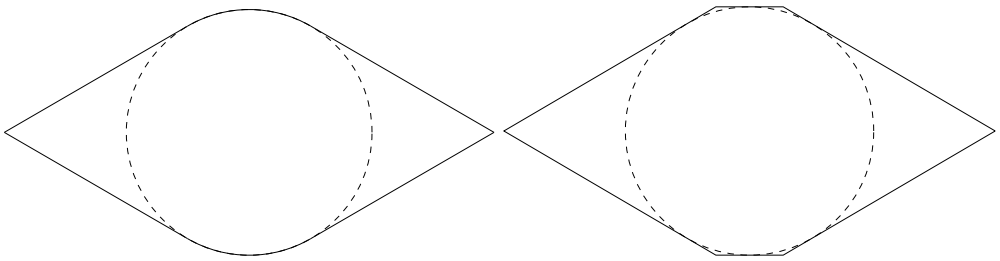

Figure 2: Gauche le two cap body, droite: l'hexagone qui pave le plan

2 Deuxième partie: Petit détour par la géométrie convexe

Dans le premier problème, nous avons exploité la partie supérieure d'un graphe que l'on appelle diagramme de Blaschke-Santaló (voir Figure 3). En effet dans cette figure est représenté en pointillés le diamètre maximal qui puisse être atteint par un corps convexe d'aire donnée égale à 4π suivant la valeur de son rayon de cercle inscrit. La courbe en trait plein ne donne qu'une borne inférieure.

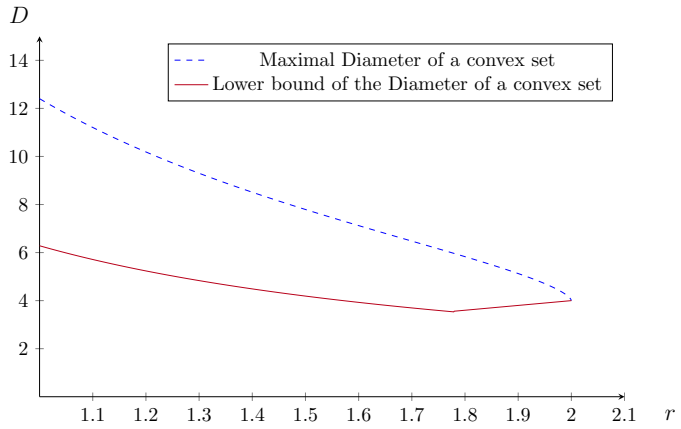

Figure 3: Diagrame de Blaschke-Santaló incomplet, $A = 4\pi$

Généralement nous préférons représenter les Diagramme de Blaschke-Santaló de telle sorte qu'aucune grandeur n'est fixée, et que l'on puisse l'inscrire dans le carré unité. Dans notre cas cela se fait en fixant $x = \frac{2r}{D}$ et $y = \frac{\pi r^2}{A}$, de sorte que le diagramme partiel a l'allure donnée par la Figure 4.

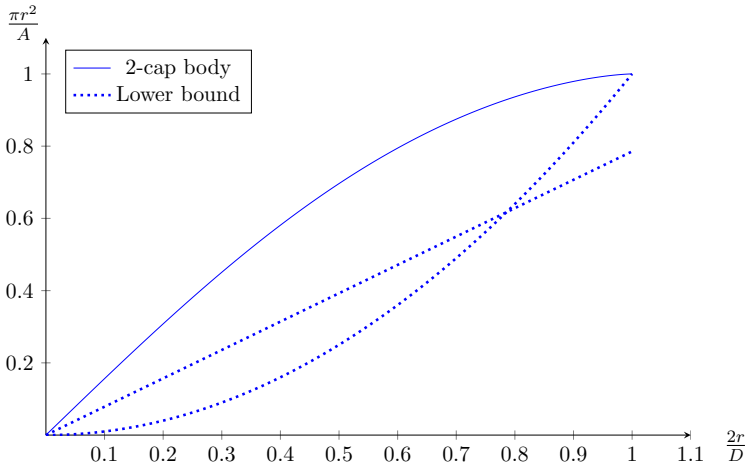

Figure 4: Une autre représentation du diagramme

Pour compléter le diagramme il faut calculer explicitement la courbe inférieure. Cela revient à résoudre le problème suivant:

$$\boxed{\sup_{K \in \mathcal{K}^2_{r,D}} |K|} \qquad (\mathcal{P}_2)$$

où $\mathcal{K}^2_{r,D}$ est l'ensemble des corps convexes du plan de diamètre égal à D et de rayon de cercle inscrit égal à r.

Theorem 2. *On fixe $r = 1$. Alors il existe une valeur $D^\star$ telle que*

- *si $D \leqslant D^\star$, alors la solution est donnée par un Ennéagone arrondi,*
- *si $D \geqslant D^\star$, alors la solution est donnée par l'intersection d'un disque de diamètre D et d'une bande d'épaisseur 2 centrée sur le centre du disque: on l'appelle symmetric slice.*

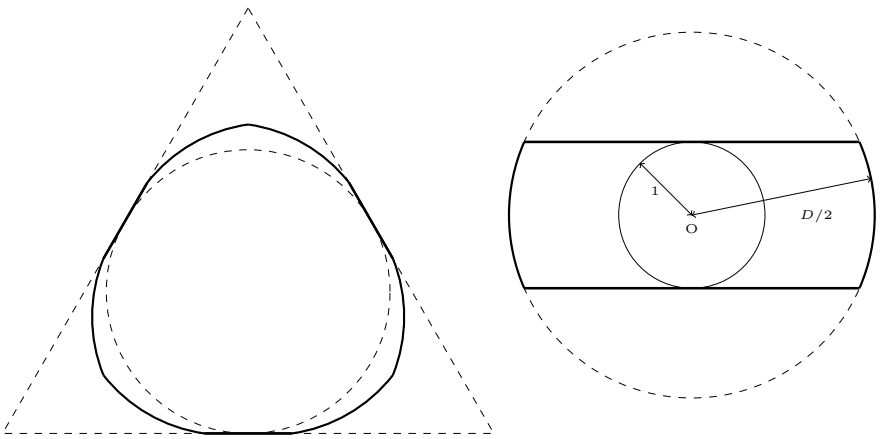

Figure 5: Gauche: le maximiser pour D petit, droite: le maximiseur pour D grand

Finalement le diagramme complet est donné par la Figure 6

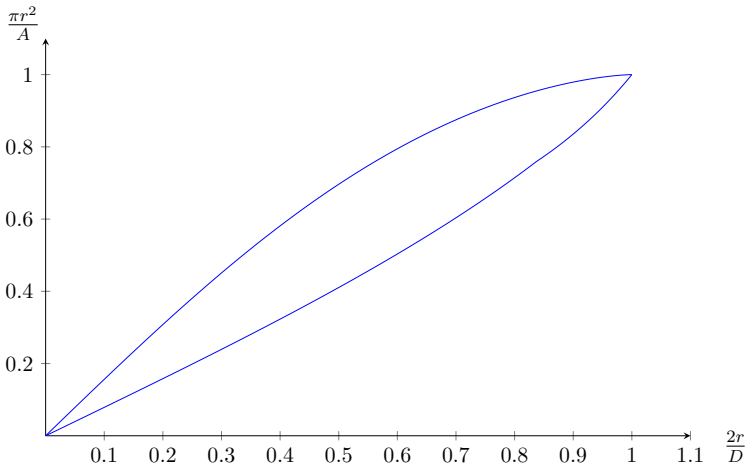

Figure 6: Diagramme complet. En pointillés les bornes inférieures. Le point rouge est la valeur seuil pour laquelle on change d'optimum.

3 Troisième partie: Un critère mettant en jeu l'élasticité linéaire

Dans cette partie nous revenons à la biologie et considérons la deuxième hypothèse biologique, à savoir un dilemme entre légèreté et solidité. Cette fois-ci on considère l'ensemble admissible Ω_{adm} des ouverts connexe de $\mathbb{R}^2$ de rayon de cercle inscrit supérieur ou égal à 1, de d'aire inférieure ou égale à A, et de masse volumique inférieur à un nombre α:

$$\delta(\Omega) = \frac{|\Omega|}{|\Omega \cup T|} \leqslant \alpha,$$

où T représente les composantes connexes bornées de $\mathbb{R}^2 \backslash \Omega$. Autrement dit, T représente les trous de la structure.

Pour mesure la resistance de la structure, on suppose que toute la partie externe de la coque est soumise à une force de pression constante $-p_0\vec{n}$, où $\vec{n}$ est le vecteur normal sortant de la frontière extérieure de Ω. On introduit la notion de compliance en élasticité linéaire:

$$C(\Omega) = \int_{\Gamma_{\text{ext}}} -p_0 u_\Omega \cdot n \; ds$$

où $u_\Omega \in L^2(\Omega)^2$ est solution de l'équation aux dérivées partielles:

$$\begin{cases} -\operatorname{div}(Ae(u_\Omega)) = 0 & \text{in } \Omega \\ Ae(u_\Omega)n = -p_0 n & \text{on } \Gamma_{\text{ext}} \\ Ae(u_\Omega)n = 0 & \text{on } \Gamma_T \end{cases} \tag{2}$$

Notre but est alors de minimiser cette quantité:

$$\boxed{\inf_{\Omega \in \Omega_{adm}} C(\Omega)} \tag{$\mathcal{P}_3$}$$

Nous disposons d'un théorème d'existence pour une version modifiée du problème:

$$\boxed{\inf_{\Omega \in \tilde{\Omega}_{adm}} C(\Omega) + \lambda Per(\Omega)} \tag{$\mathcal{P}_4$}$$

Où $Per(\Omega)$ est le périmètre de Ω, et $\tilde{\Omega}_{adm}$ est obtenu en oubliant la contrainte de connexité, et en considérant une contrainte égalité pour l'aire et la densité massique. La pénalisation par le périmètre permet de controler le nombre de trou, en évitant la prolifération, source de non compacité, et donc de non existence.

Theorem 3.
- *Le problème* $(\mathcal{P}_4)$ *a une solution.*
- *Pour le problème principal* $(\mathcal{P}_3)$ *, Si il existe une solution, alors toute les contraintes sont saturées.*

Contents

General Introduction

It is reasonable to assume that the shape of living organisms observed in nature is optimised to allow them to survive and thrive. Indeed, according to the Theory of Evolution, species are selected through the principle of natural selection, so that a species with an evolutionary advantage is more likely to propagate. This fact raises a deeper question: what is actually optimised? The question posed in this thesis is the following: can we explain the shape of the eggs of Eulmnadiae, a small crustacean living in ephemeral ponds? Shape optimisation is a mathematical discipline that may pretend to answer this question.

It is a very old discipline to find the shape that an object must have in order to be the most adapted to its use. We have been doing that in many aspects of the everyday life: the shape of any manufactured object is designed to make it as practical as possible for its use. Consider the example of a chair. A chair is supposed to remain standing when we sit on it, not to break and to be comfortable for our backs. The shape of a chair results in our will to fulfill those conditions. Yet optimisations have often been made based on intuition. But the recent developments of the modern mathematical analysis and later the advent of computers and programming led to make that discipline becoming a mathematical topic on its own, known as shape optimisation. It enabled numerous engineering feats and progresses, such as building structures capable of withstanding all the stresses applied to them, optimizing the shape of the wings of a plane, or even solving some problems that one may encounter in 3-D printing. Shape optimisation is often used to find the shape a manufactured object should have.

Our approach here is quite the opposite. We do not want to optimise the shape of an object with respect to a criterium, but we observe an object in nature that we assume to be optimal and we are looking for the criterium, by using the so-called inverse modeling method. It consists in formulating a biological hypothesis from observations, building a shape optimisation problem with a criterium (shape functional) that represents the hypothesis, then solving the problem to finally compare the resulting shape to the real one. If the two shapes fit, we may be tempted to confirm the hypothesis. If not, we can either deduce that the hypothesis is wrong, or that the model does not represent the hypothesis well enough and try to improve it.

Let us give a simple example of that approach, using a lovely geometry problem. When we look at a honeycomb, we notice that the cells have the shape of a regular hexagon. It is natural to try to explain such a regular shape. Before giving a hypothesis, note that a honeycomb is built by the bees themselves, and the material used is wax. Moreover, the shape of the cells is always the same, and it allows to tile the plane. In mathematics, such a set is called a tiling domain.

It should not come as a surprise then that bees do not want to waste wax for the structure, nor that the shape of the cell is chosen in a such way that for a given size of cell, the least quantity of wax is used. This is pretty much the hypothesis Pappus formulated in the fourth century. He wrote in its fifth book that the shape of honeycomb is a regular hexagon because it allows to store

the maximal quantity of honey for a given quantity of material to build the cell. As suggested hundred years later by the theory of evolution, the bees that used the least quantity of wax to build their honeycomb may have been naturally selected over the time because of their higher ability to survive. We can imagine for example a period in history when the living conditions were particularly tough, from which only those able to save material have been spared.

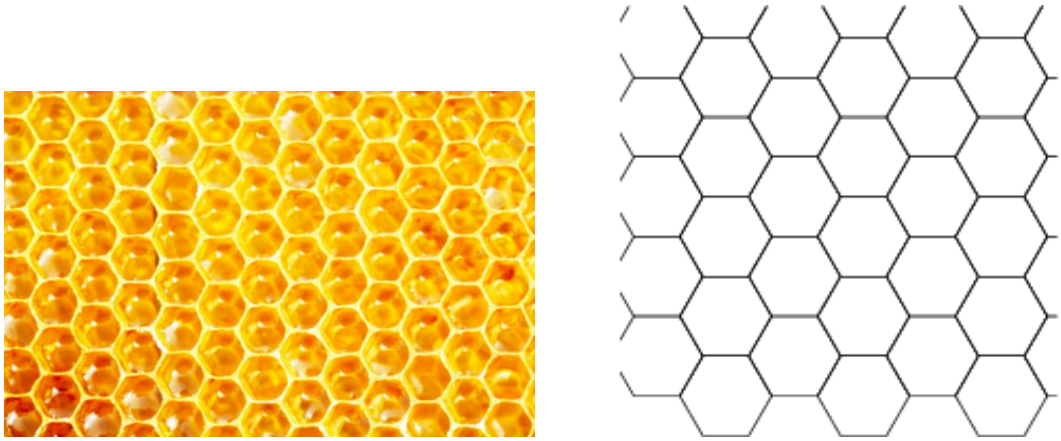

Figure 1: Left : a honeycomb structure, right: a tiling with regular hexagons.

Mathematically it is possible to model the problem as follows:

$$\inf_{K \in \mathcal{K}_{\text{adm}}} \text{Per}(K) \tag{1}$$

where K_{adm} is the set of tiling domains of $\mathbb{R}^2$ with given area A. Problem (1) is a geometrical shape optimisation problem.

Pappus implicitly conjectured that the solution is the regular hexagon. That is the very famous honeycomb conjecture. Despite many attempts to solve the problem over the centuries, a first significant step was made by Lázló Fejes Tóth in 1943 [38] where he solved the problem in the convex case. Then, while seemingly simple on the surface, it was only in 1999 that Thomas Hales completely solved that problem in [51].

From the resolution of the problem, we see that the obtained shape is the same as the original one. However we are not able to conclude that the hypothesis of Pappus was the right one. The inverse modeling method can only give a negative answer, and only enables us as far as to say that a hypothesis is plausible with regards to the results. Note for example that the honeycomb structure is also well known to be resistant to vertical compression and is widely used across industries. So what is the right hypothesis, material savings or resistance? It seems like it is a little bit of both, but a deeper analysis is required, and such analysis is not within the purview of mathematics.

Now let us go back to our problem. Our goal is to explain the shape of the eggs of small branchiopods: Eulimnadiae, also known as clam shrimps because those look like shrimps surrounded by a transparent carapace, as we shall see in Figure 2. On those figures we are also able to distinguish their eggs on the top of their back (small yellow pack)


Figure 2: Pictures of our lovely animals and their eggs on their back. Source:Nicolas Rabet

In order to give an answer to the problem we adopted the reverse modeling method and try to find practical explanation by discussing with biologists, notably with Nicolas Rabet, Maitre de conférences at Sorbonne Universités, and also with Julien Dervaux, CNRS researcher at Université de Paris Didedrot, a soft matter physician specialized in morphogenesis.

The Thesis is organized as follows: first, an introductive chapter in which we define some non-basic tools, then three distinct parts in which we study one specific shape optimisation problem. Each part contains an introductive chapter in which we expose the general motivation of the problem, biological (Part I and III) or mathematical (Part II), together with a mathematical modeling. We provide the main results together with the main ideas involved. In the end of each introductive chapter we start a discussion about the relevance of the biological and mathematical modeling with regards to the results, and suggest ways to improve the models.

Tool chapter

A first chapter of tools is written to present in a more detailed way the biological settings. We describe some species of Eulimnadiae, as well as their living environment. We also give details on their life cycle. That is an important step in order to be able to formulate a good hypothesis. In that chapter we also briefly introduce some of the mathematical non-basic tools we use in the Thesis, such as shape optimisation, packings, the support function, the system of linear elasticity, and the space of bounded variations functions. Some other are used, such as finite and infinite dimensional optimisation, but we do not develop that theory there.

Part I: Arrangements of eggs as an optimal packing

In the first Part we describe the first biological model we studied. This comes from the observation that the animal has a lot of eggs on its back, arranged in such a way as to optimise the space it needed. This led to a packing problem where the goal is to maximise a convex combination of the density $d(K)$ and the diameter $D(K)$ among the admissible set $\mathcal{A}_{r_0,A}$ of convex bodies with inradius r_0 and area A (the inradius of a convex body K is to be understood as the radius of the biggest ball that is included in K):

$$\boxed{\sup_{K\in\mathcal{A}_{r_0,A}} td(K)+(1-t)D(K)} \qquad (\mathcal{P}_1)$$

Part II: A detour to convex geometry

This Part has no direct link with the biological problem, but it came from a question that naturally arose during the resolution of $(\mathcal{P}_1)$. Indeed in the first Part we used a partial Blaschke-Santaló diagram: the (A,D,r) diagram in $\mathbb{R}^2$. In a nutshell a Blaschke-Santaló diagram represents all the values that are reachable for a given convex body. For instance it answers the question whether there exist a convex body with inradius r, diameter D and A. Such a diagram is called the (A, D, r) diagram. The latter was incomplete and we asked ourselves if it was possible to complete it. This comes through the maximisation of the area among an admissible set $\mathcal{K}^2_{r,D}$ of convex bodies in the plane with inradius r and diameter D:

$$\boxed{\sup_{K\in\mathcal{K}^2_{r,D}} |K|} \qquad (\mathcal{P}_2)$$

Part III: A criterium involving linear elasticity.

In this Part we present another biological model. By observing the life cycle of the animal, we realized that the eggs were subjected to a variety of stresses, and it appeared that it could be interesting for the eggs to be both light enough to float at the surface of the water, and resistant to external forces. So we came up with a linear elasticity model where we represented the external forces as a constant pressure stress, and we added constraints on the "holes" of the shell to ensure that the mass density of the eggs is inferior to the one of the water. This led to the following problem:

$$\boxed{\inf_{\Omega\in\Omega_{adm}} C(\Omega)} \qquad (\mathcal{P}_3)$$

where $C(\Omega)$ is the compliance, a functional that expresses the resistance of the egg to the external forces, and Ω_{adm} is a class of admissible set in which the inradius, the volume and the mass density are prescribed.

Chapter 1

Tools and Preliminary results

Contents

This chapter is devoted to the introduction of the main mathematical tools we use in the thesis. We briefly introduce those without giving much proof, but we refer to more complete lectures for details. Before talking mathematics, we are going to present more precisely *Eulimnadia* .

1.1 Some Biological Aspects

1.1.1 General description of the species

Branchiopods are a class of *Crustaceans*, mostly living in freshwater. In this class we identify a sub-order: *Spinacaudata*, also known as Clam Shrimps because of two transparent valves

surrounding their body see Figure 1.1 . The two valves, connected by a powerful muscle, provide protection against a possible predator attack: the muscle contracts, causing the membrane to close tight.

Figure 1.1: A picture of a Clam Shrimp. We can see on its back a pack of eggs. (source: https://thenaturalhistorian.com/2014/01/15/a-tale-of-taphonomy-clam-shrimp-fossils-and-the-age-of-the-earth/)

Clam shrimp are among the oldest living species on earth, with fossils dating back more than 350 million years. Moreover those are found all around the world. As a consequence It may be a very interesting tool for datation if we are able to identify the different species. Over the last few decades, the study of these animals has become increasingly important. Extensive work has been carried out to trace the phylogenetic history of the species (see e.g [13, 33]). See for example Figure 1.2 to get an overview.

From now on we focus on *Limnadiida*, sub-class of *Spinacaudata*, and more precisely on a genus of them: *Eulimnadia*, identified in 1884 by Packard. Identifying different species of *Eulimnadia* is a very hard task for at least two reasons. First it is very hard to clearly identify physiological criteria to distinguish species. The second problem is the intraspecific variability: differences may be observed within a single species. It appears that studying the shape of the eggs are a nice way to differentiate between spaces, and identify new ones, as we will see in section 1.1.3 (see e.g [80]).

1.1.2 Living environment and life cycle

Eulimnadiae are among those animals that can live in ephemeral watering places. It is possible to find them everywhere there is pond, from the small puddle on the side of the road to shallow freshwater lakes, including temporary ponds (see Figure 1.3). Their life cycle is as follows: during a period of heavy rains in a given place, all the unevenness of the relief, even the smallest ones, are temporarily filled with water, for a period ranging from a few days to a few months. In those ponds a diversified life develops, *Eulimnadiae* are among them. The animal reaches maturity within 4-5 days, and can live up to 20 days. Once mature, they measure between 1-2 millimeters to 3.5 centimeters tall and they can hatch hundreds eggs ($\simeq 350$) per day. The eggs are laid down and sink in the bottom of the pool. Once the pool dries up, every animal dies, and only the eggs survive. At this time, eggs are the last remaining life form remaining in the dried pool. If the egg

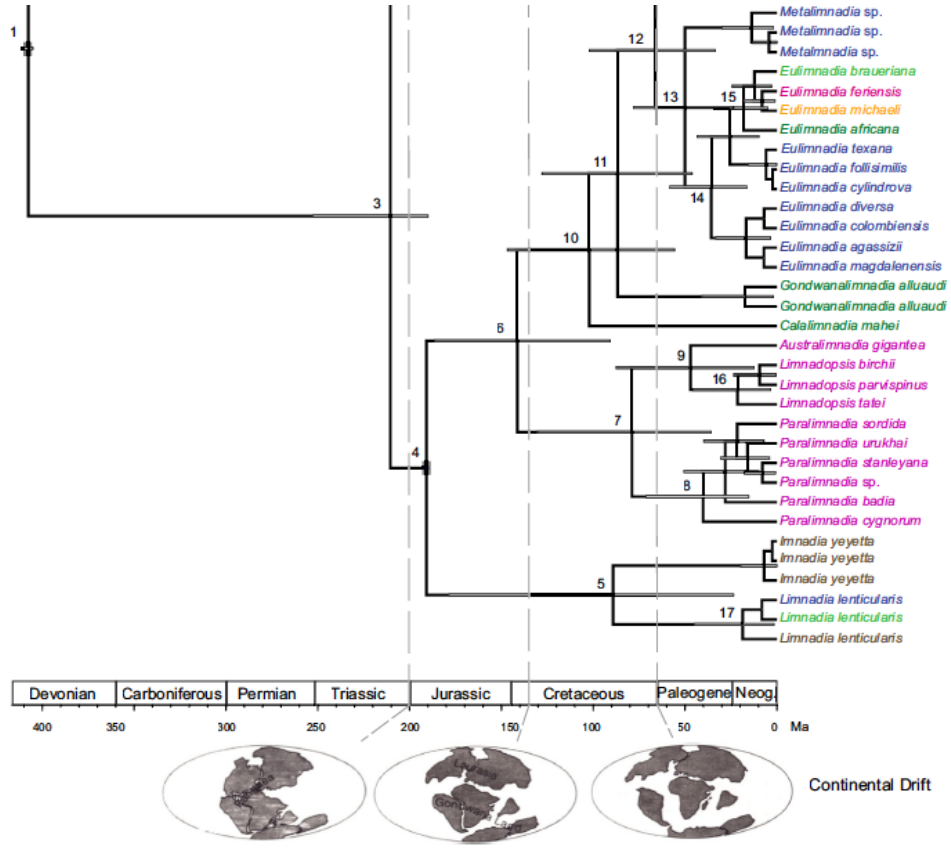

Figure 1.2: Table representing a partial phylogenetic tree involving Clam Shrimps. At node labelled 3 are Spinacaudatae. At node 4 are *Limnadiidae*. *Eulimnadiae* lie at node 12,13 and 14. The colors are used to identify the geographical location where the species live. Dark green stands for Africa, whereas light green is China/Japan. Blue is America, purple is Australia. Source [13]

is not crushed, it is able to wait for years for the water to fill the pool again, so they hatch and the life cycle continues. Actually it is even possible to collect sediments where a potential pool is identified, put it in a water tank, and find hundreds of clam shrimps a few days later. During the period when the ponds are dry, the egg is the last representative of the species. Those eggs are dessication-resistant, also named resting eggs.

1.1.3 Description of the eggs

As previously said, the shape of the egg is of a prime importance for identifying different species. In Figure 1.4 we give and example of an egg description together with the species identification that is found in [80]. The second reason why eggs are important is because it is especially crucial in allowing the survival of the species.

(a) a small water puddle

(b) A rockpool in the Australian desert (Image Credit SCW)

Figure 1.3: examples of places where we can find clam shrimps

Egg types	Figures	MNHN collection sample	Species identification
Spherical with spiral ornamentation	1A-D	MNHN-Bp316, 317, 321°	*E. acutirostris* Daday de Deés, 1926 (type specimen)
Spherical with rectangular depressions	1E-I	MNHN-Bp318	*E. aethiopica* Daday de Deés, 1926 (type specimen)
Pentagonal with large and round ridges	2A-D	MNHN-Bp319+	*E. alluaudi* Daday de Deés, 1926 (type specimen)
Cylindrical with equal border size	–	MNHN-Bp321	*E. antillarum* (Baird, 1852)?
Spherical with large depression ornamented by holes	2E-H	MNHN-Bp319°, 320°, 325-329+	*E. chaperi* (Simon, 1886) (type specimen)
Pentagonal with narrow ridges	3A-C	MNHN-Bp321°, 323, 324, 330, 331	*E. geayi* Daday de Deés, 1926 (type specimen)
Twisted	3D-I; 4A-C	MNHN-Bp320°, 328°, 332-334+, 467°	*E. mauritiana* (Guérin, 1837) (type specimen)
Spherical with large depression without ornamentation	4D, E	MNHN-Bp467°, 325+, 328+	*E. magdalensis* Roessler, 1990
Oblong with long depression	4F-I	MNHN-Bp667+	*Eulimnadia* sp.

Figure 1.4: Table identifying the species by the structure of eggs. Source: [80]

In the description of the eggs we distinguish two main aspects:

- The shape of the egg, that is the shape we guess without its ornementation. We counted three main type of shapes:

  1. The spherical shape
  2. The cylindrical shape
  3. The Pentagonal shape, also named muffin shape.

Note that variations occur among a given type of shape. For example in a cylindrical shape, the shell may be inflated or the opposite. We can also see sometimes that the top (and bottom) of the cylinder are much larger than the trunk (see Figure 1.6).

There are also shapes that do not belong to one of these three categories, but these shapes are too chaotic to be well described. Sometimes we call them twisted eggs.

Figure 1.5 shows a version of each

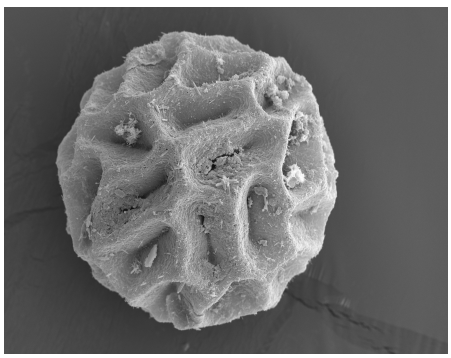

(a) Spherical shape

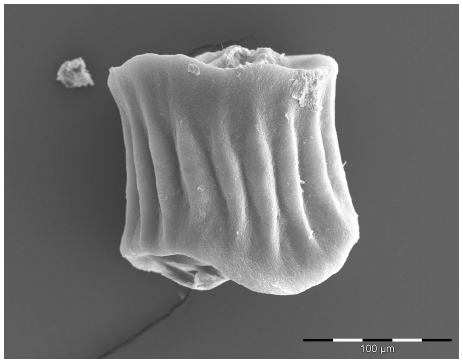

(b) Cylindrical shape

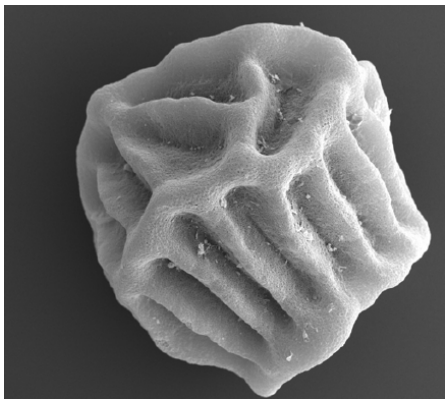

(c) Muffin shape

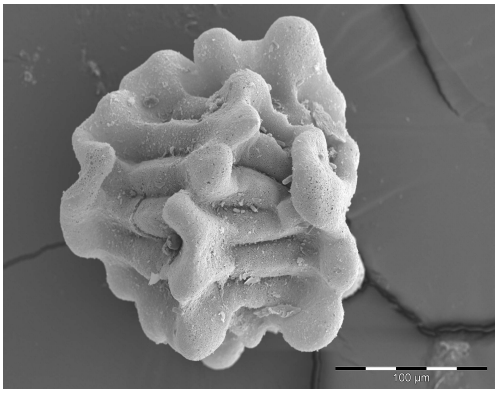

(d) Twisted shape

Figure 1.5: The different existing shapes of eggs (source: database of N.Rabet)

- The ornementation, that consists in the ridges on the egg that can be of different nature on any eggs. Those can be sharp, round, narrow, large, leaving small furrows or large circular holes. Sometimes it even can be spikes (see Figure 1.7). Note also a high variability in the number of ridges. We let the reader look at the different pictures to have an idea of the diversity of ridges.

Note that Figure 1.7 shows two eggs of the same species: *Eulimnadia magdalensis*. On Figure 1.7a the egg was obtained in laboratory condition and collected right after the laying. Egg on Figure 1.7b was collected in the natural environment, hence suffered erosion. That suggests that the shell provides a protection against erosion (and predators). We will come back to this in Part III.

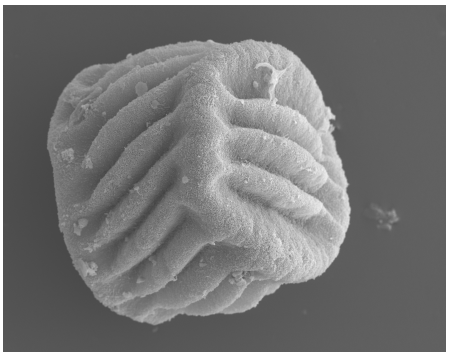

(a) Convex cylindrical Shape

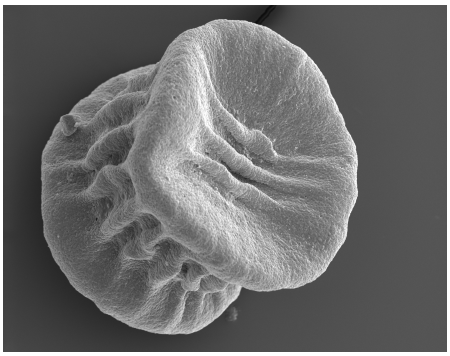

(b) Concave cylindrical shape

Figure 1.6: Different versions of a given shape

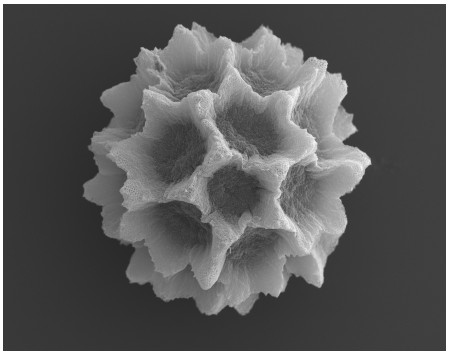

(a) Spike ridges

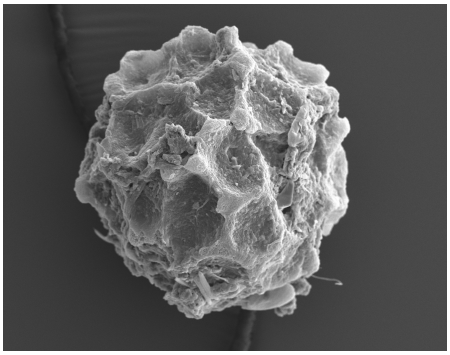

(b) Eroded spike shape

Figure 1.7: Another picture where we see the effects of erosion on the shell

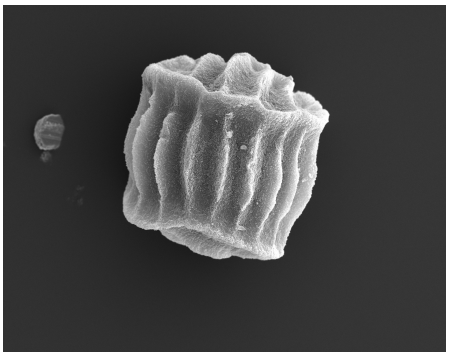

(a) Spike ridges

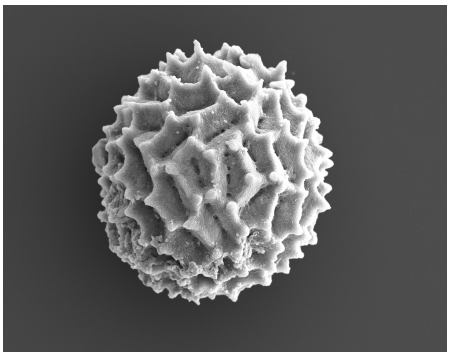

(b)

Figure 1.8: Another type of ridges

In the sequel we will consider the main shape and the ornementation to be two different things. For example in Part I we are only interested in the main shape of the eggs, whereas in

Part III we try ton consider both the main shape and the ornementation.

1.2 Elements of shape optimisation

We give here the basic framework of shape optimisation.

1.2.1 General ideas

In its broadest sense, optimisation consists in minimising a function $f : X \mapsto \mathbb{R}$ where X is any set. Three main topics can be distinguished in optimisation:

- Finite dimensional optimisation.
- Infinite dimension optimisation and calculus of variations.
- Shape optimisation.

In finite dimension optimisation, the set X is a subset of a finite dimensional vector space and we can apply every tool of finite dimension. In infinite dimension optimisation, X is subset of an infinite dimension vector space (often it is a function space). This case is much harder but many tools were developed, such as calculus of variations and functional analysis. In shape optimisation X is a class of subsets of a set Y (often it is $\mathbb{R}^N$). Even if during this thesis we use some concepts of finite dimension and infinite dimension optimisation, in this chapter we restrict ourselves to the introduction of shape optimisation.

Let $N \in \mathbb{N}$ and Ω_{adm} a class of subsets of $\mathbb{R}^N$ called class of admissible shapes and $J : \Omega_{\text{adm}} \mapsto \mathbb{R}$ a functional over Ω_{adm} called shape functional.

A shape optimisation problem consists in solving

$$\inf_{\Omega \in \Omega_{\text{adm}}} J(\Omega) \tag{$\mathcal{P}$}$$

where Ω_{adm} may be defined by topological or geometrical conditions, such as connectedness, boundedness, convexity, compactness... or thanks to an equality constraint of the kind : $\Omega_{\text{adm}} = \{\Omega \subset \mathbb{R}^N, G(\Omega) = 0\}$ where G is a shape functional.

Here are some questions that are natural to ask when studying a shape optimisation problem. A set $\Omega^\star$ such that $\Omega^\star \in \Omega_{\text{adm}}$ and

$$\forall \Omega \in \Omega_{\text{adm}}, \quad J(\Omega) \geqslant J(\Omega^\star)$$

is called a solution of the problem $(\mathcal{P})$. The resolution of the problem $(\mathcal{P})$ involves several questions:

- Existence: does the shape $\Omega^\star$ actually exists? As in finite dimension optimisation or calculus of variations the idea consists in considering a minimising sequence $(\Omega_n)_{n\in\mathbb{N}}$ such that

  $$J(\Omega_n) \underset{n\to\infty}{\to} \inf_{\Omega \in \Omega_{\text{adm}}} J(\Omega)$$

  and showing that it is compact in some sense. For that purpose we need to study the regularity of the shape functional and the compactness properties of the admissible sets. Let us just recall that in general lower semi-continuity together with a compactness argument

is enough to prove existence. Indeed, if $(\Omega_n)_{n\in\mathbb{N}}$ is a minimising sequence and $\Omega^\star$ is a limit shape of (Ω_n), then lower semi-continuity states that:

$$J(\Omega^\star) \leqslant \liminf_{n\to\infty} J(\Omega_n) = \inf_{\Omega\in\Omega_{\text{adm}}} J(\Omega)$$

therefore $\Omega^\star$ is a minimiser.

Since we are dealing with shapes, there is no natural topology, and more than ever, the choice of the topology may be of great importance. Recall that in order to have regularity for functionals, one needs many open sets in the topology whereas having compactness requires to not have too many open sets. Hence choosing a good topology is crucial for studying the existence of a solution. In sections 1.2.2 and 1.6 we introduce two choices of topology that we will mainly use: the Hausdorff convergence in part I and II and the L^1 convergence in the setting of functions of bounded variation space in part III.

- Characterization of the optimum: Geometric or topological properties such as convexity, connectedness or regularity of the solution. We may also want to provide optimality conditions. The main idea is to perform a small deformation of the hypothetical optimal shape to obtain informations on the boundary by saying that the obtained shape is necessarily worse than the optimal. One very useful right tool for this is the shape derivative. We discuss it later in the section.

- Numerical computation of the solution: is it possible to numerically compute the solution? The most classical approach is the one of geometrical optimisation which consists in a gradient descent algorithm that is looking at each step a small deformation of the boundary that decrease the functional. It is very helpful for this to provide a shape derivative. Some other tools were developed for example in structural optimisation with the SIMP method.

Each of those questions will be discussed at a certain level in this thesis.

We give two examples of a shape optimisation problem

Example 1. Suppose we have enough bricks to build a wall 2m high and 100m long and you want to build the largest enclosed property possible with those bricks. What shape should the property have to be as large as possible? Mathematically the question is which set of given perimeter (notion that will be defined in section 1.6) has the largest area? In other words let $\Omega_{\text{adm}} = \{\Omega \subset \mathbb{R}^2, \text{Per}(\Omega) = L\}$, the problem is

$$\sup_{\Omega\in\Omega_{\text{adm}}} |\Omega|.$$

Where $|\Omega|$ is the area of Ω. The problem can posed in any dimension, where $|\Omega|$ stands for the N-dimensional Lebesgue measure. This is the well-known isoperimetric problem. The answer was already formally well-known by the greeks: the ball has the largest volume among the sets of given perimeter. It is common to state this result as an universal inequality between the functionals $|\Omega|$ and $\text{Per}(\Omega)$:

$$|\Omega|^{N-1} \leqslant \frac{1}{N^N \omega_N} \text{Per}(\Omega)^N$$

with equality for the ball. ω_N is the volume of the N-dimensional unit ball. There are plenty of different proofs of this result using various tools.

It is possible to make the problem much harder in two dimensions if we add one constraint: the set has to be a tiling domain, i.e it is possible to fill the entire plane with copies of itself. This is the Honeycomb conjecture, which we exposed in the Introduction.

Example 2. A large class of problem is of a great interest since the beginning of the 20th century is the one of eigenvalue problems. The most famous one among all is about the eigenvalues of the Laplacian operator with Dirichlet boundary conditions. Recall that if Ω is an open subset of $\mathbb{R}^N$ the problem of, for a given $f \in H^{-1}(\Omega)$, finding $u \in H^1(\Omega)$ such that:

$$\begin{cases} -\Delta u = f & \text{in } \Omega \\ u = 0 & \text{on } \partial\Omega \end{cases} \tag{1.1}$$

is well posed in a weak sense. This allows us to define an operator $\Delta^{-1} : L^2(\Omega) \mapsto L^2(\Omega)$ defined by

$$-\Delta^{-1}(f) = u$$

where u is the unique solution of (1.1). This operator is symmetric, positive definite and compact. We deduce that there exists a sequence of positive numbers $(\mu_k)_{k\in\mathbb{N}^\star}$ converging to 0 and eigenfunctions $(u_k)_{k\in\mathbb{N}^\star} \in L^2(\Omega)$ such that $-\Delta^{-1}(u_k) = \mu_k u_k$ for all $k \in \mathbb{N}^\star$ (see [21] for more details about those facts). Taking $\lambda_k = 1/\mu_k$ we obtain a sequence of positive numbers converging towards infinity such that $-\Delta u_k = \lambda_k u_k$ for all $k \in \mathbb{N}^\star$. The real numbers λ_k are called the eigenvalues of the Laplacian operator with Dirichlet boundary conditions. The term Dirichlet refers to the boundary condition $u = 0$ in reference to the well known Dirichlet problem. It is possible to do the exact same thing with Neumann boundary conditions with $\frac{\partial u}{\partial n} = 0$ and we would have obtained the Neumann eigenvalues μ_k. Note that the eigenvalues depend on the set Ω. Thus we explicitly write $\lambda_k(\Omega)$.

Now in this class of problems, the most famous one is written as follows:

$$\min\{\lambda_1(\Omega),\ \Omega \subset D,\ |\Omega| = V\} \tag{1.2}$$

where D is an open subset of $\mathbb{R}^N$. The problem has the following physical formulation: find the drum of given area that has the lowest sound. To be exact, in order to have the right formulation we should add connectedness. As we will see right now this condition is naturally filled by the optimiser for λ_1, but not for λ_2. The question appeared first in the late 19th century in a book of Lord Rayleigh [82]. And was simultaneously solved in the 1920s by Faber and Krahn. The ball is the minimiser of λ_1. It is almost a corollary that the minimiser of λ_2 is the union of two disjoint identical balls. Finding the minimiser of λ_k for $k \geqslant 3$ is still an open problem. However it is proven that there exists a solution (see [23])

More generally there are plenty of operator that has the same properties than the Laplacian with Dirichlet boundary conditions and as many problems.

1.2.2 The Hausdorff distance

In this section we introduce one specific topology which is particularly convenient to deal with convex sets as we will see: the Hausdorff distance. We only deal with the basics. For a more detailed presentation we refer for example to [58, 89]. Here $\tilde{d}$ denotes the euclidian distance on $\mathbb{R}^N$.

Definition 1. *Let K_1 and K_2 be two compacts sets of $\mathbb{R}^N$. The Hausdorff distance between K_1 and K_2 and let for $x \in \mathbb{R}^n$:*

$$\tilde{d}(x, K_1) = \inf_{y \in K_1} (\tilde{d}(x, y))$$

$$\rho(K_1, K_2) = \sup_{x \in K_1} \tilde{d}(x, K_2)$$

The Hausdorff distance is then defined by:

$$d_H(K_1, K_2) = \max(\rho(K_1, K_2), \rho(K_2, K_1)) \tag{1.3}$$

One says that a sequence $(K_n)_{n \in \mathbb{N}}$ of compact sets converge to a compact set K in the sense of Hausdorff if

$$d_H(K_n, K) \underset{n \to \infty}{\longrightarrow} 0.$$

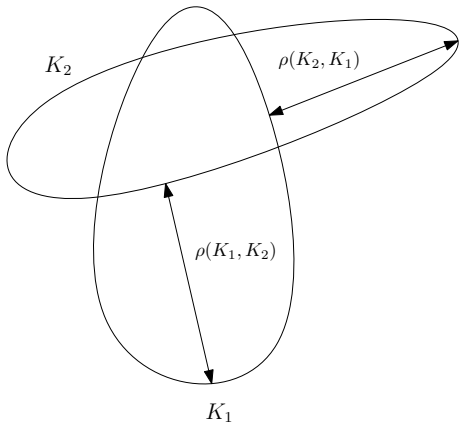

Figure 1.9: The Hausdorff distance between two compact sets.

The hausdorff distance measures how far from one set is the farthest point of the other set. It is not trivial that such functional is a distance since the triangle inequality requires some computations.

The Hausdorff convergence is equivalent to the uniform convergence for the distance function ([58] Proposition 2.2.25)

$$d_H(K_n, K) \longrightarrow 0 \Longleftrightarrow \|d(., K_n) - d(., K)\|_\infty \longrightarrow 0$$

Remark 1. This distance is only defined on compacts sets. but it is possible to define it on open sets included in a given compact set (a box) B, as the distance between their complementary (which are compacts) in B. However one cannot compute the distance between a compact set and an open set since the distance between an open set and its closure would be 0 whereas the sets are not equal. These two functions thus defined have differences, particularly in terms of regularity of some functionals that appear to be lower semi-continuous for the Hausdorff convergence on compact sets, and upper semi-continuous for the Hausdorff convergence on open sets.

We give some properties of the Hausdorff convergence for compact sets. For more properties we refer to [58, 89]

Proposition 1. *[58]*

1. *The inclusion is stable under the Hausdorff convergence.*
2. *A decreasing sequence for the inclusion of nonempty compact sets converges to its intersection.*
3. *An increasing sequence of compact sets included in a box B converges to the closure of its union*
4. *if K_n converges to K then $K = \{x, \forall n \in \mathbb{N} \exists x_n \in K_n, x_n \longrightarrow x\}$*

The main problem in choosing a topology is to have both compactness and regularity, which are opposite objectives. Indeed having compactness requires to have a few open sets while regularity is all about having a lot of open sets. The Hausdorff topology is a nice example of such a dilemma.

Indeed this topology allows compactness under small assumptions:

Proposition 2. *[[58] Th 2.2.25] The set of compacts sets K included in a compact set B is compact for the Hausdorff distance. In other words, let $(K_n)_{n\in\mathbb{N}}$ be a sequence of compacts sets included in a compact set B, then there exists a compact set $K \subset B$ and a subsequence K_{n_k} such that $K_{n_k} \underset{k\to\infty}{\longrightarrow} K$.*

But some very important functional are not continuous. This is the case of the volume, perimeter and diameter functional.

Proposition 3. *[[58] p.37]*

1. *The volume functional is upper semi-continuous for the Hausdorff convergence for compacts sets (and lower semi-continuous for the Hausdorff convergence for open sets).*
2. *The perimeter functional is neither lower semi continuous or upper semi continuous for the Hausdorff convergence.*
3. *The diameter functional is upper semi continuous for the Hausdorff convergence for compact sets.*

But as we will see later, under convexity assumption, most geometric functionals are continuous for the Hausdorff distance.

1.2.3 Shape derivative

In this section we define the derivative of a shape with respect to a given deformation. It allows to write optimality conditions. The principle is analogous as in finite or infinite dimension. Recall that if a regular functional $J : \Omega \subset \mathbb{R}^N \mapsto \mathbb{R}$ admits a minimiser $x^\star$, then $x^\star$ solves the problem $\nabla J(x^\star) \cdot h \leqslant 0$ for every admissible direction, yielding optimality conditions. In shape optimisation the idea is pretty much the same.

Several ways exist to define a shape derivative, and we rely on Hadamard's boundary variation method, a brief sketch of which is now provided; see for instance [58, 4, 76] for in-depth expositions.

From now on we suppose that Ω is an open set with Lipschitz boundary, and that the shape functional J is well defined for shapes with Lipschitz boundary. In the framework of Hadamard's

method, the sensitivity of a shape functional is assessed with respect to small perturbations of Ω. More precisely we consider the deformed shape

$$\Omega_V = (\mathrm{Id} + V)(\Omega) = \{x + V(x), x \in \Omega\} \tag{1.4}$$

where $V : \mathbb{R}^N \to \mathbb{R}^N$ is a small vector field, and Id is the identity mapping from $\mathbb{R}^N$ into itself. The shape Ω_V is obtained from initial shape Ω by transporting each element of Ω by the vector field V. V is called a deformation field.

More precisely we will chose V with some regularity. We take $V \in W^{1,\infty}(\mathbb{R}^N, \mathbb{R}^N)$ the space of functions in $L^\infty(\mathbb{R}^N, \mathbb{R}^N)$ with values in whose derivative in the sense of distribution DV is also in $L^\infty(\mathbb{R}^N, \mathbb{M}_N(\mathbb{R}))$, in other words $\frac{\partial V_i}{\partial x_j} \in L^\infty(\mathbb{R}^N)$. This space is a Banach space when endowed with the norm:

$$\|V\|_{1,\infty} = \sup_{x\in\mathbb{R}^N} |V(x)| + \sup_{x\in\mathbb{R}^N} |DV_x(x)|$$

where $|x|$ is the euclidian norm of $x \in \mathbb{R}^N$.

Note that this is precisely the set of Lipschitz functions over $\mathbb{R}^N$ with values in $\mathbb{R}^N$. A direct consequence of this choice is that whenever V is "small enough" in the sense of the $W^{1,\infty}$ norm, the set Ω_V still has a Lipschitz boundary.

Remark 2. For V small enough, at the first order, the deformation of Ω is given by the deformation of $\partial\Omega$. More precisely $\partial\Omega_V$ is obtained at the first order by taking the points $x + V \cdot n$ for $x \in \partial\Omega$. This come from the following fact: as soon as V_1 and V_2 are two deformation fields such that $V_1 \cdot n = V_2 \cdot n$ on the boundary $\partial\Omega$ of Ω, then $\Omega_{V_1} = \Omega_{V_2}$ at the first order. A proof of this fact is given in [4, prop 6.17].

We are now interested in computing directional derivatives with respect to a given deformation. For that purpose let us fix a Lipschitz deformation field V, and consider the set

$$\Omega_t = (\mathrm{Id} + tV)(\Omega).$$

The idea is to look what happens if we let t converge towards 0.

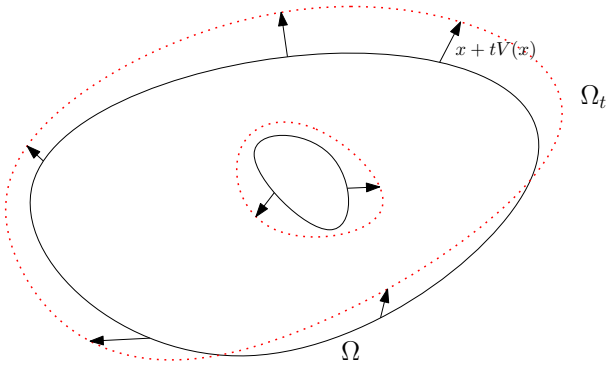

Figure 1.10: The sets Ω in black and Ω_t in red dotted.

Definition 2. *Let Ω be an open set with Lipschitz boundary. We say that J has a directional derivative with respect to a vector field V if the function $t \mapsto J(\Omega_t)$ is derivable at 0. In other words J has a directional derivative with respect to V if there exists a real number $h(V)$ such that J admits the following expansion:*

$$J(\Omega_t) = J(\Omega) + t \times h(V) + o(t). \tag{1.5}$$

The function $h(V)$ will be denoted by $\langle DJ(\Omega), V\rangle$.

If J has a directional derivative with respect to all fields $V \in W^{1,\infty}(\mathbb{R}^N, \mathbb{R}^N)$ and $V \mapsto \langle DJ(\Omega), V\rangle$ is linear continuous, then we say that J is shape differentiable at Ω.

In the future this notion will not be used a lot so we do not give too many details. Let us just mention that we are mostly dealing with integral functional of the type

$$J(\Omega) = \int_\Omega f(x, \Omega) \ \ dx, \tag{1.6}$$

or

$$J(\partial\Omega) = \int_\Omega f(x, \Omega) \ \ dx, \tag{1.7}$$

and $f(x, \Omega)$ is often given by $f(x, \Omega) = j(x, u_\Omega, Du_\Omega)$ where u_Ω is solution of a partial differential equation in Ω with boundary conditions. Under regularity assumptions over the functional j, the boundary conditions and Ω, such functional is differentiable. Moreover we have a structure theorem that states that there exists a function $\theta \in L^2(\partial\Omega)$ such that for all deformation field V,

$$\langle DJ(\Omega), V\rangle = \int_{\partial\Omega} \theta(V \cdot n) \ ds. \tag{1.8}$$

See [58] Chapter 5 for a complete course, and prop 5.9.1 for the structure theorem. In section 1.5 we provide such an example of shape derivative.

1.3 Packings, Tilings, Density

In this section we introduce the general notion of packing. It consists in studying the arrangement of a collection of geometric objects. This began more than two thousands years ago with the study of tilings domains by Archimedes and Euclid, and many raised problems such as the isoperimetric inequality in the case of tiling domains, leading to the famous honeycomb conjecture (see (1) in the general introduction). These questions have again emerged in the 17th century under the impulse of mathematicians such as Kepler, or Newton, followed by numerous until today. Kepler studied the problem of optimal packing for spheres, i.e the way of arranging spheres in the space such that the portion of the space it occupies is maximal. He conjectured that the optimal density is $\frac{\pi}{3\sqrt{2}} \simeq 0.74$, attained for the face-centered cubic packing. This is the well-known Kepler conjecture, finally proven by T.Hales in 1998 with a computer assisted proof.

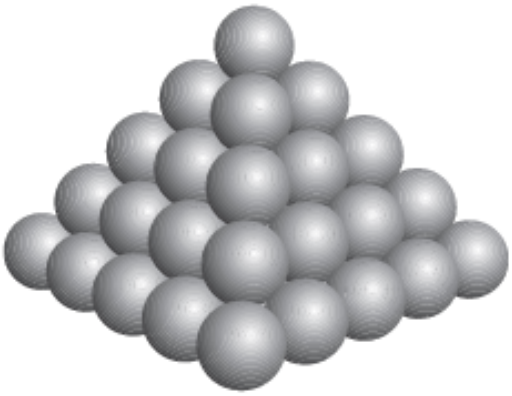

Figure 1.11: The face-centered cubic packing of spheres: the densest packing for spheres in 3 dimensions (source [52])

In what follows we briefly introduce the main concept of packing together with density, and we provide an overview over the issues related to those notions. For in-depth analysis we refer to [47, 94, 48, 87], and [15, 49, 43] for a more ludic approach, especially on tilings.

1.3.1 Definitions and basic properties

Define $\mathcal{K}^N$ as the set of convex bodies of $\mathbb{R}^N$ i.e convex compacts sets of $\mathbb{R}^N$ with non-empty interior.

Definition 3. *Let $K \in \mathcal{K}^N$. A packing with pattern K is a set*

$$\bigcup_{i\in I} \tau_i(K) \text{ such that } \operatorname{int}(\tau_i(K)) \cap \operatorname{int}(\tau_j(K)) = \emptyset, i \neq j.$$

where τ_i are affine isometries. If I is finite we call it a finite packing. If I is infinitely countable we call it an infinite packing. $\mathcal{P}(K)$ is the set of all packings of K. If $\mathbb{R}^N \in \mathcal{P}(K)$ we say that K is a tiling domain.

Remark 3. It is also possible to consider a set of patterns $\mathcal{E} = (K_j)_{j\in J}$, and a packing composed of the different patterns in $\mathcal{E}$

Remark 4. One can also study the finite packings included in a given domain Ω: $\mathcal{P}_\Omega(K)$. One very interesting problem for example is to find the maximum number of disks of a given radius r it is possible to store in disk of radius $R > r$. But in the following we will only be interested in infinite packings of $\mathbb{R}^N$

In fact there are several types of packing according to the isometries that we allow ourselves to consider. For the general definition we consider any type of direct isometries, but one can consider translative packings where only translations are authorized. In this case a packing will be denoted $K + X$ where X is a discrete set of points, each point corresponding to a translation. We could also allow inversions, i-e a rotation with angle 180 degrees. In other words we can make translations of K and $-K$ More constraining: the lattice packings, where X has to be a

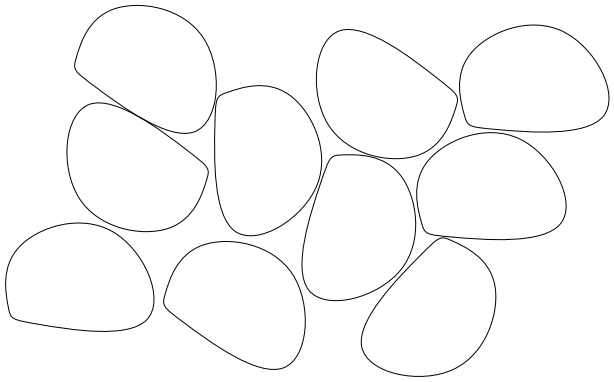

Figure 1.12: An example of packing

lattice. Recall that a lattice is any subset $\Lambda = \{\sum_{i=1}^{N} a_i v_i a_i \in \mathbb{Z}\} \subset \mathbb{R}^N$ where $(v_1, .., v_N)$ is a basis of the vector space $\mathbb{R}^N$. In other words, only two directions are allowed for a translation. Another very important packing is the double-lattice packing, where we authorize an inversion. This leads to a lattice packing of the pattern, together with the same lattice packing with $-K$. More generally, if $\mathcal{G}$ is a subgroup of the group of isometries of $\mathbb{R}^N$ we may denote by $\mathcal{P}_{\mathcal{G}}(K)$ the set of packings with pattern K obtained by taking isometries in $\mathcal{G}$.

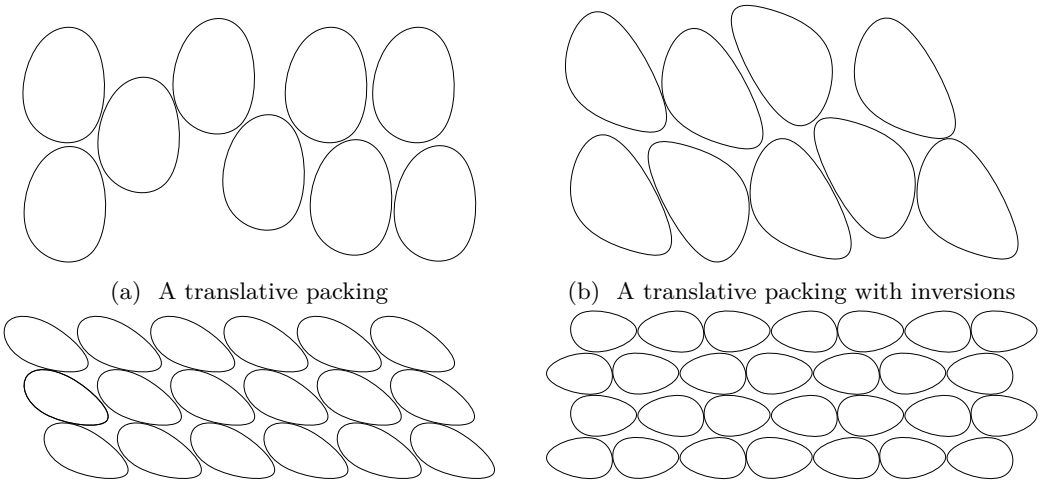

(a) A translative packing

(b) A translative packing with inversions

(c) A lattice packing

(d) A double lattice packing

Figure 1.13: Different subtypes of packings

A notion that is often associated to packings is the one of density. In a few words the density is a measure of the portion of the space a packing occupies. First we introduce the density of a packing, that is a measure of how well the space is filled by the packing, and then the density of a convex body K that is the highest density that can be reached by a packing with pattern K.

Definition 4. *let $K \in \mathcal{K}^N$ and $P(K) \in \mathcal{P}(K)$. We define the density of $P(K)$ by:*

$$\tilde{\delta}(P(K)) = \liminf_{l\to\infty} \frac{\sharp\{i \in I \mid \tau_i(K) \subset [-l/2, l/2]^N\} \times |K|}{l^N} \tag{1.9}$$

And the density of K is defined by:

$$\delta(K) = \sup_{P(K)\in\mathcal{P}(K)} \tilde{\delta}(P(K)) \tag{1.10}$$

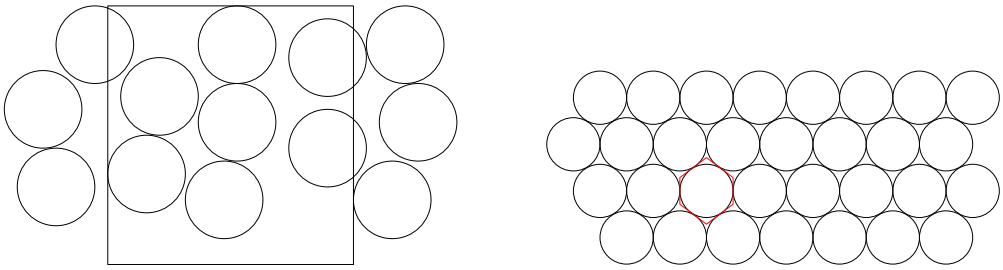

(a) The density as the ratio of the space occupied by circles in the square

(b) The Packing which maximises the density of the circle

Figure 1.14: To compute the density of a packing, take a window, divide the area of circles included in the window by the area of the square. Let the window go towards infinity. On Figure 1.14a the ratio is equal to $\frac{5\pi r^2}{l^2}$ where r is the radius of the circle and l is the length of the square. Figure 1.14b shows the packing that realizes the maximum density. It is easy to see that the density of this packing is equal to the ratio of the area of the circle divided by the area of the regular hexagon enclosing each circle (one is drawn in red). After computation it comes that $\delta(Disk) = \frac{\pi}{2\sqrt{3}}$. This latter result is far from being trivial, and was first shown by Lagrange in 1771 for lattice packings. Then Gauss proved in 1831 the results among periodic packings, and Thue in 1891 gave a proof in the general case. But the first rigorous one was given by Fejes Toth in 1940 ([38])
.

Remark 5. It is equivalent to consider for the density of a packing the number $|P(K) \cap S|$ where S is the cube, since when the length l of the N-dimensional cube goes towards infinity the number of copies of K that are partially included in C is $O(l^{N-1})$ hence the loss of volume is of the same order, whereas the growth of the cube is l^N.

Remark 6. This definition of the density does not depend of where we set the origin: we can chose the middle of the cube as any point in the space, the limit remains the same.

Similarly we can define $d_T(K)$, and the supremum taken over translative packings $\delta_{T^\star}$ when inversions are authorized. $\delta_L(K)$ the supremum taken over lattice packings, and $\delta_{L^\star}(K)$ for the double lattice packing. But if we give no precision about the density nor the packing, we consider the most general notion $\delta(K)$.

Let us first give a very simple result for the computation of the density of a lattice packing.

Proposition 4. *Let $\Lambda = \{\sum_{i=1}^N a_i v_i a_i \in \mathbb{Z}\}$ and $P = K + \Lambda$ a lattice packing. Then*

$$\tilde{\delta}(P) = \frac{|K|}{Det(v_1, .., v_N).}$$

Proof. We restrict ourselves to the dimension $N = 2$ for sake of simplicity Let $p = \{a_1v_1 + a_2v_2, a_i \in [0,1]\}$. Then p is a parallelogram named the fundamental domain of the lattice (see Figure 1.15 in red).

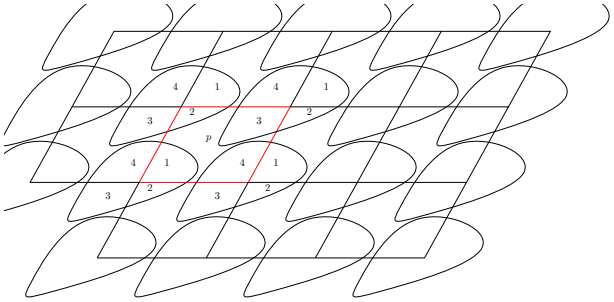

Figure 1.15: The density of a lattice packing as the ratio between the area of K and the one of the fundamental domain of the lattice.

Since the lattice packing is periodic with period p, it is sufficient to compute the density of the small region enclosed by p. Now consider $K = K + 0$. Then we can see (Figure 1.15) that the sets $p, p - a_1, p - a_1 - a_2, p - a_2$ cut K into four parts, numbered respectively 1,2,3,4. By periodicity of the packing, each part and only them is found in p as a piece of a translated copy of K. Hence the total area of the packing contained in p is exactly the one of K. Since the area of p is precisely $\mathrm{Det}(v_1, v_2)$ we get the result.

□

This is a reason why lattice packing are often considered: the density is easy to compute.

Another easy thing we can say is: If T is a tiling domain circumscribed about K, then if we consider a tiling of the space with pattern T, in each cell of the tiling we can put a copy of K (see Figure 1.16). In that way we obtain a packing of K, with density $|K|/|T|$. Hence $\delta(K) \geqslant |K|/|T|$.

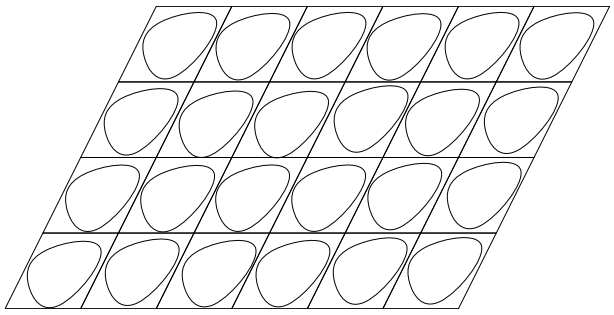

Figure 1.16: The density of K is higher than $|K|/|T|$

1.3.2 Some questions about packings

Now we stick to dimension $N = 2$. Several questions naturally arise about those functionals. Let us give some of those.

1. Is the supremum of the density over packings attained?
2. What is the regularity of the functional with respect to the Hausdorff distance?
3. It is clear that $\delta_L(K) \leqslant \delta_T(K) \leqslant \delta_{T^\star}(K) \leqslant \delta(K)$ and $\delta_{L^\star}(K) \leqslant \delta_{T^\star}(K) \leqslant \delta(K)$ for every K. What about equality cases?
4. Is there a way to compute, exactly or numerically, the density of a convex body?
5. It is obvious that the maximal density is 1, attained by tiling domains. But what is the minimal density?
6. What can we say about tiling domains?

H. Groemer in [46] gave an answer for the two first questions. Actually he proved the following:

Proposition 5 (Existence of the optimal packing and continuity of the density.[46])**.** *If $\mathcal{G}$ is any subgroup of the group of isometries of $\mathbb{R}^2$ that contains all the translations, then there exists a packing $P^\star \in \mathcal{P}_\mathcal{G}(K)$ such that $\delta(K) = \tilde{\delta}(P^\star)$. Moreover the functional $K \to \delta(K)$ is continuous for the Hausdorff distance.*

This shows that the number $\delta(K), \delta_T(K)$ and $\delta_{T^\star}(K)$ are reached. Thanks to a compactness result of about lattices due to Mahler, we can also show the result for lattice and double lattice packings ([47]).

For the third question, C.A Rogers in [86] proved that for any convex body K, one has $\delta_T(K) = \delta_L(K)$. However this results is only true in dimension $N = 2$.

In the other hand, the simple example of triangles show that if K is any triangle $\delta_T(K) = 2/3$ (see [26, 37]) whereas $\delta(T) = 1$. Nevertheless, L. Fejes Tóth proved two results about this question.

Definition 5. *A convex body K is centrally symmetric if $-K = K$.*

Proposition 6. *[40] If K is centrally symmetric, then $\delta(K) = \delta_L(K)$. In other words, the highest density of a packing with a centrally symmetric pattern is achieved by a lattice packing.*

The question now is to know how often the two density coïncinde. L. Fejes Tóth again showed the following:

Proposition 7 ([39])**.** *Let $\mathcal{N}$ be the set of convex bodies K such that $\delta(K) > \delta_L(K)$. Then $\mathcal{N}$ is a dense open subset of $\mathcal{K}$ for the Hausdorff metric.*

Regarding the minimisation of the density in dimension $N = 2$, the problem remains open, but a lot of progress has been made. Techniques for obtaining lower bounds are generally based either on the construction of a good lattice packing for which we are able to provide a density, or on the construction of a tiling domain enclosing the pattern. It has been shown that given a convex body K, there exists a triangle T such that $K \subset T$ and $|K|/|T| \geqslant 2/3$ (see [37] by M.A Fary in 1950 and [26] by R.Courant in 1965). Doing the same thing with a particular tiling (named p-hexagon), Kuperberg gave the lower bound $\delta(K) \geqslant 3/4$ for every convex body K. This lower bound has been improved in 1990 by W. and G. Kuperberg in [67], where it is shown that $\delta(K) \geqslant \sqrt{3}/2$, by building a good double lattice packing. In 1995, K.R Doheny proved in [31] the existence of $r_0 > \sqrt{3}/2$ such that $\delta(K) \geqslant r_0$ for every convex body K. Up to our knowledge, the exact value of the bound $\inf\{\delta(K),\ K \in \mathcal{K}\}$ remains unknown.

On the other side, K. Reinhardt in [84] proposed a candidate for the minimiser: a smoothed octagon with density $\simeq 0.90241$. However the best candidate up to know is the regular heptagon. The double lattice density of H is know to be $\delta_{L^\star}(H) \simeq 0.89269 < 0.90241$, and it is still an open question to know if the maximal density is attained by a double lattice packing. Y. Kallus in [64] that H is a local minimiser for $\delta_{L^\star}$.

About the computation of the exact value of the density, there is up to our knowledge no spectacular results, and the task seems very challenging. Let us also highlight the fact that up to now, there is no proof that given any convex body, the optimal packing is periodic. According to P.M Gruber ([47]), this conjecture was formulated by H. Zassenhaus. Let us point the fact that If K is centrally symmetric, then the previous proposition showed that $\delta(K) = \delta_L(K)$, and then the exact value is much easier to compute since we need to search the best packing only among the lattice packings for which we are able to provide the exact density. Another interesting result due, again, to L. Fejes Tóth shows that the density of K is always lower than $\frac{|K|}{|H(K)|}$ where $H(K)$ is the smallest hexagon enclosing K. Furthermore, if K is centrally symmetric, then $H(K)$ is symmetric, then tiling, the density is precisely $\frac{|K|}{|H(K)|}$.

Concerning the numerical computations, The methods developed in [67] actually provides an algorithm to compute the best double lattice packing. Note that there also exists a large literature on how to compute the smallest n-gon containing a given polygon. For example [78, 66, 79] provide a linear time algorithm for the computation of the minimal area triangle. In [92] , an algorithm is provided for the computation of the minimal parallelogram. It is intuitive that the more edges the enclosing polygon has, the smaller it may be. But if we look among the hexagons, it is hard to guarantee that the minimal area hexagon is a tiling domain (except if the obtained hexagon is centrally symmetric).

1.3.3 Tilings

Now we take a look at the convex tiling domains of $\mathbb{R}^2$. Without hypothesis on the convexity, there is a huge variety of tiling domains. For example the number of sides of a tiling domain is not bounded (consider a square where one side replaced by triangular spikes) and some tiling are not periodic (see [49]). Fortunately if we impose convexity, things become much easier. For example we have the following:

Proposition 8 ([48] 3.5 Theorem 6)**.** *Let K be a tiling domain. Then K is a polygon with at most 6 sides.*

Now we briefly provide the complete characterization of the convex tiling domains in the plane.

- Every triangle is a tiling domain. The tiling is achieved by a double lattice packing (see Figure 1.17). Consider a triangle: take a copy, turn it 180 degrees and stick it to the original one to form a parallelogram. Then it is easy to tile the plane by a lattice packing.

- Every quadrangle is a tiling domain. And again it is achieved by a double lattice packings. This time if we stick together a quadrangle and its inverted copy, we obtain a symmetric hexagon that tiles the plane with a Lattice packing (see Figure 1.18)

- The case of pentagons is by far the hardest. We do not provide too much details, but we know that the classification was achieved in 2017 by M. Rao ([81]). There are 15 kinds of

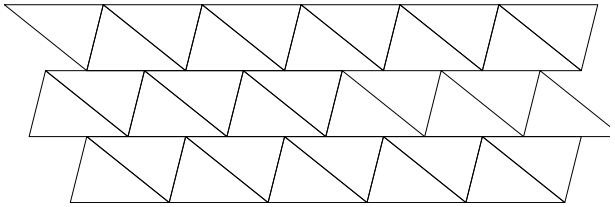

Figure 1.17: Tiling with triangles

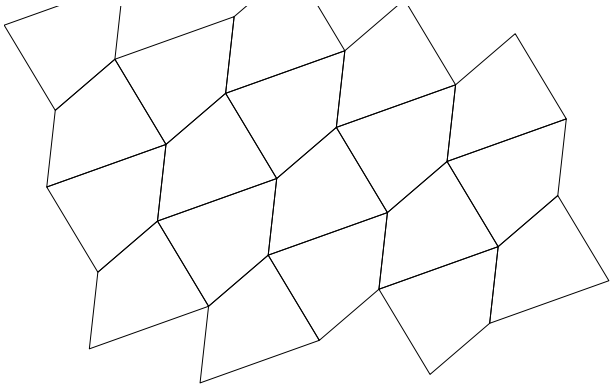

Figure 1.18: Tiling with quadrangles

Pentagonal Tilings. The search for pentagonal tiling began with K.Reinhardt in his thesis [83]. He discovered 5 types of pentagones. Fifty years after Kershner discovered in 1968 three new types ([65]). The count slowly increased until 2015 when the last one was found 2015 with the help of a computer program (see [73]). It is remarkable that each tiling is obtained by assembling a big tile, named primitive tile unit, then performing a lattice packing with this tile.

- When it comes to hexagons, the problem was solved in the early 20th century by K.Reinhardt in his thesis. There are three kinds for which we give a full description, which is made standard in [65]. Denote by a, b, c, d, e, f the length of the sides of H and A, B, C, D, E, F its angles (see Figure 1.19).

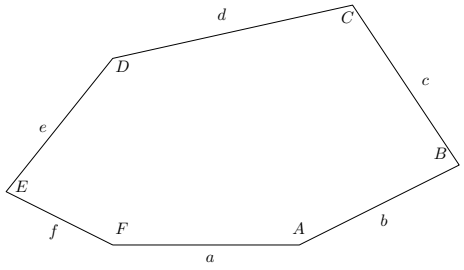

Figure 1.19: Notations for a standard hexagon

1. The first hexagon, is the easiest to obtain, and the most important for us in the sequel. It is characterized by the relations: $A + B + C = 2\pi/3$, $a = d$. It simply consists in imposing that two opposite sides are parallel and of the same size. We name it a p-hexagon

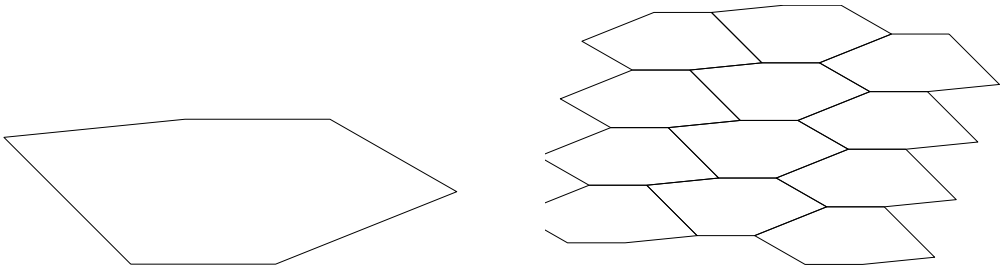

(a) Figure of the hexagon (b) The tiling with hexagons

Figure 1.20: The p-hexagon. Once the hexagon is built, we just reverse it and stick it to the original. It is now possible to obtain a lattice packing with those 2.

2. The second type is a bit more complex. It is characterized by the relations : $A + B + D = 2\pi$, $a = d$, $c = e$. It should be noted that the associated tiling contains a reflexion. Hence it cannot be fully considered as a tiling in our definition.

(a) Figure of the hexagon (b) The tiling with hexagons

Figure 1.21: The second type of tiling hexagon. Once the hexagon is built (Figure 1.21a) one must construct a block of 4 (in red in Figure 1.21b), in which 2 copies (the bottom ones) are actually the reflected hexagon. Then it is possible to build a lattice tiling with the red block.

3. The last hexagon is characterized by the relations: $A = C = E = 2\pi/3$, $a = b$, $c = d$, $e = f$.

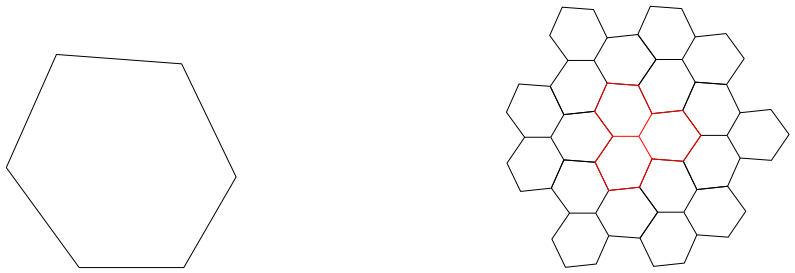

(a) Figure of the hexagon (b) The tiling with hexagons

Figure 1.22: The last type of tiling hexagon. Once the hexagon is built (Figure 1.22a), we perform two successives rotations of $2\pi/3$ and stick the equal sides together in order to obtain the red figure in 1.22b. Then we obtain a lattice tiling of the red figure.

1.4 The Support Function

The support function is useful tool to parametrize a convex set by a function defined on the unit sphere. This allows us to partially turn geometrical problem into analytical problems, see e.g [11, 54, 69, 53] (in [69] the authors actually worked with the gauge function, but the idea is the same).

We first give the main definitions and properties of the support function, among them the regularity of the support function and nice properties of the convexity with regards to the Hausdorff Distance, then we especially focus on the 2 dimensional case where we introduce the length measure of a convex body. For more details we refer to [89, 12, 70].

1.4.1 Definition and first properties

Definition 6. *Let $K \in \mathcal{K}^N$ be a convex body. the support function $\tilde{h}_K$ is defined on $\mathbb{R}^N$ by*

$$\tilde{h}_K(x) = \sup_{y \in K} (x \cdot y). \tag{1.11}$$

We give immediately properties of the support function:

Proposition 9 ([89] p.45)**.** *$\tilde{h}_K$ is a convex, Lipschitz and positively homogeneous of degree one function on $\mathbb{R}^N$.*

Thus it is enough to study $\tilde{h}_K$ as a function of the unit sphere $\mathbb{S}^{N-1}$, which is what we are going to do. Let us introduce h_K as the restriction of $\tilde{h}_K$ to $\mathbb{S}^{N-1}$.

Remark 7. It is also possible to define the support function of a non convex set. Defined in this way, it is exactly the support function of the convex hull of the latter.

The support function gives a full characterization a convex set in the following sense:

Proposition 10 ([89] Th 1.7.1)**.** *If $f : \mathbb{R}^N \mapsto \mathbb{R}$ is a linear and sub-additive function, then there exists a unique convex body $K \in K^N$ such that $f = \tilde{h}_K$.*

A good way to understand the support function is to remember that a convex K is precisely the intersection of his closed tangent hyperplane, also named support hyperplanees. Now if u is a unit vector, and H is the support hyperplane of K with outer normal vector u, $h_K(u)$ is equal to the signed distance of the origin to H (see figure 1.23).

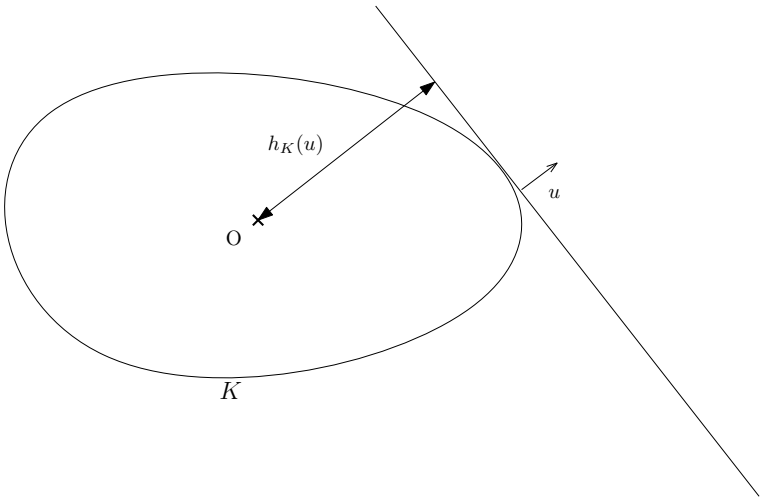

Figure 1.23: The support function as the distance function to the tangent hyperplanee

Note that it is a signed distance, since if the origin does not lie in the interior of the convex body, the support function may be negative (see Figure 1.24). We can even say that the support function is positive if and only if the origin lies in the interior of the convex body.

Let $u \in \mathbb{S}^{n-1}$ and $\alpha \in \mathbb{R}$ and define $H_u(\alpha) = \{y \in \mathbb{R}^n, x \cdot y = \alpha\}$ and $H_u^-(\alpha) = \{y \in \mathbb{R}^N, u \cdot y \leqslant \alpha\}$. Then

$$h_K(u) = \inf(\{\alpha \in \mathbb{R}, K \subset H_u^-(\alpha)\}), \tag{1.12}$$

and $H_u(h_K(u))$ is the support hyperplane of K with outer normal vector u.
For $K \in \mathcal{K}^N$ and $u \in \mathbb{S}^{N-1}$ define:

- $H_K(u) = \{y \in \mathbb{R}^n, u \cdot y = h_K(u)\}$.
- $H_K^-(u) = \{y \in \mathbb{R}^n, u \cdot y \leqslant h_K(u)\}$.

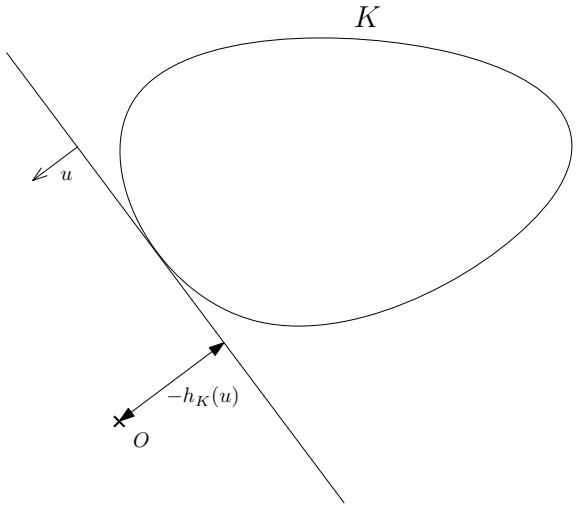

Figure 1.24: A case where the support function is negative

- $F_K(u) = H_K(u) \cap K$.

Those definitions naturally extend to $\tilde{h}_K$. Note that if x and u are colinear, then $F_K(u) = F_K(x)$ the same goes for H_K and H_K^- (see Figure 1.25).

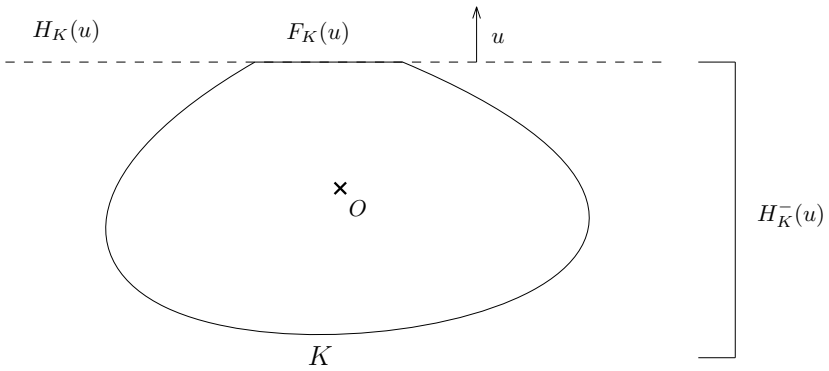

Figure 1.25: Different sets involved in the support function

$H_K(u)$ is precisely the support hyperplane of K in the direction u, $H_K^-(u)$ is the support half-space, $F_K(u)$ is called support set of K in the direction u. Let us immediately state the following fact: $F_K(u)$ is a non empty connected subset of $H_K(u)$. and we say that K is flat at u if $F_K(u)$ is not reduced to a single point. In two dimension, it means that K has a side with normal vector u. In three dimension: it is a face. This set is of primary importance for the regularity questions.

Some fundamental properties of the support function are now introduced.

Proposition 11. *Let K_1 and K_2 be two convex sets of $\mathcal{K}^N$*

- *If K is reduced to a single point $a \in \mathbb{R}^n$, then for all $u \in \mathcal{S}^{N-1}$, $h_K(u) = u \cdot a$.*
- $K = \{y \in \mathbb{R}^N, x \cdot y \leqslant h_K(x) \quad \forall x \in \mathbb{R}^N\}$
- *$K_1 \subset K_2$ if and only if $h_{K_1} \leqslant h_{K_2}$.*
- $h_{K_1 \cap K_2} = \min(h_{K_1}, h_{K_2})$.
- $h_{K_1 + K_2} = h_{K_1} + h_{K_2}$.

The second point is the direct consequence of the geometrical form of Hahn-Banach theorem: if $z \notin K$ there exists $x \in \mathbb{R}^N$ and $\alpha \in \mathbb{R}$ such that for all $y \in K$,

$$y \cdot x \leqslant \alpha < z \cdot x.$$

passing to the infinimum of the α for which the left inequality holds true (which is precisely $h_K(x)$), we get $h_K(x) < z \cdot x$.

As a direct consequence of first and last point, if $K' = K + a$, then $h_{K'}(u) = h_K(u) + u \cdot a$.

Regularity Now we briefly explain some regularity aspects of the support function. Since the support function has a direct link with the boundary ∂K of a convex body, its regularity is also directly linked to the properties of the boundary: geometrical and analytical. It is important to understand that the regularity of the boundary does not necessarily imply the regularity of the support function. For example we will see that the support function is C^1 if and only if the convex body is strictly convex. Let us now state the main theorem on the subdifferential of the support function defined on $\mathbb{R}^N$. Recall that if f is a differentiable convex function, then for all $x, y \in \mathbb{R}^n$:

$$f(y) \geqslant f(x) + \nabla f(x) \cdot (y - x). \tag{1.13}$$

Following (1.13), one is able to build a natural extension of the gradient of a convex function, known as the subdifferential:

Definition 7. *Let $f : \mathbb{R}^N \mapsto \mathbb{R}$ be any convex function. The subdifferential of f at $x \in \mathbb{R}^N$ is defined by:*

$$\partial f(x) = \{v \in \mathbb{R}^N, f(y) \geqslant f(x) + x \cdot (y - x) \forall y \in \mathbb{R}^N\}. \tag{1.14}$$

Any vector $v \in \partial f(x)$ is called a subgradient of f at x. f is differentiable at x if and only if $\partial f(x)$ is a singleton v, and in that case $v = \nabla f(x)$.

The subdifferential represents in a way the support hyperplanes of the epigraph of a convex function, i.e the convex set $\text{epi}(f) = \{(x, y) \in \mathbb{R}^N \times \mathbb{R}, y \geqslant f(x)\}$, in the following sense:

Lemma 1 (Schneider [89] Lemma 1.5.14)**.** *$v \in \mathbb{R}^N$ is a subgradient of f at x if and only if $(v, -1)$ is an outer normal vector to* $\text{epi}(f)$ *at $(x, f(x))$.*

In one dimension the subgradient is the set of the slopes of the lines passing through $(x, f(x))$ that remain below the epigraph of f.

Before giving the subdifferential of the support function, let us give its directional derivatives.

Proposition 12 ([89]). *Let $K \in \mathcal{K}^N$ and $x \in \mathbb{R}^N \backslash \{0\}$. If $v \in \mathbb{R}^N$, the derivative of $\tilde{h}_K$ at x in the direction v is*

$$\frac{\partial \tilde{h}_K}{\partial v}(x) = \tilde{h}_{F_K(x)}(v). \tag{1.15}$$

Proposition 13 ([89] Th 1.7.4). *Let $K \in K^N$ a convex body. The subdifferential of $\tilde{h}_K$ at $x \in \mathbb{R}^N \backslash \{0\}$ is precisely $F_K(x)$, and $\partial \tilde{h}_K(0) = K$*

We easily the following regularity theorem:

Proposition 14. *[89] $\tilde{h}_K$ is C^1 on $\mathbb{R}^N \backslash \{0\}$ if and only if K is strictly convex.*

Proof. The strict convexity is equivalent to the fact that $F_K(x)$ is a singleton for every $x \in \mathbb{R}^N$ □

1.4.2 Hausdorff convergence and convexity

In this section we take a closer look of convexity with regards to the Hausdorff convergence. Note first that the Hausdorff distance and the support functions are closely related:

Proposition 15 ([89] Lemma 1.8.4). *Let $K_1, K_2 \in \mathcal{K}^N$ then*

$$d_H(K_1, K_2) = \|h_{K_1} - h_{K_2}\|_\infty. \tag{1.16}$$

Together with the approximation of convex bodies polygons, we obtain an approximation of the support function of any convex body by the support function of polygons. This is a great use for proving several results that we give later

Proposition 16 ([89] Th 1.8.6). *The set of convex bodies is closed for the Hausdorff convergence, i-e if $(C_n)_{n\in\mathbb{N}}$ is a sequence of convex sets converging to a set C, then C is convex*

This follows from the point 4 of Proposition 1: if $x, y \in C$ and $t \in [0, 1]$, take $x_n \in C_n$ converges to x and $y_n \in C_n$ converges to y. it follows by convexity of C_n that $tx_n + (1-t)y_n \in C_n$, then $tx + (1-t)y \in C$.

Combined with theorem 2 we get a compactness result for convex sets:

Proposition 17. *The set of convex bodies included in a compact set D is compact for the Hausdorff distance.*

We also provide a continuity result for the volume, the diameter and the perimeter, that is a direct consequence of the link between Hausdorff convergence and support functions, together with formulas for the area and perimeter. We give more details about the two dimension case in the following subsection.

Proposition 18 ([89] Th 1.8.20). *The volume, the perimeter and the diameter defined on the set of convex bodies are continuous functionals for the Hausdorff distance.*

1.4.3 The 2d case

From now on, if there is no ambiguity we will abandon the K-index for better readability. From now we assume that $N = 2$, and the support function is defined on the unit circle

Note that the unit circle can be parametrized by the torus $\mathbb{T} = \mathbb{R}/2\pi\mathbb{Z}$. With a slight abuse of notation we write for $\theta \in \mathbb{T}$:

$$u_\theta = (\cos(\theta), \sin(\theta)) \tag{1.17}$$
$$h(\theta) = h(u_\theta) \tag{1.18}$$

hence we consider that h is a function defined on the torus. Moreover we replace the notation $H^-(\theta)$ by D_θ, and D_θ is called a support line of K. The fact that h is a Lipschitz 2π-periodic function implies that h is in $W^{1,\infty}_{per}([0, 2\pi])$, and h admits almost everywhere a derivative $h'(\theta)$.

Let us begin with some basic examples of support functions in two dimension:

Example 3. 1. If $K = D(x, r)$ where $x = (a, b)$ then for all $\theta \in [0, 2\pi]$,

$$h(\theta) = a\cos(\theta) + b\sin(\theta) + r.$$

2. If K is a segment with extremities $x_1 = (a_1, b_1)$ and $x_2 = (a_2, b_2)$. Let θ_s the angle representing the unit vector $\frac{x_2 - x_1}{\|x_2 - x_1\|}$, then

$$h(\theta) = \begin{cases} a_2\cos(\theta) + b_2\sin(\theta) & \text{if } \theta - \theta_s \in [-\pi/2, \pi/2] \\ a_1\cos(\theta) + b_1\sin(\theta) & \text{otherwise} \end{cases}$$

3. If K is the rectangle with coordinates $(\pm L, \pm l)$ then

$$h(\theta) = L|\cos(\theta)| + l|\sin(\theta)|.$$

We quickly explain how to compute the support function of a polygon. If K is a polygon, then any support line touches an edge of the polygon. Now if x is an edge of K, then it is easy to see the set of angles θ such that D_θ touches x is a segment $\Theta(x)$. On $\Theta(x)$, h is the support function of the point $x = (a, b)$, so we deduce that on each $\Theta(x)$, $h(\theta) = a\cos(\theta) + b\sin(\theta)$. Figure 1.26 illustrates this.

Notice that as mentioned earlier, the support function is not everywhere regular. Indeed, singularities can be observed when moving from one vertex of the polygon to another. Figure 1.26 also highlights that there is no link between the regularity of the boundary and the regularity and the support function. In fact the support function is smooth where the boundary has angles, and it has singularity where the boundary is flat.

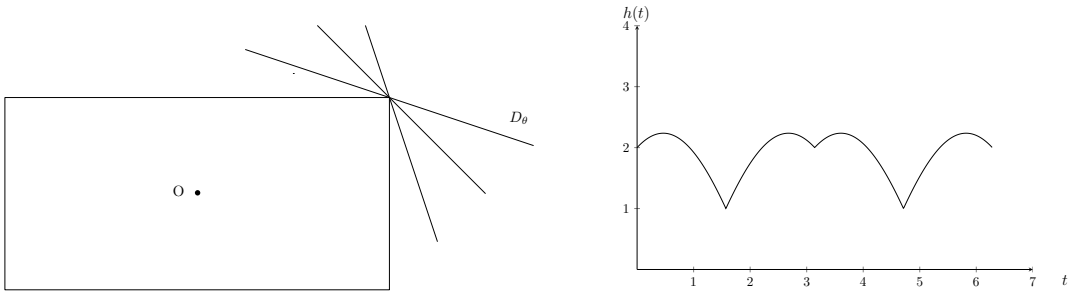

Figure 1.26: Left: A rectangle and its contact lines, right: Its support function

More Precisely, since ∂K is the intersection of its support lines, every single point x of ∂K may be represented by an (non unique) angle θ. If the angle is not unique, x is represented by

a whole segment $\Theta(x) = [\alpha(x), \beta(x)]$. In this case x is called an angular point, since the ∂K has an angle of measure $\pi - (\beta(x) - \alpha(x))$ at this point. If $\Theta(x)$ is reduced to a single point we denote it $\theta(x)$, and ∂K is regular at this point.

In contrast, at angles θ where $F(\theta)$ is a single point $M = M(\theta)$, h is derivable at θ and we can express the coordinates of $M(\theta)$ by the following formula

$$\begin{cases} x(\theta) = & h(\theta)\cos(\theta) - h'(\theta)\sin(\theta) \\ y(\theta) = & h(\theta)\sin(\theta) + h'(\theta)\cos(\theta) \end{cases} \tag{1.19}$$

As mentioned earlier, the only angles at which h is not derivable corresponds to those at which ∂K has a segment. If θ is such and angle and $A, B \in \partial K$ are the extremities of the segment, let h'_l and h'_r be the left and right derivative of h. Then:

$$\begin{cases} x_A(\theta) = & h(\theta)\cos(\theta) - h'_l(\theta)\sin(\theta) \\ y_A(\theta) = & h(\theta)\sin(\theta) + h'_l(\theta)\cos(\theta) \end{cases} \tag{1.20}$$

$$\begin{cases} x_B(\theta) = & h(\theta)\cos(\theta) - h'_r(\theta)\sin(\theta) \\ y_B(\theta) = & h(\theta)\sin(\theta) + h'_r(\theta)\cos(\theta) \end{cases} \tag{1.21}$$

We can see that the distance AB is precisely $h'_r(\theta) - h'_l(\theta)$.

Diameter and support function In what follows we introduce the links between the support function and the geometric quantities. The diameter of a convex body K is given by:

$$D(K) = \max_{\theta \in [0,2\pi]} \{h(\theta) + h(\theta + \pi)\}. \tag{1.22}$$

Proof. Notice first that θ and $\theta + \pi$ represent the same set of lines with reverse orientation. Then for every $\theta \in [0, 2\pi]$, $x \in F(\theta), y \in F(\theta + \pi)$

$$\begin{aligned} h(\theta) + h(\theta + \pi) =& x \cdot u_\theta + y \cdot u_{\theta+\pi} \\ =& (x - y) \cdot u_\theta \\ \leqslant& \|x - y\| \end{aligned}$$

Now if $x, y \in K$ are such that $D(K) = \|x - y\|$, first order optimality conditions imply that the support lines of K at x and y are parallel with the normal vector $u = \frac{x-y}{\|x-y\|}$. Otherwise it would be possible to increase the distance. We deduce that

$$\begin{aligned} \|x - y\| =& \frac{(x - y) \cdot (x - y)}{\|x - y\|} \\ =& (x - y) \cdot u \\ =& h_K(u) - h_K(-u) \\ =& h(\theta) + h(\theta + \pi). \end{aligned}$$

with θ representing u. □

Remark 8. The second argument of the proof is interesting enough to be highlighted. It says that if x and y realize the diameter, not only then their supporting hyperplanees are parallel, but also the line (xy) is orthogonal to both hyperplanees, i.e the normal vector is precisely $\frac{y-x}{\|y-x\|}$ as illustrated in Figure 1.27

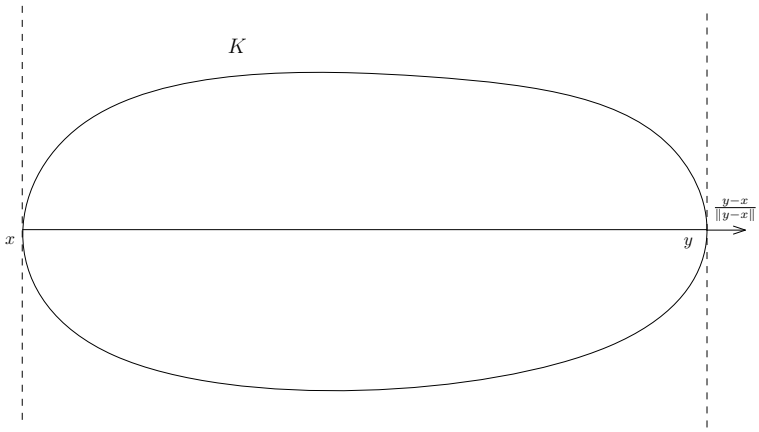

Figure 1.27: Diameter and parallel support lines.

Let us talk a bit more about the link between the diameter and the support function since this will be widely used in part II.

We say that $x \in \partial K$ realizes the diameter (or x is diametrical) if there exists $y \in \partial K$ such that $\|x-y\| = D$. If x and y are such that $\|x-y\| = D$ we say that x and y are diametrical. Note that diametrical points cannot be in the interior of a segment of ∂K because of the Pythagorean theorem. As a consequence if a point x is diametrical, then x is represented by the set $\Theta(x)$, and there exists $\theta \in \Theta(x)$ such that

$$h(\theta) + h(\theta + \pi) = D. \tag{1.23}$$

If $\theta+\pi$ is not the support line of a segment of ∂K, then $\theta+\pi$ represents the point $M(\theta+\pi) = y$ and $\|x - y\| = D$. If $\theta + \pi$ is the support line of a segment, then x is diametrical to one of both of its extremities.

It is important to underline that not every $\theta \in \Theta(x)$ satisfies (1.23).

A convex body K for which (1.23) holds everywhere is called a set of constant width.

Curvature and support function Let us introduce a last very important notion for the sequel: the radius of curvature, or equivalently the length measure. For this purpose we follow the method of G.Letac in [70].

Proposition 19 ([70] Th 3.1)**.** *For $K \in \mathcal{K}_2$ let*

$$R_l(\theta) = \int_0^\theta h(s)ds + h_l'(\theta), \tag{1.24}$$

$$R_r(\theta) = \int_0^\theta h(s)ds + h_r'(\theta). \tag{1.25}$$

Then R_r and (resp. R_l) is a non decreasing, right continuous function (resp. left continuous), and continuous at point where h has a derivative (i.e almost everywhere). Moreover if θ_1 and θ_2 with $0 \leqslant \theta_2 - \theta_1 \leqslant 2\pi$ are such that $h'(\theta_{1)}$ and $h'(\theta_2)$ exist, then $R_r(\theta_2) - R_r(\theta_1)$ is the length of the arc of ∂K defined by $\cup_{\theta_1 \leqslant \theta \leqslant \theta_2} F_\theta$.

The idea of the proof of this is that the result is obvious when K is a polygon, then use an approximation theorem.

This allows us to define a measure $R_K(d\theta)$ on $\mathbb{T}$ by the formula:

$$R_K([\theta_1, \theta_2]) = R_r(\theta_2) - R_r(\theta_1), \tag{1.26}$$

where $0 \leqslant \theta_2 - \theta_1 \leqslant 2\pi$ are such that $h'(\theta_{1)}$ and $h'(\theta_2)$ exist. R_K (R if there is no ambiguity) is called the length measure of K.

It is easy to see, by small computations, that if $K' = K + a$ then $R_K = R_{K'}$, as expected.

Remark 9.

1. If θ is a point of discontinuity of R_r and R_l then θ has a positive measure given by
$$R(\{\theta\}) = h'_r(\theta) - h'_l(\theta).$$
In other words, at angles θ where ∂K is a vertex, $R(\{\theta\})$ is precisely the length of the vertex, as expected.

2. If ∂K has an angle, let $x = (a, b)$ the angular point and $\Theta = [\alpha, \beta]$ the set of angles representing x. On Θ we have
$$h(\theta) = a\cos(\theta) + b\sin(\theta),$$
$$h'(\theta) = -a\sin(\theta) + b\cos(\theta).$$
A quick computation gives
$$R(\Theta) = 0.$$
This is what we expect of the arc length measure.

3. On strictly convex parts of K, h is C^1. Moreover if h' is absolutely continuous, then R has a density with respect to the Lebesgue measure that we note again R, defined by
$$R(\theta) = h(\theta) + h''(\theta).$$

Example 4.

1. If K is a disk of radius r, then $R(d\theta) = rd\theta$

2. The Reulaux triangle is a convex body formed from the intersection of three arc of circles of same radius, each having its center on an edge of an equilateral triangle. Up to rotation we have the following formula:
$$R(d\theta) = r\chi_A(\theta)\ d\theta$$
where $A = [0, \frac{\pi}{3}] \cup [\frac{2\pi}{3}, \pi] \cup [\frac{4\pi}{3}, \frac{5\pi}{3}]$ and r is the radius of the arc of circles and
$$\chi_A(x) = \begin{cases} 1 & \text{if } x \in A \\ 0 & \text{otherwise} \end{cases}$$

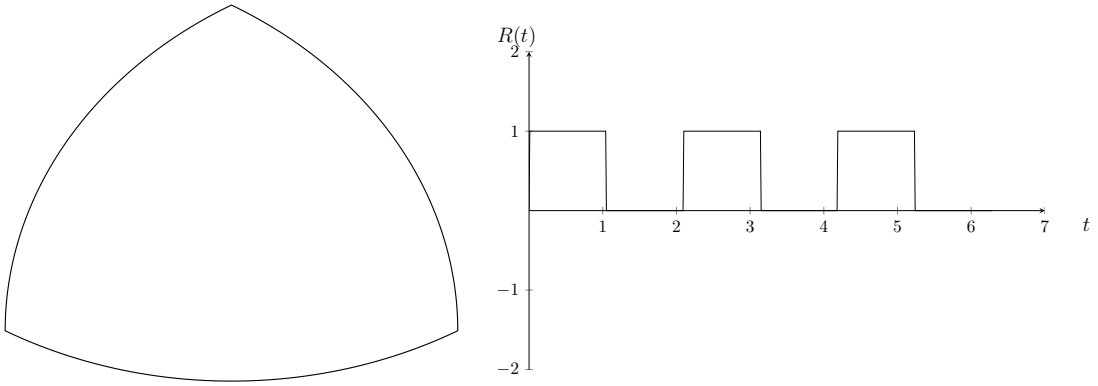

Figure 1.28: Left:The Reulaux triangle, right: its radius of curvature

We see that where $R = 1$ corresponds to an arc of circle whereas $R = 0$ corresponds to an angle.

3. If K is a polygon, let l_j, $j = 1, .., n$ the length of the vertices, and θ_j, $j = 1..n$ the angle of the vertices, then

$$R = \sum_{j=1}^{n} l_j \delta_{\theta_j},$$

where δ is the Dirac measure.

4. In this example we just show what is the shape of a convex body K whose curvature vanishes at a single point, and not on a segment (see Figure 1.29).

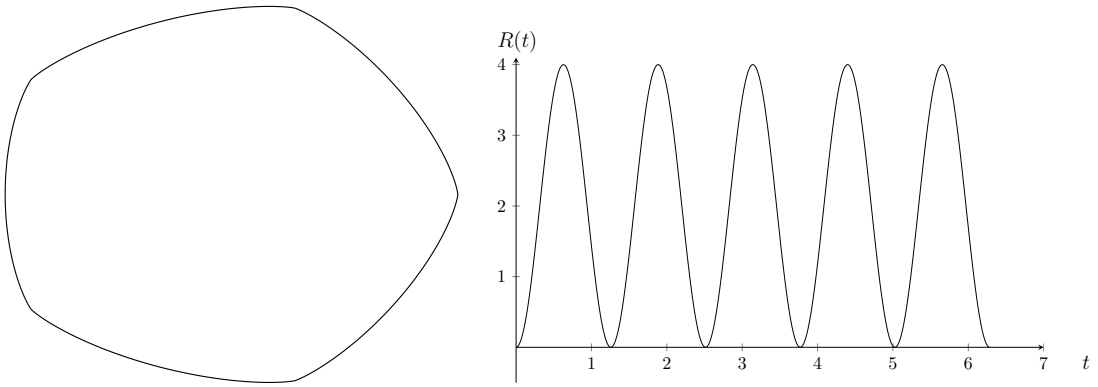

Figure 1.29: A set who has 0 curvature on one point

Another point of view consists in defining R as follows: for all $\varphi \in \mathcal{D}(\mathbb{T})$

$$\langle R, \varphi \rangle_{\mathcal{D}'(\mathbb{T}),\mathcal{D}(\mathbb{T})} = \int_0^{2\pi} h(\theta)(\varphi(\theta) + \varphi''(\theta))\, d\theta \tag{1.27}$$

Defined this way, if h is the support function of a convex body K, then $R = h + h''$ in the sense of distribution is the positive Radon measure defined above. The following proposition shows how to obtain the support function when R is given.

Proposition 20 ([70] Lemma 3.3)**.** *Let R a positive Radon measure on $\mathbb{T}$. Then there exists a convex body K such that R is the radius of curvature of K. Moreover there exists constants $a, b \in \mathbb{R}$ such that the support function h of K is given for all $\theta \in \mathbb{T}$ by*

$$h(\theta) = \int_0^\theta \sin(\theta - s)R(ds) + a\cos(\theta) + b\sin(\theta). \tag{1.28}$$

Constants a and b come from the fact that K is unique up to translation.

Now we write the area of a convex body in terms of support function.

Proposition 21 ([12],[89])**.** *Let K be a convex set with support function h. Then*

$$|K| = \frac{1}{2}\int_0^{2\pi} h(\theta)R(d\theta). \tag{1.29}$$

More generally

$$|K| = \frac{1}{2}\int_0^{2\pi} (h^2(\theta) - h'^2(\theta))\ d\theta = \frac{1}{2}\int_0^{2\pi} h(\theta)(h(\theta) + h''(\theta))\ \ d\theta. \tag{1.30}$$

where the second equality holds whenever h'' exists.

The idea behind this formula is to cut the convex K set by small angular sectors in the point of view of the support lines. Each angular sector $d\theta$ is approximated by a triangle who has $M(\theta)$ and the origin (inside K) as vertices, and a side of length $R(d\theta)$ from $M(\theta)$ and tangent to K. If the origin is not inside K then the support function will be negative on some parts, counting negatively the area of some triangles, offsetting the surplus counted by other triangles.

1.5 The system of linear Elasticity

In this section we introduce the basics of the linear elasticity, that is the basis of our mathematical modeling of Part III. We follow the way of [4]. For more details about the mathematical elasticity we refer to the book of P.G Ciarlet [24].

1.5.1 First notions

Let Ω be a bounded open domain of $\mathbb{R}^N$, and decompose $\partial\Omega = \partial\Omega_D \cup \partial\Omega_N$ in two parts with non-zero (N-1)-dimensional Hausdorff measure. On such a set we apply a volume force f in Ω and a surface force g on $\partial\Omega_N$. Those forces leads to a deformation of the domain: a point x is moved to $x + u(x)$, and u is called the displacement. The portion $\partial\Omega_D$ is considered as clamped and is not moving i.e $u(x) = 0$ (hence D stands for the Dirichlet condition). The goal is to determine the function $u : \mathbb{R}^N \to \mathbb{R}^N$, that will appear to be solution of a partial differential equation.

Let

$$e(u) = \frac{1}{2}(Du + Du^t) = \frac{1}{2}\left(\frac{\partial u_i}{\partial x_j} + \frac{\partial u_j}{\partial x_i}\right)_{1\leqslant i,j\leqslant N},$$

$e(u)$ is a symmetric matrix named stretch tensor. We also introduce the strain tensor:

$$Ae(u) = 2\mu e(u) + \lambda \operatorname{tr}(e(u)) I_N$$

A is a positive linear operator on the set $\mathbb{S}_N(\mathbb{R})$ of symmetric matrices. μ and λ are the Lamé coefficients depending of the material in Ω, verifying the relations $\mu > 0$ and $2\mu + N\lambda > 0$.

The balance of forces in the material writes:

$$\begin{cases} -\operatorname{div}(Ae(u)) = f & \text{in } \Omega \\ Ae(u)n = g & \text{on } \partial\Omega_N \\ e(u) = 0 & \text{on } \partial\Omega_D \end{cases} \tag{1.31}$$

where if σ is a matrix,

$$\operatorname{div}\sigma = \left(\sum_{j=1}^{N} \frac{\partial \sigma_{i,j}}{\partial x_j} \right)_{1 \leqslant i \leqslant N} = (\operatorname{div}(\sigma_i))_{1 \leqslant i \leqslant N}.$$

and σ_i is the i-th row of σ.

Remark 10. This is a vectorial equation, which means that there are actually N equations, each one being written for each $i = 1, .., N$:

$$\begin{cases} -\sum_{j=1}^{N} \frac{\partial}{\partial x_j} \left(\mu \left(\frac{\partial u_i}{\partial x_j} + \frac{\partial u_j}{\partial x_i} \right) + \lambda \operatorname{div}(u) \delta_{i,j} \right) = f_i & \text{in } \Omega \\ \sum_{j=1}^{N} \left(\mu \left(\frac{\partial u_i}{\partial x_j} + \frac{\partial u_j}{\partial x_i} \right) + \lambda \operatorname{div}(u) \delta_{i,j} \right) n_j = g_i & \text{on } \partial\Omega_N \\ u_i = 0 & \text{on } \partial\Omega_D \end{cases} \tag{1.32}$$

The following proposition discusses the existence and uniqueness of a solution to such a system.

Proposition 22. *[[4] Th 2.24] Assume Ω is a regular open and bounded domain of $\mathbb{R}^N$, $f \in L^2(\Omega)^N$ and $g \in L^2(\partial\Omega_N)^N$. Let $V = \{v \in H^1(\Omega)^N, v_{/\partial\Omega_D} = 0\}$.*

There exists a unique solution $u \in V$ to (1.31) and $(f, g) \in L^2(\Omega)^N \times L^2(\partial\Omega_N)^N \mapsto u \in V$ is linear and continuous.

Moreover u is the unique minimiser of the energy functional J defined by:

$$J(v) = \frac{1}{2} \int_\Omega Ae(v) : e(v) \, dx - \int_\Omega f \cdot v \, dx - \int_{\partial\Omega_N} g \cdot v \, ds.$$

where

$$M : N = \operatorname{tr}(MN^t),$$

is the classical scalar product over $\mathbb{M}_N(\mathbb{R})$.

The key argument is to provide a variational formulation to (1.31). To do this, take a test function $v \in V$ and multiply each equation by v_i and integrate over Ω, and use the Gauss Green Formula to integrate by parts.

From the N equations:

$$\int_\Omega -\operatorname{div}(Ae(u)_i) v_i \, dx = \int_\Omega f_i v_i \, dx, \tag{1.33}$$

we obtain:

$$\int_\Omega \mu \sum_{j=1}^{N} \left(\frac{\partial u_i}{\partial x_j} + \frac{\partial u_j}{\partial x_i} \right) v_i \, dx + \int_\Omega \lambda \operatorname{div}(u) \frac{\partial v_i}{\partial x_i} \, dx = \int_\Omega f_i v_i \, dx + \int_{\partial\Omega_N} g_i v_i \, ds. \tag{1.34}$$

Summing the N equation yields:

$$\int_\Omega 2\mu e(u) : e(v) \, dx + \int_\Omega \lambda \operatorname{div}(u) \operatorname{div}(v) \, dx = \int_\Omega f \cdot v \, dx + \int_{\partial\Omega_N} g \cdot v \, ds, \tag{1.35}$$

which can be rewritten as:

$$\int_\Omega Ae(u) : e(v) \, dx = \int_\Omega f \cdot v \, dx + \int_{\partial\Omega_N} g \cdot v \, ds. \tag{1.36}$$

Now it is possible to use the Lax-Milgram Theory, proving the coercivity of the bilinear form $\int_\Omega Ae(u) : e(v) \, dx$ via the Korn inequality. Notice first that via the definition of λ and μ one gets:

$$\int_\Omega Ae(v) : e(v) \, dx \geqslant \nu \int_\Omega |e(v)|^2 \, dx.$$

where $\nu = \min(2\mu, (2\mu + N\lambda)) > 0$, yielding the coercivity of the bilinear form.

Proposition 23. *[Korn inequality, [25]] Let Ω be a bounded, connected set with Lipschitz Boundary. then there exists a constant $C > 0$ such that for all $v \in V$,*

$$\|v\|_{H^1(\Omega)^N} \leqslant C \|e(v)\|_{L^2(\Omega)^N}. \tag{1.37}$$

The crucial point here is that we impose that $v = 0$ somewhere on the boundary which is ensured by the homogeneous Dirichlet condition.

As we will see in Part III, we are also interested in the case where $\partial\Omega_D = \emptyset$. In that case Lax-Milgram theory does not apply anymore. A problem arises because there exists a class of non zero functions $v \in H^1(\Omega)$ such that $e(v) = 0$ everywhere on Ω, hence the Korn inequality automatically fails. To overcome this difficulty, one can proceed as follows.

Definition 8. *A rigid transformation is a function $v \in H^1(\Omega)$ such that there exists an anti-symmetric matrix A and a constant b such that for all $x \in \Omega$,*

$$v(x) = Ax + b. \tag{1.38}$$

Denote $\mathcal{R}$ the set of all rigid transformations. It is a vector space, and $v \in \mathcal{R}$ if and only if $e(v) = 0$ a.e in Ω

Fortunately if we denote $H = H^1(\Omega)/\mathcal{R}$ the quotient space of $H^1(\Omega)$ by the rigid transformations, the second Korn inequality (see e.g [77, 25]) states that the estimate (1.37) is still valid.

We obtain the following in the full Neumann case:

Proposition 24 ([4] rem 2.27)**.** *Consider the problem of pure traction*

$$\begin{cases} -\operatorname{div}(Ae(u)) = f & \text{in } \Omega \\ Ae(u)n = g & \text{on } \partial\Omega \end{cases} \tag{1.39}$$

Then if the following equilibrium condition is verified for all $v \in \mathcal{R}$

$$\int_\Omega f \cdot v \, dx + \int_{\partial\Omega} g \cdot v ds = 0, \tag{1.40}$$

there exists a unique solution to 1.39 in H.

1.5.2 The compliance

The major interest of elasticity system is to study the stiffness of a structure, defined as the total work of the forces applied to the structure. This is called the compliance. Take again the linear elasticity system defined as (1.31). The compliance of Ω is defined as

$$C(\Omega) = \int_\Omega f \cdot u(\Omega) \, dx + \int_{\partial\Omega_N} g \cdot u(\Omega) \, ds, \tag{1.41}$$

where $u(\Omega)$ is the solution of (1.31).

By the variational formulation stated in (1.37) the compliance also writes:

$$C(\Omega) = \int_\Omega Ae(u)(\Omega) : e(u)(\Omega) \, dx > 0.$$

Remark 11. Recall that $u(\Omega)$ is also the unique minimiser of the energy

$$J(v) = \frac{1}{2} \int_\Omega Ae(v) : e(v) \, dx - \int_\Omega f \cdot v \, dx - \int_{\partial\Omega_N} g \cdot v ds.$$

replacing v by $u(\Omega)$ yields

$$C(\Omega) = -2J(u(\Omega)) = -2 \inf_{v \in V} J(v),$$

allowing a definition of the compliance without necessarily providing a solution to (1.31).

Now we provide the shape derivative of the compliance, making more clear the computation of the shape derivative of an energy functional described in 1.2.3.

Proposition 25 ([6])**.** *Let Ω a smooth open domain of $\mathbb{R}^N$ and $V \in W^{1,\infty}(\mathbb{R}^N, \mathbb{R}^N)$. Assume $f \in H^1(\mathbb{R}^N, \mathbb{R}^N)$, $g \in H^2(\mathbb{R}^N, \mathbb{R}^N)$ and $u = u(\Omega) \in H^2(\mathbb{R}^N)$. Then C admits a shape derivative with respect to V and*

$$\langle DC(\Omega), V \rangle = \int_{\partial\Omega_N} \left(2 \left(\frac{\partial(g \cdot u)}{\partial n} + Hg \cdot u + f \cdot u \right) - Ae(u) : e(u) \right) V \cdot n \, dx + \int_{\partial\Omega_D} Ae(u) : e(u) V \cdot n \, dx. \tag{1.42}$$

Note that the shape derivative writes in the form $\int_{\partial\Omega} \theta V \cdot n$.

1.6 Functions of bounded variations and finite perimeter sets

Functions of bounded variations are a very efficient tool to work with sets whose boundary is not necessary regular. Indeed, if Ω is an open set with Lipschitz boundary then its boundary can be locally represented by a Lipschitz function. By Rademacher Theorem, Lipschitz functions

are almost everywhere differentiable. Then we can define a normal vector, and do integration by parts etc... If Ω happens to be less regular, most of those properties don't stand anymore. Functions of bounded variations give some tools to extend those notions to less regular sets: the sets of finite perimeter. We restrict ourselves to some basic notions that will be useful for working in Part III, but more can be found together with the proofs e.g in [36, 8, 72] .

From now on $N \in \mathbb{N}^\star$ and Ω is an open bounded subset of $\mathbb{R}^N$.

Definition 9. *Let $f \in L^1(\Omega)$. The total variation of f in Ω is the quantity:*

$$V(f,\Omega) = \sup\left\{\int_\Omega f \mathrm{div}\varphi \; dx, \varphi \in C_c^1(\Omega,\mathbb{R})^N, \|\varphi\|_\infty \leqslant 1\right\}.$$

where $C_c^1(\Omega,\mathbb{R}^N)$ is the set $C^1(\Omega)^{\mathbb{R}^N}$ with compact support.
We say that f has bounded variation in Ω if $V(f,\Omega) < +\infty$.
If f has bounded variation in any Ω, then we say that f has bounded variation in $\mathbb{R}^N$
The set of functions with bounded variation in Ω(resp. in $\mathbb{R}^N$) is noted $BV(\Omega)$ (resp. $BV(\mathbb{R}^N)$) It is a Banach space endowed with the function norm:

$$\|f\|_{BV(\Omega)} = \|f\|_{L^1(\Omega)} + V(f,\Omega).$$

We say that a set $E \subset \mathbb{R}^N$ (not necessarely a subset of Ω) has finite perimeter in Ω if $\chi_E \in BV(\Omega)$, and we define

$$\mathrm{Per}(E,\Omega) = V(\chi_E,\Omega). \tag{1.43}$$

E has a finite perimeter in $\mathbb{R}^N$ if $\chi_E \in BV(\mathbb{R}^N)$ and we write

$$\mathrm{Per}(E) = \mathrm{Per}(E,\mathbb{R}^N). \tag{1.44}$$

$\mathrm{Per}(E,\Omega)$ is the relative perimeter of E in Ω. If E is not included in Ω, then $\mathrm{Per}(E,\Omega)$ has to be understood as the perimeter of the boundary of E that lies in Ω. We will make it clearer when we will talk about the Green-Gauss measure.

Functions of bounded variations can also be expressed in terms of derivative.

Proposition 26. *[[36] p.167]*
A function has bounded variations if its weak derivative is a signed Radon measure on $\mathbb{R}^N$: there exists a Radon measure μ and a function $\sigma : \Omega \mapsto \mathbb{R}^N$ with $|\sigma(x)| = 1$ μ-a.e such that for every test function $\varphi \in C_c^1(\Omega,\mathbb{R}^N)$,

$$\int_\Omega f \,\mathrm{div}\,\varphi \; dx = \int_\Omega \varphi \cdot \sigma d\mu.$$

The signed measure $\sigma\mu$ is noted Df and the measure μ is $|Df|$.
With this formalism, the total variation of f, $V(f,\Omega)$, is precisely $|Df|(\Omega)$.

If E has finite perimeter set, the measure $D\chi_E$ is also noted μ_E and is called the Green-Gauss measure of E. With this formalism, we have

$$\mathrm{Per}(E,\Omega) = |\mu_E|(\Omega) \quad \mathrm{Per}(E) = |\mu_E|(\mathbb{R}^N). \tag{1.45}$$

The main advantage of the set $BV(\Omega)$ is that it includes indicator functions of finite perimeter sets, which is not the case of any Sobolev space. In fact $BV(\Omega)$ is greater than any Sobolev space in the following sense:

$$\forall p \geqslant 1, W^{1,p}(\Omega) \subset BV(\Omega),$$

since any function in $L^p(\Omega)$ naturally defines a Radon signed measure.

Another interesting thing of this framework related to the L^1 convergence is some regularity propertiy that is not valid in general for the Hausdorff convergence (see Proposition 3).

Proposition 27. *[[58] prop 2.3.7] Let D be an open set in $\mathbb{R}^N$ and E_n, E measurable sets in D*

1. *If $\chi_{\mathbb{E}_n} \to \chi_E$ in $L^1_{\text{loc}}(\Omega)$, then $|E| \leqslant \liminf_{n\to\infty} |E_n|$ and $\text{Per}(E) \leqslant \liminf_{n\to\infty} \text{Per}(E_n)$.*
2. *If $\chi_{\mathbb{E}_n} \to \chi_E$ in $L^1(\Omega)$, then $|E| = \lim_{n\to\infty} |E_n|$ and $\text{Per}(E) \leqslant \liminf_{n\to\infty} \text{Per}(E_n)$.*

In other words the perimeter is l.s.c for the L^1 convergence.

Now let us quickly see what happens if E happens to be regular enough. In this case we can integrate by part as usual with a regular function compactly supported in Ω.

$$\int_\Omega \chi_E \operatorname{div} \varphi \, dx = \int_E \operatorname{div} \varphi \, dx = \int_{\partial E} \varphi \cdot n_E \, d\mathcal{H}^{N-1},$$

where ∂E is the topological boundary of E:

$$\partial E = \overline{E} \backslash \mathring{E},$$

and n_E is the outward normal vector and $\mathcal{H}^{N-1}$ is the N-1 dimensional Hausdorff measure. On the other hand by definition of the Gauss-Green measure of E,

$$\int_\Omega \chi_E \operatorname{div} \varphi \, dx = \int_\Omega \varphi \, d\mu_E.$$

We see here that the derivative of the BV function χ_E acts has a surface measure carried by the boundary of E signed with the outward normal vector. In other words:

$$\mu_E = n_E \mathcal{H}^{N-1} \llcorner \partial E.$$

The natural question that arises is to determine what is the support of the Gauss-Green measure if the set is not regular. One would be tempted to answer that it is still the topological boundary ∂E. But from the definition, if φ is a regular function compactly supported in Ω, the quantity $\int_E \operatorname{div} \varphi$ does not change if we take a set F such that $|E \Delta F| = 0$. We deduce that we should have $\mu_E = \mu_F$. But if we consider F obtained by adding or removing a small filament, then the topological boundary is different. So in general the support of the Gauss-Green measure cannot be the topological boundary. The correct object is called the reduced boundary

Definition 10. *Let $E \subset \mathbb{R}^N$ a set of finite perimeter. The reduced boundary of E is defined by:*

$$\partial_\star E = \left\{ x \in \Omega \limsup_{r\to 0} \frac{|E \cap B(x,r)|}{|B(x,r)|} > 0 \text{ and } \liminf_{r\to 0} \frac{|E \cap B(x,r)|}{|B(x,r)|} < 1 \right\}.$$

Intuitively the reduced boundary is to understand as the part of the topological boundary ∂E that has a bit of E and a bit of $\mathbb{R}^N \backslash E$ around it: the reduced boundary does not contain filament that are artificially added or removed. In other words it corresponds to the boundary a "nice" set should have.

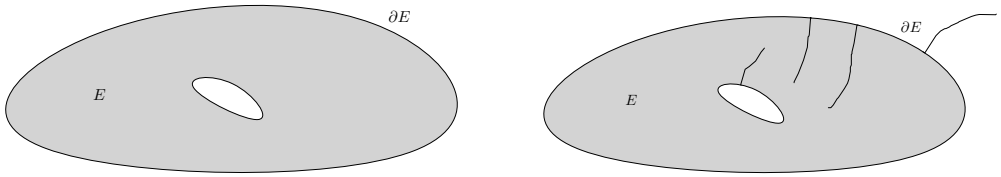

Figure 1.30: Despite having different topological boundary, those sets have the same reduced boundary: the boundary of the first set.

The following proposition shows that the reduced boundary is the right object for the Gauss-Green measure.

Proposition 28 ([72])**.** *[prop 12.19] Let $E \subset \mathbb{R}^N$ a set of finite perimeter. Then its Gauss-Green measure is supported by $\partial_\star E$.*

In the very end, we can define the normal vector to the reduced boundary, still denoted n_E, as the function σ defined in proposition 26. It is also directly defined by the measure μ_E by the following formula for $x \in \partial_\star E$

$$n_E(x) = \lim_{r \to 0} \frac{\mu_E(B(x,r))}{|\mu_E|B(x,r)}.$$

All this leads to the following formula for the Gauss-Green curvature:

$$\mu_E = n_E \mathcal{H}^{N-1} \llcorner \partial_\star E. \tag{1.46}$$

Now we also define the trace operator for BV functions, only defined for bounded domains with Lipschitz boundary, for which the reduced boundary and the topological boundary coincides and the normal vector is well defined.

Proposition 29. *[[36]] Assume Ω is an open bounded domain of $\mathbb{R}^N$ with Lipschitz Boundary. There exists a bounded linear mapping*

$$T : BV(\Omega) \mapsto L^1(\partial\Omega)$$

such that

$$\int_\Omega f \mathrm{div}\varphi \; dx = -\int_\Omega \varphi \; dDf + \int_{\partial\Omega} \varphi T f \; d\mathcal{H}^{N-1} \tag{1.47}$$

for all $f \in BV(\Omega)$ and $\varphi \in C^1(\Omega, \mathbb{R}^N)$

The operator T is the trace operator, as the usual trace operator for Sobolev functions. It defines the value of a functions with bounded variations on the boundary, thanks to a density argument.

We give a last property of the BV space about compactness:

Proposition 30 ([58] Th2.3.11)**.** *Let Ω an open bounded domain of $\mathbb{R}^N$ with Lipschitz Boundary. Then the space $(BV(\Omega), \| \bullet \|_{BV(\Omega)})$ is locally sequentially compact, i.e*
if $(f_n)_{n\in\mathbb{N}}$ is a sequence of $BV(\Omega)$ such that

$$\sup_{n\in\mathbb{N}} \|f_n\|_{BV(\Omega)} < +\infty,$$

then there exists $f \in BV(\Omega)$ *and a subsequence* $(f_{n_j})_{j\in\mathbb{N}}$ *such that*

$$\lim_{j\to\infty} f_{n_j} = f \quad \text{in } L^1(\Omega).$$

Proposition 31 (Compactness result for finite perimeter set ([72] Th 12.26))**.** *Let* $(E_n)_{n\in\mathbb{N}}$ *a sequence of set of finite perimeter such that*

$$\sup_{n\in\mathbb{N}} \mathrm{Per}(E_n) < +\infty$$

and there exists $B = B(x,r)$ *such that for all* $n \in \mathbb{N}$*:*

$$E_n \subset B,$$

then there exists a set of finite perimeter E *and a subsequence* $(E_{n_j})_{j\in\mathbb{N}}$ *such that*

$$\lim_{j\to\infty} E_{n_j} = E$$

in the sense of L^1 *convergence, or equivalently* $|E\Delta E_{n_j}| \to 0$*, and for every* $\varphi \in C_c^0(\Omega, \mathbb{R}^N)$ *,*

$$\int_\Omega \varphi \, d\mu_{E_{n_j}} \underset{j\to\infty}{\to} \int_\Omega \varphi \, d\mu_E.$$

Part I

Arrangements of eggs as an optimal packing

Chapter 2

Introduction

Contents

This Chapter is an introduction and a summary of chapter 3. We give some details on the biological modeling, and how we derive a mathematical formulation of this problem. We also provide a sketch of the work and finally we discuss the results in relation to the biological hypothesis as well as the actual shape of the eggs. All the mathematical aspects are addressed more rigorously and comprehensively in the next chapter.

2.1 Setting the problem

2.1.1 Biological aspect

In this part we introduce the first biological model that we are going to test. It comes from the observation that we made in the life cycle of the animal: when the pool of water dries up, all life disappears and only the eggs survive. In general, eggs are a primary means of survival for the species, as they are responsible for the transition between generations. In this particular case this is even more the case because it is the only representative of the species for a period of several months. A simple idea is that in order to maximise the chances of survival of its species, an animal tries to have as many offspring as possible. In that case we assume that Eulimnadia maximises the number of eggs it can carry in its brood chamber. That idea was also motivated by the observation of a pack of eggs in the brood chamber, that seemed well packed so to speak (see Figure 2.1).

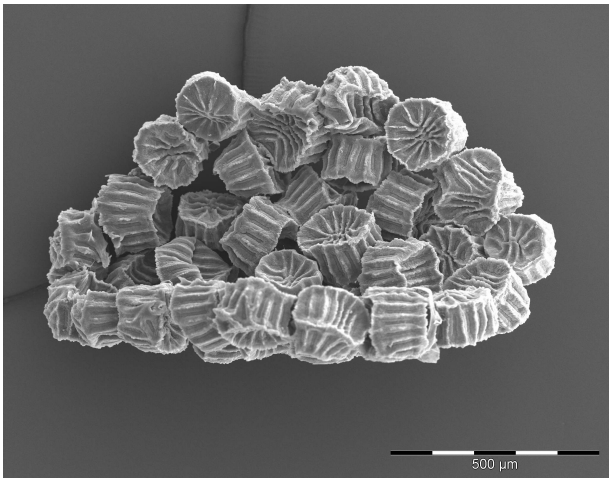

Figure 2.1: A pack of eggs in the brood chamber

2.1.2 Mathematical model

We chose to model the maximisation of the number of eggs in the brood chamber as packing problem Let us give some working hypothesis:

1. The eggs are considered as subset of $\mathbb{R}^2$.

2. The eggs are considered to be convex bodies, i.e compact convex sets with non empty interior.

3. The packings are supposed to be infinite.

The first hypothesis seems a little strange since we know that eggs are three-dimensional objects. But it is quite classical when studying a new problem to first consider simpler cases, such as studying the problem in a smaller dimension. The second hypothesis is acceptable if we ignore the folds on the eggs (see 1.1 in the Tool chapter). The third hypothesis comes from the fact that there are many eggs in the brood chamber (more than 100). Therefore consider that from the point of view of an egg, the packing is infinite. That hypothesis will be counterbalanced by an additional constraint.

Let $K \in \mathcal{K}_2$ is a convex body in $\mathbb{R}^2$. A packing with pattern K (or packing of K) is a subset of $\mathbb{R}^2$ obtained by taking the union of disjoint copies $\tau_i(K)$ of K. For each packing we can associate a number between 0 and 1 that represents the portion of the space that a packing occupies. We call it the density of a packing. In the end we define the density of K as the highest density it is possible to attain with a packing of K. That number is noted $\delta(K)$. For more details about that notion we refer to Section 1.3. As explained there, the exact definition of the density is hard to work with, because it is defined as a $\sup\inf$. Nevertheless most estimates of the real value of the density use a lower bound. One method to obtain lower bounds consists in building a sufficiently small tiling domain enclosing K. Indeed, if one can build a tiling domain T enclosing K. Then any packing consisting in tiling the plane with T, and putting a copy of K in each tile has density $|K|/|T|$. For that reason we decide to work with a more tractable object:

$$d(K) = \frac{|K|}{|K^T|} \tag{2.1}$$

where K^T is the smallest tiling domain enclosing K. We show that K^T exists in Section 3.6.1). The set K^T is called the tiling closure of K.

Clearly we have that $d(K)$ is a lower bound of $\delta(K)$, since $d(K)$ is the density of the packing obtained by putting a copy of K in each cell of the tiling. From the computation of the exact value of the density of the regular pentagon, we can prove that $d(K) < \delta(K)$. In [50] it is proven that the maximum density is attained by a double lattice packing: the pentagonal ice-ray packing (see Figure 2.2). Although it is impossible to build a tiling domain enclosing the regular pentagon in such a way that a packing with this tiling domain gives the same as the pentagonal ice-ray packing. Indeed, in the pentagonal ice-ry each sides of a pentagon is in contact with another pentagon. That means that the only polygon that may enclose the regular pentagon, and still provide the same packing as the pentagonal ice-ray packing is the regular pentagon itself.

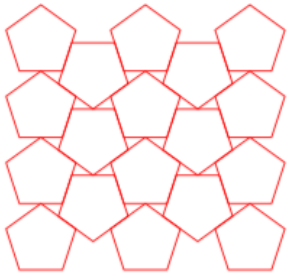

Figure 2.2: The pentagonal ice-ray packing. Source: [50]

Note that we would like this quantity to be the largest possible.

Together with the density we introduce a measure of the dispersion of a packing. The idea is to counterbalance the assumption of infinite packing by requiring that the diameter of a given packing is not too high in some sense. Miimmicking the original definition of the density we introduce an asymptotic diameter:

$$D'_\infty(K) = \inf_{P \in \mathcal{P}(K)} \limsup_{R \to \infty} \frac{2R}{\sqrt{\sharp\{i, \tau_i(K) \subset D(0,R)\} D(K)}},$$

the lim sup being used in the definition to make $D'_\infty(K)$ independent of the balls radii. More precisely, given a packing $P \in \mathcal{P}(K)$ and $R > 0$, we consider a disk with radius R and evaluate the number of copies of K within the disk. Note also that we take the square root of this integer in the definition by observing that the order ofmagnitude of the maximal number of identical copies of a convex in a disk with radius R is $\mathrm{O}(R^2)$. Finally, the diameter of K appearing in the denominator is used as a renormalization factor. That appears natural in view of defining an adimensional quantity.

It is also difficult to work with this notion. Fortunately, we show in theorem (4) (see Chapter 3) that we can replace it by

$$D_\infty(K) = \frac{2}{\sqrt{\pi}} \frac{\sqrt{|K|}}{D}(K)$$

Remark 12. In our original paper [29], theorem (4) contained a mistake because of a factor $\sqrt{\frac{2}{\sqrt{3}}}$ instead of $\frac{2}{\sqrt{3}}$. This is corrected in the present manuscript. The following in the work was not impacted by that mistake.

We want this quantity to be the lowest possible, or equivalently, its inverse to be the largest possible.

The functional that we are studying is the result of the competition between the latter two functionals that we model by a convex combination:

$$J_t(K) = td(K) + (1-t)\frac{1}{D_\infty(K)} = td(K) + (1-t)\frac{\sqrt{\pi}D(K)}{2\sqrt{|K|}}$$

where $t \in [0,1]$ is a parameter.
Now we add constraints derived from biological aspects:

- The egg is composed by a shell that must protect the embryo which we model by a ball.
- Building an egg requires material that may be costly. For that reason we fix the amount of material it takes to build an egg.

The first constraint mathematically reads as an inradius one: $r(K) \geqslant r_0$ where $r(K)$ is the radius of the biggest ball that is included in K. The second constraint is simply a volume constraint: $|K| = A$.
One denotes

$$\mathcal{A}_{r_0,A} = \{K \in \mathcal{K}^2 \mid r(K) \geqslant r_0 \text{ and } |K| = A\}.$$

The problem that we investigate is

$$\sup_{K \in \mathcal{A}_{r_0,A}} J_t(K) \tag{$\mathcal{P}_t$}$$

Note that since the area is prescribed the non-dispersal term simply rewrites as the diameter.

2.2 Results

In this section we provide the main results we obtained together with ideas on the proofs.

2.2.1 Summary of the results

First Results First of all, we studied the functional J_t for the simplest cases: $t = 0$ or $t = 1$.

- For $t = 0$, the functional rewrites

$$J_t(K) = \frac{\sqrt{\pi}}{2\sqrt{A}}D(K),$$

Hence we want to maximise the diameter among convex bodies with inradius $r(K) \geqslant r_0$ and area equal to A.

That was already solved by M. Hernandez Cifre and G.Salinas in [62]. The solution is a set named two cap body $G_{A,r}$ which is the convex hull of a disk of radius r and two points

at a distance D, whose midpoint is the center of the disk. The number D is chosen such that $|G_{A,r}| = A$ (see Figure 2.3) . We highlight the fact that that set is also the minimiser of the area when the diameter is prescribed instead of the area. In this case we write $G^{D,r}$ in order to highlights that the diameter is fixed.

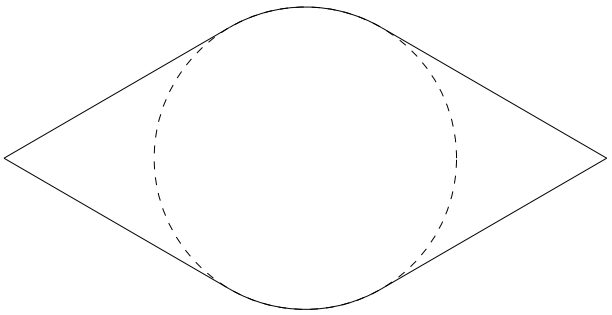

Figure 2.3: The two cap Body $G_{A,r}$

- for $t = 1$, we deal with the density only. As a consequence, every convex tiling domain is a solution. But the second term in the functional suggest that we should attach importance to the diameter. So the problem is to maximise the diameter among the convex tiling domains. We show that the unique solution of that problem is a p-hexagon (hence tiling domain) that we name $H_{A,r}$. This set looks like $G_{A,r}$ (see Figure 2.4). Similarly that set minimises the area among convex tiling domains of given diameter and inradius, and we denote it $H^{D,r}$.

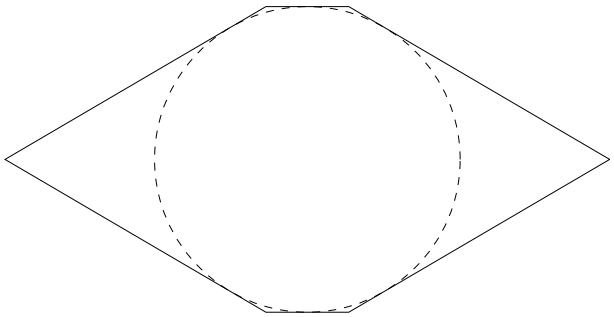

Figure 2.4: The p-hexagon $H_{A,r}$

It is important to note the following relationships that come naturally from the fact that we maximise (resp. minimise) a functional in two sets, one included in the other.

$$D(G_{A,r}) \geqslant D(H_{A,r}).$$
$$|G^{D,r}| \leqslant |H^{D,r}|.$$

Moreover we show that $G^{D,r} \subset H^{D,r}$ and that we have

$$(G^{D,r})^T = H^{D,r},$$

$H^{D,r}$ is the smallest tiling domain enclosing $G^{D,r}$. We deduce that

$$d(G^{D,r}) = \frac{|G^{D,r}|}{|H^{D,r}|}.$$

The main result [Chapter 3 Theorem 6]

We provide a result about the maximisation for any t. We show that there exits $D \geqslant 2r_0$ such that the solution is a set of area A between $G^{D,r}$ and $H^{D,r}$. More precisely we show that:

- If r_0^2/A is small enough, then there exists a number $t_\star$ depending on r_0 and A such that for all $t \leqslant t_\star$ the set G_{A,r_0} solves the problem $(\mathcal{P}_t)$.
- If r_0^2/A is even smaller, then there exists $t^\star$ such that for $t \leqslant t^\star$ The set G_{A,r_0} solves the problem, and for $t \geqslant t^\star$ the set H_{A,r_0} solves the problem $(\mathcal{P}_t)$.

2.2.2 Sketch of proofs

Proof of the maximisation of the diameter among tiling domains Since we know that the maximal number of sides for a convex tiling domain is at most 6 (see 1.3), we decided to relax the problem among convex polygons with at most six sides, hoping that some symmetry properties allow the maximiser in this larger class to be a tiling domain. The proof now articulates in two main steps.

First step: We show with geometric arguments that the optimum has 6 sides, saturates the inradius constraint, and finally has every side touching the incircle. With those results we are able to give a parametrization of a convex hexagon by giving the angles between each side (see Figure 2.5).

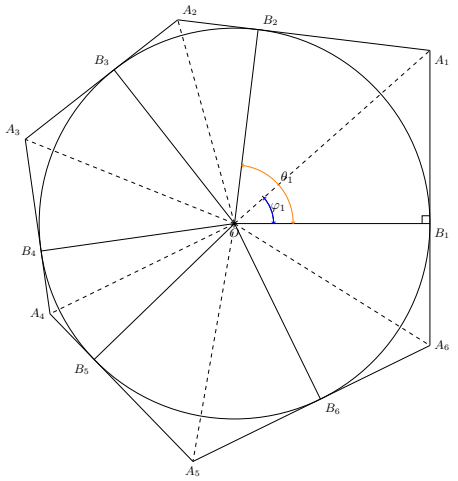

Figure 2.5: The parametrization of an hexagon whose sides are all tangent to the incircle. The angles are $\varphi_i = \widehat{B_iOA_i}$, where A_i are the vertices of the hexagon, and B_i are the projection of the center of the incircle onto the edges of the hexagon.

Second step: The parametrization in terms of angle naturally turns this shape optimisation problem, posed in the set of hexagons, into a classical finite dimension optimisation prob-

lem, where the variables are the angles φ_i in Figure 2.5. The area constraint easily writes $\sum_{i=1}^{6} \tan(\varphi_i) = A$. It is important to distinguish three sub-cases depending on what points realize the diameter. Indeed it is easy to see that if M, N are two points that realize the diameter, then those are necessarily two edges of the hexagon. That leads to three cases depending on which points realize the diameter

- the diameter is achieved by A_1A_2,
- the diameter is achieved by A_1A_3,
- the diameter is achieved by A_1A_4.

Applying the Karush-Kuhn-Tucker theory for each problem and comparing the solutions show that the solution is the p-hexagon $H_{A,r}$ achieved by the case A_1A_4, and so is a tiling domain.

Proof of the general case .

For the general case the proof articulates in three steps:

- First fix $r \in [r_0, \sqrt{\frac{A}{\pi}}]$ and $D \geqslant 2r$ and try to solve the problem $\mathcal{P}_t$ with these values of r and D. It is equivalent to maximising the density alone since $J_t(K) = td(K) + (1-t)\frac{2D}{\sqrt{\pi}}$. Note that the maximum density is not necessarily 1 anymore since we are not sure that there exists a tiling domain with inradius r, diameter D and area A.
- Once the maximal density is found write the optimum in terms of r and D. The shape optimisation can be recast into a 2D optimisation problem depending on r and D.
- Solve the optimisation problem

For that purpose we used a partial Blaschke-Santalo Diagram of the triple (A,D,r) (Figure 2.6), which is in a nutshell a map that indicates if it is possible to find a convex body with given area, diameter and inradius (see Chapter 4 for a complete definition). We split the Diagram into four zones, in each one we deal with the first step. The analysis is performed in Lemma 5 of the paper.

1. In the first zone we easily show that the functional is maximised on the red curve since the density is 1 on this curve. Under this curve, the maximal density is probably 1, but the diameter is lower, so the values of the functional are lower than the one that is attained by the p-hexagon $H_{A,r}$.
2. In the second zone,we cannot find tiling domains, so the maximal density cannot be 1 anymore, and increasing the diameter may have a cost in terms of density. We are able to show that for given r and D in that zone, the maximal density is reached by a convex body K with area A, and such that $G^{D,r} \subset K \subset H^{D,r}$. The same goes for the zone 3.
3. In the fourth zone, we have no existence of $H^{D,r}$ anymore. But we prove that the maximal density is now achieved by some set with area A whose minimal enclosing tiling domain is the regular hexagon $H_r^\star$.

The last step is tedious, and the study of a 2-dimensional functional shows that the maximal density is achieved in the second zone, and more precisely on the line $r = r_0$. A discussion over the value of the r_0^2/A yields the theorem stated above.

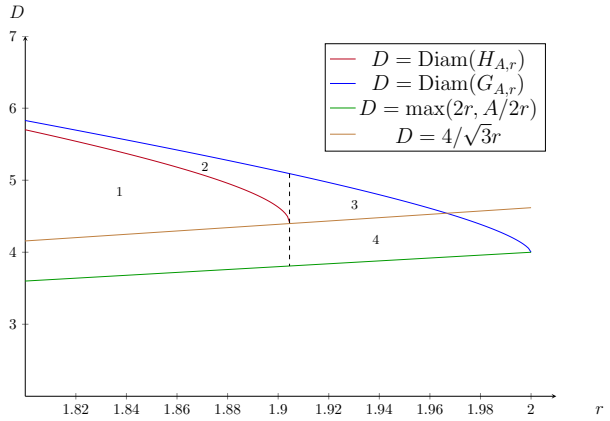

Figure 2.6: The Blaschke-Santalo Diagram for $A = 4\pi$ fixed, and r varying between 1.8 and 2. The blue curve is the curve of the diameter of $G_{A,r}$. By definition of $G_{A,r}$ it is the maximal diameter one can expects from a convex body. The red curve is the curve of the diameter of $H_{A,r}$. In Green we drew a lower curve for the diameter of a convex body, that is not optimal. Those curves delimit a region where we are susceptible to find a convex body (resp. convex tiling domain) with given quantities. Note that the maximal inradius for convex bodies is 2, corresponding to the disk, since the area equals 4π, whereas the maximal inradius for tiling domains is $\sqrt{A/2\sqrt{3}}$, corresponding to the regular hexagon of area A .The brown curve $D = 4/\sqrt{3}r$ is the curve giving the diameter of a regular hexagon with inradius r.

2.3 Discussion

2.3.1 From the biological point of view

Before discussing the result we shall discuss the biological hypothesis itself.

From the analysis we concluded that the solution of problem $(\mathcal{P}_t)$ is always a shape that looks like the 2 cap body. There is a species for which the eggs have this shape: *Australimnadia giganta* (see Figure 2.7). However it seems that it is not the case for a large part of them. So either the biological modeling is not right, or the mathematical modeling is wrong.

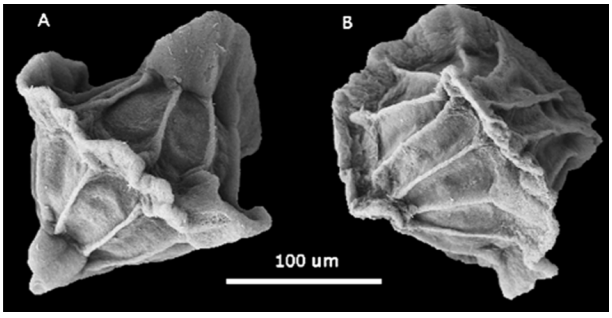

Figure 2.7: The eggs of *Australimnadia giganta* which have the shape of a 2 cap body.

It should be highlighted that despite making sense, the model we chose did not use any specificity of the species: it could be worth it for any species to maximise their egg capacity, so if that hypothesis is a good one, the shape should be seen in many other species. For that reason that hypothesis alone is not sufficient and should be reinforced by another one.

2.3.2 From the mathematical point of view

A huge remaining step is to study the three-dimensional case. It is already partly done as we provide the maximiser of the diameter for fixed inradius and area in any dimension (see Part II): it is again the two cap body. The hard part is to compute the maximiser of the diameter among tiling domains. It seems much harder than in two dimension because we do not know much about the tiling domains in $\mathbb{R}^3$. For example it is still an open problem to know whether the number of facets of a tiling domain in $\mathbb{R}^3$ is bounded or not (see [48]). Without that information it is not possible to relax the problem as we did to work among convex hexagons in $\mathbb{R}^2$. Moreover we also expected the solution to be symmetrical, and we know that a symmetric hexagon is tiling. There is no reason in higher dimension that a symmetric polyhedron is tiling. However it is reasonable to think that the solution is the tiling closure of the two cap body.

Now as far as the modeling is concerned, first of all we decided to model it as a packing problem, and take the density as the best packing density possible. That assumed that the eggs are naturally placed so that their density is maximal. That hypothesis seems hazardous and may be improved by considering random packings instead, and working on the density of a convex body that would be the expectation of the density with respect to every possible packings, under the condition that each copy of K can not be moved. The notion of random packings is not defined in the literature. There exist some notions about random packing with spheres, but we were not able to find a clear definition of it. Such a field known as random close packing is more in the interest of physicians or engineery scientists who proposed the "best value" of a random packing with spheres: around 0.64 against 0.74 for the optimal packing. Those values are experimentally or numerically obtained, (see e.g [1]).

Concerning the asymptotic diameter functional, it is quite surprising that it is equivalent to the quantity $\sqrt{|K|}/D(K)$, and hence, if our goal is to minimise the asymptotic diameter of a convex body, then we need to maximise its diameter. There is probably an issue with the renormalization term $D(K)$ in the definition. Perhaps instead we could use a definition of the asymptotic diameter of a packing such as:

$$\limsup_{n\to\infty} \frac{D((\cup_{i=1}^{n} \tau_i(K))}{n}$$

where we consider that the $\tau_i(K)$ are ordered in such a way that the distance $d(O, \tau_i(K))$ is increasing. We will see in Part II that surprisingly, when we want to minimise the diameter with the area and the inradius being fixed the solutions are shapes that look a bit more like the actual shape of the eggs.

Open problems Here we sum-up the problems related to the work we did.

- We aise a question directly related to the density. Is it clear that if $\delta(K) = 1$, then K is a tiling domain? When working with d it is obvious. But again the literature does not seem to pay much interest to this question that does not seem trivial.
- Extend the work in three dimensions. It is done through the maximisation of the diameter among tiling domains.

Chapter 3

Shape optimisation with the density functional

Contents

This chapter is issued from the article [29], joint work with A.Henrot and Y.Privat.

3.1 Introduction

This article is devoted to investigating optimal configurations of infinite packings in the two-dimensional space $\mathbb{R}^2$. Recall that a packing associated to a convex body K with non-empty interior is an arrangement of non-overlapping copies of K. More precisely, denoting by $\mathcal{K}_2$ the set of compact convex bodies of $\mathbb{R}^2$, a infinite packing $P(K)$ with pattern K is defined by

$$P(K) = \bigcup_{i \in I} \tau_i(K)$$

where I denotes either a finite or a countable set, and the mappings τ_i are affine isometries of $\mathbb{R}^2$ such that $\mathrm{int}(\tau_i(K)) \cap \mathrm{int}(\tau_j(K)) = \emptyset$ for all $i \neq j$.

Since we are interested in infinite packings, we will consider without loss of generality in what follows that $I = \mathbb{N}$ and we will denote by $\mathcal{P}(K)$ the set of all infinite packings of the plane with pattern K.

A close notion that will be much discussed in the sequel is the one of tiling domains. Recall that, as a consequence of the definition of packings, a convex K defines a tiling domain of the plane whenever $\mathbb{R}^2 \in \mathcal{P}(K)$.

In the whole article, the notation $|\cdot|$ will denote the Lebesgue measure in $\mathbb{R}^2$.

Let us make the shape optimisation problem we will deal with precise. The criterion to minimise involves two geometrical functionals denoted d and D_∞. Let us define them.

- The first one models the *density of a packing*. We choose to define it as follows, see Section 3.2.1 for a discussion and the link with another quantity for the density.

$$d(K) = \frac{|K|}{|K^T|} \tag{3.1}$$

  for every convex set K, where K^T denotes the smallest convex set tiling the plane and containing K (we refer to Section 3.6.1 for the proof that such a set exists). In some sense, the quantity $d(K)$ stands for a quantitative measure of the tiling ability of K. Roughly speaking, we can consider that the highest $d(K)$ is and the most tiling will be the convex set K. Notice in particular that if K is tiling, then $d(K) = 1$.

- The second functional is defined by

$$D_\infty(K) = \frac{2\sqrt{|K|}}{\sqrt{\pi} D(K)}, \tag{3.2}$$

  for every convex set K, where $D(K)$ denotes the diameter of K. As this will be highlighted in the sequel, the quantity $D_\infty(K)$ is a *measure of non-dispersal of any packing associated to the convex K*. Indeed, this quantity is obtained by introducing the restriction of a packing with pattern K to a disk with diameter $R > 0$, by comparing the diameter of this set with the diameter of the disk, and by letting R tend to $+\infty$. Hence, trying to minimise $D_\infty(K)$ will allow to obtain a convex K and an associated packing as "compact" as possible.

Note that modelling issues and in particular the functionals choices will be discussed and commented in Section 3.2.1.

Finally, for a given $t \in [0, 1]$, we will consider in the sequel a convex combination of both previous criteria. The resulting criterion, denoted J_t reads

$$J_t(K) = td(K) + (1-t)\frac{1}{D_\infty(K)}.$$

Let us define the admissible set. We will deal with three kinds of constraints:

(i) the considered sets will be compact and convex subsets of $\mathbb{R}^2$,

(ii) to avoid that the shapes collapse, we impose to the considered convex sets to have a minimal inradius r_0. In what follows, we will denote by $r(K)$ the inradius of any convex set K.

(iii) since the functionals we will deal with are invariant by homothety, it is relevant to assume the area of the patterns are prescribed, equal to a positive constant A.

We now introduce the complete shape optimisation problem we will solve.

Let $t \in [0,1]$, $r_0 > 0$ and $A \geqslant \pi r_0^2$ be fixed and let $\mathcal{A}_{r_0,A}$ denote the set of compact convex sets having an inradius larger than r_0 and an area equal to A, namely

$$\mathcal{A}_{r_0,A} = \{K \in \mathcal{K}_2 \mid r(K) \geqslant r_0 \text{ and } |K| = A\}.$$

The shape optimisation problem we will consider reads

$$\boxed{\sup_{K \in \mathcal{A}_{r_0,A}} J_t(K).} \qquad (\mathcal{P}_t)$$

It is notable that this problem is also motivated by applied considerations. Some explanations about the biological framework in which this problem naturally arises are provided at the end of this section.

Let us roughly state hereafter the main results of this article. More detailed (and technical) versions of these theorems are provided in Section 3.2.2.

Our first result deals with generalities about tiling domains. it seems to us interesting in its own :

Theorem A. *The (convex) tiling set with given diameter and inradius minimising its area is a p-hexagon, in other words a hexagon with two parallel opposite sides with same length. By duality, one shows that the (convex) tiling set with given area and inradius maximising its diameter is a p-hexagon.*

Our second result deals with the solution of Problem $(\mathcal{P}_t)$. For the sake of clarity, we state it informally.

Theorem B. *Under a smallness assumption on the ratio r_0^2/A, the solutions of Problem $(\mathcal{P}_t)$ are either a p-hexagon or a symmetric 2-cap body (the convex hull of a disk and two points lined-up with the center of the disk), depending on the values of the parameter t.*

Complete and extensive versions of these results are provided in Theorems 5 and 6.

We end this section by giving an interpretation of this problem in Biology. The shape optimisation problem $(\mathcal{P}_t)$ is related to the understanding of the eggs shape of a class of crustaceans, subclass branchiopoda, called eulimnadia.

In a clutch, the eggs are placed in the brood chamber, which is located dorsally beneath the carapace and which is closed by the abdominal processes. To understand eggs geometry, it appears relevant to interpret the observed arrangements as the result of an optimisation process. This way, assuming that resulting shapes allow to the crustacean to incubate the largest number of eggs, we look for configurations guaranteeing at the same time that shapes and arrangements make the resulting packing the most "dense" (this word meaning here the "most tiling", see the definition of $d(K)$) and the most "compact" (in the sense that the restriction of the packing to a given ball with large radius will contain the largest number of elements). In a nutshell, denoting by K the egg shape and assuming that the clutch contains the largest possible number of eggs, it is plausible that eggs arrangements look at maximising at the same time $d(K)$ and $D_\infty(K)$. We formalize this idea by looking for patterns K maximising a convex combination of these functionals, whence the writing of Problem $(\mathcal{P}_t)$.

Structure of the article. This article is organized as follows. Section 3.2.1 is devoted to several remarks about our motivations for considering Problem $(\mathcal{P}_t)$, as well as our functional and admissible set choices. The main results of this article are gathered in Section 3.2.2. Section 3.3 is devoted to the proof of Theorem 5, whereas Section 3.4 is devoted to the proof of Theorem 6.

3.2 Modelling and solving the optimisation problem

3.2.1 Modelling issues and state of the art

Density of convex sets. Let $K \in \mathcal{K}_2$ and $P(K)$ be a packing with pattern K. It is standard (see [94]) to define the **density of** $P(K)$ as

$$\tilde{\delta}(P(K)) = \liminf_{r \to +\infty} \frac{\sharp\{i \in \mathbb{N} \mid \tau_i(K) \subset [-r/2, r/2]^2\}|K|}{r^2}. \tag{3.3}$$

For a fixed $r > 0$, the ratio $\sharp\{i \in \mathbb{N} \mid \tau_{i\in I}(K) \subset [-r/2, r/2]^2\}|K|/r^2$ represents the rate of the area occupied by the elements of the packing $P(K)$ contained in $[-r/2, r/2]^2$ with respect to the total area of a square with side r. Letting $r \to +\infty$ makes this definition independent of the window in which this rate is evaluated.

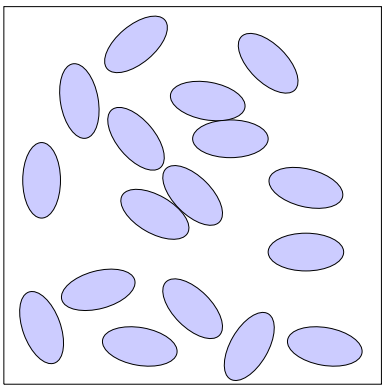

Figure 3.1: An example of a packing with ellipses, we can see the density as the ratio between the blue area and the entire square

Having in mind to look for packings maximising (among other criteria) the density functional, it is relevant to introduce a criterion depending only on the pattern choice, by setting

$$\delta(K) = \sup_{P(K) \in \mathcal{P}(K)} \tilde{\delta}(P(K)),$$

corresponding to the optimal density of a packing associated to the pattern K. This quantity is called **density of the convex** K [94].

Notice that the following elementary properties about δ are direct consequences of the definition.

Proposition 32. *For every $K \in \mathcal{K}_2$, one has $\delta(K) \in [0, 1]$. Moreover,*

1. *if D is a disk, $\delta(D) = \frac{\pi}{2\sqrt{3}} \simeq 0.9$ [38].*
2. *if K is a tiling domain, $\delta(K) = 1$.*
3. *if $K \in \mathcal{K}_2$ and T is a convex tiling domain such that $K \subset T$ then $\delta(K) \geqslant \frac{|K|}{|T|}$ [68].*

The last property will be crucial in the sequel, since it allows to provide a lower bound for δ. Roughly speaking, the main ingredient consists in considering a tiling domain T such that

$K \subset T$, the family of sets $\{\tau_i(T)\}_{i\in\mathbb{N}}$ defining the associated packing. We then define a packing with pattern K by placing a copy of K in each cell $\tau_i(T)$, and observe that the density of this packing will be larger than $|K|/|T|$. Moreover, it has been shown that given a convex body K, there exists a triangle T such that $K \subset T$ and $|K|/|T| \geqslant 2/3$ (see [37] by M.A Fary in 1950 and [26] by R.Courant in 1965). By considering parallelograms instead of triangles, Kuperberg obtained in 1982 in [68] the same conclusion, and this way the lower bound $\delta(K) \geqslant 3/4$ for every convex body K. This lower bound has been improved in 1990 by W.Kuperberg and G. Kuperberg in [67], where it is shown that $\delta(K) \geqslant \sqrt{3}/2$, by using a particular tiling hexagon. In 1995, K.R Doheny proved in [31] the existence of $r_0 > \sqrt{3}/2$ such that $d_1(K) \geqslant r_0$ for every convex body K. Up to our knowledge, the exact value of the bound $\inf\{\delta(K),\ K \in \mathcal{K}_2\}$ remains unknown.

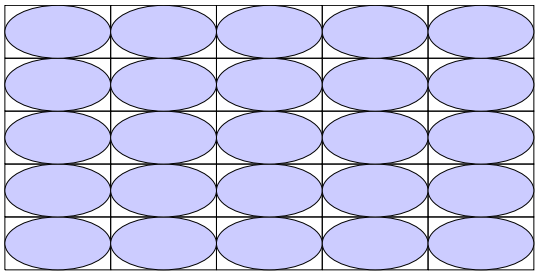

Figure 3.2: A packing with ellipses in a tiling with rectangles. It is intuitive that the density of this packing is equal to the ratio of the area of the ellipse over the area of the rectangle

Unfortunately, the precise value of $\delta(K)$ is almost never computable, even for simple choices of K. More annoying, having in mind to consider it as criterion of an optimisation problem, the quantity $\delta(K)$ appears intricate to handle. These considerations lead us to consider as an alternative and more workable definition of the density the functional d defined by (3.1) involving the smallest convex tiling domain containing K. Obviously there holds $d(K) \leqslant \delta(K)$ for every convex body K and it is notable that all the properties gathered in Proposition 32 above remain satisfied with this new definition of density.

Non-dispersal properties of convex sets. Let us first model the notion of non-dispersion for packings. We start from the observation that balls are the "less dispersed" bodies, in the sense that, among all nonempty convex sets, they minimise the ratio of the diameter by the square of their area. this leads us to define the notion of "non-dispersion" of packings by comparing their diameter to the one of balls. More, precisely, we introduce, mimicking the definition of δ in (3.3):

$$D'_\infty(K) = \inf_{P\in\mathcal{P}(K)} \limsup_{R\to\infty} \frac{2R}{\sqrt{\sharp\{i, \tau_i(K) \subset D(0,R)\}D(K)}},$$

the lim sup being used in the definition to make $D'_\infty(K)$ independent of the balls radii. More precisely, given a packing $P \in \mathcal{P}(K)$ and $R > 0$, we consider a disk with radius R and evaluate the number of copies of K within the disk. Note also that we take the square root of this integer in the definition by observing that the maximal number of identical copies of a convex order of magnitude in a disk with radius R is $\mathrm{O}(R^2)$[1]. Finally, the diameter of K appearing in the

[1]Indeed, let us provide a sketch of argument. Let us consider a rectangle tiling the plane and containing the convex body. We denote by L and ℓ its dimensions. If $R >> L$, the number of rectangles that can be packed

denominator is used as a renormalization factor. This appears natural in view of defining an adimensional quantity.

First an elementary reasoning shows that, in a disk of radius R, there cannot be more than $\pi R^2/|K|$ copies of K. As a consequence, we infer that

$$D'_\infty(K) \geqslant \frac{2\sqrt{|K|}}{\sqrt{\pi}D(K)} = D_\infty(K), \tag{3.4}$$

for every $K \in \mathcal{K}$, where $D_\infty(K)$ is defined by (3.2). The following result provides fine estimates of $D'_\infty(K)$.

Theorem 4. *Let $K \in \mathcal{K}$. One has*

$$\frac{2\sqrt{|K|}}{\sqrt{\pi}D(K)} \leqslant D'_\infty(K) \leqslant \frac{2}{\sqrt{3}}\frac{2\sqrt{|K|}}{\sqrt{\pi}D(K)}. \tag{3.5}$$

Furthermore, if K is tiling, then one has $D'_\infty(K) = D_\infty(K)$.

According to the result above, one has $D'_\infty(K)/D_\infty(K) \in [1, 1.15)$. We infer that, in order to consider workable quantities, it will be relevant in the sequel to consider D_∞ as criterion of non-dispersal.

Convex tiling domains. The previous remarks suggest that we take a short interest about convex tiling domains. Notice that a convexity argument allows to show that a two-dimensional convex domain which is tiling in $\mathbb{R}^2$ is necessarily a polygon. More precisely, thanks to Euler's formulae, it is known that a polygon with more than six vertices cannot be tiling [15]. Moreover, any triangle or quadrilateral tiles the plane, but there exist only three kinds of tiling hexagons. The case of pentagons is more intricate. It has been recently solved in [81], by leading an exhaustive search of all families of convex pentagons tiling the plane. In particular, the authors state that there are no more than fifteen kinds of pentagons tiling the plane.

3.2.2 Solving the optimisation problems

Notations. Recall that we use the following notations throughout this article:

$\|K\|$	area of a convex body K
$r(K)$	inradius of a convex body K
$D(K)$	diameter of a convex body K
H_r^*	regular hexagon with inradius r

Let us now define particular convex sets that will play a crucial role in the sequel.

Definition 11 (The hexagons $H_{A,r}$ and $H^{D,r}$)**.** *Let $r > 0$ and $A \geqslant 2\sqrt{3}r^2$. Let $\mathcal{C}$ be a circle centered at the origin O with radius r and $H_{A,r}$ be the hexagon defined as follows:*

(i) each side of $H_{A,r}$ is tangent to $\mathcal{C}$.

(ii) Denoting by $\{B_i\}_{i=1,\dots,6}$ the tangential points between $H_{A,r}$ and $\mathcal{C}$ and by θ_i the angle $\widehat{B_iOB_{i+1}}$ (with the convention that $B_7 = B_1$), one has

$$\begin{cases} \theta_1 = \theta_4 = 4\arctan\left(\frac{2r_0^2+\sqrt{A^2-12r_0^4}}{4r_0^2+A}\right) \\ \theta_2 = \theta_3 = \theta_5 = \theta_6 = \frac{\pi-\theta_1}{2} \end{cases}$$

within a disk with radius R is $\mathrm{O}(\pi R^2)/(L\ell) = \mathrm{O}(R^2)$. Therefore, the number of copies of a convex K that can be packed within a disk is less than $\pi R^2/|K| = \mathrm{O}(R^2)$

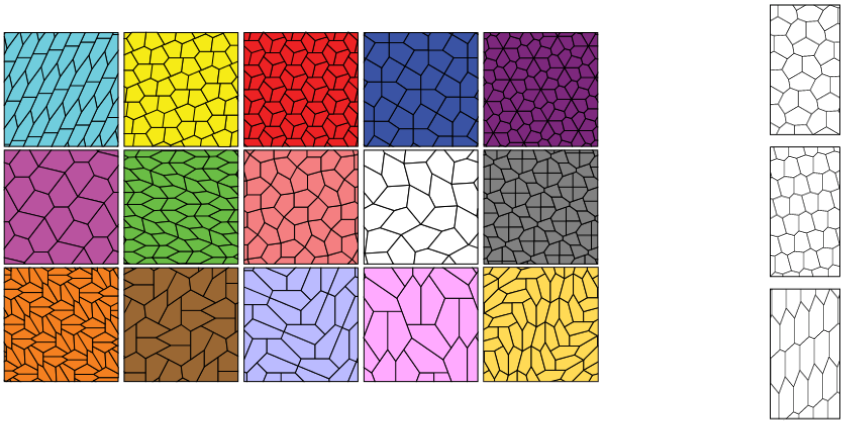

Figure 3.3: (Left) The fifteen kinds of tiling pentagons (Source `https://commons.wikimedia.org/wiki/File:PentagonTilings15.svg`). (Right) The three kinds of tiling hexagon (Source `http://mathworld.wolfram.com/HexagonTiling.html`)

It is notable that $H_{A,r}$ is a a p-hexagon, in other words a hexagon with two parallel opposite sides with same length (see Figure 3.4).

Moreover, let D and r be two positive numbers. Noting that one has[2]

$$D(H_{A,r}) = \frac{1}{3r}\left(2A + \sqrt{A^2 - 12r^4}\right),$$

one defines the hexagon $H^{D,r}$ by $H^{D,r} = H_{A(D),r}$, where $A(D)$ is the unique solution of the equation

$$D = \alpha(A(D), r) \quad \textit{with} \quad \alpha(A, r) = \frac{1}{3r}\left(2A + \sqrt{A^2 - 12r^4}\right). \tag{3.6}$$

Furthermore, one has $|H^{D,r}| = 2rD - r\sqrt{D^2 - 4r^2}$ (see Appendix 3.6.3).

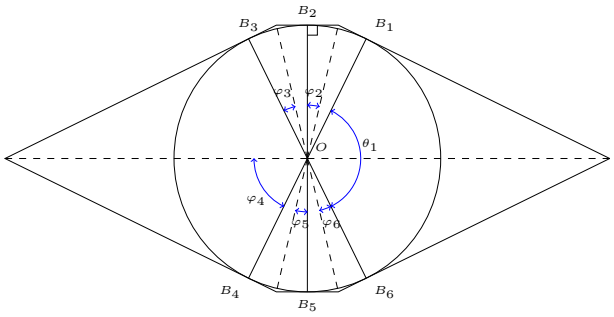

Figure 3.4: The p-hexagon $H_{A,r}$ and its inscribed circle.

[2]We refer to Appendix 3.6.3 for a proof of this claim.

Definition 12 (The symmetric 2-cap bodies $G^{D,r}$ and $G_{A,r}$)**.** *Let D and r be two positive numbers such that $D \geqslant 2r$. We denote by $G^{D,r}$ the convex hull of a circle with radius r and two points at a distance of D, lined up with the circle center (see Figure 3.5). Such a convex set will be called symmetric 2-cap body of diameter D and inradius r.*

Similarly let A and r be two positive numbers. One defines the symmetric 2-cap body $G_{A,r}$ by $G_{A,r} = G_{D(A),r}$, where $D(A)$ is the unique positive solution of

$$A = r\left(\sqrt{D(A)^2 - 4r^2} + 2r \arcsin\left(\frac{2r}{D(A)}\right)\right).$$

Remark 13. Let A, D, r, be three positive numbers. In [62], it is shown that for every convex set with area A, inradius r and diameter D, one has

$$A \geqslant r\left(\sqrt{D^2 - 4r^2} + 2r \arcsin\left(\frac{2r}{D}\right)\right) \tag{3.7}$$

and this inequality is an equality if, and only if $K = G^{D,r}$ (and thus, $A = |G^{D,r}|$). This inequality can also be interpreted as follows: the convex set with diameter D and inradius r having the lowest area is $G^{D,r}$. By duality, this also means that the convex set with area A and inradius r having the maximal diameter is the convex hull of a circle with radius r and two points, lined up with the circle center

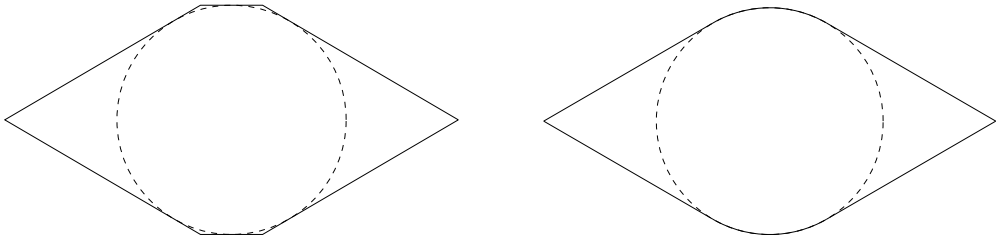

Figure 3.5: Left: the hexagon $H_{A,r}$ and its inscribed circle. Right: the symmetric 2-cap body $G^{D,r}$ and its inscribed circle.

Remark 14. It follows easily from geometrical observations or simple computations that

- there exists a unique hexagon fulfilling the conditions of Definition 11, and this construction can be led if, and only if $A \geqslant 2\sqrt{3}r^2$;
- the hexagon $H_{A,r}$ is of area A and inradius r;
- the sides of $H_{A,r}$ are two by two parallels. In particular, $H_{A,r}$ is a p-hexagon (see Theorem A for the definition).

Statement of the main results. In the following theorem, we state several sharp inequalities for tiling domains of the plane. These results constitute key ingredients of the proof of Theorem 6.

Theorem 5. *Let T be a tiling domain of $\mathbb{R}^2$*

1. *There holds*
$$|T| \geqslant 2\sqrt{3}r(T)^2 \quad \textit{and} \quad D(T) \geqslant \frac{4}{\sqrt{3}}r(T),$$
with equality if only if T is a regular hexagon.

2. *One has*
$$D(T) \leqslant \frac{1}{3r(T)}\left(2|T| + \sqrt{|T|^2 - 12r(T)^4}\right), \tag{3.8}$$
with equality if, and only if $T = H_{A,r}$

Remark 15. Let $r > 0$. As a byproduct of Theorem 5, using in particular that the mapping $[2\sqrt{3}r^2, +\infty) \ni A \mapsto \alpha(A, r)$ (where α is given by (3.6)) is increasing, we get that

- the (convex) tiling set with diameter D and inradius r minimising its area is the hexagon $H^{D,r}$;
- the (convex) tiling set with area A and inradius r maximising its diameter is the hexagon $H_{A,r}$.

The first claim is a direct consequence of Theorem 5. The second point comes from the following observation: let $A \geqslant 2\sqrt{3}r^2$ for some $r > 0$. Then, the map $F_r : A \mapsto \alpha(A, r) = \frac{1}{3r}\left(2A + \sqrt{A^2 - 12r^4}\right)$ is increasing and defines a bijection from $[2\sqrt{3}r^2, +\infty)$ to $[4/\sqrt{3}, +\infty)$. Its inverse mapping is $F_r^{-1} : [4/\sqrt{3}, +\infty) \ni D \mapsto 2rD - r\sqrt{D^2 - 4r^2}$.

Now, let T be a tiling domain of $\mathbb{R}^2$. According to the considerations above, the inequality (3.8) is equivalent to $D(T) \leqslant F_{r(T)}(|T|)$, which rewrites $F_r^{-1}(D(T)) \leqslant |T|$. This shows that the inequality
$$2r(T)D(T) - r(T)\sqrt{D(T)^2 - 4r(T)^2} \leqslant |T| \tag{3.9}$$
holds true for every tiling domain of $\mathbb{R}^2$. The expected conclusion follows.

Theorem 6. *Let r_0 and A be two positive numbers such that $2\sqrt{3}r_0^2 < A$.*

Let us denote by X_0 ($\simeq 3.1847$) be the unique zero of the function $X \mapsto \sqrt{X^2 - 4}(14 - 5X^2) + 4X(X^2 - 3)$ on $[4/\sqrt{3}, +\infty)$ and set
$$t_{A,r_0} = \frac{\sqrt{\pi}/(2\sqrt{A})}{\sqrt{\pi}/(2\sqrt{A}) + A\gamma_0/r_0^3} \in (0, 1). \tag{3.10}$$
with
$$\gamma_0 = \frac{\left(2\sqrt{X_0^2 - 4} - X_0\right)}{\sqrt{X_0^2 - 4}(2X_0 - \sqrt{X_0^2 - 4})^2} \simeq 0.0472. \tag{3.11}$$

1. *If $t \in [0, t_{A,r_0}]$, the symmetric 2-cap body G_{A,r_0} solves Problem $(\mathcal{P}_t)$;*

2. *Let us assume moreover that*
$$r_0 \leqslant \gamma\sqrt{A} \qquad \textit{where} \qquad \gamma = \frac{1}{\sqrt{2X_0 - \sqrt{X_0^2 - 4}}} \in [0.5069, 0.5070]) \tag{3.12}$$
and define
$$t^*_{A,r_0} = \frac{\frac{\sqrt{\pi}}{2\sqrt{A}}\left(D(G_{A,r_0}) - D(H_{A,r_0})\right)}{\frac{\sqrt{\pi}}{2\sqrt{A}}\left(D(G_{A,r_0}) - D(H_{A,r_0})\right) + A\left(\frac{1}{|D(G_{A,r_0})|} - \frac{1}{|D(H_{A,r_0})|}\right)} \tag{3.13}$$

One has $t^*_{A,r_0} \geqslant t_{A,r_0}$. Moreover, if $t \in [0, t^*_{A,r_0})$, the symmetric 2-cap body G_{A,r_0} solves Problem $(\mathcal{P}_t)$, and if $(t^*_{A,r_0}, 1]$, the p-hexagon H_{A,r_0} solves Problem $(\mathcal{P}_t)$. If $t = t^*_{A,r_0}$, the two convex sets H_{A,r_0} and G_{A,r_0} solve Problem $(\mathcal{P}_t)$.

Remark 16 (Comment on the assumption (3.12))**.** The assumption $2\sqrt{3}r_0^2 < A$ is natural since it is a sufficient and necessary condition for ensuring the existence of the p-hexagon H_{A,r_0} (see the first item of Theorem 5). Note that writes also $r_0 \leqslant \hat{\gamma}\sqrt{A}$ with $\hat{\gamma} \simeq 0.5373$.

The assumption (3.12) appears a bit technical (although relevant from an applied point of view). A refined analysis can show that if $r_0/\sqrt{A} \in (\gamma, \hat{\gamma})$, there exists $\tilde{t}_{A,r_0} \geqslant t_{A,r_0}$ such that for $t \geqslant \tilde{t}_{A,r_0}$, either the symmetric 2-cap body G_{A,r_0} or the p-hexagon H_{A,r_0} solves the problem $(\mathcal{P}_t)$.

3.3 Proof of Theorem 5

Proving Theorem 5 is equivalent to determine the optimal value of the problems

$$\inf\{|K|,\ K \in \mathcal{T},\ r(K) \geqslant r_0\} \quad \text{and} \quad \inf\{D(K),\ K \in \mathcal{T},\ r(K) \geqslant r_0\}, \tag{3.14}$$

and

$$\sup\{D(K),\ K \in \mathcal{T},\ r(K) \geqslant r_0,\ |K| = A\}, \tag{3.15}$$

where $\mathcal{T}$ denotes the set of tiling domains in $\mathbb{R}^2$. In what follows, we will solve a relaxed version of these problem, namely

$$\inf\{|K|,\ K \in \mathcal{P}_6,\ r(K) \geqslant r_0\} \quad \text{and} \quad \inf\{D(K),\ K \in \mathcal{P}_6,\ r(K) \geqslant r_0\}, \tag{3.16}$$

and

$$\sup\{D(K),\ K \in \mathcal{P}_6,\ r(K) \geqslant r_0,\ |K| = A\}, \tag{3.17}$$

where $\mathcal{P}_6$ denotes the set of polygons of the plane having at most six sides, and show that the solutions are tiling domains. As a consequence, and since the new admissible set contains the previous one, the optimal values between the problems (3.14) and their relaxed version will coincide.

Before dealing with each problem separately, let us state some preliminary results allowing to reduce the search of optimal domain to a simpler class. The arguments used in Step 1 below hold indifferently for each problem of (3.16).

As a preliminary remark, notice that the two problems of (3.16) have a solution since $\mathcal{P}_6$ is compact for the Hausdorff topology and the functionals $K \mapsto |K|$, $K \mapsto r(K)$, $K \mapsto D(K)$ restricted to convex sets are continuous for this topology, see [58, chapter 2].

Step 1. Restricting the set of admissible domains. The following lemmas are in order.

Lemma 2. *For any problem of* (3.16) *and* (3.17)*, every solution is a hexagon.*

Proof. Let us assume by contradiction that K^* has N sides, with $N < 6$. Consider two diametral points D_1 and D_2 of K^* and let M be any vertex of K^* different from D_1 and D_2. Then, we change K^* into $\hat{K}^*$ by removing the vertex M and creating two new vertices as follows: we cut K^* with a well-chosen hyperplane at a distance of M small enough so that the diameter and the inner radius of K^* are not modified.

- **minimising the area:** the area of $\hat{K}^*$ is strictly lower than the area of K^* which contradicts the optimality of K^*. The conclusion follows.

- **minimising the diameter:** the diameter of $\hat{K}^*$ being equal to the one of K^*, we infer that it is possible to restrict our search to hexagons.

- **maximising the diameter:** consider the set $t\hat{K}^*$ where $t > 1$ is chosen in such a way that $|t\hat{K}^*| = |K^*|$. Then, one has $r(t\hat{K}^*) = tr(\hat{K}^*) = tr_0 > r_0$ and $D(t\hat{K}^*) = tD(\hat{K}^*) > D(\hat{K}^*)$, which contradicts the optimality of K^*. The conclusion follows.

□

Remark 17. It will follow from the proof that all the solutions of Problems (3.16) and (3.17) are hexagons.

The proofs of the two next lemmas are exactly similar for each problems of (3.14) and (3.15). Since this last problem is more constrained and in some sense, more intricate, we prove this lemma for the problem of maximising the diameter. An easy adaptation of the proof below shows the same result for the issue of minimising the area or the diameter.

Lemma 3. *Let K^* be a solution of any problem of* (3.16) *and* (3.17)*. Then, necessarily, $r(K^*) = r_0$.*

Proof. Let K^* be a solution of Problem (3.17) and let us assume by contradiction that $r(K^*) > r_0$. Since K^* is a convex polygon, there exists two vertices B and C of K^* such that $D(K^*) = BC$. For $t \in [0,1]$ let ρ_t be the stretching with ratio t and direction the axis (BC). Then, one has $|\rho_t(K^*)| = t|K^*|$ and $D(\rho_t(K^*)) = D(K^*)$. Noting that $[0,1] \ni t \mapsto r(\rho_t(K^*))$ is a continuous increasing function such that $r(0) = 0$ and $r(1) = r(K^*)$, consider $r \in (r_0, r(K^*))$ and $t \in (0,1]$ such that $r(\rho_t(K^*)) = r$. Let K_t be the range of K^* by the homothety centered at O, the center of the incircle, with scale factor $1/\sqrt{t} > 1$. Hence, one has $|K_t| = |K^*|$, $D(K_t) = D(K^*)/\sqrt{t}$ and $r(K_t) = r(K^*)/\sqrt{t} > r_0$. It follows that K_t is a admissible hexagon and moreover $D(K_t) > D(K^*)$. We have then reached a contradiction.

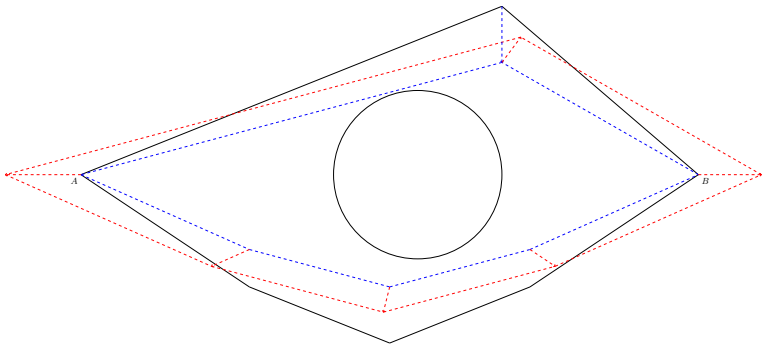

Figure 3.6: Illustration of the proof of Lemma 3: the hexagon K^* (black), the hexagon $\rho_t(K^*)$ (blue) and the hexagon K_t (red).

□

Lemma 4. *Let K^* be a solution of any problem of* (3.16) *and* (3.17)*. Then, necessarily K^* is tangent at each side to any inscribed circle.*

Proof. We argue by contradiction, by assuming that there exist an inscribed circle $\mathcal{C}$ and a side of K^* that does not meet. To reach a contradiction, we will show that one can transform K^* into a new admissible set $\hat{K}$ having a strictly larger diameter.

Consider first the case where there exists a location of an inscribed circle $\mathcal{C}$ and a side $[MM']$ at positive distance of K^* such that $D(K^*) > MM'$. Assume without loss of generality the existence of two vertices of K^* different from M and reaching its diameter. This property will allow to construct a new set $\tilde{K}$ from K^* by slightly modifying the location of M, and such that $D(\tilde{K}) = D(K^*)$. Let N be the vertex of K^* such that M is adjacent to N and M'. Let $\lambda \in (0,1)$ and $M_\lambda = \lambda N + (1-\lambda)M$. For $\lambda > 0$ small enough, there holds $(M'M_\lambda) \cap \mathcal{C} = \emptyset$. Hence, denoting by $\tilde{K}$ be the hexagon obtained by replacing M by M_λ, one has $r(\tilde{K}) = r(K^*)$. Moreover, since $\tilde{K} \subset K^*$ and , one has $|\tilde{K}| < |K^*|$. To get $\hat{K}$, we now apply a homothety to $\tilde{K}$ where the scale factor is chosen in such a way that $|\hat{K}| = |K^*|$ (see Figure 3.7). We then have $r(\hat{K}) > r(K^*)$ and $D(\hat{K}) > D(K^*)$, whence the contradiction.

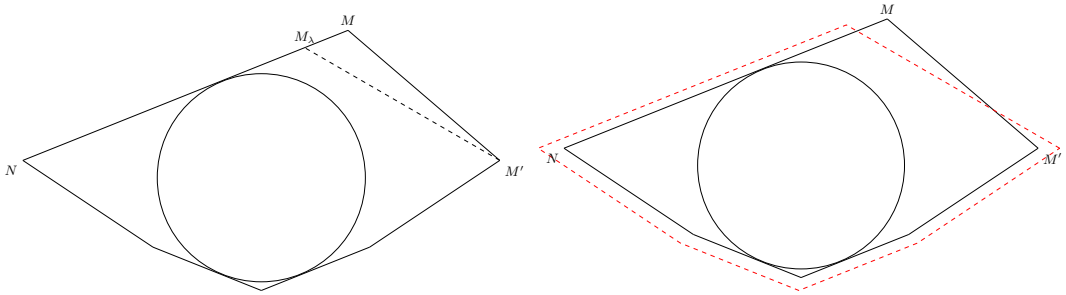

Figure 3.7: Geometrical illustration of the method: construction of $\tilde{K}$ (left) and construction of $\hat{K}$ (dotted line) from $\tilde{K}$ (right).

Consider now the complementary case where the diameter is realized by the only side $[AB]$ of K^* which does not meet $\mathcal{C}$ tangentially. Denote by O be the center of $\mathcal{C}$ and by M the orthogonal projection of O on (AB). Then, M belongs to the segment $[AB]$ and the distance δ of M to $\mathcal{C}$ is positive (by compactness). The new circle $\mathcal{C}'$ obtained from $\mathcal{C}$ by translation of vector $\delta\frac{\vec{OM}}{OM}$ is tangent to (AB) (see Figure 3.8). Let us prove that $\mathcal{C}' \subset H$. Let $(A, \vec{i}, \vec{j})$ be the orthonormal basis such that $\vec{i} = \overrightarrow{AB}/AB$ and K^* be contained in $\mathbb{R}^2_+$. Then, $\partial K^* \backslash (AB)$ is parametrized by a positive concave function $f : [0,1] \mapsto \mathbb{R}_+$. For $u \in [0,1]$, let D_u be the vertical axis with equation $x = u$. Then, defining $x_1 = \min\{u \in [0,1], D_u \cap \mathcal{C} \neq \emptyset\}$ and $x_2 = \max\{u \in [0,1], D_u \cap \mathcal{C} \neq \emptyset\}$, the region $\mathcal{R} = \{(x,y), x_1 \leqslant x \leqslant x_2, 0 \leqslant y \leqslant f(x)\}$ is contained in K^* with an easy convexity argument and by construction, $\mathcal{C}' \subset \mathcal{R}$. Hence, $\mathcal{C}' \subset K^*$. We are then led to the previous case, and we conclude as previously.

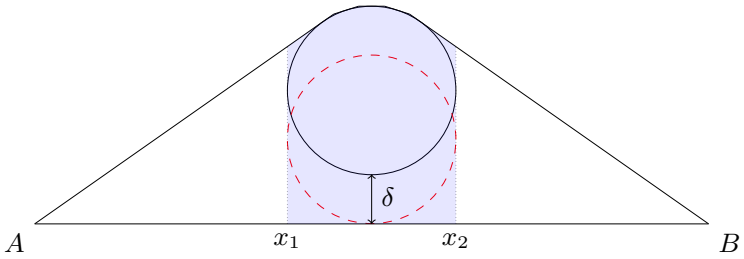

Figure 3.8: case where the diameter is realized by the only side $[AB]$ of K^* which does not meet $\mathcal{C}$ tangentially.

□

By combining the three lemmas we have just proved, we will recast both problems of (3.16) in a simpler way by using a convenient parametrization and some analytical arguments. For homogeneity reasons and according to Lemma 3, we will assume from now on that $r_0 = 1$, the solutions for the general case being easily inferred from that case.

Let K^* be a hexagon solution of a problem of (3.16). Since each problem is invariant under rotation or translation of K, we will assume without loss of generality that the center of the inscribed circle (which is uniquely located inside K^*, according to Lemma 4) is the origin O and that one side of K^* is included in the axis $x = 1$. Let $\{B_i\}_{i=1..6}$ be the projections of O on each side of K^* with the convention that B_1 is the projection of O on the side included in the axis $x = 1$, and the other points are located by following the trigonometric sense.

Let $\{A_i\}_{i=1..6}$ be the vertex of K^* having positive coordinates in the basis $(O; \overrightarrow{OB_i}, \overrightarrow{OB_{i+1}})$, let $\theta_i = \widehat{B_iOB_{i+1}}$ and $\varphi_i = \widehat{B_iOA_i}$, so that

$$\sum_{i=1}^{6} \theta_i = 2\pi \quad \text{and} \quad \sum_{i=1}^{6} \varphi_i = \pi.$$

Notice that $0 \leqslant \theta_i \leqslant \pi$ and since the two triangles B_iOA_i and A_iOB_{i+1} are similar, one has $\varphi_i = \theta_i/2$ (see Figure 3.9).

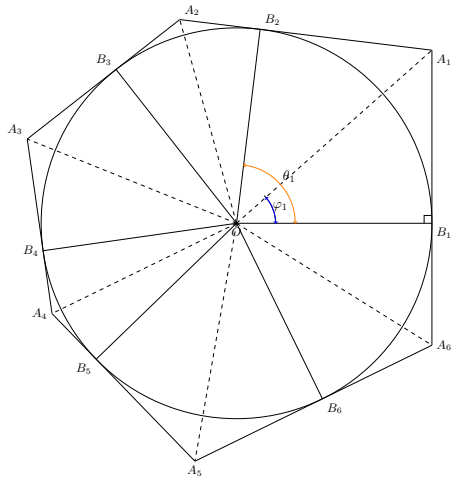

Figure 3.9: Parametrization of hexagons

Using this parametrization, let us rewrite each optimisation problem in terms of the variables φ_i. Decomposing the hexagon K^* into the six quadrilaterals $OB_iA_iB_{i+1}$ $(i = 1, \dots, 6)$ and each quadrilateral into two similar triangles B_iOA_i and $B_{i+1}OA_i$ (whose area is equal to $\frac{OB_i.B_iA_i}{2} = \frac{\tan(\varphi_i)}{2}$), we get

$$|K^*| = \sum_{i=1}^{6} \tan \varphi_i.$$

Introduce the set

$$\Theta^0 = \left\{ \Phi = (\varphi_1, ..., \varphi_6) \in [0, \pi/2]^6,\ \sum_{i=1}^{6} \varphi_i = \pi \right\} \quad \text{and} \quad \Theta_A = \left\{ \Phi \in \Theta^0,\ \sum_{i=1}^{6} \tan \varphi_i = A \right\}.$$

The two problems of (3.16) rewrite

$$\min_{\Phi \in \Theta^0} \sum_{i=1}^{6} \tan(\varphi_i) \qquad \text{and} \qquad \min_{\Phi \in \Theta^0} D(H(\Phi)) \tag{3.18}$$

whereas Problem (3.17) rewrites

$$\max_{\Phi \in \Theta_A} D(H(\Phi)), \tag{3.19}$$

where $H(\Phi)$ denotes the hexagon tangent at each side to the unit circle, whose semi circle center angles are the φ_i's.

Step 2. Solving the two problems of (3.18)**.** Let us consider the first problem of (3.18). The proof is straightforward. Indeed, noting that the point-wise constraint $\varphi_i \leqslant \pi/2$ cannot be active, it follows from the Karush-Kuhn-Tucker theorem the existence of a Lagrange multiplier $\lambda \in \mathbb{R}$ such that

$$1 + (\tan \varphi_i)^2 = \lambda$$

for all the non-zero angles φ_i. As a consequence, all the non-zero angles are necessarily equal. Investigating hence separately the cases where three, four, five and six angles are non-zero yields easily the expected result.

Let us now solve the second problem of (3.18). Let K be a hexagon and let us use the notations of Figure 3.9. One has

$$\min_{\Phi\in\Theta^0} D(H(\Phi)) \quad = \quad \min_{K\in\mathcal{P}_6} \max_{(x,y)\in K^2} |x-y| \geqslant \min_{K\in\mathcal{P}_6} \max_{i=1,2,3} A_iA_{i+3}.$$

Let us now solve the problem $\min_{K\in\mathcal{P}_6} \max_{i=1,\dots,3} A_iA_{i+3}$. We will show that the chain of inequalities above is in fact a chain of equalities. We start by several remarks allowing to reduce the problem. Notice that the preliminary remarks of Step 1 still hold for this problem. Consider a solution denoted K^*, associated to $\Phi^* \in \Theta^0$.

- Let us assume without loss of generality that the maximum is reached by A_1A_4. Consider the hexagons $\hat{K}_i$, $i = 1, 2$, obtained by symmetrizing the quadrilaterals $A_1A_2A_3A_4$ and $A_4A_5A_6A_1$ with respect to the axis (A_1A_4). Assume by contradiction that A_1, A_4 and O are not aligned. Then, it is obvious that either the inradius of $\hat{K}_1$ or the one of $\hat{K}_2$ is strictly lower than 1. Assume that the inradius of $\hat{K}_1$ is strictly lower than 1. Then, applying a well-chosen homothety to $\hat{K}_1$ provides a hexagon with inradius 1 having a diameter larger than the one of K^*, which is absurd. Hence, A_1, A_4 and O are necessarily aligned and this argument can be extended to any length reaching the maximum.

- In fact, one can show that the three lengths A_1A_4, A_2A_5 and A_3A_6 are equal. Indeed, in the converse case, assume that A_1A_4 does not reach the maximum. We replace A_1 and A_4 by $\hat{A}_1$ and $\hat{A}_4$ that are the respective images of A_1 and A_4 by a homothety centered at the middle of $[A_1A_4]$ in such a way that $\hat{A}_1\hat{A}_4 > A_1A_4$, and the maximum remains unchanged. This is a contradiction with the conclusion of Lemma 4.

As a result, one has necessarily $A_1A_4 = A_2A_5 = A_3A_6$ and moreover, the points O, A_i and A_{i+3} are aligned for $i = 1, 2, 3$. According to the considerations above, and since $OA_i = 1/\cos\varphi_i^*$, $i = 1, \dots, 6$, one has $\widehat{A_iOA_{i+3}} = \pi[2\pi]$, and

$$A_iA_{i+3}^2 = OA_i^2 + OA_{i+3}^2 = \left(\frac{1}{\cos\varphi_i^*} + \frac{1}{\cos\varphi_{i+3}^*}\right)^2,$$

by using the Al-Kashi formula in the triangle A_iOA_{i+3}. Therefore, we infer that

$$\min_{\Phi\in\Theta^0} D(H(\Phi)) \quad \geqslant \quad \min_{K\in\mathcal{P}_6} \max_{i=1,2,3} A_iA_{i+3} = \max_{i=1,2,3} \left(\frac{1}{\cos\varphi_i^*} + \frac{1}{\cos\varphi_{i+3}^*}\right).$$

Moreover, one has

$$\max_{i=1,2,3} \frac{1}{\cos\varphi_i^*} + \frac{1}{\cos\varphi_{i+3}^*} \quad \geqslant \quad \frac{1}{3}\sum_{i=1}^{6} \frac{1}{\cos\varphi_i^*} \geqslant \frac{1}{3} \min_{K\in\mathcal{P}_6} \sum_{i=1}^{6} \frac{1}{\cos\varphi_i}.$$

For this last problem, let $\tilde{\Phi}$ be a solution. Notice that one has necessarily $\tilde{\varphi}_i < \pi/2$. Let us assume that $\tilde{\varphi}_i$ is positive. Hence, it follows from the Karush-Kuhn-Tucker theorem the existence of a Lagrange multiplier $\lambda \in \mathbb{R}$ such that

$$-\frac{\sin\varphi_i}{\cos^2\varphi_i} = \lambda,$$

and therefore, all the non-zero angles must be equal. For $N = 3, 4, 5, 6$, assume that there are $6 - N$ zero angles and N nonzero angles (therefore equal to π/N according to the equality constraint). One shows easily that

$$\sum_{i=1}^{6} \frac{1}{\cos\tilde{\varphi}_i} = \frac{N}{\cos(\pi/N)} + (N-6) \geqslant \frac{6}{\cos(\pi/6)} = \frac{12}{\sqrt{3}}.$$

This proves that the only solution of the problem $\min_{K\in\mathcal{P}_6} \sum_{i=1}^{6} \frac{1}{\cos^2\varphi_i}$ is $\tilde{\Phi} = \frac{\pi}{6}(1,1,1,1,1,1)$. We infer from this reasoning that

$$\min_{\Phi\in\Theta^0} D(H(\Phi)) \geqslant \frac{4}{\sqrt{3}}.$$

We conclude by noting that this inequality is an equality as soon as $\Phi = \tilde{\Phi}$ (in other words, whenever K^* is a regular hexagon with inradius 1).

Step 3. Solving Problem (3.19)**.** Assume that K^* is the hexagon plotted on Figure 3.9. The diameter can be realized in three ways: (i) on a side, (ii) on a diagonal of the kind A_1A_4, or (iii) on a diagonal of the kind A_1A_3. In what follows, we will first consider separately each of these three cases and combine them in a second time to get the expected result. In the sequel, we will denote by $\Phi^* = (\varphi_1^*, ..., \varphi_6^*)$ a solution of (3.19) associated to a hexagon K^*.

Case (i): the diameter is realized by a side

Assume without loss of generality that the diameter of K^* is given by A_1A_2 (this is always possible by re-indexing the vertices). For $\Phi \in \Theta_A$, denote by $D_{1,2}(\Phi)$ the length A_1A_2 in the hexagon $H(\Phi)$. One has $D_{1,2}(\Phi) = \tan(\varphi_1) + \tan(\varphi_2)$, and we are therefore led to solve the optimisation problem

$$\max_{\Phi\in\Theta} \tan(\varphi_1) + \tan(\varphi_2).$$

It is notable that for the hexagon K^*, one has necessarily $0 < \varphi_i < \pi/2$. Indeed, the left inequality is a direct consequence of Lemma 2, and the right one comes from the area constraint. According to the Karush-Kuhn-Tucker theorem, there exists $(\lambda, \mu) \in \mathbb{R}^2$ such that

$$\begin{pmatrix} 1+\tan^2(\varphi_1^*) \\ 1+\tan^2(\varphi_2^*) \\ 0 \\ 0 \\ 0 \\ 0 \end{pmatrix} = \lambda \begin{pmatrix} 1+\tan^2(\varphi_1^*) \\ 1+\tan^2(\varphi_2^*) \\ 1+\tan^2(\varphi_3^*) \\ 1+\tan^2(\varphi_4^*) \\ 1+\tan^2(\varphi_5^*) \\ 1+\tan^2(\varphi_6^*) \end{pmatrix} + \mu \begin{pmatrix} 1 \\ 1 \\ 1 \\ 1 \\ 1 \\ 1 \end{pmatrix}$$

The two first equations yield $(\lambda, \mu) \neq (0, 0)$ and we easily infer that

$$\varphi_1^* = \varphi_2^* \quad \text{and} \quad \varphi_3^* = \varphi_4^* = \varphi_5^* = \varphi_6^*.$$

Denoting by φ the angle φ_1^* and by Ψ the angle φ_3^*, it follows from the equality constraint on the φ_i's and from the area constraint that

$$\psi = \frac{\pi}{4} - \frac{\varphi}{2} \quad \text{and} \quad 2\tan(\varphi) + 4\tan(\psi) = A.$$

Let $t = \tan(\varphi/2)$. Since

$$\tan(\psi) = \tan(\frac{\pi}{4} - \frac{\varphi}{2}) = \frac{1 - \tan(\varphi/2)}{1 + \tan(\varphi/2)} = \frac{1-t}{1+t},$$

the second equation rewrites $4\left(\frac{t}{1-t^2} + \frac{1-t}{1+t}\right) = A$, and hence

$$t^2\left(1 + \frac{A}{4}\right) - t + 1 - \frac{A}{4} = 0.$$

Since $A \geqslant 2\sqrt{3}$, this equation has two real roots, and the largest one is

$$t = \frac{1 + \sqrt{\frac{A^2}{4} - 3}}{2(1 + \frac{A}{4})}.$$

We then get

$$\max_{\Phi \in \Theta_A} D_{1,2}(\Phi) = D_{1,2}(\Phi^*) = \frac{4t}{1-t^2}.$$

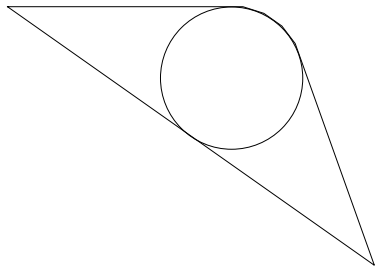

Figure 3.10: Hexagon maximising $D_{1,2}(\Phi)$ for $A = 4\sqrt{3}$

Case (ii): the diameter is realized by A_1A_4

Since $OA_1 = 1/\cos\varphi_1$, $OA_4 = 1/\cos\varphi_4$ and $\widehat{A_1OA_4} = \varphi_1 + 2\varphi_2 + 2\varphi_3 + \varphi_4$, one has

$$A_1A_4^2 = OA_1^2 + OA_2^2 - 2\cos(\widehat{A_1OA_4})OA_1.OA_4 = \frac{1}{\cos^2\varphi_1} + \frac{1}{\cos^2\varphi_4} - \frac{2\cos(\varphi_1 + 2\varphi_2 + 2\varphi_3 + \varphi_4)}{\cos\varphi_1\cos\varphi_4},$$

by using the Al-Kashi formula in the triangle A_1OA_4. For $\Phi \in \Theta_A$, we introduce

$$D_{1,4}(\Phi) = \frac{1}{\cos^2\varphi_1} + \frac{1}{\cos^2\varphi_4} - \frac{2\cos(\varphi_1 + 2\varphi_2 + 2\varphi_3 + \varphi_4)}{\cos\varphi_1\cos\varphi_4}$$

Notice that for all $\Phi \in \Theta$, one has

$$D_{1,4}(\Phi) \leqslant \frac{1}{\cos^2\varphi_1} + \frac{1}{\cos^2\varphi_4} + \frac{2}{\cos\varphi_1\cos\varphi_4} = \left(\frac{1}{\cos\varphi_1} + \frac{1}{\cos\varphi_4}\right)^2 = G(\varphi_1, \varphi_4)^2, \qquad (3.20)$$

where $G(x,y) = \frac{1}{\cos(x)} + \frac{1}{\cos(y)}$ for all $x, y \in [0, \pi/2]^2$.

To solve the problem of maximising $D_{1,4}$ over Θ_A, we will maximise $\Phi \mapsto G(\varphi_1, \varphi_4)^2$ over Θ_A and use (3.20) to prove that both the optimal values and the maximisers of the aforementioned problems coincide. Hence, we investigate the optimisation problem

$$\max_{\Phi \in \Theta_A} G(\varphi_1, \varphi_4).$$

With a slight abuse of notation, we denote by Φ^* a solution to this problem. Reasoning similarly as for the case (i), we first notice that one has necessarily $\varphi_i^* \in (0, \frac{\pi}{2})$. Applying the Karush-Kuhn-Tucker theorem, we infer the existence of $(\lambda, \mu) \in \mathbb{R}^2$ such that

$$\begin{pmatrix} \frac{\sin(\varphi_1^*)}{\cos^2(\varphi_1^*)} \\ 0 \\ 0 \\ \frac{\sin(\varphi_4^*)}{\cos^2(\varphi_4^*)} \\ 0 \\ 0 \end{pmatrix} = \lambda \begin{pmatrix} 1+\tan^2(\varphi_1^*) \\ 1+\tan^2(\varphi_2^*) \\ 1+\tan^2(\varphi_3^*) \\ 1+\tan^2(\varphi_4^*) \\ 1+\tan^2(\varphi_5^*) \\ 1+\tan^2(\varphi_6^*) \end{pmatrix} + \mu \begin{pmatrix} 1 \\ 1 \\ 1 \\ 1 \\ 1 \\ 1 \end{pmatrix}$$

By exploiting these equalities, we get successively that $\varphi_2^* = \varphi_3^* = \varphi_5^* = \varphi_6^*$, $\mu = -\lambda(1+\tan^2(\varphi_2))$, and that φ_1^* and φ_4^* solve the equation

$$\frac{\sin\theta}{\cos^2\theta} = \lambda(\tan^2\theta - \tan^2(\varphi_2^*)). \tag{3.21}$$

Notice that $\varphi_1^* \neq \varphi_2^*$. Indeed, in the converse case, one has $\varphi_1^* = 0 = \varphi_2^* = \varphi_3^* = \varphi_5^* = \varphi_6^*$ and then $\varphi_4^* = \pi$, which is absurd. Similarly, one has $\varphi_4^* \neq \varphi_2^*$. Equation (3.21) hence rewrites

$$\frac{\sin\theta}{\cos^2\theta(\tan^2\theta - \tan^2(\varphi_2))} = \lambda.$$

We claim that the function h defined by

$$h : \theta \in [0, \varphi_2^*[\cup]\varphi_2^*, \frac{\pi}{2}[\mapsto \frac{\sin\theta}{\cos^2\theta(\tan^2\theta - \tan^2(\varphi_2^*))}.$$

is one-to-one[3]. As a result, one has $\varphi_1^* = \varphi_4^*$, and we infer that

$$\varphi_1^* = \varphi_4^* = 2\arctan\left(\frac{1+\sqrt{\frac{A^2}{4}-3}}{2(1+\frac{A}{4})}\right) \quad \text{and} \quad \varphi_2^* = \varphi_3^* = \varphi_5^* = \varphi_6^* = \frac{\pi}{4} - \frac{\varphi_1^*}{2}.$$

Noticing that $\varphi_1^* + 2\varphi_2^* + 2\varphi_3^* + \varphi_4^* = \pi$ and according to the previous considerations, it follows that

$$\max_{\Phi \in \Theta_A} D_{1,4}(\Phi) = D_{1,4}(\Phi^*) = \left(\frac{1}{\cos\varphi_1^*} + \frac{1}{\cos\varphi_4^*}\right)^2 = G^2(\varphi_1^*, \varphi_4^*) = \max_{\Phi \in \Theta_A} G^2(\varphi_1, \varphi_4).$$

[3]Indeed, since h is negative on $[0, \varphi_2[$ and positive on $]\varphi_2^*, \pi/2[$, we can deal separately with the intervals $[0, \varphi_2^*[$ and $]\varphi_2^*, \pi/2[$. On $[0, \varphi_2^*[$, one has $h(\theta) = \sin\theta \frac{1+\tan^2\theta}{\tan^2\theta - \tan^2(\varphi_2^*)}$. It follows that h is the product of the positive increasing sine function by $\theta \mapsto \frac{1+\tan^2\theta}{\tan^2\theta - \tan^2(\varphi_2^*)}$, which is negative decreasing. The conclusion follows.

On $]\varphi_2^*, \pi/2[$, one has $h(\theta) = \frac{1}{\sin\theta}\left(1 - \frac{\tan^2(\varphi_2^*)}{\tan^2\theta}\right)^{-1}$, and therefore, h is the product of two positive decreasing functions, whence the result.

Moreover, the maximal value of A_1A_4 is $2/\cos\varphi_1^*$.

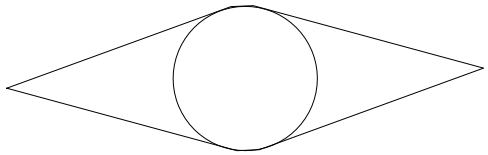

Figure 3.11: Hexagon maximising A_1A_4 for $A = 4\sqrt{3}$

Case (iii): the diameter is realized by A_1A_3

Using similar computations as for A_1A_4, we get

$$A_1A_3^2 = D_{1,3}(\varphi), \quad \text{with} \quad D_{1,3}(\varphi) = \frac{1}{\cos^2\varphi_1} + \frac{1}{\cos^2\varphi_3} - \frac{2\cos(\varphi_1 + 2\varphi_2 + \varphi_3)}{\cos\varphi_1\cos\varphi_3}.$$

Following exactly the same lines as for the case (ii), and using the same notations, one shows successively that

$$\forall \Phi \in \Theta_A, \quad D_{1,3}(\Phi) \leqslant G^2(\varphi_1, \varphi_3)$$

and

$$D_{1,4}(\Phi^*) = \max_{\Phi\in\Theta_A} D_{1,4}(\Phi)) = \max_{\Phi\in\Theta_A} G^2(\varphi_1, \varphi_4) = \max_{\Phi\in\Theta_A} G^2(\varphi_1, \varphi_3)$$

As a consequence, there holds

$$\max_{\Phi\in\Theta_A} D_{1,3}(\Phi)) \leqslant \max_{\Phi\in\Theta_A} D_{1,4}(\Phi)$$

with equality if, and only if there exists $\Phi^* \in \Theta$ such that $\pi = \varphi_1^* + 2\varphi_2^* + \varphi_3^*$. Because of the first equality constraint on the angles φ_i, it follows that $\varphi_2^* = \varphi_4^* + \varphi_5^* + \varphi_6^*$. Now, writing the optimality conditions for the problem of maximising $D_{1,3}$ over Θ_A as for the case (ii), we infer that $\varphi_2^* = \varphi_4^* = \varphi_5^* = \varphi_6^*$. Thus, these angles are necessarily equal to 0, which contradicts Lemma 2. This shows that the case (iii) cannot arise.

Comparison between the three cases

According to the previous analysis, one has $A_1A_4 > A_1A_3$ for any optimal set K^*. Notice moreover that

$$\max_{\Phi\in\Theta_A} A_1A_2 = 2\tan(\Phi^*) \text{ and } \max_{\Phi\in\Theta_A} A_1A_4 = \frac{2}{\cos(\Phi^*)} \text{ with } \Phi^* = 2\arctan\left(\frac{1+\sqrt{\frac{A^2}{4}-3}}{2(1+\frac{A}{4})}\right).$$

We then infer that the solution of Problem (3.19) corresponds to the case (ii).

Therefore, the optimisation problem has a unique solution (whenever $A \geqslant 2\sqrt{3}r_0^2$) given by the hexagon with inner radius r_0, which is tangent at every side to its inner circle, and such that the semi circle center-angles are given by

$$\varphi_1^* = \varphi_4^* = 2\arctan\left(\frac{1+\sqrt{\frac{A^2}{4r_0^4}-3}}{2(1+\frac{A}{4r_0^2})}\right) \quad \text{and} \quad \varphi_2^* = \varphi_3^* = \varphi_5^* = \varphi_6^* = \frac{\pi}{4} - \frac{\varphi_1^*}{2}.$$

3.4 Proof of Theorem 6

Before solving Problem $(\mathcal{P}_t)$, we first investigate the following auxiliary problem:

$$\max\{d(K),\ |K| = A,\ r(K) = r,\ D(K) = D\}, \tag{3.22}$$

where (A, D, r) denote the triple of positive numbers.

To help the forthcoming analysis and since several cases must be distinguished, let us plot on Figure 3.12 some elements of the Blashke diagram for the diameter and inradius, the area being fixed.

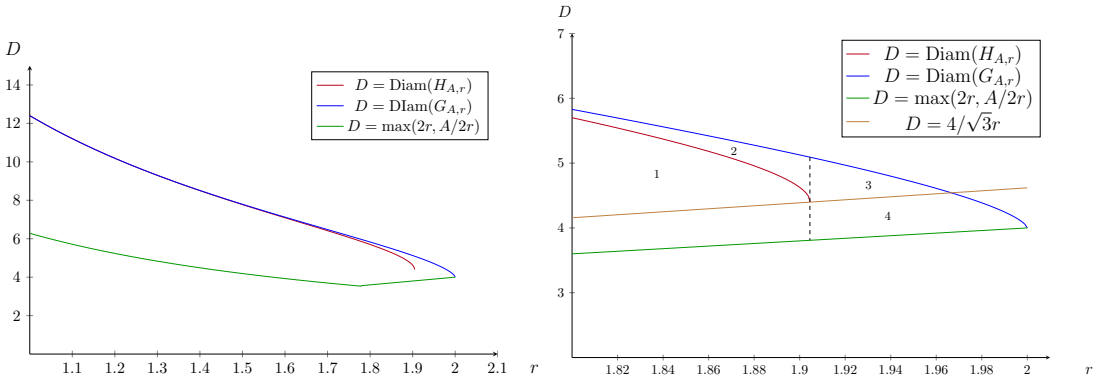

Figure 3.12: Left: Blaschke Diagram for $(r(K), D(K))$ under the condition $A = |K| = 4\pi$. Right: zoom on the right part of the diagram.

Remark 18. Let us comment on the construction of Figure 3.12. The green boundary consists of two parts. The first one is obtained by using that for every convex set K, one has

$$|K| < 2D(K)r(K),$$

with equality if, and only if $\mathrm{int}(K) = \emptyset$ (see [56]), and the (straight) right one is obtained by using that $D(K) \geqslant 2r(K)$ with equality if, and only if K is a ball. The red boundary is determined by using the second item of Theorem 5. Finally, the blue boundary is obtained by using (3.7) in Remark 13.

First, notice that, according to the so-called isodiametric inequality, one has $r \leqslant D(K)/2 \leqslant \sqrt{A/\pi}$ and $D(K) \leqslant D(G_{A,r})$ for every convex body K having as inradius r and area A, where the ice-cone $G_{A,r}$ has been introduced in Definition 12.

The main ingredient of the proof of Theorem 6 is the following lemma about the maximisation of the density functional $d(\cdot)$, whose proof is postponed at the end of this section for the sake of clarity.

Lemma 5. *Let $A > 0$ and $D > 0$.*

1. *Let $r \in (0, \sqrt{A/2\sqrt{3}}]$ and $D = D(H_{A,r})$. One has*
$$\max\{d(K),\ r(K) = r,\ D(K) \leqslant D,\ |K| = A\} = 1.$$
2. *Let $r \in (0, \sqrt{A/2\sqrt{3}})$ and $D \geqslant D(H_{A,r})$ or $(r, D) \in \{(r, D) \mid r \geqslant \sqrt{A/2\sqrt{3}}$ and $D \in [4/\sqrt{3}r, D(G_{A,r})]\}$. Then, one has*
$$\max\{d(K),\ r(K) = r,\ D(K) = D,\ |K| = A\} = \frac{A}{|H^{D,r}|}.$$
3. *Let $(r, D) \in \{(r, D) \mid r \geqslant \sqrt{A/2\sqrt{3}}$ and $D \leqslant \min\{4/\sqrt{3}r, D(G_{A,r})\}\}$. Then, one has*
$$\max\{d(K),\ r(K) = r,\ D(K) = D,\ |K| = A\} = \frac{A}{|H_r^*|}.$$

Let us come back to the solution of Problem $(\mathcal{P}_t)$.

Let us distinguish between several cases, depending on the possible values of $r(K)$ and $D(K)$. For that purpose, let us notice that

$$\sup_{K \in \mathcal{A}_{r_0,A}} J_t(K) \quad = \quad \max_{1 \leqslant i \leqslant 4} \sup_{K \in \mathcal{A}^i_{r_0,A}} J_t(K);$$

with the following partition of $\mathcal{A}_{r_0,A}$:

$$\begin{aligned}
\mathcal{A}^1_{r_0,A} &= \{K \in \mathcal{A}_{r_0,A} \mid r(K) = r,\ r_0 \leqslant r \leqslant \sqrt{A/(2\sqrt{3})} \text{ and } D(K) \leqslant D_{H_{A,r}})\} \\
\mathcal{A}^2_{r_0,A} &= \{K \in \mathcal{A}_{r_0,A} \mid r(K) = r,\ r_0 \leqslant r \leqslant \sqrt{A/(2\sqrt{3})} \text{ and } D(K) \in (D_{H_{A,r}}, D_{G_{A,r}})\} \\
\mathcal{A}^3_{r_0,A} &= \{K \in \mathcal{A}_{r_0,A} \mid r(K) = r,\ r > \sqrt{A/(2\sqrt{3})} \text{ and } D(K) \in (4/\sqrt{3}r, D_{G_{A,r}})\} \\
\mathcal{A}^4_{r_0,A} &= \{K \in \mathcal{A}_{r_0,A} \mid r(K) = r,\ r > \sqrt{A/(2\sqrt{3})} \text{ and } D(K) \leqslant 4/\sqrt{3}r\}.
\end{aligned}$$

where we introduce the notations $D_{H_{A,r}} = D(H_{A,r})$ and $D_{G_{A,r}} = D(G_{A,r})$, for the sake of readability. $\mathcal{A}^i_{r_0,A}$ corresponds to the zone i in Figure 3.12.

Let us investigate each problem separately.

Solution of Problem $\sup_{K \in \mathcal{A}^1_{r_0,A}} J_t(K)$. Let $r \in [r_0, \sqrt{A/(2\sqrt{3})}]$ and $K \in \mathcal{A}^1_{r_0,A}$ such that $r(K) = r$. According to Lemma 5, one has

$$J_t(K) \quad \leqslant \quad t + (1-t)\frac{\sqrt{\pi} D_{H_{A,r}}}{2\sqrt{A}} = t + (1-t)\frac{\sqrt{\pi}}{2\sqrt{A}} \left(\frac{1}{3r} \left(2A + \sqrt{A^2 - 12r^4} \right) \right)$$

with equality whenever $K = H_{A,r}$. Moreover, the mapping $r \mapsto \frac{1}{3r}\left(2A + \sqrt{A^2 - 12r^4}\right)$ is decreasing on $(0, +\infty)$. As a consequence, we infer that

$$\boxed{\max_{K \in \mathcal{A}^1_{r_0,A}} J_t(K) = J_t(H_{A,r}) = t + (1-t)\frac{\sqrt{\pi}}{2\sqrt{A}} \left(\frac{1}{3r_0} \left(2A + \sqrt{A^2 - 12r_0^4} \right) \right)},$$

and the maximum is reached by the p-hexagon H_{A,r_0}.

Solution of Problem $\sup_{K\in\mathcal{A}^2_{r_0,A}\cup\mathcal{A}^3_{r_0,A}} J_t(K)$**.** Let $K \in \mathcal{A}^2_{r_0,A}$ and $r = r(K)$ be such that $r \in [r_0, \sqrt{A/(2\sqrt{3})}]$. According to Lemma 5, one has

$$J_t(K) \leqslant t\frac{A}{|H^{D,r}|} + (1-t)\frac{\sqrt{\pi}D}{2\sqrt{A}} \tag{3.23}$$

Let us first maximise the function in the right-hand side, by solving the problem

$$\max_{(D,r)\in\mathcal{Z}} \psi_{t,A}(r,D) \quad \text{where} \quad \psi_{t,A}(r,D) = t\frac{A}{|H^{D,r}|} + (1-t)\frac{\sqrt{\pi}D}{2\sqrt{A}}, \tag{3.24}$$

with

$$\mathcal{Z} = \{(r,D) \mid r_0 \leqslant r \leqslant \sqrt{A/(2\sqrt{3})} \text{ and } D \in (D_{H_{A,r}}, D_{G_{A,r}}) \text{ or } r > \sqrt{A/(2\sqrt{3})} \text{ and } D \geqslant 4/\sqrt{3}r\}.$$

This corresponds to deal with the zone 2 and 3 of Figure 3.12. First, note that

$$\frac{d\psi_{t,A}}{dr}(r,D) = \frac{-tA(2D\sqrt{D^2-4r^2} - D^2 + 8r^2)}{\sqrt{D^2-4r^2}\left(2Dr - r\sqrt{D^2-4r^2}\right)^2}.$$

Moreover, if $D^2 \leqslant 8r^2$, we conclude directly that $2D\sqrt{D^2-4r^2} - D^2 + 8r^2)$ is positive. in the converse case, the sign of $2D\sqrt{D^2-4r^2} - D^2 + 8r^2$ is also the sign of $4D^2(D^2-4r^2) - (D^2-8r^2)^2$, namely $3D^4 - 64r^4$. Notice that, in that zone, one has $D \geqslant 4r/\sqrt{3} \geqslant r\sqrt{8/\sqrt{3}}$, which means precisely that $3D^4 - 64r^4 > 0$. In all cases, we then have $2D\sqrt{D^2-4r^2} - D^2 + 8r^2 > 0$, and we infer that $\frac{d\psi_{t,A}}{dr}(r,D) < 0$. It follows that either $D = D_{H_{A,r}}$ or $r = r_0$. The case $D = D_{H_{A,r}}$ has been investigated when solving Problem $\sup_{K\in\mathcal{A}^1_{r_0,A}} J_t(K)$ above. As a consequence, one has necessarily $r = r_0$ at the maximum.

It then remains to investigate the variations of the criterion with respect to the parameter D, at $r = r_0$. One has

$$\frac{d^2\psi_{t,A}}{dD^2}(r_0,D) = -\frac{2At\left(\sqrt{D^2-4r_0^2}(14r_0^2 - 5D^2) + 4D(D^2-3r_0^2)\right)}{r_0(D^2-4r_0^2)^{3/2}(2D - \sqrt{D^2-4r_0^2})^3}.$$

Note that $\sqrt{D^2-4r_0^2}(14r_0^2 - 5D^2) + 4D(D^2-3r_0^2) = r_0^3\left(\sqrt{X^2-4}(14-5X^2) + 4X(X^2-3)\right)$ with $X = D/r_0$. Recall that the function $X \mapsto \sqrt{X^2-4}(14-5X^2) + 4X(X^2-3)$ has a unique zero X_0 on $[4/\sqrt{3}, +\infty)$. Moreover, a tedious but easy analysis yields that $\sqrt{X^2-4}(14-5X^2) + 4X(X^2-3) \geqslant 0$ on $[4/\sqrt{3}, X_0]$ and $\sqrt{X^2-4}(14-5X^2) + 4X(X^2-3) < 0$ elsewhere (see Figure 3.13).

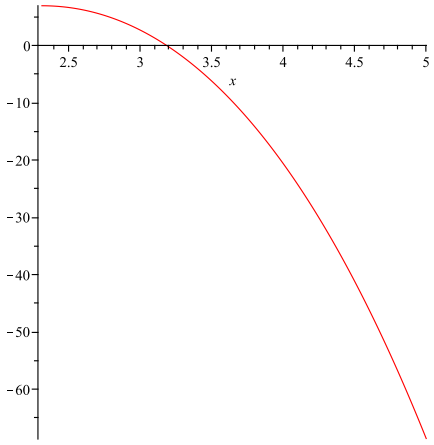

Figure 3.13: Plot of the function $X \mapsto \sqrt{X^2-4}(14-5X^2)+4X(X^2-3)$.

It follows that the mapping $D \mapsto \frac{d}{dD}\psi_{t,A}(r_0,\cdot)$ is decreasing on $[4\sqrt{3}r_0, X_0r_0]$ and increasing on $[X_0r_0,+\infty)$. Its minimal value is

$$\frac{d\psi_{t,A}}{dD}(r_0, X_0r_0) \quad = \quad \frac{-A\gamma_0}{r_0^3}t + (1-t)\frac{\sqrt{\pi}}{2\sqrt{A}}$$

where γ_0 is defined by (3.11).

The minimal value of $\frac{d\psi_{t,A}}{dD}(r_0,\cdot)$ is then non-negative whenever $t \in [0, t_{A,r_0}]$ and negative whenever $t \in (t_{A,r_0}, 1]$, where t_{A,r_0} is given by (3.10).

- If $t \in [0, t_{A,r_0}]$, we infer from the above analysis that $D \mapsto \psi_{t,A}(r_0, D)$ is increasing on $(D_{H_{A,r}}, D_{G_{A,r}})$ and the maximum is achieved at $D = D_{G_{A,r}}$.

- If $t \in (t_{A,r_0}, 1]$, the minimal value of $\frac{d\psi_{t,A}}{dD}\psi_{t,A}(r_0,\cdot)$ is negative. Notice moreover that

$$\frac{d\psi_{t,A}}{dD}(r_0, 4r_0/\sqrt{3}) = \lim_{D\to+\infty}\frac{d\psi_{t,A}}{dD}(r_0, D) = \frac{(1-t)\sqrt{\pi}}{2\sqrt{A}}.$$

  Combining these informations about $\frac{d\psi_{t,A}}{dD}$ yields the existence[4] of $z^1_{t,r_0,A} \in [4/\sqrt{3}, X_0)$ and $z^2_{t,r_0,A} \in [X_0,+\infty)$ such that the mapping $D \mapsto \psi_{t,A}(r_0,\cdot)$ is increasing on $(4/\sqrt{3}r_0, z^1_{t,r_0,A}r_0)$, decreasing on $(z^1_{t,r_0,A}, z^2_{t,r_0,A})$ and increasing on $(z^2_{t,r_0,A},+\infty)$.

  Now, using that $D(H_{A,r_0}) = \frac{1}{3r_0}\left(2A + \sqrt{A^2-12r_0^4}\right)$ and that the mapping $[2\sqrt{3},+\infty) \ni A \mapsto \frac{1}{3r_0}\left(2A+\sqrt{A^2-12r_0^4}\right)$ is increasing, we claim that

$$\frac{A}{r_0^2} \geqslant 2X_0 - \sqrt{X_0^2-4} \Longleftrightarrow \mathrm{D}_{H_{A,r_0}} \geqslant X_0r_0$$

[4]Moreover, $z^1_{t,r_0,A}$ and $z^2_{t,r_0,A}$ are the two solutions of the equation $d\psi_{t,A}/dD(r_0, r_0z) = 0$ with unknown z on $[4/\sqrt{3},+\infty)$

$$\frac{2\sqrt{z^2-4}-z}{\sqrt{z^2-4}(2z-\sqrt{z^2-4})^2} = \frac{(1-t)\sqrt{\pi}r_0^3}{2tA^{3/2}}.$$

Since $\psi_{t,A}(r_0,\cdot)$ is decreasing on $[X_0 r_0, z^2_{t,r_0,A}]$ and increasing on $(z^2_{t,r_0,A},+\infty)$, we infer that, under the smallness condition (3.12) on r_0, one has successively

$$\begin{aligned}\max_{(D,r)\in\mathcal{Z}} \psi_{t,A}(r,D) &= \max_{D\in(D_{H_{A,r_0}},D_{G_{A,r_0}})} \psi_{t,A}(r_0,D)\\ &= \max\{\psi_{t,A}(r_0,D_{H_{A,r_0}}),\psi_{t,A}(r_0,D_{G_{A,r_0}})\}\end{aligned}$$

To solve the problem arising in the right-hand side, let us introduce

$$\Delta_{r_0,A}(t)=\psi_{t,A}(r_0,D_{G_{A,r_0}})-\psi_{t,A}(r_0,D_{H_{A,r_0}}).$$

One computes

$$\begin{aligned}\Delta_{r_0,A}(0) &= \frac{\sqrt{\pi}}{2\sqrt{A}}(D_{G_{A,r_0}}-D_{H_{A,r_0}})\\ \Delta_{r_0,A}(1) &= A\left(\frac{1}{|D_{G_{A,r_0}}|}-\frac{1}{|D_{H_{A,r_0}}|}\right).\end{aligned}$$

Hence, since $\Delta_{r_0,A}$ is affine, $\Delta_{r_0,A}(0)>0$, $\Delta_{r_0,A}(1)<0$, we infer the existence of $t^*_{A,r_0}\in[0,1]$ such that

- on $[0,t^*_{A,r_0}]$, $\max\{\psi_{t,A}(r_0,D_{H_{A,r_0}}),\psi_{t,A}(r_0,D_{G_{A,r_0}})\}=\psi_{t,A}(r_0,D_{G_{A,r_0}})$;
- on $(t^*_{A,r_0},1]$, $\max\{\psi_{t,A}(r_0,D_{H_{A,r_0}}),\psi_{t,A}(r_0,D_{G_{A,r_0}})\}=\psi_{t,A}(r_0,D_{H_{A,r_0}})$.

Notice that, by construction, one has $\Delta_{r_0,A}(t^*_{A,r_0})=0$ leading to the expression (3.13) of t^*_{A,r_0} and one has necessarily $t^*_{A,r_0}\geqslant t_{A,r_0}$ according to the analysis of the case where $t\in[0,t_{A,r_0}]$.

Let us come back to the solution of Problem $\sup_{K\in\mathcal{A}^2_{r_0,A}\cup\mathcal{A}^3_{r_0,A}} J_t(K)$. We proved that, under the smallness assumption (3.12) on r_0, G_{A,r_0} and H_{A,r_0} are the only possible solutions of Problem $\max_{(D,r)\in\mathcal{Z}}\psi_{t,A}(r,D)$. Noting that (3.23) is an equality whenever K is either equal to G_{A,r_0}, or H_{A,r_0}, we infer to the end that

$$\boxed{\max_{K\in\mathcal{A}^2_{r_0,A}\cup\mathcal{A}^3_{r_0,A}} J_t(K)=\begin{cases}J_t(G_{A,r_0}) & \text{if } t\in[0,t^*_{A,r_0}]\\ J_t(H_{A,r_0}) & \text{if } t\in(t^*_{A,r_0},1].\end{cases}}$$

Estimate of $\sup_{K\in\mathcal{A}^4_{r_0,A}} J_t(K)$**.** According to Lemma 5, one has

$$J_t(K)\leqslant t\frac{A}{|H^*_r|}+(1-t)\frac{\sqrt{\pi}D}{2\sqrt{A}}=t\frac{A\sqrt{3}}{2r^2}+(1-t)\frac{\sqrt{\pi}D}{2\sqrt{A}}. \tag{3.25}$$

Since $D\mapsto t\frac{A\sqrt{3}}{2r^2}+(1-t)\frac{\sqrt{\pi}D}{2\sqrt{A}}$ is increasing, we infer that the solutions of the problem

$$\max_{(r,D)\in\hat{\mathcal{Z}}} t\frac{A\sqrt{3}}{2r^2}+(1-t)\frac{\sqrt{\pi}D}{2\sqrt{A}}$$

with

$$\hat{\mathcal{Z}}=\{(r,D)\mid \sqrt{A/(2\sqrt{3})}\leqslant r\leqslant\sqrt{A/\pi}\text{ and }2r\leqslant D\leqslant 4/\sqrt{3}r\}.$$

satisfy necessarily $D = 4r/\sqrt{3}$. According to Lemma 5, we deduce successively that

$$\begin{aligned}\max_{K\in\mathcal{A}^4_{r_0,A}} J_t(K) &= \max_{(r,D)\in\hat{\mathcal{Z}}} t\frac{A\sqrt{3}}{2r^2} + (1-t)\frac{\sqrt{\pi}D}{2\sqrt{A}} \\ &\leqslant \max_{K\in\mathcal{A}^2_{r_0,A}\cup\mathcal{A}^3_{r_0,A}} J_t(K).\end{aligned}$$

Moreover, we have proved that every solution of the last problem in the right-hand side must satisfy $r(K) = r_0$, proving that the last inequality is in fact strict.

This concludes the proof of Theorem 6.

Proof of Lemma 5. We investigate the three different cases:

1. For $r \in (0, \sqrt{A/2\sqrt{3}})$ (zone 1 of Figure 3.12), since $H_{A,r}$ is admissible and since $d(K) \leqslant 1$ for every convex body K, the first equality is obvious, by choosing $K = H_{A,r}$.

2. Let us deal with the zone 2 and 3 of Figure 3.12. We first assume that $r \in (0, \sqrt{A/2\sqrt{3}})$ and $D \geqslant D(H_{A,r})$. Let K be a maximiser for the problem

$$\max\{d(K),\ r(K) = r,\ D(K) = D,\ |K| = A\}.$$

Denoting by K^T the smallest convex set tiling the plane and containing K, one has

$$D(K^T) \geqslant D, \qquad r(K^T) \geqslant r.$$

Then, by using Theorem 5 and by monotonicity of $|H^{D,r}|$ with respect to D and r, we have

$$|K^T| \geqslant |H^{D(K^T),r(K^T)}| \geqslant |H^{D,r}|,$$

As a consequence, we infer that

$$d(K) = \frac{|K|}{|K^T|} \leqslant \frac{A}{|H^{D,r}|}.$$

Notice that the mapping $A \mapsto D(H_{A,r})$ is increasing on its definition set. Using this remark and according to Remark 13, since $D \in [D(H_{A,r}), D(G_{A,r})]$, we have $|G^{D,r}| \leqslant A \leqslant |H^{D,r}|$. Moreover, there holds $G^{D,r} \subset H^{D,r}$ by construction. Let us show that $(G^{D,r})^T = H^{D,r}$. Since

$$D((G^{D,r})^T) \geqslant D \quad \text{and} \quad r((G^{D,r})^T) \geqslant r,$$

one has $|(G^{D,r})^T| \geqslant |H^{D,r}|$, showing that $(G^{D,r})^T = H^{D,r}$. Now, consider a convex set K of area A chosen such that $G^{D,r} \subset K \subset H^{D,r}$. Then, since $(G^{D,r})^T = H^{D,r}$, one has $K^T = H^{D,r}$ by continuity and $d(K) = \frac{A}{|H^{D,r}|}$. Therefore the supremum is reached, whence the conclusion.

Let us now assume that $(r, D) \in \{(r, D) \mid r \geqslant \sqrt{A/2\sqrt{3}}$ and $D \in [4/\sqrt{3}r, D(G_{A,r})\}$. Then, a convex set K with inradius r and area A cannot be tiling according to Theorem 5. Nevertheless, one checks easily that the diameter of the hexagon $H^{D,r}$ is equal to D if, and only if $D \geqslant 4/\sqrt{3}r$. Therefore, the same argument as below allows to conclude similarly.

3. If $(r, D) \in \{(r, D) \mid r \geqslant \sqrt{A/2\sqrt{3}}$ and $D \leqslant \min\{4/\sqrt{3}r, D(G_{A,r})\}\}$ (zones 4 of Figure 3.12), then the diameter of $H^{D,r}$ differs from D[5].

   We claim (see below for a proof) moreover that *the regular hexagon H_r^* is the tiling convex set with inradius r and area A having the lowest diameter*, or similarly that *the regular hexagon H_r^* is the tiling convex set with inradius r and diameter D having the lowest area.*

   Let K be a convex set such that $r(K) = r$ and $D(K) = D$, with (r, D) belonging to the zone described above. One has $D(K^T) \geqslant D$ and $r(K^T) \geqslant r$. As a consequence of the claim above, one has necessarily $D(K^T) \geqslant D(H^\star_{r(K^T)})$. Since K^T is tiling, one has

$$|K^T| \geqslant |H_{D(K^T),r(K^T)}| \geqslant |H_r^*|.$$

   according to Theorem 5 and the claim above. It follows that for every convex K in the aforementioned zone of the Blaschke diagram, one has $d(K) \leqslant \frac{A}{|H_r^*|}$.

   Let K be a convex set of area A such that $G_{D(K^T),r(K^T)} \subset K \subset H_r^*$. We infer from the previous analysis that $K^T = H_r^*$, and $\delta(K) = A/|H_r^*|$, so that it maximises the density.

   To conclude, it remains to prove the claim above. For a given $r > 0$, we investigate the problem

$$\inf\{D(T),\ T \text{ tiling and } r(T) \geqslant r\}.$$

   Notice first that, by mimicking the arguments used to prove Theorem 5, one shows that there exists a solution T^* to this problem, and necessarily, $r(T^*) = r$.

   Moreover, according to Theorem 5, the solution of the more constrained problem

$$\inf\{D(T),\ T \text{ tiling, } r(T) = r \text{ and } |T| = A\},$$

   with $A \geqslant 2\sqrt{3}r^2$, is the p-hexagon described in Definition 11. Then, by writing

$$\inf\{D(T),\ T \text{ tiling and } r(T) \geqslant r\} = \inf_{A \geqslant 2\sqrt{3}r^2} \inf\{D(T),\ T \text{ tiling, } r(T) = r \text{ and } |T| = A\},$$

   and using that the area of the p-hexagon introduced in Definition 11 is an increasing function of the diameter (see Remark 15), we infer that T^* is such that $|T^*| = 2\sqrt{3}r^2$. In other words, $T^* = H_r^*$ and we are done.

□

3.5 Conclusion and perspectives

In this paper, we solve several problems in convex geometry, paying attention to the class of plane tiling domains. These problems were motivated by issues in biology related to the shape of eggs os some crustaceans. Of course, the 3D situation is certainly more relevant but a complete mathematical analysis, like in this paper, seems out of range. Nevertheless, some numerical simulations will be done for this problem.

We foresee to investigate a related issue in a forthcoming paper, namely the precise determination of the Blaschke-Santalò diagram, see Figure 3.12 for the area, diameter and inradius (sometimes known as the A, D, r problem).

Acknowledgement. The first and the third authors were partially supported by the Project "Analysis and simulation of optimal shapes - application to life-sciences" of the Paris City Hall. The authors warmly thank Nicolas Rabet for very stimulating discussions about modelling issues.

[5]Indeed, this is an easy consequence of the first item of Theorem 5.

3.6 Appendix

3.6.1 Existence of K^T

Since the set of convex bodies contained in a compact D is itself compact for the Hausdorff topology and since the restriction of the Lebesgue measure to this set is continuous [58], it is enough to show that the set of convex tiling domains T with $T \geqslant \varepsilon > 0$ is closed for the Hausdorff topology. To prove this claim, let $(T_n)_{n\in\mathbb{N}}$ be a sequence of convex tiling domains converging to T. Then T is necessarily convex. Since T_n is tiling for every n, there exist a sequence $(\tau_{n,i})_{i\in\mathbb{N}}$ of affine isometries such that $R^2 \subset \bigcup_{i\in\mathbb{N}} \tau_{n,i}(T_n)$, in other words

$$\forall R > 0, \qquad B(0,R) \subset \bigcup_{i\in\mathbb{N}} \tau_{n,i}(T_n)$$

Without loss of generality, we assume that the distance of $\tau_{n,i}(T_n)$ (i-th copy of T_n) to the origin is non-decreasing.

Let $D = \sup(D(T_n))$, $A = \sup(|T_n|)$, $R > 0$, $N = \left[\frac{|B(0,R)|}{\varepsilon}\right]$ (the bracket notation standing for the integer part) and $I_N = \{0, ..., n\}$. Then, we claim that

$$\forall n \in \mathbb{N}, \qquad B(0,R) \subset \bigcup_{i\in I_N} \tau_{n,i}(T_n) \subset B(0, R+2D).$$

Decomposing $\tau_{n,i}$ as $\tau_{n,i} = r_{n,i} + t_{n,i}$ where $r_{n,i}$ is a rotation and $t_{n,i}$ is a translation assimilated (with a slight abuse of notation) to a vector such that $\|t_{n,i}\| \leqslant R + 2D$ for all $n \in N$ and $i \leqslant N$. Applying a compactness argument yields the existence of τ_i and $\varphi : \mathbb{N} \mapsto \mathbb{N}$ such that $\tau_{\varphi(N),i} \to \tau_i$ for all $i \leqslant N$. Therefore, one has $\tau_{\varphi(n),i)}(T_{\varphi(n)}) \to \tau_i(T)$ as $n \to +\infty$. Furthermore, since $\mathrm{int}(\tau_{\varphi(n),i}(T_{\varphi(n)})) \cap \mathrm{int}(\tau_{\varphi(n),j}(T_{\varphi(n)})) = \emptyset$ for $i \neq j$, we get $\mathrm{int}(\tau_i(T)) \cap \mathrm{int}(\tau_j(T)) = \emptyset$ and $\bigcup_{i\in I_N} \tau_{\varphi(n),i}(T_{\varphi(n)}) \to \bigcup_{i\in I_N} \tau_i(T)$. Finally by stability of the inclusion for the Hausdorf metric, one has $B(0,R) \subset \bigcup_{i\in I_N} \tau_i(T)$.

Using that the last inclusion holds true for every $R > 0$, we infer that T is a convex tiling domain.

3.6.2 Proof of Theorem 4

Let us first consider the case of tiling domains.

Case of tiling domains. Let K be a tiling domain and set $D = D(K)$. There exists a family $\{\tau_i\}_{i\in\mathbb{N}}$ of isometries such that

$$\mathbb{R}^2 = \bigcup_{i\in\mathbb{N}} \tau_i(K).$$

For $R > 2D$, define

$$P(R) = \bigcup_{\tau_i(K)\subset D(0,R)} \tau_i(K).$$

Then, by maximality of the diameter, and since K is tiling, one has necessarily $D(0, R-D) \subset P(R)$, and therefore $\sharp\{i, \tau_i(K) \subset D(0,R)\}|K| \geqslant \pi(R-D)^2$ and

$$\frac{2R}{\sqrt{\sharp\{i, \tau_i(K) \subset D(0,R)\}}D(K)} \leqslant \frac{2R\sqrt{|K|}}{\sqrt{\pi}(R-D)D(K)}.$$

Letting $R \to \infty$, we obtain

$$\limsup_{R\to+\infty} \frac{2R}{\sqrt{\sharp\{i, \tau_i(K) \subset D(0,R)\}}D(K)} \leqslant \frac{2\sqrt{|K|}}{\sqrt{\pi}D(K)}.$$

Finally, passing to the infimum over all packings yields

$$D'_\infty(K) \leqslant \frac{2\sqrt{|K|}}{\sqrt{\pi}D(K)}.$$

The conclusion follows by combining this estimate with (3.4).

We now investigate the general case.

General case. In view of proving (3.5), we will use the following result due to Kuperberg's in [68].

Proposition 33. *Every convex set $K \in K$ is contained in a tiling hexagon K_{kup} satisfying $|K_{kup}|/|K| \leqslant 4/3$*[6].

Let $K \in \mathcal{K}$ and consider the tiling K_{kup} provided by Proposition 33. We define a packing of K by placing adequately a copy of K in each cell of K_{kup}. Denoting by $\{\tau_i\}_{i\in\mathbb{N}}$ the family of isometries used to define this packing, we deduce that

$$\begin{aligned} D'_\infty(K) &\leqslant \limsup_{R\to\infty} \frac{2R}{\sqrt{\sharp\{i, \tau_i(K_{kup}) \subset D(0,R)\}}D(K)} \\ &= \frac{D(K_{kup})}{D(K)} \limsup_{R\to\infty} \frac{2R}{\sqrt{\sharp\{i, \tau_i(K_{kup}) \subset D(0,R)\}}D(K)} \\ &= \frac{2\sqrt{|K_{kup}|}}{\sqrt{\pi}D(K)} \leqslant \sqrt{\frac{2}{\sqrt{3}}} \frac{2\sqrt{|K|}}{\sqrt{\pi}D(K)}, \end{aligned}$$

by using the computation above in the case of tiling sets and Proposition 33.

The expected conclusion follows.

3.6.3 Diameter of $H_{A,r}$ and area of $H^{D,r}$

To avoid any confusion with the notations we will use within this proof, let us denote temporarily by d the diameter of the hexagon $H^{d,r}$ we will consider. Let us introduce the points A, B, C, D and O, as plotted on Figure 3.14.

[6] Moreover, K_{kup} is a p-hexagon, in other words a hexagon with two opposite parallel sides having the same length. Recall that every p-hexagon tiles the plane.

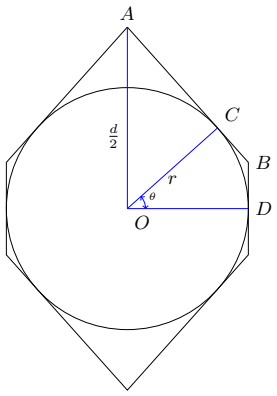

Figure 3.14: The hexagon $H^{d,r}$

The area $|H^{d,r}|$ is equal to 4 times the area of the pentagon $ACBDO$, which is the sum of the area of ACO and the area of $CBDO$, which is twice the area of the triangle BDO. Hence, one has

$$|H^{d,r}| = 4 \times (|ACO| + 2|BDO|)$$

Let $\theta = \widehat{COD}$. On has $\sin\theta = 2r/d$. Then, we compute

$$|ACO| = \frac{dr}{4}\cos\theta = \frac{r}{4} \times \sqrt{d^2 - 4r^2}.$$

Consider the orthonormal basis $(O; \frac{\overrightarrow{OD}}{OD}, \frac{\overrightarrow{OA}}{OA})$. Then the coordinates of B are $(r, r\frac{1-\cos(\theta)}{\sin(\theta)})$ and since $\theta = \arcsin(2r/d)$, we get

$$|BDO| = \frac{r^2}{2}\frac{1 - \sqrt{1 - \frac{4r^2}{d^2}}}{\frac{2r}{d}} = \frac{r}{4}(d - \sqrt{d^2 - 4r^2})$$

Finally, we get that $|H^{d,r}| = 2rd - r\sqrt{d^2 - 4r^2}$. By inverting the relation $A = 2rd - r\sqrt{d^2 - 4r^2}$ (whenever $A \geqslant 2\sqrt{3}r^2$ and $d \geqslant 2r$), we get that

$$d = \alpha(A, r) = \frac{1}{3r}\left(2A + \sqrt{A^2 - 12r^4}\right),$$

whence the expression of $D(H_{A,r})$ with respect to the parameter A.

Part II

A detour to convex geometry

Chapter 4

Introduction

Contents

This Chapter is an introduction and a summary of the next chapter, which has been submitted to an international journal[30]

4.1 Setting the problem

In the last Part we investigated the problem of maximising a convex combination of the density and the diameter. A key element was the diagram representing the different values of the area, the diameter, or the inradius that a convex body in $\mathbb{R}^2$ can take. Indeed the diagram was very useful because we needed to know what is the highest possible diameter for a convex of given area and inradius.

As previously said, this result was given in [62]. They actually found a general inequality involving the diameter, the inradius and the area, that shows that the 2-cap body 4.1 is the minimiser of the area for fixed diameter and inradius. More precisely, define

$$\mathcal{K}^N_{r,D} = \{K \in \mathcal{K}_N \mid r(K) = r \text{ and } D(K) = D\}.$$

Theorem 7. *[62] For every $K \in \mathcal{K}^2_{r,D}$,*

$$|K| \geqslant r\left(\sqrt{D^2 - 4r^2} + 2r \arcsin\left(\frac{2r}{D}\right)\right) \tag{4.1}$$

with equality if $K = G^{D,r}$ the 2-cap body

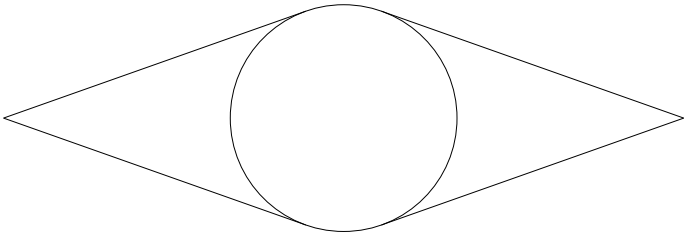

Figure 4.1: The minimiser of the Area among convex sets of given diameter and inradius.

It is possible to inverse that inequality with fixed r to deduce an upper bound for the diameter, and we obtain that the 2-cap body is also the maximiser of the diameter for a fixed inradius and area. Since we didn't need to know about the minimisation of the diameter, we were able to work on the following incomplete diagram 4.2

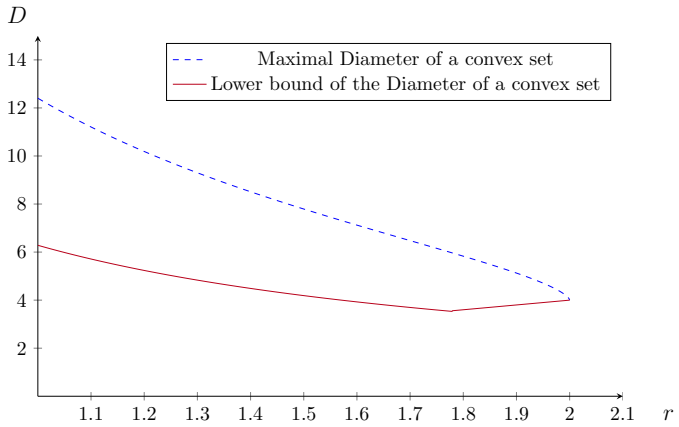

Figure 4.2: Incomplete (A,D,r) diagram. The red curve only gives a lower bound to the diameter

When we look at this diagram, a natural that arises is what is its minimal curve. Answering that question allows us to answer a bigger question:

Question: Given r, D and A three positive numbers, is it possible to find a convex body with area A, inradius r and diameter D?

This kind of questions was first formally introduced by W. Blaschke in [17] in which the fundamental question was to find complete systems of inequalities between the six main geometric quantities: the area A, the diameter D, the circumradius R, the inradius r, the minimum width w, and the perimeter P. The *Blaschke-Santaló diagram* is a way to represent those inequalities, and also gives a map that indicates what the possible values that a set can take are.

Definition 13. *Let $\Omega_{adm} \subset \mathcal{P}(\mathbb{R}^N)$, a class of admissible subset of $\mathbb{R}^N$ and let X, Y two functionals $\Omega_{adm} \mapsto \mathbb{R}$. The corresponding Blaschke-Santaló diagram is the region of the plane:*

$$\mathcal{B}(\Omega_{adm}, X, Y) = \{(x, y) \in \mathbb{R}^2, \exists K \in \Omega_{adm} \mid X(K) = x, Y(K) = y\}$$

Note that X and Y are usually functionals of three quantities (q_1, q_2, q_3) such that the diagram stores the complete system of inequalities between those quantities in the square $[0,1] \times [0,1]$. A *Blaschke-Santaló diagram* that involves (q_1, q_2, q_3) is called the (q_1, q_2, q_3) diagram.

Since there are 6 main geometric quantities, there are 20 possible diagrams. L. Santaló solved six of them : (A, P, w), (A, P, r), (A, P, R), (A, D, w), (P, D, w), (D, r, R) and gave a partial solution to (D, R, w) and (r, R, w). The two last cases were eventually solved by M. Hernandez Cifre and S. Segura Gomis in [61]. In a series of papers with collaborators, M. Hernandez Cifre has also been able to prove complete systems of inequalities in the cases (A, D, R), (P, D, R) [60], in the cases (A, r, R), (P, r, R) [19] and finally in the case (D, r, w) [59].

To the best of our knowledge, (A, P, D), (A, D, r), (A, r, w), (A, R, w), (P, D, r), (P, r, w) and (P, R, w) were not solved yet.

Remark 19. It is worth noticing that *Blaschke-Santaló diagrams* involving less geometrical quantities such as λ_1 and λ_2 have also been investigated. For example, the $(A, \lambda_1, \lambda_2)$ Diagram is studied in [22, 10], or the (λ_1, P, D) diagram in [41]. Let us also mention a diagram involving a physical quantity such as the Torsion: (λ_1, T, A) in [71].

Considering our main objective, solving the (A, D, r) diagram, we decided to work with $X = 2r/D$ and $Y = \pi r^2/A$. That choice comes from the fact that trivially, for any convex set, $2r \leqslant D$ with equality for the disk, and $A \geqslant \pi r^2$ with equality for the disk. It ensures that the diagram lies in the square $[0,1] \times [0,1]$. Now if we fix a geometric quantity, say r, we see that Y is directly linked to $1/A$ and X is directly linked to $1/D$. Hence a bottom curve would give the maximiser of the area for given inradius and diameter, whereas a top curve gives its minimiser. As we shall see during the construction of the diagram, The only remaining question is to build the bottom curve of the diagram. For that purpose, we solve the following problem

Problem: For $r > 0$ and $D \geqslant 2 > r$, let $\mathcal{K}^2_{r,D}$ be the set of convex bodies with inradius r and diameter D. Then we would aim at solving:

$$\boxed{\sup_{K \in \mathcal{K}^2_{r,D}} |K|} \qquad (\mathcal{P}_{\max})$$

4.2 Results

4.2.1 The theorems

We were able to give the complete (A, D, r) Diagram by solving the maximisation area problem. The problem being scale invariant we decided to work with a fixed inradius $r = 1$.

We obtained this result, for which we give a more detailed statement in Chapter 5 (Theorem 11).

Theorem 8. *There exists $D^\star \simeq 2.388$ such that for $D \leqslant D^\star$ the solution of $(\mathcal{P}_{\max})$ is by the set $K_E(D)$ (see Figure 4.3a) and for $D \geqslant D^\star$ the solution of $(\mathcal{P}_{\max})$ is the symmetric slice $K_S(D)$ (Figure 4.3b)*

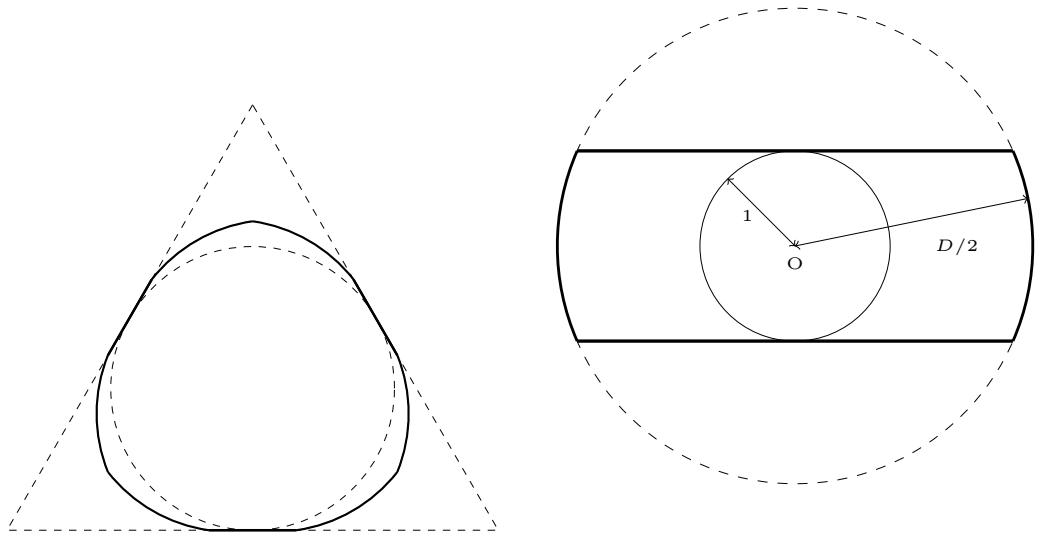

(a) $K_E(D)$ the solution of $(\mathcal{P}_{\max})$ for small D. (b) $K_S(D)$ the solution of $(\mathcal{P}_{\max})$ for large D

Figure 4.3: The two solutions of $(\mathcal{P}_{\max})$ depending on the value of D

We were also able to extend the result of Theorem (7) in any dimension. If we define the N-dimensional 2-cap body $K_2^N(r, D)$ as the convex hull of a ball of radius r and two points at a distance of D and whose middle is the center of the ball, then we proved the following theorem (see Theorem 10 in Chapter 5 for a complete statement):

Theorem 9. *Among all the convex bodies of $\mathcal{K}^N$ with diameter $D \geqslant D_0$ and inradius $r \geqslant r_0$, the 2-cap body $K_2^N(r_0, D_0)$ (see Figure 4.4) has the lowest volume.*

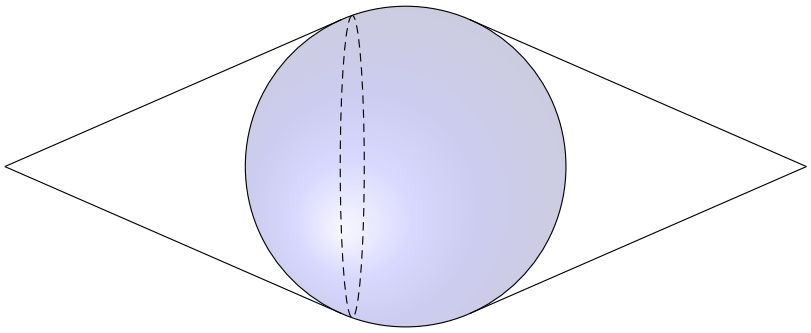

Figure 4.4: the 2-cap body $K_2^N(r, D)$

As a consequence of the theorem we provided the complete *Blaschke-Santaló diagram* of (A, D, r), which is given in Figure 4.5

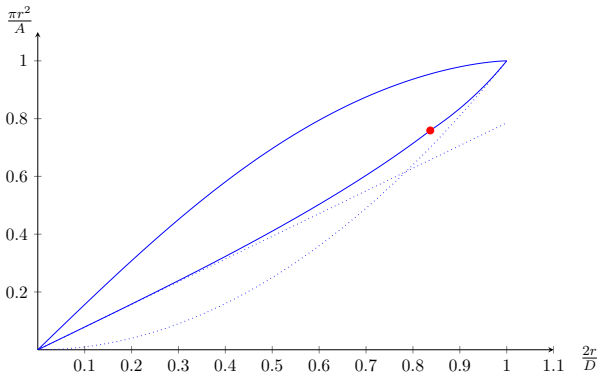

Figure 4.5: The complete (A,D,r) Diagram. The dotted lines are the old lower bound that were already known. . The point (1,1) correspond to any disk. The point (0,0) is any infinite set included in the strip. On the top curve is represented the 2-cap body, whereas on the left part of the bottom curve is the symmetric slice, and on the right part is the set K_E
. The red dot is the value for which the optimum changes

4.2.2 Main ideas of the proof

Proof of Theorem (9) First we show that the diameter and the inradius constraints are saturated. Then observe that the solution is always the convex hull of two points A and B at a distance D and a ball. We need only to show that the center of the ball O is in the middle of the two points.

Then we show that the diameter $[A, B]$ necessarily crosses the ball. It allows to prove through a Steiner symmetrization that A, B are lined up with O. Finally, we are able to show that the set obtained when O is in the middle of $[A, B]$ has always a lower volume than in any other case.

Proof of Theorem (8) The main tool for this proof is the support function:

$$h_K(\theta) = \sup_{y \in K} y \cdot u_\theta, \tag{4.2}$$

where $u_\theta = (\cos(\theta), \sin(\theta))$.

We give some details about this function in 1.4. This is a natural choice since there exists natural formulae to compute the diameter and the area of a convex set with the support function.

However the main difficulty here is to deal with the inradius constraint. Indeed without this constraint we feel that the optimal set would tend to saturate the diameter constraint everywhere on the boundary. We can show that in those conditions, the width of K is always constant, equal to D, where the width of a convex body in the direction θ is defined by $w(\theta) = |h(\theta) + h(\theta + \pi)|$. In other words, the width of K in the direction θ is the distance between the two contact lines with normal vector oriented by u_θ. Actually, without the inradius constraint, the solution is trivially the disk of diameter D.

Before working on our problem, let us first consider a related problem that is the minimisation of the area among the convex bodies of constant width. The Blaschke-Lebesgue Theorem states that the Reuleaux triangle is the solution. There is a handful of proofs of this result, let us simply cite [11],[54]. T.Bayen in his thesis proposed a proof of that theorem using optimal control theory

together with the support function, using the radius of curvature of the convex as the control and proving that it is bang-bang: the curvature is either 0 or D with finite number of switches. E.Harrell obtained the same conclusion, but with calculus of variations arguments on the support function.

It is easy to see that on some part of the boundary, the diameter constraint is saturated, hence it has a constant curvature. But the inradius constraint forces the set to stick to its incircle. The intuition is then that the optimal shape is made of flat parts that stick to the incircle, and constant width parts to maximise the area in this zone. We would like to use the same kind of argument as T.Bayen and E.Harrell did, but since we worked on sets with only locally constant width, it was not possible to totally exploit their work. However we found a proof that is mixing the calculus of variations arguments together with some geometrical arguments to show that the constant width part has radius of curvature $D/2$.

The first important step is to find the right model to work with the inradius. We distinguish two cases:

1. There are two parallel contact lines between the incircle and the convex set, and the convex is included in the strip formed by those two lines. That is the strip case.

2. There are at least three non-parallel contact, and the convex set is included in the triangle formed by those three lines.

Those two different cases lead to two subproblems for each of which we provide a solution.

In both cases the main interest is to describe the part of the boundary where the diameter constraint is saturated. Name it the free boundary.

The first case is easier because a symmetrization argument works. Indeed, in this case it is possible to perform two steiner symmetrization in the direction of the strip and in the orthogonal direction, without changing the inradius. Adding the saturation of the diameter constraints on the free boundary yields that the solution is the symmetric slice.

Unfortunately such argument does not work in the second case because in general the Steiner symmetrization increases the inradius. In that second case we provide the following informations on the optimal shape:

- There are three contact segments and their middle is the contact point between the incircle and the shape.

- There are three connected components in the free boundary, each one between two contact segments. We name it free zones.

- Each free zone is made of at most two arcs of circle of diameter D, each arc of circle is diametrical to another one.

The last step is itself decomposed into three sub-steps: First prove that the radius of curvature is either $0, D/2$ or D, then prove that having arc of radius D is never optimal, to finally conclude that the radius of curvature is always $D/2$.

By applying the optimality conditions we finally show that there are only two sets that can fulfill all those conditions, the set $K_E(D)$ and another set, $K_C(D)$ (see Figure 4.6). The difference between those two sets is that $K_E(D)$ is made of six arcs of circles and has 3 axes of symmetry, whereas $K_C(D)$ has four arcs of circles and only one axe of symmetry.

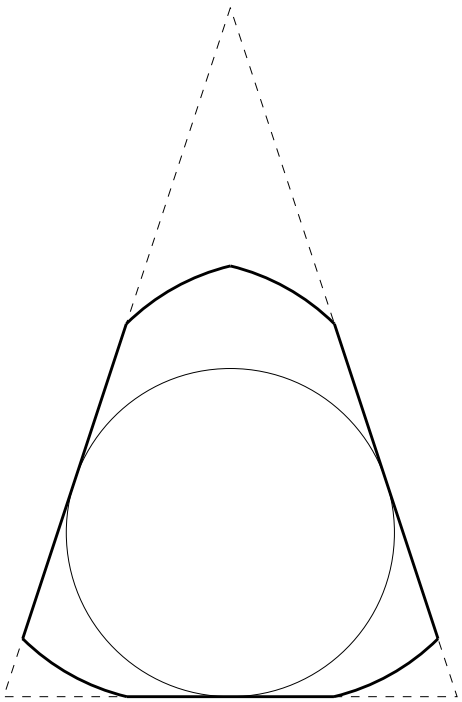

Figure 4.6: The set $K_C(D)$

4.3 Numerical insights

General setting While working on the theoretical solution we also made a numerical investigation following a technique developed in [9]. The main idea is to optimise the Fourier coefficients of the support function h and use the Plancherel theorem to compute the area of K using those coefficients, together with a discretization of $[0, 2\pi]$ in order to write the local constraints on h. It is a very practical method to deal with convexity or diameter constraint because those constraints are naturally expressed as local constraints on h, plus the fact that the functional to optimise is quadratic, with linear constraints.

Since h is a H^1, periodic function, it admits a decomposition

$$h(\theta) = a_0 + \sum_{n=1}^{+\infty} a_n(h)\cos(n\theta) + b_n(h)\sin(n\theta) \tag{4.3}$$

where $(a_n)_{n\in\mathbb{N}}$ and $(b_n)_{n\in\mathbb{N}^\star}$ denote the Fourier coefficients defined by

$$a_0 = \frac{1}{2\pi}\int_0^{2\pi} h(\theta)d\theta,$$

and for $n \geqslant 1$,

$$a_n = \frac{1}{\pi}\int_0^{2\pi} h(\theta)\cos(n\theta)d\theta$$
$$b_n = \frac{1}{\pi}\int_0^{2\pi} h(\theta)\sin(n\theta)d\theta$$

We wish to limit to the N first coefficient, hence work on the set

$$\mathcal{H}_N = \{h \mid \exists (a_n)_{0\leqslant n\leqslant N}, (b_n)_{1\leqslant n\leqslant N}, \forall\theta\in[0,2\pi], h(\theta) = a_0 + \sum_{n=1}^{N} a_n\cos(n\theta) + b_n\sin(n\theta)\} \quad (4.4)$$

That approach is justified by the following approximation theorem:

Lemma 6 ([89]). *Let $K \in \mathcal{K}_2$ and $\varepsilon > 0$. Then there exists N_ε and K_ε with support function $h \in \mathcal{H}_{N_\varepsilon}$ such that $d_H(K, K_\varepsilon) < \varepsilon$.*

As in the theoretical analysis of the optimisation problem, the main difficulty is to deal with the inradius constraint. To do this, we consider all possible cases triangle inclusion, considering that the strip case is a limit case of the triangle inclusion. Hence we consider the problem:

$$\sup_{T\in\mathcal{T}} F(T), \quad (4.5)$$

where F(T) is the solution of the area maximisation problem under the additional constraint that K is included in $T \in \mathcal{T}$. Recall that we can define T by fixing $\eta_1 = 0, \eta_2 \in]0,\pi[, \eta_3 \in]\pi, 2\pi[$. The limit case $\eta_2 \to \pi$ and $\eta_3 \to \pi$ represents the strip case. Hence we have the identification

$$\mathcal{T} \simeq]0,\pi[\times]\pi,2\pi[. \quad (4.6)$$

And so we propose the following strategy:

- Use a discretization of $]0,\pi[\times]\pi,2\pi[$.
- For each η_2, η_3 in the discretized square solve the area maximisation problem in the triangle $T(0,\eta_2,\eta_3)$.
- Find η_2, η_3 for which $F(T)$ has the biggest value.

If, as expected for some values of D, it turns out that the solution is the symmetric slice, and the discretization step is small enough, we expect η_2 and η_3 to be as close as possible to π

Solving one subproblem From now on $T = T(0,\eta_2,\eta_3)$ is a fixed triangle. We will use the notation $a = (a_0, ..., a_N), b = (b_1, ..., b_N)$ and $X = (a, b) \in \mathbb{R}^{2N+1}$

Now if a positive integer N is chosen to fix the workspace $\mathcal{H}_N$ as well as a positive integer M to define a discretization $\{m\tau, m = 0..M-1\}$ of $[0, 2\pi]$ where $\tau = 2\pi/M$, it is possible to express the problem as follows.

Let $A \in \mathcal{M}_{M,2N+1}(\mathbb{R})$ the matrix containing all the values $\cos(nm\tau)$ and $\sin(nm\tau)$ with $\tau = 2\pi/M$, such that $AX = (h(m\tau))_{m=0,..M-1}$:

$$(A_{m,n})_{m=1..M,n=1..2N+1} \begin{cases} \cos((m-1)(n-1)\tau) & \text{if } 1\leqslant n\leqslant N+1 \\ \sin((m-1)(n-N-1)\tau) & \text{if } N+2\leqslant n\leqslant 2N+1 \end{cases} \quad (4.7)$$

Now let us explicit the objective function and the constraints in terms of $X = (a, b)$

- The condition $h + h'' \geqslant 0$ which ensures that h is the support function of a convex set.

  If we denote C the matrix containing the values $(1-n^2)\cos(nm\tau)$ and $(1-n^2)\sin(nm\tau)$, then the constraint rewrites:

$$CX \geqslant 0 \tag{4.8}$$

- The area of K. Recalling that if h is the support function of K, then

$$|K| = \frac{1}{2}\int_{[0,2\pi]} h^2 - h'^2 \, d\theta,$$

  we get

$$J(X) = \pi a_0^2 + \frac{\pi}{2}\sum_{n=1}^{N}(1-n^2)(a_n^2 + b_n^2) \tag{4.9}$$

- The inradius constraint $1 \leqslant h \leqslant h_T$, which writes

$$1 \leqslant AX \leqslant H_T \tag{4.10}$$

  where H_T is the vector with values of h_T

We see that the objective function is quadratic, and the constraints are linear. This problem is solved using fmincon in matlab.

Once we solved the problem for every possible triangle, we just select the triangle for which the maximal area is the greatest.

Remark 20. We could object that this method is not totally valid since the strip case is not explored. Actually, if it happens that the resulted triangle has η_2 and η_3 as close as possible to π, we will consider that the solution is in the strip case.

Results Now let us take a look at the numerical results. The following figures show the numerical solution for different values of the parameters D, N, M and n. Recall that D is the diameter, N is the number of Fourier coefficients we consider for the support function. M is the discretization of $[0, 2\pi]$ for the computation of the support function. And n stands for the discretization step of the different angles defining the triangles we investigate. Note that the higher the values of N and M, the more accurate the calculation of the solution. However one of the weakness of this method is that the convex bodies with flat parts are poorly described with a finite number of Fourier coefficients, because the support function of a flat part is not smooth.

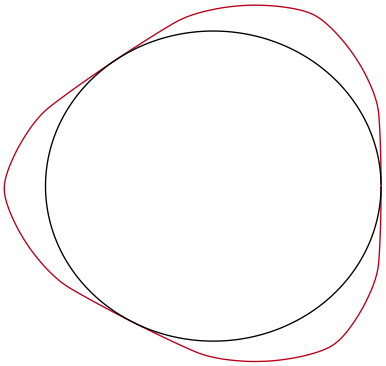

Figure 4.7: The numerical solution for $D = 2.3$, $N = M = n = 50$

For $D = 2.3$ The real solution is K_e, the deformed equilateral triangle. The numerical solution fits pretty well with the optimal shape.

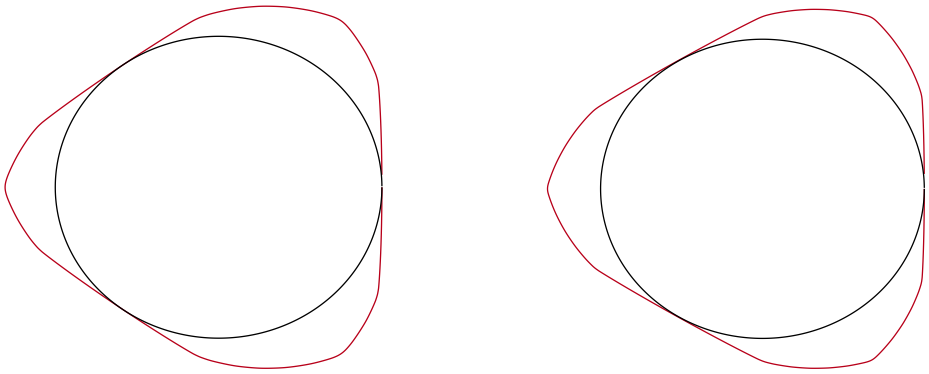

(a) $D = 2.4$, $N = M = n = 50$ (b) $D = 2.4$, $N = M = n = 70$

Figure 4.8: The numerical solution for $D = 2.4$ and different discretization steps

$D = 2.4$ is very close to the threshold that is approximately 2.388. Hence the algorithm has difficulties to change its optimum. Note that moreover, the strip case is not explicitly computed since we only do the computations for triangles and the strip case is seen as a triangle whose angles are almost $\pi, 0$ and 0. Here with different values of the discretization steps we obtain some approximation of the set K_E. We can notice that it is not really K_E since the arc of circle are not the same size. Even with better discretization we were not able to obtain the symmetric slice. The computation time is already quite long.

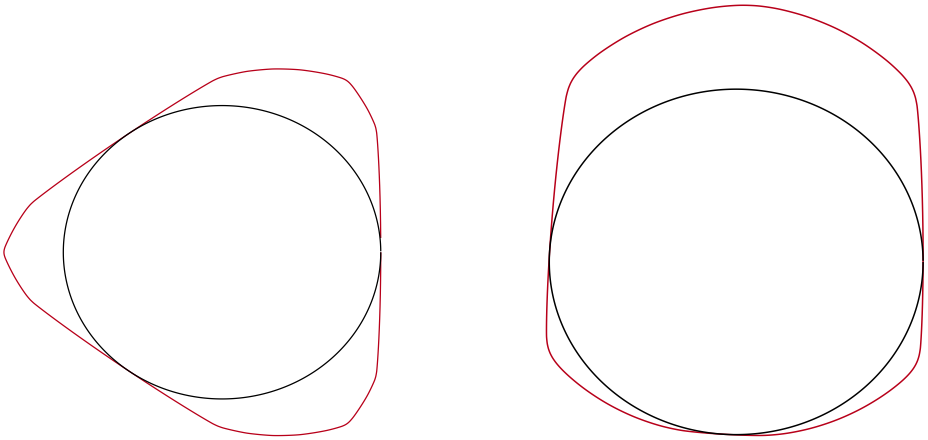

(a) $D = 2.5$, $N = M = n = 50$ (b) $D = 2.5$, $N = 70$, $M = n = 50$

Figure 4.9: The numerical solution for $D = 2.5$ and different discretization steps

In this case, $D = 2.5$ is farther than the threshold and for a small discretization we obtain some bad approximation of K_E, but if we increase a bit the discretization step, we finally obtain some kind of Symmetric slice. We see that a triangle with angles almost $\pi, 0, 0$ is almost a strip.

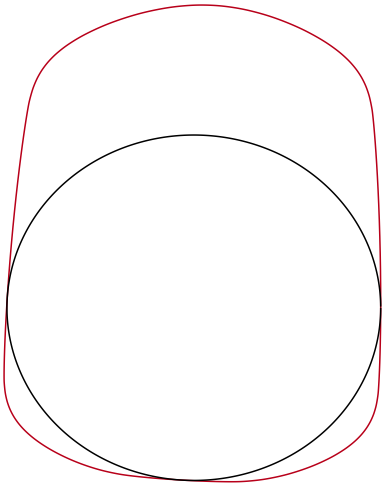

Figure 4.10: The numerical solution for $D = 2.8$, $N = M = n = 50$

For D=2.8, there is no problem and the obtained shape is close to the symmetric slice K_S.

4.4 Discussion

At first it was expected that the solution of $(\mathcal{P}_{\max})$ would be the symmetric slice. It is quite a surprise indeed that the set K_E is better for low values of D.

Let us note that at first that problem did not arise from a biological modeling, but from a natural question seeing the incomplete (A,D,r) diagram.

Even if this work is not directly related to our biology problem, it is interesting to notice that the solutions of $(\mathcal{P}_{\max})$ actually look a bit like some shapes of eggs (see Figure 4.11) even though it is not totally convincing for the set K_E. It must be taken into account that we worked in the 2D case, and the 3D case may give another figures. But it would not be surprising the 3-dimensional symmetric slice (a ball cutted by a cylindrical tube) would be a nice candidate. That shape is pretty close to the cylinder. One might also consider working with a maximisation of the density together with minimising the diameter instead of maximising the diameter. It would remain to seek a good biological reason for the minimisation of it.

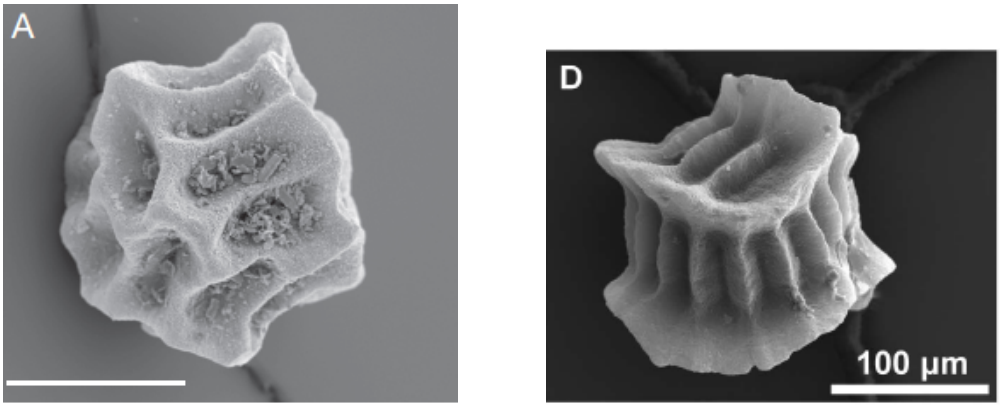

(a) The muffin shape that could look like the set K_E in 3D

(b) The cylinder shape, looking like the symmetric slice K_S in 3D

Figure 4.11

Related and open problems Here we give some problems related to the (A,D,r) diagram

- Solve the (P,D,r) diagram. In [62] $(A, \bullet, \bullet)$ and $(P, \bullet, \bullet)$ problems are discussed together. We did not pay much attention to the (P, D, r) diagram yet but the problem seems worth investigating. It should be underlined though that this time there is no reason for the free boundary to saturate the diameter constraint.

- Investigate the (A,D,r) diagram in 3 dimensions or more. This is partially solved with Theorem 9 but it remains at least to maximise the volume for given diameter and inradius. However it is common in geometry problems that passing from two dimensions to three or more raises major difficulties, cite for exemple two famous problems that were solved in 2D, and that are still desperately open in 3D: the 3D version of the honeycomb problem, or the Meissner conjecture on the Blaschke-Lebesgue theorem in 3D (see [12]).

- Do the same work as it was done in the previous chapter, but consider instead a minimisation of the diameter instead of a maximisation. Following the method we employed, we should first solve the minimisation of the diameter among convex tiling domains.

Chapter 5

A complete Blashke-Santalo Diagram

Contents

This chapter is an article submitted a journal ([30]), joint work with A.Henrot and Y.Privat.

5.1 Introduction

Let $N \in \mathbb{N}^*$. In the whole article, we will denote by $\mathcal{K}_N$ the set of all convex bodies (i.e. compact convex sets with non-empty interior) in $\mathbb{R}^N$.

In convex geometry, the search for optimal inequalities between the six standard geometrical quantities which are the surface A (or volume V), the perimeter P, the diameter D, the radius r, the circumradius R and the (minimal) width[7] w of any convex body, is a very old activity that dates back to the work of W. Blaschke ([16], [17]) and has been extensively studied by L. Santaló in [88]. For a list of such inequalities known in 2000, we refer to the classical review paper [90].

The general idea is to consider three of the aforementioned quantities (q_1, q_2, q_3) and to determine a complete system of inequalities relating them, in other words a system of inequalities describing the set

$$\{(q_1(K), q_2(K), q_3(K)),\ K \in \mathcal{K}_N\}.$$

[7] In other words, the smallest distance between any two different parallel supporting hyperplanes of a convex body.

In general, it is convenient to summarize it into a diagram, usually called *Blaschke-Santaló diagram*. It represents the set of possible values of the triple that can be reached by a convex set (suitably normalized). Among the 20 possible choices of this three geometric quantities, L. Santaló completely solved in his work the 6 cases (A, P, w), (A, P, r), (A, P, R), (A, D, w), (P, D, w), (D, r, R) and gave a partial solution to (D, R, w) and (r, R, w). These two last cases were eventually solved by M. Hernandez Cifre and S. Segura Gomis in [61]. In a series of papers with collaborators, M. Hernandez Cifre has also been able to prove complete systems of inequalities in the cases (A, D, R), (P, D, R) [60], in the cases (A, r, R), (P, r, R) [19] and finally in the case (D, r, w) [59].

In spite of all these efforts, several Blaschke-Santaló diagrams (or complete systems of inequalities) remain unknown. To the best of our knowledge, this is the case for the diagrams (A, P, D), (A, D, r), (A, r, w), (A, R, w), (P, D, r), (P, r, w) and (P, R, w). Let us mention that several interesting inequalities for (P, D, r) and (P, R, w) can be found in [62].

In this paper, we focus on the case (A, D, r) and completely solve it in the two-dimensional case ($n = 2$), and partially in the general case $n \geqslant 3$. More precisely in the case $n = 2$, we obtain universal inequalities involving the area of a plane convex set, its diameter and inradius, and we plot the corresponding Blaschke-Santaló diagram:

$$\mathcal{D} = \left\{(x, y) \in \mathbb{R}^2,\ x = 2\frac{r(K)}{D(K)},\ y = \pi\frac{r^2(K)}{A(K)},\ K \in \mathcal{K}_2\right\}.$$

To this aim, we will introduce two families of optimisation problems for the area (or the volume in higher dimension) and then solve them. More precisely, we will tackle the issue of maximising and minimising the area with prescribed diameter and inradius. It turns out that the minimisation problem has already been solved in the two dimensional case by M. Hernandez Cifre and G. Salinas [62]. The optimal set is known to be a two-cap body defined as the convex hull of a disk of radius r with two points that are symmetric with respect to the center of the ball and at a distance D. This result has been extended in three dimensions in [93] but with an additional assumption. In this paper, we solve this minimisation problem in full generality (see Theorem 10).

Regarding the maximisation problem, it is much harder and we are only able to solve it in the two-dimensional case. At first glance, it seems intuitive that the optimal shape should be a *spherical slice* defined as the intersection of a disk of diameter D with a strip of width $2r$ (symmetric with respect to the center of the disk). Surprisingly, this is only true for "large" values of D (more precisely for $D \geqslant \alpha r$ with $\alpha \simeq 2.388$, see Theorem 11), while the optimal set is some kind of nonagon made of 3 segments and 6 arcs of circle inscribed in an equilateral triangle for small values of D. For the precise definition of this set, we refer to Definition 15 hereafter. It is likely that this unexpected solution explains why this elementary *shape optimisation* problem remained unsolved up to now.

The article is organized as follows. Section 5.1.1 is devoted to introducing the optimisation problems we will deal with and stating the main results. In Section 5.1.2, the Blaschke-Santaló diagram $\mathcal{D}$ for the triple (A, D, r) is plotted. The whole sections 5.2 and 5.3 are respectively concerned with the proofs of Theorems 10 and 11. Because of the variety and complexity of optimisers, the proofs appear really difficult and involve several tools of convex analysis, optimal control and geometry.

Let us end this section by gathering some notations used throughout this article:

- $\mathcal{H}^{N-1}$ is the $N-1$ dimensional Hausdorff measure.
- if K is a convex set of $\mathbb{R}^2$, we call respectively $A(K)$ (or $|K|$), $D(K)$ and $r(K)$ (or alternatively A, D and r if there is no ambiguity) the area, diameter and inradius of K.

- in the more general n-dimensional case, we keep the same notations, except for the volume of K which will be either denoted $V(K)$ or $|K|$.
- $x \cdot y$ is the Euclidean inner product of two vectors x and y in $\mathbb{R}^n$.
- $B(O,r)$ (or $D(O,r)$ in dimension $N=2$) denotes the open ball of center O and radius r while $S(O,r)$ is the sphere (its boundary).
- The boundary of the biggest ball included into a convex set will be called *incircle* in dimension 2, *insphere* in higher dimension.

5.1.1 optimisation problems and main results

Let us first make the notations precise. Let $r>0$, $D>2r$ be given and let $\mathcal{K}^N_{r,D}$ be the set of convex bodies of $\mathbb{R}^N$ having as inradius r and as diameter D, namely

$$\mathcal{K}^N_{r,D} = \{K \in \mathcal{K}_N \mid r(K) = r \text{ and } D(K) = D\}.$$

We are interested in the following maximisation problem

$$\boxed{\sup_{K \in \mathcal{K}^2_{r,D}} |K|} \qquad (\mathcal{P}_{\max})$$

and minimisation problem

$$\boxed{\inf_{K \in \mathcal{K}^N_{r,D}} |K|.} \qquad (\mathcal{P}_{\min})$$

Note that the condition $D>2r$ guarantees that the set $\mathcal{K}^N_{r,D}$ is non-empty. If $D=2r$, problems are obvious since only the ball belongs to the set of constraints $\mathcal{K}^N_{r,D}$. Without loss of generality, by using an easy rescaling argument, one can deal with sets of constraints with unitary inradius, in other words $r=1$ and with diameter $D>2$.

Let us first observe, since we are working with convex sets, that existence of solutions for Problems $(\mathcal{P}_{\max})$ and $(\mathcal{P}_{\min})$ is straightforward.

Proposition 34. *Let (r,D) be two given parameters such that $D>2r$. Problems $(\mathcal{P}_{\max})$ and $(\mathcal{P}_{\min})$ have a solution.*

Proof. Let us deal with the minimisation problem $(\mathcal{P}_{\min})$, the case of the maximisation problem $(\mathcal{P}_{\max})$ being exactly similar. Let us consider a minimising sequence $(K_m)_{m\in\mathbb{N}}$. Since we are working with sets of diameter D, up to applying a well-chosen translation to each element of the sequence, one can assume that every convex set K_m is included in a (compact) box B of $\mathbb{R}^n$. Since the set of convex sets included in a given box is known to be compact for the Hausdorff distance [58], there exists a subsequence (still denoted $(K_m)_{m\in\mathbb{N}}$) converging to a convex set K. It remains to prove that the objective function (the area) is continuous with respect to the Hausdorff distance and that the diameter and inradius constraints are stable for the Hausdorff convergence. It is well-known that the volume and diameter functionals are not continuous for the Hausdorff distance. Nevertheless, when dealing with convex sets, the continuity property becomes true (see [58, 89]). Let us show that the inradius constraint is in some sense stable. Assume, without loss of generality, that $r(K_m)=1$ for every $m\in\mathbb{N}$. By applying well-chosen translations of K_m, one can moreover assume that $B(0,1)\subset K_m$ for every $m\in\mathbb{N}$. By stability of the inclusion for the Hausdorff convergence, one gets $B(0,1)\subset K$ and $r(K)\geqslant 1$. Assume by contradiction that $r(K)>1$. Hence, there exists $x\in K$ and $\alpha>1$ such that $B(x,\alpha)\subset K$. Let

us consider the closed ball $\hat{B} = \overline{B}(x, (1+\alpha)/2$. By stability of the Hausdorff convergence [58], one has $\hat{B} \subset K_m$ whenever m is large enough, which implies that $r(K_n) \geqslant (1+\alpha)/2$. We have then reached a contradiction. □

As underlined in the Introduction, Problem $(\mathcal{P}_{\min})$ has already been solved in the two-dimensional case in [62]. In what follows, we will generalize it to the general case $\mathbb{R}^n$, by proving that the two-cap body is the only solution in any dimension.

Theorem 10. *The (unique) optimal shape for Problem $(\mathcal{P}_{\min})$ is the convex hull of a ball of radius 1 and two points apart of distance D and whose middle is the center of the ball. In other words, any convex set in $\mathbb{R}^n$ with volume V, diameter D and inradius r satisfies:*

$$V \geqslant 2\omega_{N-1} r^N \int_{\arccos(2r/D)}^{\pi/2} \sin^N t dt + \frac{\omega_{N-1} r^{N-1}}{N D^N} \left(D^2 - 4r^2\right)^{(N+1)/2} \tag{5.1}$$

where ω_{N-1} is the volume of the unit ball in dimension $N-1$. In particular, any convex set in $\mathbb{R}^2$ with area A, diameter D and inradius r satisfies:

$$A \geqslant r\sqrt{D^2 - 4r^2} + r^2 \left(\pi - 2\arccos\left(\frac{2r}{D}\right)\right). \tag{5.2}$$

Let us turn to the maximisation Problem $(\mathcal{P}_{\max})$. Let us introduce particular convex sets of $\mathcal{K}^N_{r,D}$ that will be shown to be natural candidates to solve the maximisation problem.

Definition 14 (The symmetric spherical slice $K_S(D)$)**.** *Let $D > 2$. We call symmetric spherical slice and denote by $K_S(D)$ the convex set defined as the intersection of the disc $D(O, D/2)$ with a strip of width 2 centered at O (see Figure 5.1). We have*

$$|K_S(D)| = \sqrt{D^2 - 4} + \frac{D^2}{2} \arcsin\left(\frac{2}{D}\right).$$

Definition 15 (The smoothed regular nonagon $K_E(D)$)**.** *Let $D \in]2, 2\sqrt{3}[$. We denote by $K_E(D)$ the convex set enclosed in an equilateral triangle Δ_E of inradius 1 and made of segments and arcs of circle of diameter D in the following way (see Figure 5.2): let η_i be the normal angles to the sides of Δ_E (where one sets for example $\eta_1 = -\pi/2$). Let us introduce*

$$\tau = (3 + \sqrt{D^2 - 3})/2 \quad \text{and} \quad h = \sqrt{D^2 - \tau^2}$$

and the points A_i, B_i and M_i, $i = 1, 2, 3$ defined through their coordinates by

$$A_i = \begin{pmatrix} \cos\eta_i + \tau \sin\eta_i \\ \sin\eta_i - \tau\cos\eta_i \end{pmatrix}, \quad B_i = \begin{pmatrix} \cos\eta_i - h\sin\eta_i \\ \sin\eta_i + h\cos\eta_i \end{pmatrix}, \quad M_i = (1-\tau) \times \begin{pmatrix} \cos\eta_i \\ \sin\eta_i \end{pmatrix}, \ i = 1, 2, 3.$$

The set $K_E(D)$ is then obtained as follows:

- *the points A_1, B_1, M_3, A_2, B_2, M_1, A_3, B_3, M_2, A_1 belong to its boundary;*
- *$\widehat{B_1M_3}$ and $\widehat{M_1A_3}$ are diametrally opposed arcs of the same circle of diameter D, and similarly for the two other pairs of arcs of circle $\widehat{B_2M_1}$ and $\widehat{M_2A_1}$, $\widehat{M_2B_3}$ and $\widehat{M_3A_2}$.*
- *the boundary contains the segments $[A_iB_i]$, $i = 1, 2, 3$. Note that the contact point I_i with the incircle is precisely the middle of $[A_iB_i]$,*

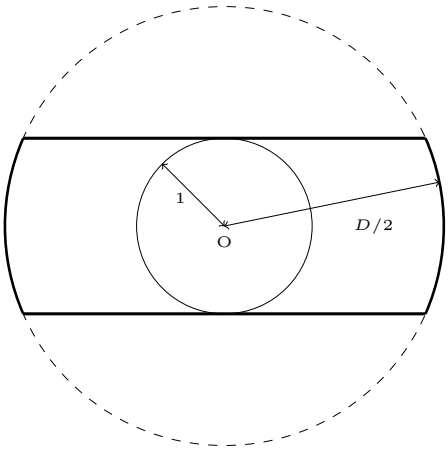

Figure 5.1: The symmetric slice $K_S(D)$ and its (non unique) incircle.

Moreover, setting

$$t_1 = \arccos\left(\frac{\sqrt{3}}{D}\right) = \arcsin\left(\frac{2\tau - 3}{D}\right), \quad t_2 = \arccos\left(\frac{\sqrt{3}(\tau - 2)}{D}\right) = \arcsin\left(\frac{\tau}{D}\right)$$

one has

$$|K_E(D)| = \frac{3}{4}D^2(t_2 - t_1) + \frac{3\sqrt{3}}{2}(\sqrt{D^2 - 3} - 1) = \frac{3}{2}D^2\left(\frac{\pi}{3} - t_1\right) + \frac{3\sqrt{3}}{2}\left(\sqrt{D^2 - 3} - 1\right). \quad (5.3)$$

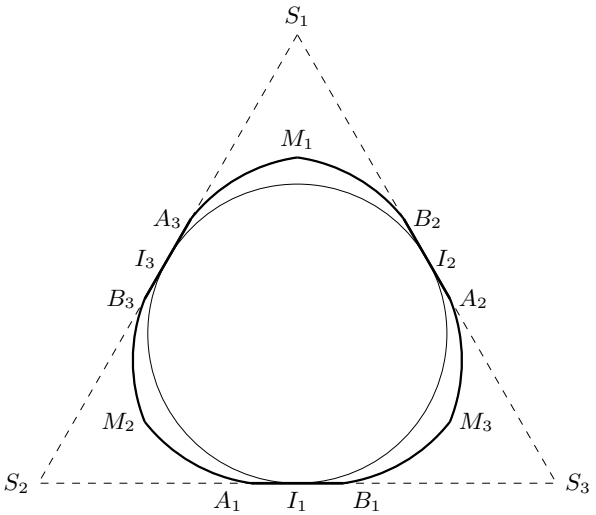

Figure 5.2: The set $K_E(D)$ and its incircle

In a nutshell, we will prove that the set is $K_E(D)$ is optimal for small values of D whereas the solution is the symmetric slice for bigger values of D.

Theorem 11. *There exists $D^\star \simeq 2.3888$ such that if $D < D^\star$, the (unique) solution of Problem $(\mathcal{P}_{\max})$ is $K_E(D)$, and for $D > D^\star$ the unique solution is $K_S(D)$. For $D = D^\star$ the two solutions coexist.*

In other words, for every plane convex set with area A, diameter D and inradius r, one has

$$A \leqslant \psi(D,r) \quad \textit{where} \quad \psi(D,r) = \begin{cases} \frac{3\sqrt{3}r}{2}\left(\sqrt{D^2-3r^2}-r\right) + \frac{3D^2}{2}\left(\frac{\pi}{3} - \arccos\left(\frac{\sqrt{3}r}{D}\right)\right) & \textit{if } D \leqslant rD^\star \\ r\sqrt{D^2-4} + \frac{D^2}{2}\arcsin\left(\frac{2r}{D}\right) & \textit{if } D \geqslant rD^\star. \end{cases} \tag{5.4}$$

5.1.2 The Blashke-Santaló Diagram for (A, D, r)

Usually, Blaschke-Santaló diagrams are normalized to fit into the unit square $[0,1]\times[0,1]$. Thus, starting from the straightforward inequalities $D \geqslant 2r$ and $A \geqslant \pi r^2$ (where A, D and r denote respectively the area, diameter and inradius of any two-dimensional convex set), drives us to choose the system of coordinates $x = 2r/D$ and $y = \pi r^2/A$. We then define the Blashke-Santaló diagram $\mathcal{D}$ as the set of points

$$\mathcal{D} = \left\{(x,y) \in \mathbb{R}^2, x = 2\frac{r(K)}{D(K)},\ y = \pi\frac{r^2(K)}{A(K)},\ K \in \mathcal{K}_2\right\}.$$

The point $(1,1)$ corresponds to the disk, while the point $(0,0)$ corresponds to an infinite strip. The solution of the minimisation problem $(\mathcal{P}_{\min})$ provided in Theorem 10 leads to the upper curve of $\mathcal{D}$. Using (5.2), we claim that the upper curve is the graph of y^+, defined by

$$y^+(x) = \frac{\pi x}{x(\pi - 2\arccos x) + 2\sqrt{1-x^2}}, \quad x \in [0,1].$$

According to Theorem 11, the lower curve is the graph of y^-, piecewisely defined by

$$y^-(x) = \begin{cases} \dfrac{\pi x}{2\sqrt{1-x^2} + 2\frac{\arcsin x}{x}} & \text{if } x \leqslant 2/D^\star \\ \dfrac{\pi x^2}{2\pi - 6\arccos(\frac{\sqrt{3}x}{2}) + \frac{3\sqrt{3}x}{2}\left(\sqrt{4-3x^2}-x\right)} & \text{if } x \geqslant 2/D^\star. \end{cases}$$

Were already known the inequalities:

- $4A \leqslant \pi D^2$ (see [63]) which corresponds to the inequality $y \geqslant x^2$ on the diagram,
- $A \leqslant 2rD$ (see [57]) which is equivalent to $y \geqslant \frac{\pi x}{4}$ on the diagram.

These two inequalities are shown with a dotted line on the diagram hereafter.

To plot the Blaschke-Santaló diagram, it remains to prove that the whole zone between the two graphs $\{(x, y^-(x)),\ x \in [0,1]\}$ and $\{(x, y^+(x)),\ x \in [0,1]\}$ is filled, meaning that each point between these two graphs corresponds to at least one plane convex domain.

Let us start with the part of the diagram on the left of $x \leqslant x^\star := 2/D^\star$. For a given diameter D and inradius r, let K^- denote the convex set with minimal area (the two-cap body) and K^+ the convex set with maximal area (the symmetric slice). We have $K^- \subset K^+$ and for any $t \in [0,1]$ the convex set K_t : constructed according to the Minkowski sum $K_t = tK^+ + (1-t)K^-$ with

$t \in [0,1]$, is known to satisfy $K^- \subset K_t \subset K^+$. Therefore, all the sets K_t share the same diameter D, the same inradius r and their area is increasing from $A(K^-)$ to $A(K^+)$. This way, it follows that the whole vertical segment joining $(2r/D, y^-(2r/d))$ to $(2r/D, y^+(2r/d))$ is included in $\mathcal{D}$ as soon as $2r/D \leqslant 2/D^\star$.

Let us consider the remaining case $x \geqslant x^\star := 2/D^\star$. Starting from the optimal domain K^+ which maximises the area with given D and r (recall that K^+ is the convex set inscribed in the equilateral triangle introduced in Definition 15), we fix one of its diameter, say $[A, B]$ and we shrink continuously K^+ to the set K_{AB} defined as the convex hull of the points A, B and the disk of radius r contained in K^+. Then, in a second time, we move the points A, B continuously to the points A', B' at distance D, oppositely located with respect to the center of the disk (in the sense that the center is the middle of A', B') by keeping the convex hull with the disk at each step. The final step is therefore the two-cap body K^- and we have constructed a continuous path between K^+ and K^- keeping the diameter and the inradius fixed: it follows that the whole segment joining $(2r/D, y^-(2r/d))$ to $(2r/D, y^+(2r/d))$ for $2r/D \geqslant 2/D^\star$ is included in $\mathcal{D}$. At the end, $\mathcal{D}$ has only one connected component.

The complete Blaschke-Santaló diagram is plotted on Figure 5.3 below.

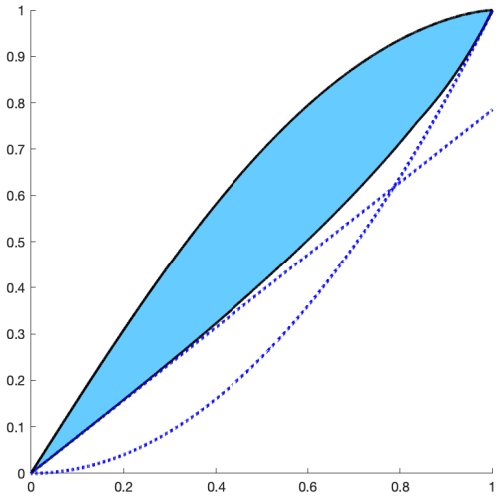

Figure 5.3: The Blaschke-Santaló diagram $\mathcal{D}$ for (A, D, r) (colored picture). The dotted lines represents the known inequalities $4A \leqslant \pi D^2$ and $A \leqslant 2rD$.

Remark 21. It is notable that the two-cap body has been showed to solve a shape optimisation problem motivated by the understanding of branchiopods eggs geometry in biology, and involving packings (see [29]).

5.2 Proof of Theorem 10

Let us first introduce several notations. For a generic convex set K, we will denote by A and B the points of K realizing the diameter, and respectively by O and r the center and radius of an insphere (the boundary of the biggest ball included in K). Introduce $\mathcal{B} = (e_1, ..., e_N)$ an

orthonormal basis such that $e_1 = \overrightarrow{AB}/AB$, so that the coordinates of A and B in $\mathcal{B}$ are

$$A = (0, 0, ..., 0) \quad \text{and} \quad B = (D, 0, ..., 0).$$

More generally, we will denote by $(x_1, \ldots, x_N)$ the coordinates of a generic vector X in $\mathcal{B}$.

First, in order to relax the conditions $D(K) = D$ and $r(K) = r$ in Problem $(\mathcal{P}_{\min})$, we show that it is equivalent to deal with the conditions $r(K) \geqslant r$ and $D(K) \geqslant D$, which are always saturated at the optimum.

Lemma 7. *Let $r > 0$ and $D > 2r$. Let us consider the minimisation problem*

$$\inf_{K \in \widehat{\mathcal{K}}^N_{r,D}} |K|. \tag{$\widehat{\mathcal{P}}_{\min}$}$$

where $\widehat{\mathcal{K}}^N_{r,D} = \{K \in \mathcal{K}_N \mid r(K) \geqslant r \text{ and } D(K) \geqslant D\}$. Then, Problem $(\widehat{\mathcal{P}}_{\min})$ has at least a solution $K^\star$ and moreover, one has $D(K^\star) = D$ and $r(K^\star) = r$.

Proof. Existence of $K^\star$ follows by an immediate adaptation of the proof of Proposition 34 (if the diameter goes to $+\infty$ it is easy to prove that the volume must blow up).

Regarding the second part of the statement, let us argue by contradiction, assuming that $r(K^\star) > r$. We use the coordinate system associated to the basis $\mathcal{B}$ introduced above, constructed from a diameter $[AB]$ of $K^\star$. Defining $\lambda = r/r(K^\star) < 1$ and applying to $K^\star$ the linear transformation whose matrix in $\mathcal{B}$ is $\mathrm{diag}(1, \lambda, ..., \lambda)$, we obtain a new convex set K' with diameter D and inradius r. Moreover, its volume is $\lambda^{N-1}|K^\star| < |K^\star|$. This is in contradiction with the minimality of $K^\star$.

Similarly, arguing still by contradiction, let us assume that $D(K^\star) > D$. Since $D > 2r = 2r(K^\star)$, there exist A' and B' in $[A, B]$ such that $A'B' = D$. Given O, the center of an insphere, we consider the set K' defined as the convex hull of A', B' and $B(O, r)$. From this construction and by convexity, K' is strictly included in K, $D(K') \geqslant D$ and $r(K') \geqslant r$. Therefore, one has $K' \in \widehat{\mathcal{K}}^N_{r,D}$ and $|K'| < |K|$, which is in contradiction with the optimality of K. The conclusion follows. □

It follows in particular from this result that the solutions of Problems $(\mathcal{P}_{\min})$ and $(\widehat{\mathcal{P}}_{\min})$ coincide.

Furthermore, if K is a general convex body in $\mathcal{K}^N_{r,D}$, by repeating the argument used to deal with the diameter constraint in the proof of Lemma 7, one sees that the convex hull of A, B and $B(O, r)$ also belongs to $\mathcal{K}^n_{r,D}$ and has a lower measure than the one of K.

Therefore, any minimiser $K^\star$ is necessarily the convex hull of two points A and B realizing its diameter, and $B(O, r)$, whose boundary is an insphere. The next result proves a symmetry property of $K^\star$.

Lemma 8. *Let us denote by $x_O \in [0, D]$ the first coordinate of O in the basis $\mathcal{B}$ introduced above. Let us introduce K' as the convex hull of A, B and $B(O', r)$ where the coordinates of O' in $\mathcal{B}$ are $(x_O, 0, .., 0)$ (in other words, O' is the orthogonal projection of O on the axis $(A; e_1)$). Then K' belongs to $\mathcal{K}^N_{r,D}$ and there holds $|K'| \leqslant |K^\star|$ with equality if, and only if $O = O'$.*

Proof. Assume that $O \neq O'$. Two cases may happen.

1. The ball $B(O, r)$ does not meet the diameter $[AB]$.

2. The ball meets the diameter $[AB]$.

In the first case let $a = OO' - r > 0$, and assume that $e_2 = \overrightarrow{OO'}/OO'$. Let us consider $S(K)$ the Steiner symmetrization of $K^\star$ with respect to the hyperplane with normal vector e_2 and containing A and B. It is a well known result (see [18]) that $S(K)$ is still convex with same Area as K. Furthermore it contains $B(O', R), A$ and B. So it contains K'. Let us finally remark that $K^\star \cap (OO')$ has length $2r + a$, and so $S(K)$ contains the point $C = (x_O, r + a/2, 0, .., 0)$ which is not in K'. This proves that $|K'| < |K^\star|$. We conclude that the first case does not occur

In the second case, consider the upper part $K^\star_+$ of $K^\star$, namely $K^\star \cap \{X \in \mathbb{R}^n \mid X \cdot e_1 \in [x_O, D]\}$. Let Γ_B be the set of points of $S(O, r)$ whose tangent hyperplane contains B, and Γ'_B be the set of points of $S(O', r)$ whose tangent hyperplane contains B. By symmetry, all the points of Γ'_B share the same first coordinate x'. Let x_1 and x_2 denote respectively the minimal and maximal first coordinate of points of Γ_B. Hence, one has $x_O + r > x_2 > x_1 > x_O$ and moreover, $x' \in (x_1, x_2)$.

Let us distinguish between three zones of $K^\star_+$:

- *On* $K^\star_+ \cap \{X \in \mathbb{R}^N \mid X \cdot e_1 \in [x_O, x_1]\}$. It is easy to see that $B(O', r) \cap \{X \in \mathbb{R}^N \mid X \cdot e_1 \in [x_O, x_1]$ is exactly the image of

$$K^\star_+ \cap \{X \in \mathbb{R}^N \mid X \cdot e_1 \in [x_O, x_1]\} = B(O', r) \cap \{X \in \mathbb{R}^N \mid X \cdot e_1 \in [x_O, x_1]\}.$$

  by the translation vector $\overrightarrow{O'O}$. These two sets have therefore the same measure.

- *On* $K^\star_+ \cap \{x \in [x_1, x']\}$. For $x \in \mathbb{R}$, let H_x be the affine hyperplane whose equation in $\mathcal{B}$ is $\{X \in \mathbb{R}^N \mid X \cdot e_1 = x\}$, and introduce $K_x = K^\star \cap H_x$. If $x \in [x_O - r, x_O + r]$, let B_x be the $n-1$ dimensional ball $B(O', r) \cap H_x$. By construction, one has $\mathcal{H}^{N-1}(B_x) < \mathcal{H}^{N-1}(K_x)$ for all $x > x_1$. As a consequence

$$|B(O, r) \cap \{X \in \mathbb{R}^N \mid X \cdot e_1 \in [x_1, x']\}| < |K \cap \{X \in \mathbb{R}^n \mid X \cdot e_1 \in [x_1, x']\}|.$$

- *On* $K^\star_+ \cap \{X \in \mathbb{R}^n \mid X \cdot e_1 \in [x', D]\}$. Define $C_{x'}$ as the cone with vertex B and basis $B_{x'} = B(O', r) \cap H_{x'}$. Since $C_{x'}$ is the convex hull of $B_{x'}$ and B, it follows that $|C_{x'}| < |K^\star \cap \{X \in \mathbb{R}^n \mid X \cdot e_1 \in [x', D]\}|$.

It follows that $|K' \cap \{x \in [x_0, D]\}| < |K \cap \{x \in [x_0, D]\}|$. Doing the same construction on the lower part of $K^\star$ yields at the end that $|K'| < |K^\star|$. The expected result follows. □

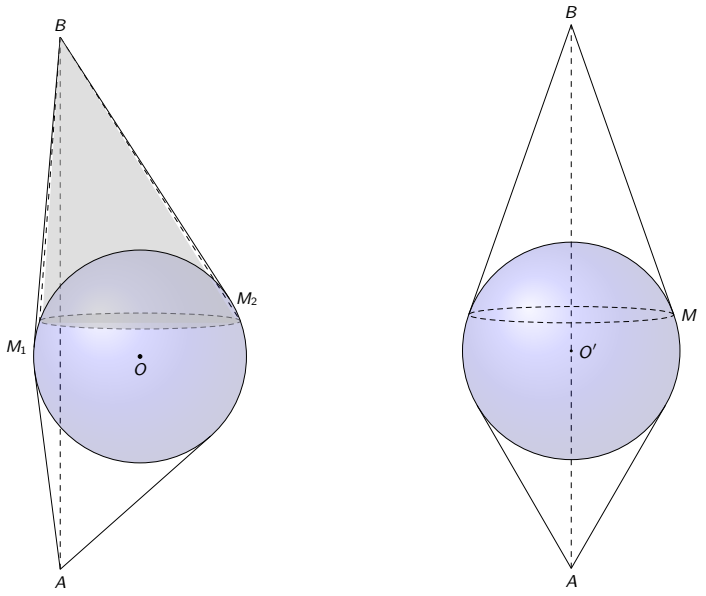

Figure 5.4: Illustration of the proof of Lemma 8. The convex set on the right has the same inradius and diameter as the one on the left but a lower volume.

To sum-up, we know that any minimiser $K^\star$ is the convex hull of A, B and $B(O,r)$, where $AB = D$ and A, B and O are colinear. It remains to show that the minimum is reached whenever O is in the middle of the segment $[AB]$. This can be done by an explicit computation, but we propose a more geometrical proof based again on Steiner symmetrization.

Let us argue by contradiction, considering $O \in [AB]\backslash\{I\}$, where I is the middle of $[AB]$ and assuming that $K^\star = \mathrm{hull}(A, B, B(O,r))$. Let $\mathcal{H}$ be the hyperplane containing I with normal vector $\overrightarrow{AB}$. Let K' be the Steiner symmetrized of $K^\star$ with respect to $\mathcal{H}$. We claim that $K' \in \mathcal{K}^N_{r,D}$. Indeed, by monotonicity of the Steiner symmetrization with respect to the inclusion and since the range of $B(O,r)$ by the Steiner symmetrization is $B(I,r)$, one has necessarily $r(K') \geqslant r(K^\star)$. In the same way, observe that the strip $\mathcal{S} := \{x \in \mathbb{R}^N \mid x_N \in [-r/2, r/2]\}$ is invariant by the Steiner symmetrization and contains $K^\star$. By using again the aforementioned monotonicity property, one has also $K' \subset \mathcal{S}$, and therefore, $r(K') \leqslant r = r(\mathcal{S})$. Therefore, one has $r(K') = r$.

It is standard that Steiner symmetrization reduces diameter. By using the aforementioned monotonicity property, since $[AB]$ is invariant by the Steiner symmetrization and contains $K^\star$, we get $[AB] \subset K'$ and thus, $D(K') = D$. Since $|K'| = |K^\star|$ by property of the Steiner symmetrization, it follows that K' solves Problem $(\mathcal{P}_{\min})$.

In the basis $\mathcal{B}$, let $x_n^* \in (0,r)$ be such that $\mathrm{hull}(A, B, B(I,r)) \cap \{x_N \geqslant x_N^\star\} = B(I,r) \cap \{x_N \geqslant x_N^\star\}$ and $B(O,r) \cap \{x_n \geqslant x_N^\star\} \subsetneq \mathrm{hull}(A, B, B(O,r)) \cap \{x_N \geqslant x_n^\star\}$. The existence of $x_N^\star$ follows from the dissymmetry of $\mathrm{hull}(A, B, B(O,r))$ with respect to $\mathcal{H}$. Using one more time the monotonicity property of the Steiner symmetrization with respect to the inclusion, one has

$$B(I,r) \cap \{x_N \geqslant x_N^\star\} \subsetneq K' \cap \{x_N \geqslant x_N^\star\},$$

which implies that the volume of K' is strictly larger than the one of $\mathrm{hull}(A, B, B(I,r))$. We

have thus reached a contradiction and it follows that one has necessarily $O = I$, meaning that $K^\star = \text{hull}(A, B, B(I, r))$, which concludes the proof.

5.3 Proof of Theorem 11

In the whole proof, for a given set $K \in \mathcal{K}_2$, we will denote by C_K an incircle of K. It is standard that K is tangent to C_K at two points at least.

Definition 16. *Let $K \in \mathcal{K}_2$. A point $x \in K$ is said to be diametral if there exists $y \in K$ such that $\|x - y\| = D(K)$.*

Obviously, if x is diametral, then it belongs necessarily to ∂K. Denoting by y its counterpart, if the boundary of K is $\mathscr{C}^1$ at x, the outward unit normal vector at x on ∂K is $n(x) = (x - y)/\|x - y\|$.

In what follows, we will consider a solution $K^\star$ to Problem $(\mathcal{P}_{\max})$, whose existence is provided by Proposition 34.

Since the area is maximised, it seems natural to look for the largest possible set and thus to saturate the diameter constraint at each point. Nevertheless, the inradius constraint tends to stick the convex body onto the circle. M. Belloni and E. Oudet in [14] worked on the minimal gap between the first eigenvalue of the Laplacian λ_2 and the first eigenvalue of the $\infty-$Laplacian λ_∞. Since $\lambda_\infty(\Omega) = 1/r(\Omega)$ and λ_2 is decreasing for the inclusion, some of their results were obtained by constructing bigger sets while maintaining the inradius and the diameter. The following lemma is an example.

Lemma 9 ([14])**.** *Let $x \in \partial K^\star$. Then, one has the following alternative:*

1. *x is non diametral and belongs to the interior of a segment of $\partial K^\star$.*
2. *x is diametral and is not in the interior of a segment of $\partial K^\star$.*
3. *x is in the intersection of two segments of $\partial K^\star$.*

To locate the flat parts of $\partial K^\star$ and provide an estimate of their numbers, we need the notion of *contact point*.

Definition 17. *A contact point of $\partial K^\star$ is a point x at the intersection of $\partial K^\star$ and an incircle $C_{K^\star}$ of $K^\star$. Similarly, a contact line is a support line of $K^\star$ passing by a contact point. Note that it is also a support line of $C_{K^\star}$.*

Observe that the relative interior of a flat portion of $\partial K^\star$ is necessarily made of non diametral points.

Note that the incircle is *a priori* not unique. Let us consider all the possibilities:

- **case 1:** The incircle is not unique. In that case the convex $K^\star$ is necessarily included in a strip of width 2, and every incircle touches both lines of the strip.

  Indeed, let C_1 and C_2 be two incircle and O_1 and O_2 their center. We consider a basis in which the coordinates of O_1 are $(-a, 0)$ and those of O_2 are $(a, 0)$. Let N_i (resp S_i) be the north (resp. south) pole of C_i. By convexity the rectangle $N_1N_2S_2S_1$ is included in $K^\star$. Now suppose that $K^\star$ is not included in the strip formed by the lines (N_1N_2) and (S_1S_2). Then there exist a point $M(x, y) \in K^\star$ with $-a \leqslant x \leqslant a$ and $y > 1$. By construction, the pentagon $N_1MN_2S_2S_1$ is convex, included in $K^\star$, and its inradius is larger than 1 (see Figure 5.5) which contradicts the inradius constraint.

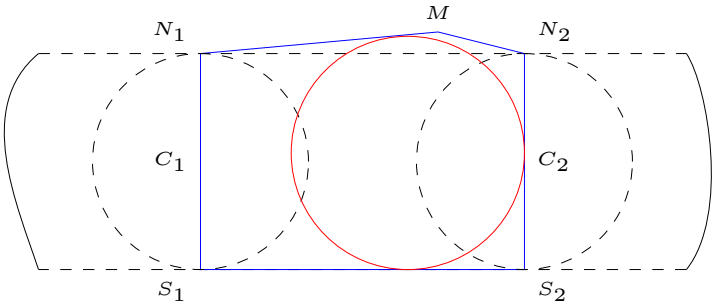

Figure 5.5: The middle circle is larger than the others, so the inradius is larger than 1.

- **case 1bis:** The incircle is unique, but still inscribed between two strips. In this case it is even included in a square, which is covered by the case 1.
- **case 2 :** The incircle is unique, and there are exactly three contact lines, forming a triangle containing both the circle and the convex.

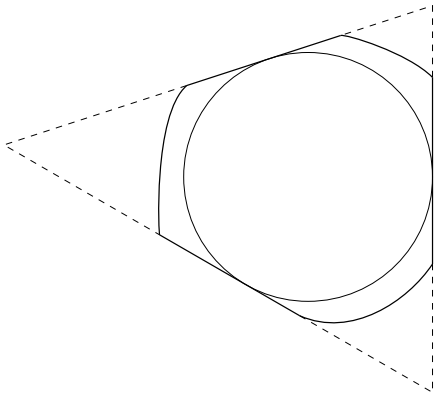

Figure 5.6: A convex set with three contact points

We sum-up these information in the following lemma.

Lemma 10. *Any segment of $\partial K^\star$ contains a contact point. Furthermore, $\partial K^\star$ contains at most three segments.*

Proof. If a segment of $\partial K^\star$ does not touch an incircle, it would be possible to inflate this part without changing the inradius nor violating the diameter constraint. The upper bound on the number of segment is a direct consequence of the previous analysis: if K has more than the minimal numbers of segments that are useful to prescribe the incircle, then some are useless and can be inflated without consequences on the constraints. □

In what follows, we will work separately on the cases 1 and 2. Section 5.3.1 deals with the first case, whereas Section 5.3.2 is devoted to the investigation of the second case.

Thanks to an easy renormalization argument, we will assume without loss of generality that the inradius of the considered convex sets is equal to 1 ($r = 1$).

5.3.1 First case: $K^\star$ is included in a strip

Let $C_{K^\star}$ be an incircle of $K^\star$. To investigate the case where $K^\star$ is included in a strip, we consider a basis $\mathcal{B}$ whose origin O is the center of $C_{K^\star}$ and such that the equations of the two contact points support lines are $x = 1$ and $x = -1$ (see Figure 5.7). Let us denote by $\mathcal{S}$, the closed strip $\{(x, y) \in \mathbb{R}^2 \mid |x| \leqslant 1\}$.

We investigate in this section a constrained version of Problem $(\mathcal{P}_{\max})$, namely

$$\sup_{\substack{K \in \mathcal{K}^2_{1,D} \\ K \subset \mathcal{S}}} |K|. \tag{$\mathcal{P}'$}$$

Proposition 35. *The symmetric slice $B(O, D/2) \cap \mathcal{S}$, where $B(O, D/2)$ denotes the open ball centered at O with radius $D/2$, is the unique solution of Problem $(\mathcal{P}')$. The optimal area is*

$$\max_{\substack{K \in \mathcal{K}^2_{1,D} \\ K \subset \mathcal{S}}} |K|. = \sqrt{D^2 - 4} + \frac{D^2}{2} \arcsin\left(\frac{2}{D}\right)$$

The set $K^\star$ is plotted on Figure 5.7 right.

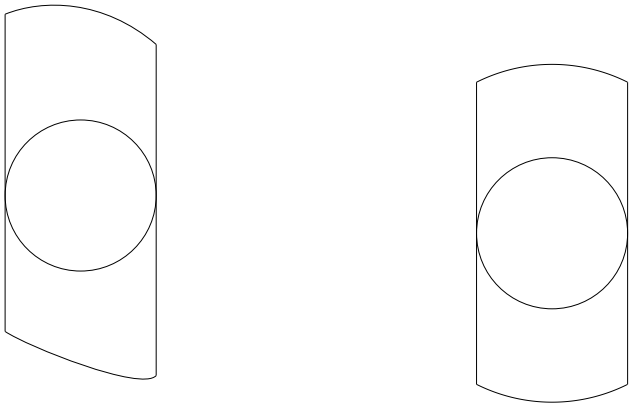

Figure 5.7: Left: a convex set whose (non unique) incircle has two parallel contact lines. Right: the optimal domain among convex sets included in a slice.

The end of this section is devoted to the proof of Prop. 35. It is straightforward that, if a convex set K belongs to $\mathcal{K}^2_{r,D}$ and is included in $\mathcal{S}$, then there exist two concave nonnegative functions f and g on $[-1, 1]$ such that

$$K = \{(x, y) \in \mathbb{R}^2, x \in [-1, 1], -g(x) \leqslant y \leqslant f(x)\}. \tag{5.5}$$

With these notations, the optimal set $K^\star$ introduced in Prop. 35 corresponds to the choices

$$f = y_D, \quad g = y_D \quad \text{where} \quad y_D(x) = \sqrt{D^2/4 - x^2}.$$

The proof consists of two steps: first, we provide necessary optimality conditions on an optimal pair (f, g) and show in particular that the aforementioned symmetric slice is a solution. Then, we investigate uniqueness properties of the optimum.

Lemma 11. *Let $K^\star$ be a solution of Problem $(\mathcal{P}')$. Then, $K^\star$ is of the form* (5.5) *and satisfies*

$$f(x) + g(x) + f(-x) + g(-x) = 4y_D(x), \quad x \in [-1, 1]. \tag{5.6}$$

Furthermore, the convex set $\tilde{K}$ of the form (5.5) *with $f = g = y_D$ solves Problem $(\mathcal{P}')$.*

Proof. We already know that $K^\star$ writes as (5.5) for some positive concave functions f and g.

First, by lemma 9, every point of the free boundary part $\partial K^\star_{\text{free}} := \partial K^\star \cap \{(x, y) \in \mathbb{R}^2 \mid x \in (-1, 1)\}$ is necessarily diametral. As a consequence, the functions f and g are strictly concave. Indeed, observe that a flat part of the boundary of a convex set contains at most two diametral points.

From the parametrization of $K^\star$, we get

$$D^2 = \max_{(x,x')\in[-1,1]^2} (x - x')^2 + (f(x) + g(x'))^2 \quad \text{and} \quad |K^\star| = \int_{-1}^{1} (f + g). \tag{5.7}$$

Let us introduce the set $\hat{K}$ of the form (5.5) where f and g are both replaced by $(f + g)/2$. Hence, one has obviously $|K^\star| = |\hat{K}|$ and moreover, by using an easy convexity argument,

$$\begin{aligned}
D(\hat{K})^2 &= \max_{(x,x')\in[-1,1]^2} (x - x')^2 + ((f(x) + g(x))/2 + (f(x') + g(x')/2))^2 \\
&= \max_{(x,x')\in[-1,1]^2} (x - x')^2 + ((f(x) + g(x'))/2 + (f(x') + g(x)/2))^2 \\
&\leqslant \frac{1}{2} \max_{(x,x')\in[-1,1]^2} (x - x')^2 + (f(x) + g(x'))^2 + \frac{1}{2} \max_{(x,x')\in[-1,1]^2} (x - x')^2 + (f(x') + g(x))^2 \\
&= \max_{(x,x')\in[-1,1]^2} (x - x')^2 + (f(x) + g(x'))^2 = D^2
\end{aligned}$$

Moreover, if $D(\hat{K}) < D(K^\star)$, then $\hat{K}$ is a convex set having the same area as $K^\star$, but a strictly lower diameter. Mimicking the argument used in the proof of Lemma 7 allows us to obtain a convex set in $\mathcal{K}^2_{1,D}$ with a larger area than $K^\star$, which is impossible. It follows that one has necessarily $D(\hat{K}) = D(K^\star)$.

Let us set $f^\star = (f + g)/2$ and let $x \in [-1, 1]$. Let $K_{f^\star}$ be a set of the form (5.5) where f and g are both replaced by $\tilde{f}$ defined by

$$\tilde{f}(x) = \frac{f^\star(x) + f^\star(-x)}{2}, \quad x \in [-1, 1].$$

Then, one has obviously $|K^\star| = |K_{f^\star}|$ and moreover,

$$\begin{aligned}
D(K_{f^\star})^2 &= \max_{(x,x)'\in[-1,1]^2} (x - x')^2 + (\tilde{f}(x) + \tilde{f}(x'))^2 \\
&= \max_{(x,x')\in[-1,1]^2} (x - x')^2 + ((f^\star(x) + f^\star(x'))/2 + (f^\star(-x) + f^\star(-x'))/2)^2 \\
&\leqslant \frac{1}{2} \max_{(x,x')\in[-1,1]^2} (x - x')^2 + (f^\star(x) + f^\star(x'))^2 + \frac{1}{2} \max_{(x,x')\in[-1,1]^2} (-x + x')^2 + (f^\star(-x) + f^\star(-x'))^2 \\
&= \max_{(x,x')\in[-1,1]^2} (x - x')^2 + (f^\star(x) + g^\star(x'))^2 = D^2
\end{aligned}$$

If $D(K_{f^\star}) < D$, then $K_{f^\star}$ is a convex set having the same area as $K^\star$, but a strictly lower diameter. Mimicking the argument used in the proof of Lemma 7 yields a contradiction and we therefore infer that one has necessarily $D(K_{f^\star}) = D$. Therefore, we have constructed a solution with two axis of symmetry.

As we have seen at the beginning of the proof, any point of coordinates $(x, \tilde{f}(x))$ is diametral. Let $x' \in [-1, 1]$ be such that $\|(x, \tilde{f}(x)) - (x', -\tilde{f}(x'))\| = D$. We claim that one has necessarily $x' = -x$. Indeed, assume by contradiction that $x' \neq -x$. By strict concavity of $\tilde{f}$, one has

$$\begin{aligned} D^2 &= (x-x')^2 + (\tilde{f}(x) + \tilde{f}(x'))^2 = (x-x')^2 + (\tilde{f}(x) + \tilde{f}(-x'))^2 \\ &< ((x-x')/2 + (x-x')/2)^2 + (\tilde{f}((x-x')/2) + \tilde{f}((x-x')/2))^2 \\ &= ((x-x')/2 - (x'-x)/2)^2 + (\tilde{f}((x-x')/2) + \tilde{f}((x'-x)/2))^2 \\ &\leqslant \max_{(x,x')\in[-1,1]^2} (x-x')^2 + (\tilde{f}(x) + \tilde{f}(x'))^2 = D^2, \end{aligned}$$

by using that $\tilde{f}$ is even. We have thus obtained a contradiction, which proves that necessarily, $x' = -x$.

It follows that $K_{f^\star}$ solves Problem $(\mathcal{P}')$. Furthermore, using that $\tilde{f}$ is even and that each point $(x, \tilde{f}(x))$ is diametral, associated to $(-x, -\tilde{f}(x))$, we finally infer that $x^2 + \tilde{f}(x)^2 = D^2/4$ for all $x \in [-1, 1]$. Noting that

$$\tilde{f}(x) = \frac{1}{4}(f(x) + g(x) + f(-x) + g(-x)),$$

every solution $K^\star$ is of the form (5.5) satisfies (5.6).

Proposition 35 follows. □

It remains to investigate the uniqueness of the optimal set, which is the purpose of the next result.

Lemma 12. *Let $K^\star$ be a solution of Problem $(\mathcal{P}')$. Then, $K^\star$ is of the form* (5.5)*, and for every parametrization (f, g), there exists $\varepsilon > 0$ such that:*

$$f(x) = y_D(x) + \varepsilon, \qquad g(x) = y_D(x) - \varepsilon, \quad x \in [-1, 1].$$

Proof. Let (f, g) be a pair of concave positive functions solving Problem $(\mathcal{P}')$. In particular, (f, g) satisfies (5.6). It follows from the proof of Lemma 11 that there exists a continuous odd function φ_o on $[-1, 1]$ such that

$$\frac{f(x) + g(x)}{2} = y_D(x) + \varphi_o(x).$$

Let K be the convex set defined by (5.5) where f and g are both replaced by $(f + g)/2$. Recall that, according to the proof of Lemma 11, K is also a solution of Problem $(\mathcal{P}')$. Let us focus on the diameter constraint. Since K solves Problem $(\mathcal{P}')$, then one has necessarily

$$\begin{aligned} D^2 &= \max_{(x,x')\in[-1,1]^2} (x-x')^2 + \left(y_D(x) + y_D(x') + \varphi_o(x) + \varphi_o(x')\right)^2 \\ &\geqslant \max_{x\in[-1,1]} (2x)^2 + \left(y_D(x) + y_D(-x)\right)^2 = D^2. \end{aligned}$$

In particular, since every point of $\partial K \cap \{(x, y) \in \mathbb{R}^2 \mid x \in (-1, 1)\}$ is diametral, the function $[-1, 1] \ni x' \mapsto (x - x')^2 + \left(y_D(x) + y_D(x') + \varphi_o(x) + \varphi_o(x')\right)^2$ is maximal at $x' = -x$. Note that

the function $y_D + \varphi_o$ is (concave and therefore) differentiable almost everywhere in $(-1,1)$, and therefore so is φ_o. Let us consider $x \in [-1,1]$ at which φ_o is differentiable. One has

$$\frac{d}{dx'}\left((x-x')^2 + (y_D(x) + y_D(x') + \varphi_o(x) + \varphi_o(x'))^2\right)\Big|_{x'=-x} = 0$$

which reads $-4x + 4y_D(x)(-y_D'(x) + \varphi_o'(x)) = 0$, and after calculation, implies that $\varphi_o'(x) = 0$. We infer that $\varphi_o'(x) = 0$ for a.e. $x \in (-1,1)$. Since φ_o is absolutely continuous (and even belongs to $W^{1,\infty}(-1,1)$), we infer that φ_o is constant on $(-1,1)$, equal to $\varphi_o(0) = 0$. It follows that $(f+g)/2 = y_D$ and we infer that

$$f(x) = y_D(x) + \varphi_e(x) \quad \text{and} \quad g(x) = y_D(x) - \varphi_e(x),$$

where φ_e denotes a continuous function on $[-1,1]$. One has for every $x \in [-1,1]$,

$$\begin{aligned} D^2 &= \max_{(x,x')\in[-1,1]^2} (x-x')^2 + (y_D(x) + y_D(x') + \varphi_e(x) - \varphi_e(x'))^2 \\ &\geqslant D^2 + 4y_D(x)\left(\varphi_e(x) - \varphi_e(-x)\right) + \left(\varphi_e(x) - \varphi_e(-x)\right)^2. \end{aligned}$$

and therefore, $4y_D(x)\left(\varphi_e(x) - \varphi_e(-x)\right) + \left(\varphi_e(x) - \varphi_e(-x)\right)^2 \leqslant 0$ so that

$$-4y_D(x) \leqslant \varphi_e(x) - \varphi_e(-x) \leqslant 0.$$

Inverting the roles played by x and $-x$ in this relation yields that $\varphi_e(x) - \varphi_e(-x) = 0$ and therfore, φ_e is even.

By using the same reasoning as above, one shows that for almost every x in $(-1,1)$, the derivative of the diameter functional vanishes at $x' = -x$, so that one has $\varphi_e'(x) = 0$ a.e. x in $(-1,1)$. Since φ_e belongs to $W^{1,\infty}(-1,1)$ and is in particular absolutely continuous, we infer that φ_e is constant on $[-1,1]$. The expected conclusion follows noticing that the converse sense is immediate: every pair (f,g) chosen as in the statement of Lemma 12 obviously drives to a solution of Problem $(\mathcal{P}')$. □

Remark 22 (Geometric interpretation of the proof)**.** The proof of Lemma 11 can be understood geometrically: indeed, from a solution, we performed two Steiner symmetrizations: one along the strip, and the other in an orthogonal direction. From the standard properties of Steiner symmetrization (that we proved for the sake of completeness), the inradius remains unchanged, as well as the area, but the diameter decreases. The difficulty lies in proving that the diameter is strictly decreasing, whence the uniqueness.

5.3.2 Second case: the convex is included in a triangle

In that case, the incircle is unique (see Figure 5.6). We assume without loss of generality that it is the unit circle. There are exactly three contact lines (see Def. 17), forming a triangle called $T(K)$.

Definition 18. *We will call "free boundary γ of $\partial K^\star$" the union of all non flat parts of $\partial K^\star$ and "free zone" every connected component of the free boundary.*

Recall that according to Lemma 10, there are at most three freezones located between the contact segments.

A crucial tool for the analysis is the so-called *support function* of the convex body K denoted h_K. Recall that h_K is defined for every $\theta \in \mathbb{T}$ by

$$h_K(\theta) = \sup_{y \in K} y \cdot u_\theta \tag{5.8}$$

where $u_\theta = (\cos(\theta), \sin(\theta))$, and $\mathbb{T}$ is the torus $\mathbb{R}/[0, 2\pi)$. The straight line D_θ whose cartesian equation is $x\cos(\theta) + y\sin(\theta) = h_K(\theta)$ is precisely the support line of the convex body K in the direction u_θ (in what follows, we will also name this direction θ with a slight abuse of language).

It follows that $F_\theta := D_\theta \cap K$. F_θ is a segment, possibly reduced to a point. Furthermore, F_θ is a segment if, and only if K is flat on this portion. In the case where F_θ is reduced to a point, we will denote this point by $M(\theta)$.

Let us finally recall some basic facts on the support function. For a complete survey about this notion, we refer for instance to [89]. When there will be no ambiguity, we will sometimes write h instead of h_K.

The support function h associated to a convex body K is periodic, belongs to $H^1(\mathbb{T})$ and is C^1 on the strictly convex parts of K. Furthermore, the diameter $D(K)$, area $|K|$ and radius of curvature R_K are respectively given in terms of h by

$$D(K) = \sup_{(0,2\pi)} \left(h(\theta) + h(\theta+\pi)\right), \quad |K| = \frac{1}{2}\int_{(0,2\pi)} (h^2 - h'^2), \quad R_K = h + h'' \tag{5.9}$$

where h'' has to be understood in the sense of distributions.

Let $\mathcal{T}$ be the set of triangles with unit inradius enclosing K. In this section, we will investigate the optimisation problem

$$\sup_{T \in \mathcal{T}} \sup_{\substack{K \in \mathcal{K}^2_{r,D} \\ K \subset T}} |K|, \tag{5.10}$$

which can be recast in terms of support functions as

$$\boxed{\sup_{h \in \mathcal{H}} \frac{1}{2}\int_{(0,2\pi)} (h^2 - h'^2)} \tag{$\mathcal{P}_h$}$$

with

$$\mathcal{H} = \{h \in H^1(0,2\pi), h + h'' \geqslant 0 \text{ in } \mathcal{D}'(\mathbb{T}),\ \exists T \in \mathcal{T} \mid 1 \leqslant h \leqslant h_T, \sup_{\theta \in \mathbb{T}} h(\theta) + h(\theta+\pi) \leqslant D\},$$

where h_T is its support function of T. Note that $h + h''$ is a positive Radon measure. It is essential to ensure that h is the support function of a convex set. The condition $1 \leqslant h \leqslant h_T$ simply means that K, whose support function is h, contains the disk $D(0,1)$ and is included in the triangle T.

Before stating the main result of this section, let us introduce another particular smoothed nonagon, denoted $K_C(D)$.

Definition 19 (The smoothed nonagon $K_C(D)$)**.** *Let $D \in]2, 2\sqrt{3}[$. We denote by $K_C(D)$ the convex set enclosed in an isosceles triangle Δ_I of inradius 1 and made of segments and arcs of circle of diameter D in the following way (see Figure 5.8): the normal angles to the sides of Δ_I are*

$$\eta_1 = -\pi/2, \quad \eta_2 = \arcsin(\tau/2 - 1) \quad \textit{and} \quad \eta_3 = \pi - \eta_1$$

where τ is the unique root of the equation

$$-\tau^3 + \left(D^2/2 + 5\right)\tau^2 - \left(2D^2 + 4\right)\tau + D^2 = 0.$$

Let us introduce the points A_i, B_i, $i = 1, 2, 3$ and M_3 defined through their coordinates by

$$A_i = \begin{pmatrix} \cos\eta_i + h_i \sin\eta_i \\ \sin\eta_i - h_i \cos\eta_i \end{pmatrix}, \quad B_i = \begin{pmatrix} \cos\eta_i - h_i \sin\eta_i \\ \sin\eta_i + h_i \cos\eta_i \end{pmatrix}, \ i = 1, 2, 3, \quad M_1 = (1-\tau) \times \begin{pmatrix} \cos(\eta_1) \\ \sin(\eta_1) \end{pmatrix}.$$

with $h_1 = \sqrt{D^2 - \tau^2}$ and $h_2 = h_3 = \frac{h_1}{4}(\tau - 2)$. The set $K_C(D)$ is then obtained as follows:

- *the points A_1, B_1, A_2, B_2, M_1, A_3, B_3 belong to its boundary;*
- *$\widehat{B_2M_1}$ (resp. $\widehat{M_1A_3}$) and $\widehat{A_1B_3}$ (resp. $\widehat{B_1A_2}$) are diametrally opposed arcs of the same circle of diameter D.*
- *the boundary contains the segments $[A_iB_i]$, $i = 1, 2, 3$. Note that the contact point I_i with the incircle is precisely the middle of $[A_iB_i]$,*

Moreover, setting

$$t_1 = \arcsin\left(\frac{2(\sin\eta_1 + h_1\cos\eta_1) - \tau + 2}{D}\right) \quad \textit{and} \quad t_2 = \arcsin\left(\frac{\tau}{D}\right),$$

we have the formula

$$|K_C(D)| = \frac{\tau}{\tau - 2}\sqrt{D^2 - \tau^2} + \frac{D^2}{2}(t_2 - t_1). \tag{5.11}$$

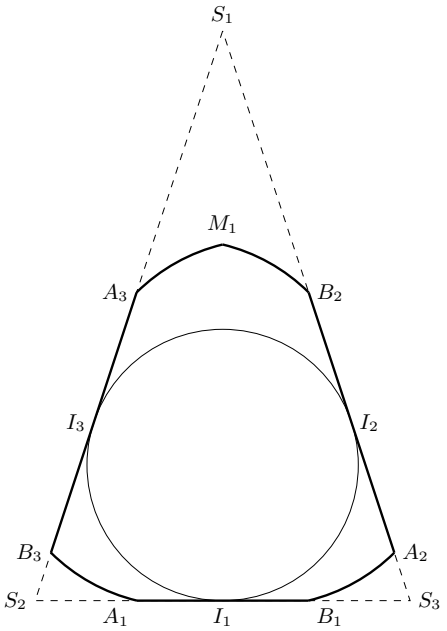

Figure 5.8: The set $K_C(D)$ and its incircle.

Proposition 36. *Let $D > 2$ be given and assume that Problem* (5.10) *has a solution $K^\star$. Then, $K^\star$ is either the set $K_C(D)$ or $K_E(D)$.*

The end of this section is devoted to proving Proposition 36. Hence, let us assume that Problem (5.10) has a solution denoted K (instead of $K^\star$) for the sake of simplicity. Let T be the triangle of inradius 1 containing K. Let D_{η_i} be the three tangent lines to the unit circle defining T, where η_i is the angle between the abscissa axis and the normal vector to each side of T. We assume that $\eta_1 < \eta_2 < \eta_3$ and we introduce the contact points I_i between the lineD_{η_i} and the unit circle. We also define φ_1, φ_2, φ_3 as the demi angles at the center (see Figure 5.9). The problem being rotationally invariant, we will impose without loss of generality that $\eta_1 = -\pi/2$, and $\varphi_1 \leqslant \varphi_2 \leqslant \varphi_3$. Identifying the index i with the index $i+3$, one has

$$\varphi_i = \frac{\eta_{i+2} - \eta_{i+1}}{2}, \quad i = 1, 2, 3.$$

The set $K \cap D_{\eta_i}$ is a segment (possibly reduced to the point I_i) denoted $[A_i, B_i]$. The free boundary γ being strictly convex according to Lemma 10, we parametrize it with the help of a function $\theta \mapsto M(\theta)$ defined on $I_\gamma = (0, 2\pi)\backslash\{\eta_i\}_{i=1,2,3}$, where θ is the angle between the normal to the support line of the point $M(\theta)$ and the abscissa axis. A point M of the free boundary may have several support lines. More precisely, two cases may arise: either a point has a unique supporting line or a point has at least two supporting lines.

Each point M of the second kind is a kind of vertex of K called "angular point" of ∂K. Moreover, considering the smallest and the largest angle made by its supporting lines, one can associate to M a closed interval $J_M \subset I_\gamma$. Notice that two consecutive vertices M and N cannot admit overlapping intervals J_M and J_N since it would mean that γ contains a segment violating the property that every point in γ saturates the diameter constraint. It also implies that angular points of γ are isolated, whereas points of ∂K of the first kind are represented by a unique angle.

This remark rewrites in the following way in terms of the support function h of K:

(i) if $M(\theta)$ has a unique supporting line, then $\theta + \pi \in I_\gamma$ and $h(\theta) + h(\theta + \pi) = D$;

(ii) in the converse case, there exists $\theta \in J_M$ such that $\theta + \pi \in I_\gamma$ and $h(\theta) + h(\theta + \pi) = D$.

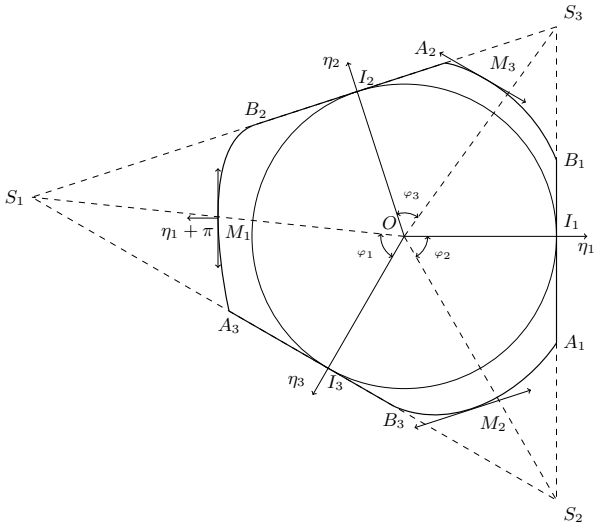

Figure 5.9: Example of a convex K and the triangle $T(K)$.

Regarding the flat parts $[A_i, B_i]_{i=1,2,3}$, one has

$$A_i = M(\eta_i^-) = \lim_{\theta \to \eta_i, \theta < \eta_i} M(\theta) \quad \text{and} \quad B_i = M(\eta_i^+) = \lim_{\theta \to \eta_i, \theta > \eta_i} M(\theta)$$

For $i = 1, 2, 3$, let α_i and β_i be such that $M(\theta) = A_i$ for all $\theta \in [\eta_i - \alpha_i, \eta_i]$ and $M(\theta) = B_i$ for all $\theta \in (\eta_i, \eta_i + \beta_i]$. Since angular points are isolated, the free boundary γ near A_i and B_i is made of points of ∂K having a unique supporting line. An easy continuity argument shows that A_i and B_i saturate the diameter constraint. Let us make their diametral point(s) precise. Recall that we introduced F_θ as $D_\theta \cap K$ and let us characterize $F_{\eta_i+\pi}$. Since $\eta_{i+1} - \eta_i < \pi$, $\eta_i + \pi$ cannot belong to $\{\eta_j\}_{j=1,2,3}$, then $F_{\eta_i+\pi}$ is a point denoted $M(\eta_i + \pi)$ or more simply M_i. Considering for instance the point M_1, we have to distinguish between three cases:

- if $\eta_1 + \pi \in (\eta_2 + \beta_2, \eta_3 - \alpha_3)$, meaning that M_1 lies in the interior of the free boundary, then M_1 is diametral with both A_1 and B_1
- if $\eta_1 + \pi \in (\eta_2, \eta_2 + \beta_2)$, then $M_1 = B_2$ and one easily infers that $M_1A_1 = D$
- if $\eta_1 + \pi \in (\eta_3 - \alpha_3, \eta_3)$, then $M_1 = A_3$ and it follows that $M_1B_1 = D$

Geometrical description of optimisers

Lemma 13. *Let $i \in [\![1, 3]\!]$. The contact points I_i between the line D_{η_i} and the incircle is the middle of the segment $[A_i, B_i]$.*

Proof. To prove this, we will use a small perturbation of an angle η_i and get optimality conditions. Let us consider I_1 and introduce the lengths $l_A = I_1A_1$ and $l_B = I_1B_1$. Let us do the following perturbation: replace η_1 by $\eta_1 + \varepsilon$ for $\varepsilon > 0$ small. We denote by $L_{\eta_1+\varepsilon}$ the corresponding tangent line of the unit disk. Now introduce J_ε the intersection point between D_{η_1} and $L_{\eta_1+\varepsilon}$. This point satisfies $J_\varepsilon = I_1 + \frac{\varepsilon}{2}(-\sin\eta_1, \cos\eta_1)$. Let T_ε be this new triangle. We build a new convex set included in the triangle T_ε by slightly modifying the previous one : replace A and B by A_ε and B_ε located on $L_{\eta_1+\varepsilon}$ in such a way that the diameter constraint is still fulfilled (see Figure 5.10). We explicit the construction of A_ε below as the intersection of $L_{\eta_1+\varepsilon}$ with a well chosen line issued from A; while B_ε is the intersection of $L_{\eta_1+\varepsilon}$ with the boundary of K We have to make the balance between

- the area we gain: this is triangle $T(AJ_\varepsilon A_\varepsilon)$
- the area we lose: this is the intersection of $K^\star$ with the half-space $\{x \cdot u_{\eta_1+\varepsilon} \geqslant 1\}$. At first order, this area is the same than the area of the triangle $T(BJ_\varepsilon B_\varepsilon)$

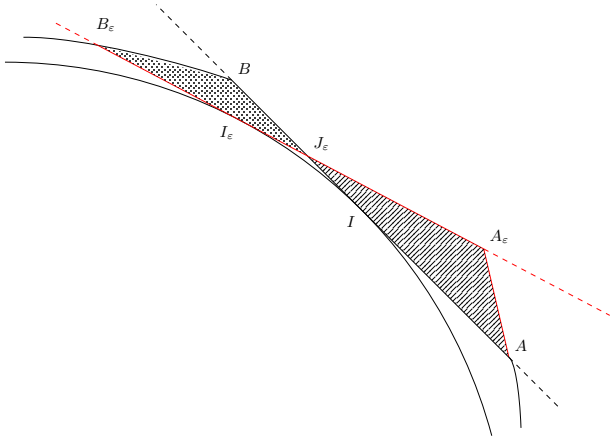

Figure 5.10: Gain of area (strips) vs loss of area (dots)

The two triangles share the same angle ε, therefore the balance of area is

$$\delta A := \frac{1}{2}\sin\varepsilon\,(J_\varepsilon A.J_\varepsilon A_\varepsilon - J_\varepsilon B.J_\varepsilon B_\varepsilon)$$

Now we can explicitly compute these lengths and get the expansions

$$J_\varepsilon A = l_A + O(\varepsilon), \qquad J_\varepsilon B = l_B + O(\varepsilon),$$

Let us introduce the angle $\theta_A^\varepsilon = \widehat{J_\varepsilon A A_\varepsilon}$. Using elementary trigonometry, we can rewrite the length $J_\varepsilon A_\varepsilon$ as

$$J_\varepsilon A_\varepsilon = \frac{AJ_\varepsilon}{\cos\varepsilon + \sin\varepsilon\cot\theta_A^\varepsilon} = l_A(1 - \varepsilon\cot\theta_A^\varepsilon + o(\varepsilon)).$$

Now let us prove that we can choose an angle θ_A^ε which does not go to zero while keeping the diameter constraint satisfied. Suppose $\eta_1 \in [0, \pi/2]$. Recall that A is represented by an interval of angles $I_A = [\eta_1 - \alpha, \eta_1]$. Let D_A be the set of points that are diametrical to A and $\Theta_A \subset I_A + \pi$ the set of angles representing elements of D_A:

$$\Theta_A = \{\theta \in I_\gamma, M(\theta) \in D_A \text{ and } h(\theta) + h(\theta + \pi) = D\} \subset [0, 2\pi).$$

We claim that there exists $\gamma > 0$ such that for all $\theta' \in [\eta_1 + \pi - \gamma, \eta_1 + \pi]$, $\theta' \notin \Theta_A$. Otherwise the diameter constraint on I_1 would be broken. Let $\zeta = \max(\Theta_A) < \pi + \eta_1$. Choosing $\theta_A^\varepsilon = (\pi + \eta_1 - \zeta)/2$ fulfills the desired condition for ε small enough and provides a gain of area as $l_A^2\varepsilon/2 + o(\varepsilon)$).

On the side of B there is no problem with the diameter constraint, thus we simply observe that $J_\varepsilon B_\varepsilon = l_B + O(\varepsilon)$ by construction. Therefore we get a loss of area as $l_B^2\varepsilon/2 + o(\varepsilon)$).

Thus we infer that the difference of areas is equal to $\delta A = \frac{\varepsilon}{2}(l_A^2 - l_B^2) + o(\varepsilon)$ which has to be non-positive, which leads to $l_A \leqslant l_B$ at the optimum. We repeat the argument with $\varepsilon < 0$ to get $l_B \leqslant l_A$, whence the equality.

□

Now we are going to prove that the free boundary is made of arc of circle of radius $D/2$ by working on the radius of curvature R. It consists of three steps. We show first that this radius can only take the values 0, $D/2$ or D on the free boundary. Then we prove that the set $\{R = D\}$

is necessarily of empty interior to finally deduce that the radius of curvature on non angular points can only be $D/2$.

Lemma 14. *On the free boundary γ of $K^\star$, the radius of curvature is almost everywhere equal to either 0, $D/2$ or D.*

Proof. According to the above discussion, we will distinguish between points of the free boundary γ having a unique support line, and angular points. Since angular points are isolated on $\partial K^\star$, it means that points of γ having a unique support line define an open subset γ_1 of γ or equivalently that their angle parametrization define an open subset I_1 of $I_\gamma = (0, 2\pi)\backslash\{\eta_i\}_{i=1,2,3}$. Any point of the complement set of γ_1 is an angular point, and therefore its radius of curvature is zero. Thus, it remains to look at points of γ_1.

Recall that, since $K^\star$ is a convex set, its radius of curvature defines a nonnegative Radon measure. For any $\theta \in I_1$ one has $h(\theta) + h(\theta + \pi) = D$. Differentiating twice this equality and since $R = h + h''$, one gets that $R + \tau_\pi R = D$ in the sense of measures in I_1, where τ_π is the translation operator given by $\tau_\pi(f) = f(\pi + \cdot)$ for every continuous function f. It follows that $0 \leqslant R(\theta) \leqslant D$ for a.e. θ in $\mathbb{T}$ and thus, R is a bounded function, allowing us to write

$$\forall \theta \in I_1, \quad R(\theta) + R(\theta + \pi) = D. \tag{5.12}$$

Let us now prove that for almost every $\theta \in I_1$, one has $R(\theta) \in \{0, D/2, D\}$. Let us assume that the set $\omega = \{\theta \in I_1 \mid 0 < R(\theta) < D\}$ has a positive measure, otherwise it means that $R = 0$ or $R = D$ a.e. and we are done. Let us first show that R is necessarily constant on ω. Let us argue by contradiction: assume there exist two disjoint subsets ω_1 and ω_2 of ω such that $|\omega_1| = |\omega_2| > 0$ and

$$\int_{\omega_1} R(\theta)\, d\theta > \int_{\omega_2} R(\theta)\, d\theta. \tag{5.13}$$

Let us consider a regularization ξ of the function v defined by

$$v(\theta) = \begin{cases} +1 & \text{if } \theta \in \omega_1, \quad -1 \quad \text{if } \theta \in \omega_1 + \pi \\ -1 & \text{if } \theta \in \omega_2, \quad 1 \quad \text{if } \theta \in \omega_2 + \pi \end{cases}$$

and $v = 0$ elsewhere. We will deal with the perturbation $h + \varepsilon v$ of the support function h for $\varepsilon > 0$ small. In what follows, we should deal with the regularization ξ, work on a subset of ω on which $0 < \eta \leqslant h(\theta)$, and finally pass to the limit $\eta \searrow 0$. To avoid technicalities, we will directly write the asymptotic of the derivative of the area under this perturbation, with a slight abuse of notation.

Since the area of the domain is

$$|K| = J(h) \quad \text{where } J(h) = \frac{1}{2}\int_0^{2\pi} (h^2(\theta) - h'^2(\theta))\, d\theta,$$

the first derivative of the area under the perturbation above reads as

$$\langle dJ(h), \xi\rangle = \int_{\omega_1 \cup \omega_2 \cup (\omega_1+\pi) \cup (\omega_2+\pi)} h\xi - h'\xi' = \int_{\omega_1 \cup \omega_2 \cup (\omega_1+\pi) \cup (\omega_2+\pi)} (h + h'')\xi.$$

By definition of ξ, one gets

$$\langle dJ(h), \xi\rangle = \int_{\omega_1} R - \int_{\omega_2} R - \int_{\omega_1+\pi} R + \int_{\omega_2+\pi} R$$

and according to (5.12), it comes

$$\langle dJ(h), \xi \rangle = \int_{\omega_1} R - \int_{\omega_2} R - \int_{\omega_1} (D - R) + \int_{\omega_2} (D - R) = 2 \left(\int_{\omega_1} R - \int_{\omega_2} R \right) > 0$$

leading to a contradiction. It follows that R is necessarily constant on ω. Let us moreover show that the constant value of R is precisely $D/2$. We proceed similarly: let us choose a perturbation ξ equal to 1 on a subset ω_1 and -1 on $\omega_1 + \pi$. The same computation as above leads to

$$\langle dJ(h), \xi \rangle = \int_{\omega_1} R - \int_{\omega_1} (D - R) = \int_{\omega_1} (2R - D),$$

and we conclude since this derivative must be zero (indeed, if this derivative would not vanish, either the admissible perturbation ξ or $-\xi$ would make the area increase). We conclude that necessarily $R \in \{0, D/2, D\}$ on I_1.

□

From this lemma we deduce that if the boundary ∂K^* contains an arc of circle of radius $D/2$, it also contains its antipodal part (in other words the set of points of $\partial K^\star$ diametrically opposed to those of the arc of circle), and if it contains an arc of circle of radius D, it also contains its center. Let us show that this second case cannot occur, following an idea in [14].

Lemma 15. *The two assertions are incompatible:*

- *the free boundary γ contains an arc of circle of radius D;*
- *its center belongs to $\partial K^\star$.*

Proof. Let us argue by contradiction. Let us denote by C the circle of radius D one arc of which belongs to γ and by $P \in \partial K^\star$ its center. Note that since C saturates the diameter constraint, according to lemma 9, it belongs to the free boundary γ or lies in the intersection of two segments. In this last case K has only two free zones and C is an edge of T. Anyway C is not in the neighborhood of any contact point. By choosing adequately an orthonormal basis, assume that the coordinates of P are $(-D/2, 0)$ and the coordinate of the center of the arc, denoted by Q, are $(D/2, 0)$. Now for $\varepsilon > 0$ consider Q_ε whose coordinates are $(D/2 + \varepsilon, 0)$ and define

$$K_\varepsilon = \text{hull}(K^\star \cup Q_\varepsilon) \cap B(Q_\varepsilon, D).$$

where $B(Q_\varepsilon, D)$ is the disc of center Q_ε and radius D.

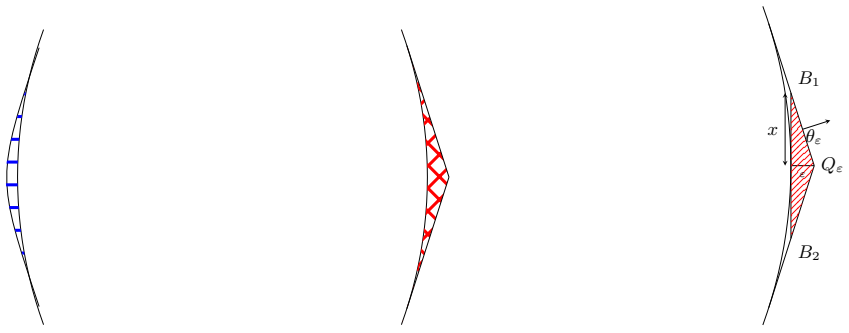

Figure 5.11: Left: gain of area (red crosshatch) vs loss of area (blue horizontal lines). Right: calculus of the gain .

Since the free boundary is modified locally, far from the contact point, the inradius remains unchanged and the diameter also by construction. This transformation drives to a gain of area on the right part, and a loss on the left part (see Figure 5.11). Let us show that the gain is $O(\varepsilon\sqrt{\varepsilon})$ and the loss is $O(\varepsilon^2)$.

- **gain:** using the notations on the right part of Figure 5.11, one determine a lower bound of the area gain by computing the area of the triangle $B_1Q_\varepsilon B_2$. Here $x = \varepsilon/\tan(\theta_\varepsilon)$ with $\cos(\theta_\varepsilon) = D/(D+\varepsilon)$, and therefore, $x = \mathrm{O}(\sqrt{\varepsilon})$, and thus, a lower bound on the area gain is $\mathrm{O}(\varepsilon\sqrt{\varepsilon})$.
- **loss:** note that if the radius of curvature is D on an open interval, thus it is equal to 0 on its antipodal interval. It means that the center of the corresponding arc of circle is an angular point, and hence it admits two different tangent lines. By convexity, the loss area is less than the one of the triangle formed by the point P, and the two intersection points of the tangent with the circle $C(Q_\varepsilon, D)$. Now the angle of the tangents does not depend on ε, and the same kind of calculus shows that the area loss is $\mathrm{O}(\varepsilon^2)$.

Hence, choosing $\varepsilon > 0$ small enough guarantees that $|K_\varepsilon| > |K^\star|$ and we have thus reached a contradiction. □

Let us complete the description of the free boundary with the help of two lemmas.

Proposition 37. *The free boundary γ of $K^\star$ is the union of arc of circles of diameter D (i.e. the radius of curvature is equal almost everywhere to $D/2$ on γ), that are mutually antipodal.*

Proof. As usual, we denote the optimal set by K in this proof. We will consider its radius of curvature R as a variable. Recall that, globally, R is a Radon measure on $\mathbb{T}$ such that

$$\langle R, \cos\rangle_{\mathcal{M}(\mathbb{T}),\mathscr{C}^0(\mathbb{T})} = 0 = \langle R, \sin\rangle_{\mathcal{M}(\mathbb{T}),\mathscr{C}^0(\mathbb{T})} = 0 \tag{5.14}$$

(we choose to fix the origin at the Steiner point of the convex set K). Its associated support function h solves the ODE

$$\begin{cases} h + h'' = R & \text{in } \mathbb{T} \\ \int_0^{2\pi} h(\theta) e^{i\theta}\, d\theta = 0 \end{cases} \tag{5.15}$$

Let F be the associated resolvent operator, in other words,

$$F : \mathcal{R}_D \ni R \mapsto F[R] = h \in H^1(\mathbb{T}),$$

where h is the unique solution to System (5.15) and

$$\mathcal{R}_D = \left\{ R \in \mathcal{M}(\mathbb{T}) \mid \langle R, \cos + i\sin\rangle_{\mathcal{M}(\mathbb{T}),\mathscr{C}^0(\mathbb{T})} = 0 \text{ and } F[R](\theta) + F[R](\theta+\pi) \leqslant D,\ \theta \in \mathbb{T} \right\}.$$

In what follows and for the sake of notational simplicity, we will denote the quantity $\langle R, f\rangle_{\mathcal{M}(\mathbb{T}),\mathscr{C}^0(\mathbb{T})}$, where f is a continuous function in $\mathbb{T}$, by $\int_0^{2\pi} R(\theta) f(\theta)\, d\theta$ with a slight abuse.

We recall that the area of K is given by

$$|K| = J(R) \quad \text{where } J(R) = \int_0^{2\pi} F[R](\theta) R(\theta)\, d\theta. \tag{5.16}$$

Let R be the radius of curvature function of the optimal set K, and $h = F(R)$. Let I denote a subset of $(0,\pi)$ of positive measure (assumed to contain an interval without loss of generality

since angular points are isolated) on which there holds $h(\theta) + h(\theta + \pi) = D$. According to Lemma 14, R is bounded on I, such that $R(\theta) + R(\theta + \pi) = D$ and $R \in \{0, D/2, D\}$ a.e. on I. Moreover, according to Lemma 15, the interiors of $I \cap \{R = 0\}$ and $I \cap \{R = D\}$ are empty.

We want to write the optimality conditions satisfied by R locally on the interval I. For that purpose we need to use admissible deformations: these are precisely deformations ξ belonging to the tangent cone at R, we recall this definition: *the tangent cone* to the set $L^\infty(I; [0, D])$ at R, (also called the *admissible cone*) denoted $\mathcal{T}_R$ is the set of functions $\xi \in L^\infty(I)$ such that, for any sequence of positive real numbers $(\eta_n)_{n\in\mathbb{N}}$ decreasing to 0, there exists a sequence of functions $\xi_n \in L^\infty(I)$ converging to ξ as $n \to +\infty$, and $R + \eta_n \xi_n \in L^\infty(I; [0, D])$ for every $n \in \mathbb{N}$.

Let us now give the first order optimality condition. This a quite classical result in control theory, but for sake of completeness, we postpone the proof of the following Lemma to Appendix 5.4.1.

Lemma 16. *There exist three real numbers (μ, α, β) (Lagrange multipliers), which are not all zero, such that the radius of curvature R of the optimal domain and its support function h satisfy*

$$\forall \xi \in \mathcal{T}_R, \quad \int_I (\mu(2h(\theta) - D) + \alpha \cos\theta + \beta \sin\theta)\, \xi(\theta)\, d\theta \leqslant 0. \tag{5.17}$$

To finish the proof of Proposition 37, let us introduce the switching function

$$\Psi_R : \theta \mapsto \mu(2h(\theta) - D) + \alpha \cos\theta + \beta \sin\theta,$$

where h is the solution to (5.15) associated to R. The first order necessary condition can be recast as

$$\forall \xi \in \mathcal{T}_R, \quad \int_I \Psi_R \xi \leqslant 0.$$

Let $y_0 \in I$ be a Lebesgue point of $I \cap \{R = 0\}$ and let $(G_n)_{n\in\mathbb{N}}$ denote a subset of $I \cap \{R = 0\}$ containing y_0. Then, $\xi = \mathbb{1}_{G_n}$ belongs to $\mathcal{T}_R$ and therefore

$$\int_{G_n} \Psi_R \leqslant 0$$

By dividing this inequality by $|G_n|$ and letting G_n shrink to y_0 as $n \to +\infty$, we infer that $\Psi_R(y_0) \leqslant 0$ according to the Lebesgue density theorem.

Generalizing this reasoning to the sets $I \cap \{R = D\}$ and $I \cap \{0 < R < D\}$, it follows that

- on $I \cap \{R = 0\}$, $\Psi_R \leqslant 0$;
- on $I \cap \{R = D\}$, $\Psi_R \geqslant 0$;
- on $I \cap \{0 < R < D\}$, $\Psi_R = 0$.

Note that Ψ_R is continuous. Let us distinguish between two cases. If $\mu = 0$, then $\Psi_R(\theta) = \alpha \cos\theta + \beta \sin\theta$ with $(\alpha, \beta) \neq (0, 0)$ and then, $\{\Psi_R = 0\}$ has zero measure. It follows that R is bang-bang, equal to 0 and D almost everywhere in I. By continuity, since I contains an interval, one has either $R = 0$ or $R = D$ on an interval, which is in contradiction with Lemma 15. In the same way, if $\psi_R < 0$ (or $\psi_R > 0$) somewhere, it will remain negative (or positive) on an interval, implying that $R = 0$ on that interval, in contradiction with Lemma 15. Therefore, we deduce that ψ_R is identically zero which implies that

$$h = \frac{D}{2} + \frac{\alpha}{\mu}\cos + \frac{\beta}{\mu}\sin \quad \text{on } I.$$

The same identities hold true on $I + \pi$, which corresponds to an antipodal arc of circle. The expected result follows. Notice finally that, since angular points are isolated (which allowed us to assume that I contained an open interval), γ is the union of arcs of circle of diameter D. □

Another necessary point is to determine when ones switches from an arc of circle to another one.

Lemma 17. *Arc of circles only end at an angular point of the free boundary. Furthermore, the only angular points in the interior of the free boundary are the points M_i, $i = 1, 2, 3$.*

Proof. We have seen that a piece of γ whose points have a unique supporting line corresponds to an arc of a given circle with diameter D. All such points are represented by a unique angle. Hence, denoting by I the corresponding interval of angles, the relation $h(\cdot) + h(\cdot + \pi) = D$ holds true on I. It follows that an arc of circle breaks in the interior of γ if, and only if there exists an angular point M represented by an interval J_M on which the relation $h(\cdot) + h(\cdot + \pi) = D$ is not satisfied (otherwise we would necessarily have $R = D$ on J_M because of Lemma 14, which is impossible because of Proposition 37). Therefore, only an angular point can break an arc of circle and we claim that such a point is necessarily one of the points M_1, M_2, M_3. Indeed, let us write $J_M = [\alpha, \beta]$ with $\alpha \leqslant \beta$ and recall that for $\varepsilon > 0$ small enough, $\theta \in [\alpha - \varepsilon, \alpha]$ (and respectively $\theta \in [\beta, \beta + \varepsilon]$) is associated to a point on an arc of circle with diameter D. Let A (resp. B) be the points of $\partial K^\star$ corresponding by $\alpha + \pi$ (resp. $\beta + \pi$). If $A = B$, there are two pairs of arc of circle with same center, same radius meeting with a nonzero angle, which is impossible. Thus, one has $A \neq B$ and there is a point in the boundary between A and B which does not saturate the diameter constraint (otherwise, using the same arguments as above, there would exist an arc of circle of radius D between A and B). This point belongs necessarily to a contact line, which proves that J_M contains one of the angles $\eta_i + \pi$, $i = 1, 2, 3$. It follows that M corresponds to a point M_i, $i = 1, 2, 3$. □

According to Proposition 37 and Lemma 17, each free zone of γ is made of one or two arc of circles, and for each one, the antipodal arc of circle is in γ.

We end our study by distinguishing between two cases, depending on whether γ is made of two or three free zones.

Case of two free zones

First of all, let us remark that the case where the boundary contains only one free zone cannot occur. Indeed, it would mean that all the points in this free zone, that we know to be diametral, would be at the distance D of one vertex of the triangle. But this is impossible, according to Lemma 15. Thus, it remains to look at the case of two free zones. In that case, one of the vertices of the triangle belongs to the boundary $\partial K^\star$. Exactly for the same reason, it is impossible that one piece of the free boundary is diametral to this vertex. Therefore, the two remaining free zones that we denote Z_1 and Z_2 are mutually diametral, which means that for each M_1 in Z_1 there exists M_2 in Z_2 with $M_1M_2 = D$.

The case of two free zones arises whenever some points A_i and B_i on Figure 5.9 coincide with a vertex S_i. According to Lemma 13, the contact point are the middle of the contact segments. Moreover, two segments have a vertex as endpoint, and it is necessary for the contact segments to be included in the edges of the triangle that this vertex is closer to the contact points than the other vertices. With the notations previously introduced (and summed-up on Figure 5.9), we have $S_iI_j = \tan\varphi_i$ for $i \neq j$. Since we assumed that $0 < \varphi_1 \leqslant \varphi_2 \leqslant \varphi_3 < \pi/2$, the vertex is necessarily S_1 and one has $I_2A_2 = I_3B_3 = \tan\varphi_1$.

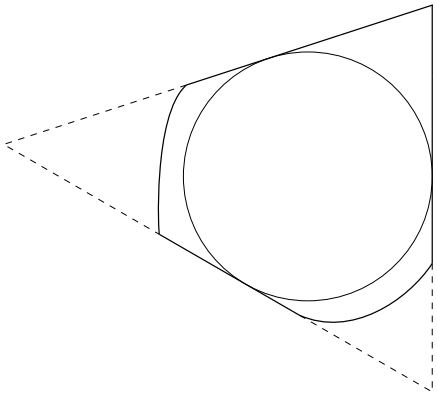

Figure 5.12: A convex set with two free zones

Assume hence without loss of generality that Z_1 contains A_1. Since A_1 is diametral, there exists $M \in Z_2$ such that $MA_1 = D$. We are going to prove that M is unique and equal to A_2. Assume by contradiction that it is not the case. Then there exists an angle $\theta \notin [\eta_2 - \alpha_2, \eta_2]$ representing M with $\theta+\pi \in [\eta_1-\alpha_1, \eta_1]$ and $h(\theta)+h(\theta+\pi) = D$. Consider $\varepsilon > 0$ small such that $\eta_2 - \alpha_2 - \varepsilon > \theta$. Since the only angular point is a point M_i, every angle $\theta' \in]\eta_2 - \alpha_2 - \varepsilon, \eta_2 - \alpha_2[$ uniquely represents a point that is diametral. We deduce that for all $\theta' \in]\eta_2 - \alpha_2 - \varepsilon, \eta_2 - \alpha_2[$, $h(\theta') + h(\theta' + \pi) = D$. From the inequalities: $\theta + \pi \geqslant \eta_1 - \alpha_1$ and $\theta' > \theta$ we obtain that $\theta' + \pi \geqslant \eta_1 - \alpha_1$. The inequality $\eta_2 - \eta_1 < \pi$ guarantees that $\theta' + \pi \in [\eta_1 - \alpha_1, \eta_1]$, which means that every point represented by the angles $\theta' \in]\eta_2 - \alpha_2 - \varepsilon, \eta_2 - \alpha_2[$ are diametral to A_1, hence the existence of an arc of radius D, which is impossible.

Recall that that the free zones are only made of arc of circles of diameter D. Let us show that each free zone is one arc of circle, that is antipodal to the other free zone. If it were not the case, one point M_i with $i = 2, 3$ would be in the interior of the free zone. Let us consider without loss of generality that M_3 belongs to the interior of the free boundary. Let N be a point of γ strictly between B_1 and M_3. Let θ be the corresponding angle of the associated supporting line, which is unique. Then, $\theta < \eta_3 + \pi$ and N is diametral with a point whose angles set of its supporting line(s) is included in (η_2, η_3). It is necessarily S_1. But this is impossible according to Lemma 15 since γ cannot contain an arc of circle of radius D whose center is a vertex of T.

Therefore, the free zones are antipodal arcs of circle of radius $D/2$. Since the points A_1, B_1, A_2, B_3 belong to the same circle and are two by two diametral, they are the vertices of a rectangle, meaning that T is an isosceles triangle (we use here the fact that the incircle and the rectangle share the same axis of symmetry). Taking the convention that $\eta_1 = -\pi/2$, we have $\eta_3 = \pi - \eta_2$ and $\varphi_1 = \pi/2 - \eta_2$ (see Fig 5.13).

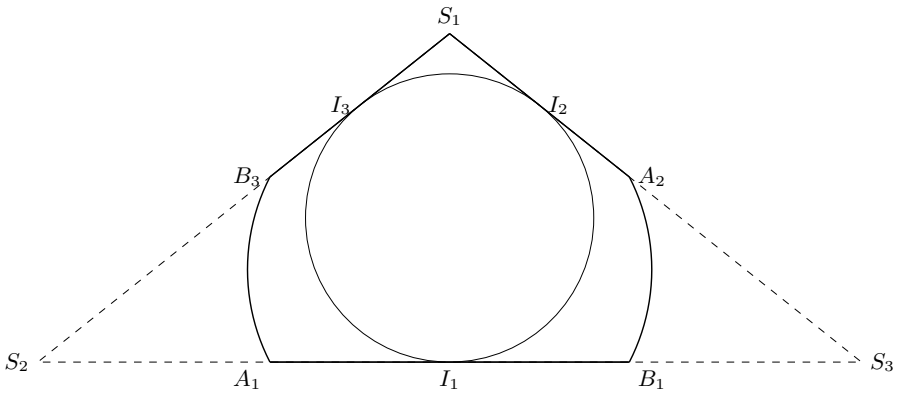

Figure 5.13: Picture of an admissible set with two free zones

Now let us compute the exact value of η_2 with respect to D. Since $\varphi_1 \leqslant \pi/3$, one has necessarily $\eta_2 \geqslant \pi/6$.

Let us consider the orthonormal basis $(O; \frac{\overrightarrow{A_1B_1}}{A_1B_1}, \frac{\overrightarrow{A_1B_3}}{A_1B_3})$ centered at O, the incircle center. Since the abscissa of A_1 is the same as the one of B_3 and since I_3 is the middle of $[S_1B_3]$ (and resp. I_2 is the middle of $[S_1A_2]$), we infer that the coordinates of A_1 and A_2 are then

$$A_1 = (-2\cos\eta_2, -1) \quad \text{and} \quad A_2 = \left(2\cos\eta_2, \frac{\cos(2\eta_2)}{\sin\eta_2}\right).$$

Solving the equation $A_1A_2 = D$ leads to the polynomial equation:

$$P(\sin\eta_2) = 0 \quad \text{with } P(X) = X^3 - \frac{D^2-1}{4}X^2 - \frac{1}{2}X + \frac{1}{4}. \tag{5.18}$$

We need to determine a solution in $[1/2, 1]$. Assume that $D > 2$. Let us observe that $P(1) = \frac{4-D^2}{4} < 0$ and $P(1/2) = \frac{3-D^2}{16} < 0$. Furthermore, one shows easily that P is either decreasing on $(1/2, 1)$ or decreasing and then increasing on $(1/2, 1)$. Thus the equation $P(\sin\eta_2) = 0$ has no solution on $[1/2, 1]$. We conclude that this is not possible to build an optimal set with two free zones.

Case of three free zones

Let us distinguish between two cases.

Subcase 1: all the points M_i, $i = 1, 2, 3$ belong to the interior of γ.

In this case, the previous study has shown that the free boundary is as follows (see Fig. 5.14)

- $\widehat{A_3M_1}$ and $\widehat{B_1M_3}$ are antipodal arcs of circle of radius $D/2$,
- $\widehat{A_2M_3}$ and $\widehat{B_3M_2}$ are antipodal arcs of circle of radius $D/2$,
- $\widehat{A_1M_2}$ and $\widehat{B_2M_1}$ are antipodal arcs of circle of radius $D/2$,
- I_i is on the middle of $[A_i, B_i]$
- M_i is on the perpendicular bisector of $[A_i, B_i]$ (or I_i, O and M_i are aligned).

We deduce the relationships

$$\overrightarrow{M_3B_1} = \overrightarrow{M_1A_3}, \quad \overrightarrow{M_1B_2} = \overrightarrow{M_2A_1}, \quad \text{and} \quad \overrightarrow{M_2B_3} = \overrightarrow{M_3A_2}. \tag{5.19}$$

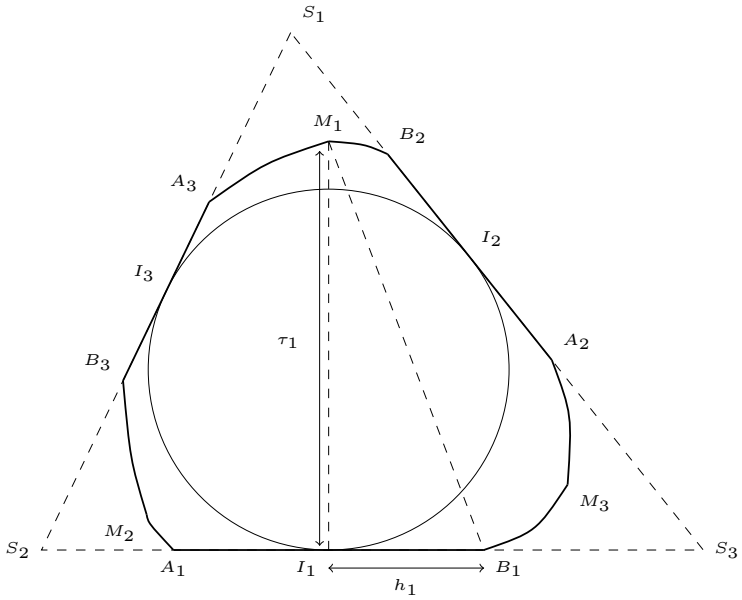

Figure 5.14: Case of three free zones and the M_i's belong to the interior of the free zones.

Let $\tau_i = M_iI_i$ and $h_i = I_iA_i$. Then necessarily $\tau_i > 2$ and we have the relationship

$$h_i = \sqrt{D^2 - \tau_i^2} \tag{5.20}$$

Let us consider the orthonormal basis $(O; \frac{\overrightarrow{I_1B_1}}{I_1B_1}, \frac{\overrightarrow{I_1O}}{I_1O})$ centered at O, the incircle center. For $i = 1, 2, 3$, the coordinates of A_i, B_i and M_i are

$$A_i = \begin{pmatrix} \cos\eta_i + h_i \sin\eta_i \\ \sin\eta_i - h_i \cos\eta_i \end{pmatrix}, \quad B_i = \begin{pmatrix} \cos\eta_i - h_i \sin\eta_i \\ \sin\eta_i + h_i \cos\eta_i \end{pmatrix}, \quad M_i = (1-\tau_i) \times \begin{pmatrix} \cos\eta_i \\ \sin\eta_i \end{pmatrix}.$$

By assimilating the index i with $i+3$, the vector relationships above rewrites

$$i = 1, 2, 3, \quad \begin{cases} 2 - \tau_i &= (2-\tau_{i+1})\cos(\eta_i - \eta_{i+1}) + h_{i+1}\sin(\eta_i - \eta_{i+1}) \\ h_i &= (2-\tau_{i+1})\sin(\eta_i - \eta_{i+1}) - h_{i+1}\cos(\eta_i - \eta_{i+1}) \end{cases} \tag{5.21}$$

from which we infer that

$$\begin{cases} (2-\tau_1)\tan(\eta_3 - \eta_2) &= h_1 \\ (2-\tau_2)\tan(\eta_1 - \eta_3) &= h_2 \\ (2-\tau_3)\tan(\eta_2 - \eta_1) &= h_3 \end{cases} \tag{5.22}$$

With the value of h_i given by (5.20), we have the quadratic equation on τ_1:

$$(2-\tau_1)^2 \tan^2(\eta_3 - \eta_2) = D^2 - \tau_1^2 \tag{5.23}$$

and similarly for the others. This yields

$$2-\tau_1 = 2\cos^2(\eta_3-\eta_2) \pm \cos(\eta_3-\eta_2)\sqrt{D^2-4\sin^2(\eta_3-\eta_2)} \tag{5.24}$$

Since $2-\tau_1$ is negative, we can choose the sign depending on the value of cos. Recall that $\eta_{i+1}-\eta_i \in (0,\pi)$ and $\eta_3-\eta_2 \leqslant \eta_1-\eta_3 \leqslant \eta_2-\eta_1$. Furthermore, $\eta_{i+1}-\eta_i \in (0,\pi/2)$ means that the triangle has an obtuse angle. This can happen only once, and for $\eta_3-\eta_2$. So at least $\eta_1-\eta_3$ and $\eta_2-\eta_1$ are in $(\pi/2,\pi)$ and their cosine is negative. Assuming now that we have $\eta_3-\eta_2 > \pi/2$ leads to

$$\begin{cases} 2-\tau_1 = 2\cos^2(\eta_3-\eta_2) + \cos(\eta_3-\eta_2)\sqrt{D^2-4\sin^2(\eta_3-\eta_2)} \\ 2-\tau_2 = 2\cos^2(\eta_1-\eta_3) + \cos(\eta_1-\eta_3)\sqrt{D^2-4\sin^2(\eta_1-\eta_3)} \\ 2-\tau_3 = 2\cos^2(\eta_2-\eta_1) + \cos(\eta_2-\eta_1)\sqrt{D^2-4\sin^2(\eta_2-\eta_1)}. \end{cases} \tag{5.25}$$

By replacing h_i by its value (5.22) in (5.19), we obtain after calculation

$$\begin{cases} (2-\tau_3)\cos(\eta_3-\eta_2) &= (2-\tau_1)\cos(\eta_1-\eta_2) \\ (2-\tau_2)\cos(\eta_2-\eta_1) &= (2-\tau_3)\cos(\eta_3-\eta_1) \\ (2-\tau_1)\cos(\eta_1-\eta_3) &= (2-\tau_2)\cos(\eta_2-\eta_3) \end{cases} \tag{5.26}$$

Finally, replacing $2-\tau_i$ by his expression in (5.26) and using that $\cos(\eta_{i+1}-\eta_i) \neq 0$, we get

$$\begin{cases} 2\cos(\eta_2-\eta_1) + \sqrt{D^2-4\sin^2(\eta_2-\eta_1)} &= 2\cos(\eta_3-\eta_2) + \sqrt{D^2-4\sin^2(\eta_3-\eta_2)} \\ 2\cos(\eta_2-\eta_1) + \sqrt{D^2-4\sin^2(\eta_2-\eta_1)} &= 2\cos(\eta_1-\eta_3) + \sqrt{D^2-4\sin^2(\eta_1-\eta_3)} \end{cases} \tag{5.27}$$

Let $f : x \mapsto 2\cos x + \sqrt{D^2-4\sin^2 x}$. One easily shows that f is decreasing on $(\pi/2,\pi)$ and hence injective (see Fig. 5.15). We thus infer that

$$\eta_3-\eta_2 = \eta_1-\eta_3 = \eta_2-\eta_1 = \frac{2\pi}{3}.$$

The triangle T is therefore equilateral and one has $\tau_1=\tau_2=\tau_3=(3+\sqrt{D^2-3})/2$. We recover the smoothed nonagon introduced in Def. 15.

Assume now that $\eta_3-\eta_2 \leqslant \pi/2$. If $\eta_3-\eta_2=\pi/2$, then $\tau_1=2$ and M_1 is on in the incircle, which is impossible for $D>2$, otherwise the arc of circle would cross the incircle.

Now we have

$$\begin{cases} 2-\tau_1 = 2\cos^2(\eta_3-\eta_2) - \cos(\eta_3-\eta_2)\sqrt{D^2-4\sin^2(\eta_3-\eta_2)} \\ 2-\tau_2 = 2\cos^2(\eta_1-\eta_3) + \cos(\eta_1-\eta_3)\sqrt{D^2-4\sin^2(\eta_1-\eta_3)} \\ 2-\tau_3 = 2\cos^2(\eta_2-\eta_1) + \cos(\eta_2-\eta_1)\sqrt{D^2-4\sin^2(\eta_2-\eta_1)} \end{cases} \tag{5.28}$$

The same computations as above yield

$$2\cos(\eta_3-\eta_2) - \sqrt{D^2-4\sin^2(\eta_3-\eta_2)} = 2\cos(\eta_1-\eta_3) + \sqrt{D^2-4\sin^2(\eta_1-\eta_3)} \tag{5.29}$$

Now, let us introduce $g : x \mapsto 2\cos x - \sqrt{D^2-4\sin^2 x}$. One easily sees that g is negative while f is positive and therefore, the equation $f(x)=g(y)$ has no solution. We conclude that this case cannot happen.

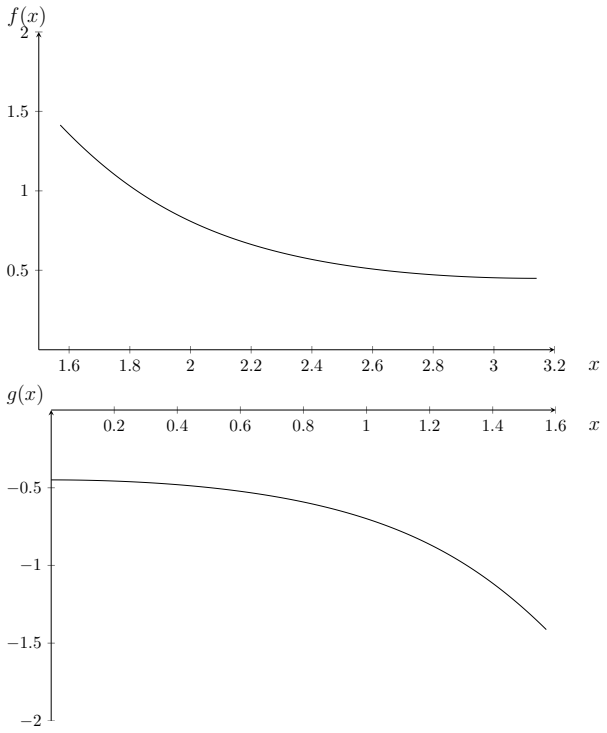

Figure 5.15: $D^2 = 6$. Left: plot of the function f. Right: plot of the function g.

Finally, the solution for this sub-case is $K_E(D)$ defined in Def. 15. Observe that since $K_E(D)$ is inscribed in the equilateral triangle, we need to have $h < \sqrt{3}$, ie $\tau < 3$ and $D < 2\sqrt{3}$, whence the requirement on D for the sake of the definition of $K_E(D)$.

Subcase 2: at least one point M_i is on the boundary of the free zone, namely it is one of the points A_j or B_j.

Assume here that a point M_i, say M_1 is not in the interior of the free zone. Then $M_1 = B_2$ or $M_1 = A_3$, say $M_1 = B_2$. The free zone Z_1 is an arc of circle of radius $D/2$ whose antipodal arc is $\widehat{B_1M_3}$. If M_3 is also on the boundary of Z_3 then Z_1 and Z_3 would be antipodal and Z_2 would not have any antipodal arc of circle. This is impossible. So M_3 lies in the interior of Z_3 and it has a second arc of circle: $\widehat{M_3A_2}$ which antipodal arc is $\widehat{M_2B_3}$. We claim that $M_2 = A_1$ otherwise $\widehat{M_2A_1}$ would not have antipodal arc.

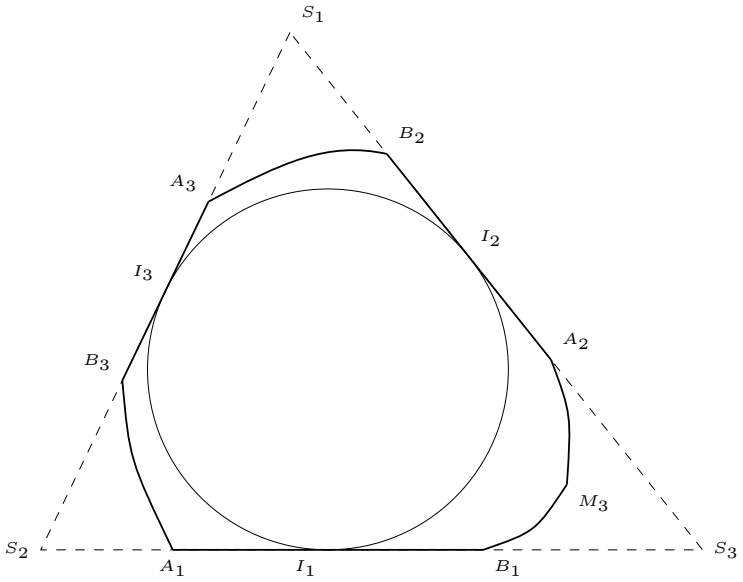

Figure 5.16: An approximate illustration of the case of three free zones and M_1 in the boundary of the free zone.

Now, in comparison with the first case, only two vector relation are valid, namely

$$\overrightarrow{B_1M_3} = \overrightarrow{A_3B_2} \quad \text{and} \quad \overrightarrow{A_2M_3} = \overrightarrow{B_3A_1}. \tag{5.30}$$

Taking the same notations as in the first case with $\tau = \tau_3$, one has

$$\begin{cases} \cos\eta_2 - h_2\sin\eta_2 - \cos\eta_3 - h_3\sin\eta_3 = (1-\tau)\cos\eta_3 - \cos\eta_1 + h_1\sin\eta_1 \\ \sin\eta_2 + h_2\cos\eta_2 - \sin\eta_3 + h_3\cos\eta_3 = (1-\tau)\sin\eta_3 - \sin\eta_1 - h_1\cos\eta_1 \end{cases} \tag{5.31}$$

and

$$\begin{cases} \cos\eta_1 + h_1\sin\eta_1 - \cos\eta_3 + h_3\sin\eta_3 = (1-\tau)\cos\eta_3 - \cos\eta_2 - h_2\sin\eta_2 \\ \sin\eta_2 - h_1\cos\eta_1 - \sin\eta_3 - h_3\cos\eta_3 = (1-\tau)\sin\eta_3 - \sin\eta_2 + h_2\cos\eta_2 \end{cases} \tag{5.32}$$

The same kind of computations as in the first case lead to the following statements:

$$\begin{cases} \eta_3 - \eta_2 = \eta_1 - \eta_3 = y \\ h_1 = h_2 \\ 2 - \tau = 2\cos y < 0 \\ \tau^2 + h_3^2 = D^2 \\ 2h_1 = -h_3\cos y. \end{cases} \tag{5.33}$$

Now set $\eta_3 = -\pi/2$. then $\eta_1 = y - \pi/2 \in [0, \pi/2]$ and $\eta_2 = \pi - \eta_1$. Observe that$A_2M_3A_1B_3$ is a rectangle which leads to the new equation $\overrightarrow{A_1M_3} \cdot \overrightarrow{A_2M_3} = 0$. It rewrites

$$(\tau-1)^2 - 2(\tau-1)\sin\eta_1 + (h_1^2+1)(2\sin^2\eta_1 - 1) = 0 \tag{5.34}$$

and using that

$$\sin\eta_1 = \tau/2 - 1 \quad \text{and} \quad h_1^2 + 1 = \frac{D^2-\tau^2}{(\tau-2)^2} + 1, \tag{5.35}$$

Equation (5.34) becomes

$$-\tau^3 + \left(D^2/2 + 5\right)\tau^2 - \left(2D^2 + 4\right)\tau + D^2 = 0. \tag{5.36}$$

Since τ has to be a root of the polynomial in $[2,3]$, a calculus argument shows that for $D \in [2, 2\sqrt{3}]$, the polynomial has a unique root in $[2,3]$, with $\tau(2) = 2$, $\tau(2\sqrt{3}) = 3$ and τ is an increasing function.

Finally this leads to the construction of the set $K_C(D)$ shown in Fig. 5.8.

Furthermore, if we set $t_1 = \arcsin\left(\frac{2(\sin\eta_1 + h_1\cos\eta_1) - \tau + 2}{D}\right)$ and $t_2 = \arcsin(\tau/D)$ then we have the formula

$$|K_C(D)| = \frac{\tau}{\tau - 2}\sqrt{D^2 - \tau^2} + \frac{D^2}{2}(t_2 - t_1) \tag{5.37}$$

Let us remark that, using (5.35), we have $\cos^2 t_2 = (D^2 - \tau^2)/D^2$ and $(\tau - 2)^2 = 4\sin^2\eta_1$, thus

$$h_1^2 = \frac{D^2 - \tau^2}{(\tau - 2)^2} = \frac{D^2\cos^2 t_2}{4\sin^2\eta_1} \Longrightarrow h_1 = \frac{D\cos t_2}{2\sin\eta_1}$$

and replacing in the definition of t_1, it provides the alternative formula

$$t_1 = \arcsin\left(\frac{\cos t_2}{\tan\eta_1}\right). \tag{5.38}$$

5.3.3 Comparison

Now we have to determine what is the optimal shape for a given D. Previous analysis show that for $D \geqslant 2\sqrt{3}$ it is not possible to construct the sets K_E and K_S. Hence the stadium K_S is optimal for such D. Let us have a look to the graphics of the area of the three domain for $D \in [2, 2\sqrt{3}]$. Now let us investigate the case $D \in [2, 2\sqrt{3}]$. Graphics 5.17 suggest that the set K_E is optimal for small values of D and K_S is optimal for high values of D. In the following we prove two facts:

1. The domain $K_C(D)$ is never optimal,

2. the existence of $D^\star$ such that for $D \leqslant D^\star$, $|K_E(D)| \geqslant |K_S(D)|$ and for $D \geqslant D^\star$, $|K_S(D)| \geqslant |K_E(D)|$.

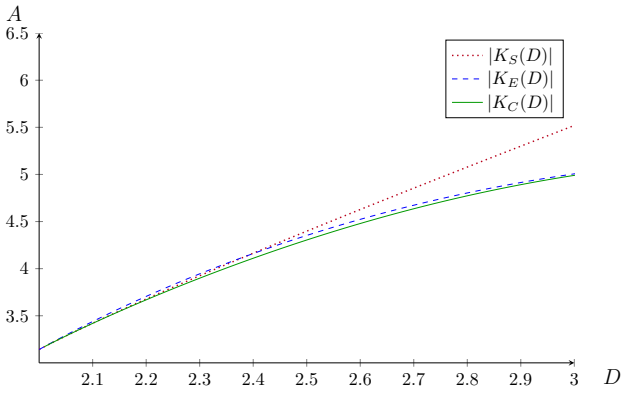

(a) $D \in (2, 2.5)$

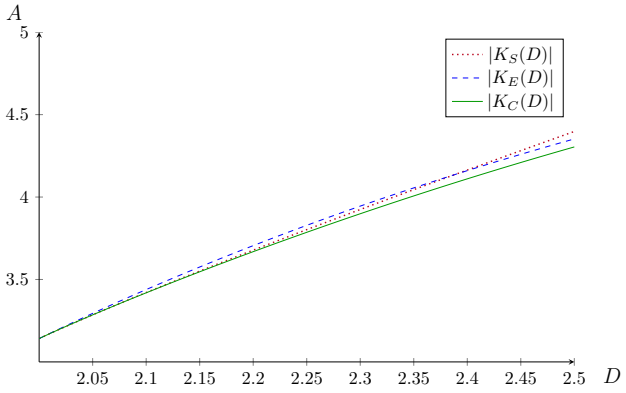

(b) $D \in (2, 2.1)$

Figure 5.17: Comparison of the three areas

Proof that $K_C(D)$ is never optimal

We are going to prove that $K_C(D) < K_S(D)$ for $D \in (2, 2\sqrt{3}]$ by comparing their derivatives (we know that $K_C(2) = K_S(2) = \pi$). Let us write Equation (5.36) in the following way

$$D^2 = \tau \frac{\tau^2 - 5\tau + 4}{\frac{\tau^2}{2} - 2\tau + 1} := \tau g(\tau) \tag{5.39}$$

where the function $g : x \mapsto (x^2 - 5x + 4)/(x^2/2 - 2x + 1)$ is increasing. Thus we make the change of variable $D \to \tau$ and rewrite the areas $K_C(D)$ and $K_S(D)$ in terms of $\tau \in [2, 3]$. More precisely, we write $\tau = 2 + h$ with $h \in [0, 1]$ and we write all quantities in term of h. Let us observe that

$$g(2 + h) = 2 + \frac{h}{1 - h^2/2}. \tag{5.40}$$

We start with $K_C(D)$ given by (5.37). By (5.40)

$$D^2 - \tau^2 = (2 + h)g(2 + h) - (2 + h)^2 = h^2 \frac{h + h^2/2}{1 - h^2/2}$$

and then the first term of $K_C(D)$ is

$$\frac{\tau}{\tau-2}\sqrt{D^2-\tau^2} = (2+h)\sqrt{\frac{h+h^2/2}{1-h^2/2}}. \tag{5.41}$$

A simple computation gives its derivative with respect to h:

$$\frac{d}{dh}\left(\frac{\tau}{\tau-2}\sqrt{D^2-\tau^2}\right) = \sqrt{\frac{2+h}{2h(1-h^2/2)}}\frac{1+2h+h^2/2-h^3/2}{1-h^2/2}. \tag{5.42}$$

Now we look at the other term in $K_C(D)$:

$$t_2 = \arcsin\left(\sqrt{\frac{\tau}{g(\tau)}}\right) = \arcsin\left(\sqrt{\frac{2+h-h^2-h^3/2}{2+h-h^2}}\right). \tag{5.43}$$

Now, let us express t_1 using (5.38):

$$\cos t_2 = \sqrt{1-\frac{\tau^2}{D^2}} = \sqrt{1-\frac{2+h}{g(2+h)}} = h\sqrt{\frac{h/2}{2+h-h^2}}$$

while , from $\sin\eta_1 = h/2$, we get

$$\tan\eta_1 = \sqrt{\frac{1}{1-\sin^2\eta_1}-1} = \frac{h}{4-h^2}.$$

From this, we infer:

$$t_1 = \arcsin\left(\sqrt{\frac{h(2+h)}{2(1+h)}}\right). \tag{5.44}$$

Now using the formula $\arcsin b - \arcsin a = \arcsin\left(b\sqrt{1-a^2}-a\sqrt{1-b^2}\right)$ (all numbers a and b are between 0 and 1), we finally get thanks to (5.43) and (5.44):

$$t_2 - t_1 = \arcsin\left((1-h)\sqrt{\frac{2+h}{2-h}}\right). \tag{5.45}$$

In particular, we have

$$\frac{d}{dh}(t_2-t_1) = \frac{h^2-2h-2}{(2-h)\sqrt{2h(2+h)(1-h^2/2)}}.$$

Thus, one has

$$\frac{D^2}{2}\frac{d}{dh}(t_2-t_1) = \frac{(1+h)(2-h)(2+h)}{2(1-h^2/2)}\frac{h^2-2h-2}{(2-h)\sqrt{2h(2+h)(1-h^2/2)}} = \sqrt{\frac{2+h}{2h(1-h^2/2)}}\frac{-1-2h-h^2/2+h^3/2}{1-h^2/2}$$

which is exactly the opposite of (5.42). Therefore

$$\frac{d}{dh}K_C(2+h) = D\frac{dD}{dh}\arcsin\left((1-h)\sqrt{\frac{2+h}{2-h}}\right).$$

On the other hand, since

$$\frac{d}{dD}K_S(D) = D\arcsin\left(\frac{2}{D}\right)$$

we have

$$\frac{d}{dh}K_S(2+h) = D\frac{dD}{dh}\arcsin\left(\frac{2}{D}\right)$$

and to compare the derivatives, it suffices to compare the arguments in the arcsin. Now

$$\frac{2}{D} = \sqrt{\frac{2(1-h^2/2)}{(1+h)(2-h)(2+h)}}$$

and squaring and simplifying amounts to prove

$$\frac{4(1-h^2/2)}{(1+h)(2+h)} > (1-h)^2(2+h) \Leftrightarrow h^2(5+h-3h^2-h^3) > 0$$

which is true for $0 < h \leqslant 1$. This finishes the proof of $K_S(D) > K_C(D)$ for $D > 2$.

Existence of $D^\star$

Note that $|K_S(2)| = |K_E(2)| = \pi$. Now we compute the derivative of $D \mapsto |K_E(D)| - |K_S(D)|$ which is given by

$$\frac{d}{dD}(|K_E(D)| - |K_S(D)|) = \frac{3}{2} \times D\left(\frac{2\pi}{3} - 2\arccos(\frac{\sqrt{3}}{D})\right) - D\arcsin\left(\frac{2}{D}\right),$$

which has the same sign as $\pi - 3\arccos(\frac{\sqrt{3}}{D})) - \arcsin(2/D) = g(D)$.

Now, we have

$$g'(D) = -\frac{3\sqrt{3}}{D\sqrt{D^2-3}} + \frac{2}{D\sqrt{D^2-4}}$$

which is positive if and only if $D \in [2, \sqrt{\frac{96}{23}}]$. Together with $g(0) = 0$ and $g(2\sqrt{3}) = -\arcsin(\frac{1}{\sqrt{3}}) < 0$ we get that g is positive then negative. Finally we deduce that $D \mapsto |K_E(D)| - |K_S(D)|$ is increasing then decreasing with value 0 at 2 and taking negative value at $2\sqrt{3}$. We finally get the existence of some $D^\star \in [2, 2\sqrt{3}]$ such that for $D \leqslant D^\star$, $|K_E(D)| \geqslant |K_S(D)|$ and for $D \geqslant D^\star$, $|K_E(D)| \leqslant |K_S(D)|$. This conclude the proof.

5.4 appendix

5.4.1 Proof of Lemma 16

To prove the Lemma, we will introduce an auxiliary problem whose unknown is the restriction of R to the set I. Let us introduce $J = [0, 2\pi]\backslash(I \cup (I+\pi))$. Let us decompose R as $R = R_0\mathbb{1}_J + u^\star\mathbb{1}_I + (D - u^\star(\cdot - \pi))\mathbb{1}_{I+\pi}$, and observe that

$$J(R) = \int_I (2F[R]u^\star - DF[R] - Du^\star + D^2) + \int_J F[R]R_0.$$

and

$$\int_I u^\star(\theta)\cos\theta\, d\theta = \alpha \quad \text{and} \quad \int_I u^\star(\theta)\sin\theta\, d\theta = \beta,$$

with $\alpha = -\frac{1}{2}\int_J R_0(\theta)\cos\theta\,d\theta + \frac{D}{2}\int_I \cos\theta\,d\theta$ and $\beta = -\frac{1}{2}\int_J R_0(\theta)\sin\theta\,d\theta + \frac{D}{2}\int_I \sin\theta\,d\theta$.

We will now characterize $u^\star$ by exploiting that it solves the optimisation problem

$$\sup_{u\in\widetilde{\mathcal{R}}_D} \widetilde{J}(u) \quad \text{where} \quad \widetilde{J}(u) = \int_I (2hu - Dh - Du + D^2) + \int_J hR_0 \tag{5.46}$$

where h solves the ODE

$$\begin{cases} h + h'' = R_0\mathbb{1}_J + u\mathbb{1}_I + (D - u(\cdot-\pi))\mathbb{1}_{I+\pi} & \text{in } (0,2\pi) \\ \int_0^{2\pi} h(\theta)e^{i\theta}\,d\theta = 0 \\ h(0) = h(2\pi),\ h'(0) = h'(2\pi) \end{cases} \tag{5.47}$$

and

$$\widetilde{\mathcal{R}}_D = \left\{ u \in L^\infty(I;[0,D]) \mid \int_I u(\theta)e^{i\theta}\,d\theta = \alpha + i\beta \right\}.$$

Let us now derive the first order necessary optimality conditions for this problem. Since the method is standard, we briefly comment on the method allowing us to write such conditions: first, the mapping $\widetilde{\mathcal{R}}_D \ni u \mapsto h$, where h solves (5.47), being linear it is Gâteaux-differentiable at $u^\star$ in every direction ξ belonging to the tangent cone to the set $\widetilde{\mathcal{R}}_D$ at $u^\star$. Furthermore, its differential $\dot{h}$ is the unique solution of the ODE

$$\begin{cases} \dot{h} + \dot{h}'' = \xi\mathbb{1}_I - \xi(\cdot-\pi)\mathbb{1}_{I+\pi} & \text{in } (0,2\pi) \\ \int_0^{2\pi} \dot{h}(\theta)e^{i\theta}\,d\theta = 0 \\ \dot{h}(0) = \dot{h}(2\pi),\ \dot{h}'(0) = \dot{h}'(2\pi) \end{cases}$$

It follows that $\widetilde{\mathcal{R}}_D \ni u \mapsto \widetilde{J}(u)$ is Gâteaux-differentiable at $u^\star$ and its differential reads

$$\begin{aligned} \langle d\widetilde{J}(u^\star), \xi\rangle &= \lim_{\eta\searrow 0} \frac{\widetilde{J}(u^\star+\eta\xi) - \widetilde{J}(u^\star)}{\eta} = \int_I (2\dot{h}u^\star + 2h\xi - D\dot{h} - D\xi) + \int_J \dot{h}R_0 \\ &= \int_I (2h - D)\xi + \int_I \dot{h}(2u^\star - D) + \int_J \dot{h}R_0 = 2\int_I (2h-D)\xi, \end{aligned}$$

by using several times integration by parts and the relation $h(\theta) + h(\theta+\pi) = D$ on I.

We now have to deal with two kinds of constraints in $\widetilde{\mathcal{R}}_D$: a global L^1 one and point-wise ones, since u belongs to $[0,D]$ almost everywhere. Although such constraints are standard, we briefly explain how to derive the Euler inequation for this problem with the help of a penalization approach, for the sake of completeness. For $\varepsilon > 0$, let us introduce $\widetilde{J}_\varepsilon$ as the penalized functional

$$\widetilde{J}_\varepsilon(u) = \widetilde{J}(u) + \frac{1}{\varepsilon}\left| \int_I u(\theta)e^{i\theta}\,d\theta - (\alpha + i\beta) \right|^2.$$

We consider the optimisation problem

$$\sup_{u\in L^\infty(I;[0,D])} \widetilde{J}_\varepsilon(u). \tag{5.48}$$

On what follows, we will need to consider an element ξ to the tangent cone $\mathcal{T}_u$ to $L^\infty(I;[0,D])$ at u, that we describe hereafter.

Since they follow from a basic variational analysis, we do not provide all the details to the following claims:

- Since $L^\infty(I;[0,D])$ is compact for the weak-star convergence in L^∞, the resolvent operator $\widetilde{\mathcal{R}}_D \ni u \mapsto h \in L^2(\mathbb{T})$ is compact and therefore, the penalized problem (5.48) has a solution $u_\varepsilon \in L^\infty(I;[0,D])$.
- Let h_ε be the solution to (5.47) associated to u_ε. There exists a sequence $(\varepsilon_n)_{n\in\mathbb{N}}$ decreasing to 0, there exists $\widetilde{u} \in L^\infty(I;[0,D])$ such that $(u_{\varepsilon_n})_{n\in\mathbb{N}}$ converges weakly-star to $\widetilde{u}$ in $L^\infty(I;[0,D])$ and $(h_{\varepsilon_n})_{n\in\mathbb{N}}$ converges strongly to $\widetilde{h} \in H^1(0,2\pi)$ and uniformly in $\mathscr{C}^0([0,2\pi])$ as $n \to +\infty$. Furthermore, one has necessarily $\int_I u_{\varepsilon_n}(\theta)e^{i\theta}\,d\theta = \alpha + i\beta + \mathrm{O}(\varepsilon_n)$ and therefore, $\widetilde{u}$ belongs to $\widetilde{\mathcal{R}}_D$.
- Let $\xi \in \mathcal{T}_{\widetilde{u}}$. There exists $\xi_n \in \mathcal{T}_{u_{\varepsilon_n}}$ such that $(\xi_n)_{n\in\mathbb{N}}$ converges weakly-star to ξ as $n \to +\infty$ (this follows from the definition of the tangent cone and the fact that pointwise inequalities are preserved by the weak-star convergence).

Let $\xi \in \mathcal{T}_{\widetilde{u}}$. According to the computations above, the necessary first order optimality conditions for the penalized problem (5.48) read: for every $n \in \mathbb{N}$, since $\xi \in \mathcal{T}_{u_{\varepsilon_n}}$, one has

$$\int_I (2h_{\varepsilon_n}(\theta) - D + \alpha_n \cos\theta + \beta_n \sin\theta)\,\xi_n(\theta)\,d\theta \leqslant 0.$$

where

$$\alpha_n = \frac{1}{\varepsilon_n}\left(\int_I u_{\varepsilon_n}(s)\cos s\,ds - \alpha\right) \quad \text{and} \quad \beta_n = \frac{1}{\varepsilon}\left(\int_I u_{\varepsilon_n}(s)\sin s\,ds - \beta\right).$$

Let us divide the inequality above by $\sqrt{1+\alpha_n^2+\beta_n^2}$. Since the quantities $\sqrt{1+\alpha_n^2+\beta_n^2}$, $\alpha_n/\sqrt{1+\alpha_n^2+\beta_n^2}$ and $\beta_n/\sqrt{1+\alpha_n^2+\beta_n^2}$ are uniformly bounded with respect to n, one can assume that they respectively converge (up to a new extraction) to $\mu \geqslant 0$, $\bar{\alpha} \in \mathbb{R}$ and $\bar{\beta} \in \mathbb{R}$ such that $(\mu,\bar{\alpha},\bar{\beta}) \neq (0,0,0)$. Since ξ was arbitrarily chosen, by passing to the limit as $n \to +\infty$, we get at the end that the first order necessary conditions associated to Problem (5.47) read

$$\forall \xi \in \mathcal{T}_{\widetilde{u}}, \quad \int_I \left(\mu(2\widetilde{h}(\theta) - D) + \bar{\alpha}\cos\theta + \bar{\beta}\sin\theta\right)\xi(\theta)\,d\theta \leqslant 0 \tag{5.49}$$

Now, since $\widetilde{J}_{\varepsilon_n}(u) = \widetilde{J}(u)$ for every $u \in \widetilde{\mathcal{R}}_D$, it follows that

$$\widetilde{J}_{\varepsilon_n}(u_\varepsilon) = \max_{u\in L^\infty(I;[0,D])} \widetilde{J}_{\varepsilon_n}(u) \geqslant \max_{u\in L^\infty(I;[0,D])} \widetilde{J}(u) = \widetilde{J}(u^\star) \geqslant \widetilde{J}(u_{\varepsilon_n}).$$

Passing to the limit in this inequality yields $\widetilde{J}(u^\star) \geqslant \widetilde{J}(\widetilde{u})$. Using that $\widetilde{u}$ belongs to $\widetilde{\mathcal{R}}_D$, we infer that $\widetilde{u}$ solves Problem (5.46). Therefore, we can assume without loss of generality that $\widetilde{u} = u^\star$.

Part III

A criterium involving linear elasticity

Chapter 6

Introduction

Contents

This chapter is an introduction over an ongoing work where we studied a biological modeling involving a compliance functional in the field of linear elasticity. For the moment we only obtained some partial results, and the existence result is mostly an adaptation of an already established result.

6.1 A biological motivation

Recall a very important aspect of the life cycle of the Clam Shrimps. Once laid down in the pool, the eggs sink to the bottom of the pond, all the animals die and only the resting eggs remain. At this stage the eggs are the only representatives of the species. In a second stage the pond fills up again with water, and we observe that the eggs are now floating at the surface.

It is a widespread hypothesis that the floating of the egg on the surface favours the spread of species because they are more easily transported, especially by an animal that comes to the pond to quench its thirst and swallows the egg by accident, or the egg simply clings to the animal's hair ([75, 45]).

This suggests that the shell has cavities that are filled with water or some liquid at start, then the liquid evaporates (see Figure 6.1). Once the water comes back in the pond, there is no liquid in the shell and the eggs becomes less dense than water. It is important to notice that such a perforated structure might be fragile to external stresses. Indeed, it is well observed that the main danger for the eggs is not erosion, but being crushed by the external environment ([55, 42]). Note that it is a recurring problem in construction to build light and resistant materials, hence the study of porous micro-structures. We suggest that the structure of the shell makes the egg more resistant to external forces.

It is not uncommon to assume that an egg must be resistant to external forces. A lot of work has been done on the study of the microstructure of hens' eggs (see e.g [85]). From what we learnt, the resistance of an egg is closely related to the thickness of the shell, its density of

material, and its micro-structure. As we wish to control the quantity of material used as well as the density of material to allow the egg to float, mass density and thickness are considered to be penalizing in our context. By this modeling we hope to explain the micro-structure of the egg modeling, and possibly see if an overall shape emerges to improve resistance since very little is imposed on the geometry.

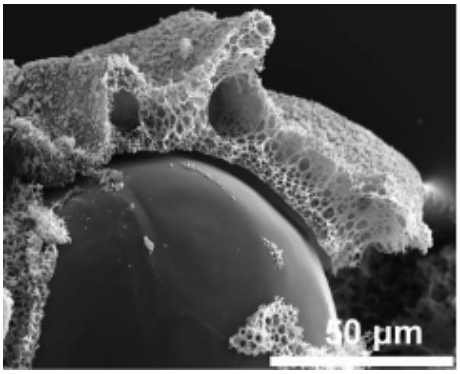

(a) A picture where the perforated structure is highlighted, with the embryo clearly appearing

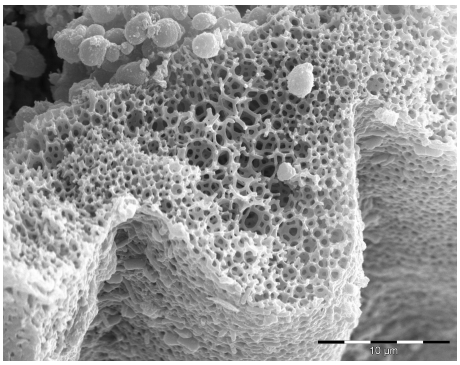

(b) A zoom over the perforated structure

Figure 6.1: Those pictures show how porous the shell is, explaining why it is floating at the surface.

6.2 Mathematical modeling

Let $N \geqslant 2$ (in the future N will be 2) and Ω be an open set of $\mathbb{R}^N$. The holes of Ω are defined as the bounded conected components of $\mathbb{R}^N \backslash \Omega$. We name them T. It follows that $|\Omega|$ is the volume occupied by the material of the egg, and $|\Omega \cup T|$ is the total volume occupied by the egg. We assume that the shell and the embryo have the same mass density, and the holes have mass density 0. Then we define the mean mass density of Ω as follows.

$$\Delta(\Omega) = \frac{|\Omega|}{|\Omega \cup T|}. \tag{6.1}$$

The floatability of the egg on the surface is mathematically translated into the constraint:

$$\Delta(\Omega) \leqslant \alpha, \tag{6.2}$$

where $\alpha \in (0, 1)$ is a constant depending on the mass density of the material. For example if the mass density of the material is $\mu > 1$ then the floatability conditions states that the ratio $\mu|\Omega|/|\Omega \cup T|$ has to be less than 1, hence, $\Delta(\Omega) \leqslant \frac{1}{\mu}$. The assumption that $\mu > 1$ comes from that the observation that when the eggs are laid in the pool by the shrimps, the cavities are filled with water, and sink. We deduce that the material of Ω is denser that the water.

Now the resistance of the eggs is modeled by the compliance of Ω. Let $\Gamma_T = \partial T$, and $\Gamma_{\text{ext}} = \partial(\Omega \cup T)$. We summarize the forces applied to the egg by a constant pressure force on Γ_{ext}:

$$F = -p_0 n.$$

Here n denotes the outward normal vector of the boundary and p_0 is a constant. It follows that the force depends on Ω.

The compliance of Ω is then defined by

$$C(\Omega) = \int_{\Gamma_{\text{ext}}} -p_0 u \cdot n \; ds \tag{6.3}$$

Where $u = u(\Omega) \in L^2(\Omega)^N$ solves the linear elasticity equation:

$$\begin{cases} -\operatorname{div}(Ae(u)) = 0 & \text{in } \Omega \\ Ae(u)n = -p_0 n & \text{on } \Gamma_{\text{ext}} \\ Ae(u)n = 0 & \text{on } \Gamma_T \end{cases} \tag{6.4}$$

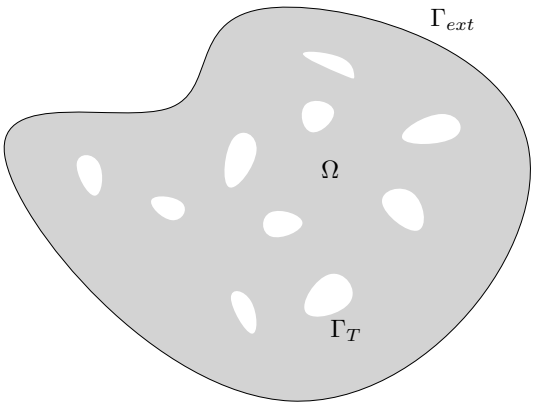

Figure 6.2: Modelisation of the egg

The basics of linear elasiticity were introduced in 1.5. Notice that here we only have a Neumann boundary condition, so we wish to apply Proposition 24. For that purpose we must prove the compatibility conditions: for all $v \in \mathcal{R}$,

$$\int_{\Gamma_{\text{ext}}} v \cdot n = 0.$$

Recall that $v \in \mathcal{R}$ writes $v(x) = Ax + b$ where $A \in \mathbb{M}_N(\mathbb{R})$ is antisymmetric. We apply the Gauss-Green formula:

$$\int_{\Gamma_{\text{ext}}} (Ax + b) \cdot n \; ds = \int_{\Omega \cup T} \operatorname{div}(Ax + b) \; dx.$$

The results immediately follows because A has 0 as diagonal elements.

Proposition 38. *Equation* (6.4) *admits solution* $u \in H^1(\Omega, \mathbb{R}^N)$ *that is unique up to a rigid transformation, and* u *verifies the variational formulation :* $\forall v \in H^1(\Omega, \mathbb{R}^N)$*:*

$$\int_\Omega Ae(u) : e(v) \; dx = -p_0 \int_{\Gamma_{\text{ext}}} v.n \; ds \tag{6.5}$$

Moreover u *is the (unique up to a rigid transformation) minimiser over* $H^1(\Omega, \mathbb{R}^N)$ *of the energy*

$$\mathcal{E}(\Omega, v) = \frac{1}{2} \int_\Omega Ae(v) : e(v) \; dx + p_0 \int_{\Gamma_{\text{ext}}} v.n \; ds \tag{6.6}$$

Remark 23. Notice that the energy of v is not modified by replacing v by $v + r$ where $r \in \mathcal{R}$.

Defining u as the minimiser of the energy allows a new definition for the compliance:

$$C(\Omega) = -2 \inf_{v \in H^1(\Omega, \mathbb{R}^N)} \mathcal{E}(\Omega, V) \tag{6.7}$$

Let

$$\Omega_{\text{adm}} = \{\Omega \subset \mathbb{R}^N, \text{open, connected, with Lipschitz boundary }, |\Omega| \leqslant V_0, r(\Omega) \geqslant 1, \Delta(\Omega) \leqslant \alpha\}.$$

The shape optimisation is then

$$\boxed{\inf_{\Omega \in \Omega_{adm}} C(\Omega)} \tag{$\mathcal{P}_{\text{elast}}$}$$

6.3 Theoretical analysis

For our results we worked in dimension $N = 2$.

It is well known that without further hypothesis, the minimisation of the compliance has no solution because of the creation of small holes. In fact a minimising sequence tends in some sense to a homogenized material, and one way to study the minimisation of the compliance is via homogenization (see e.g [3] or [4] Theorem 7.30). Another way is to prevent the proliferation of holes by adding a perimeter constraint. Indeed creating holes has a cost in terms of perimeter, and this mathematically translates as a compactness property (see Proposition 31). L. Ambrosio and G. Butazzo give in [7] an exemple of the use of compactness properties under a perimeter constraint to show the existence of a solution to a shape optimisation problem. This methods allows the creation of holes, but gives a control to the number of those, which can be modulated by modifying the coefficient of the perimeter penalization. We chose this method.

In this framework we mostly adapted a paper of Blaise Bourdin and Antonin Chambolle [20] who provide an existence result together with an algorithm. The idea is as follows: Observe that the problem may be written a three phase problem. Consider a bounded regular domain D, for example a ball of large radius. In D we distinguish three phases: a solid phase S, a liquid phase L and a void phase V. S represents the egg (Ω in our model), L is the exterior environment from where the outer forces apply, and V are the holes in the shell (T in our model). Note that the proportion of each phase is fixed by a paramter $\theta = (\theta_S, \theta_L, \theta_V)$ such that $|S| = \theta_S |D|$ etc, hence we force an equality constraint instead of an inequality constraint. We can define for each partition S, L, V of D an energy that is similar to the one we defined in (6.6):

$$\mathcal{E}_{S,L,V}(u) = \frac{1}{2} \int_S Ae(u) : e(u)\ dx - \int_{\partial L \cap D} p_0 u \cdot n_L\ ds \tag{6.8}$$

And the compliance $C(S, L, V)$ is naturally defined as the infimum of this energy (see (6.7)).

In order to deal with this perimeter penalization, we work in the setting of functions of bounded variations (BV) and the L^1 convergence of the characteristic functions. The energy is rewritten in this setting (see equation (7.4)) and the problem we consider is the minimisation of the compliance with a perimeter penalization written as:

$$P(S, L, V) = \mathcal{H}^1(\partial_\star L) + \mathcal{H}^1(\partial_\star V),$$

So that the problems writes:

$$\boxed{\inf_{(S,L,V)\in\mathcal{P}_D} C(S,L,V) + \lambda\overline{P}(S,L,V)} \tag{6.9}$$

where $\mathcal{P}_D$ takes into account the fact that we impose that the liquid phase is the external environment and that we prescribe the area of each phase.

Theorem 12. *There exists a partion S, L, V that solves the problem* (6.9)

To prove this theorem we use a fictitious material approach that is pretty classical in optimal design (see e.g [6]), together with a phase-field approximation. In a nutshell, in the fictitious material approach we consider that the liquid and void phases are filled with an elastic material with very low Hooke law: in other words on $L \cup V$ we consider δA with δ small. And the phase field approach consists in replacing the three sets by a function ideally taking value in $\{-1, 0, 1\}$ and then consider a relaxation in $L^1(D)$ of the problem. The authors relied on an adaptation of the Modica-Mortola theory ([74]) for the approximation of the perimeter to make it work in a three phases model, whereas the study of the fictitious material was performed with the help of duality theory in convex optimisation. The convergence of the approximated problems are in the setting of Γ-convergence. In section 7.1 we set the formulation of the main problem and the approximated problems and state the results. Section 7.1.4 is devoted to the proof of the theorems. Note that since this analysis results from a direct adaptation of [20] we only provide the main ideas and refer to the main article for the technical aspects of the proof.

In section 7.2 we go back to the original problem and study the optimality conditions of a possible connected minimiser that we assume to be smooth enough to allow to compute shape derivatives. We prove that at the optimum, under hypothesis over the incircle, every constraint is saturated.

6.4 Discussion

Unfortunately we still do not have solutions to compare with the real shapes, but numerical investigations are being made in order to provide a numerical solution. Nevertheless, we highlight a weakness in the modeling. Choosing a constant pressure force is not well suited for testing the resistance of an egg: most often the force applied is localised, for example on the top and bottom of the egg when it is trampled. Furthermore it is reasonable to assume that the force is only applied to the parts that protrude beyond the egg, in other words, the force would be applied on $\partial\Omega \cap \partial(\text{hull}(\Omega))$. Up to our knowledge, this kind of problem was not treated yet. Let us remark that without further hypothesis, the problem is trivially solved by any set Ω such that $\partial\Omega \cap \partial(\text{hull}(\Omega))$ has 0 length. However, it could be interesting for explaining the ornamentation.

From the mathematical point of view, the approach developed by B. Boudin and A. Chambolle does not guarantee that the optimal shape is connected, even though the perimeter penalization prevents the emergence of a multitude of connected components (for the same reasons as holes). Work is in progress to include in the functional a penalisation for non-connectedness through the following functional:

$$\overline{P_{\mathcal{C},D}}(E) = \inf\{\liminf_{n\to\infty} \text{Per}(E_n), E_n \to E \text{ in } L^1(D), E_n \subset D, E_n \text{ connected and } C^\infty\} \tag{6.10}$$

Then if E is connected, the latter functional is precisely the perimeter of E. If E has two connected components, then $\overline{P_{\mathcal{C},D}}(E)$ is equal to the classical perimeter of E to which we add twice the length of the minimal path in D that joints the connected components ([28]).

In [32] the authors prove a $\Gamma-$convergence of some $\varepsilon-$indexed functional to $\overline{P_{\mathcal{C},D}}$ in a two phase model. Our goal is to adapt this proof to our three phase model to prove the existence of a solution with the new functional

$$\overline{\Lambda}(S, L, V) = \overline{P}(S, L, V) + \overline{P_{\mathcal{C},D}}(S), \tag{6.11}$$

so we can adapt the general proof of [20] based on a $\Gamma-$convergence argument. With this penalization there is a good chance that the solution is connected. However it may still not be convincing since the obtained solution could be given as two shapes connected by a small tube, and thus being "artificially connected".

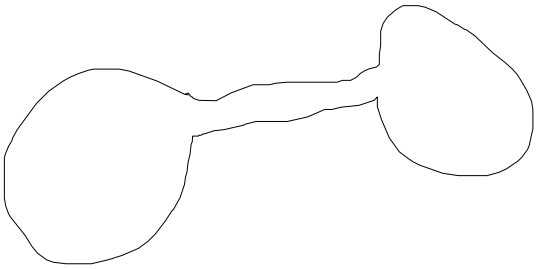

Figure 6.3: A set that is artificially connected

Besides, numerical simulations are being carried out, first by a classical geometrical optimisation that is not handling hole creation, and then by implementing the algorithm provided by the proof of the existence of a solution.

Chapter 7

minimisation of a compliance functional

Contents

Let us recall the problem we are dealing with. We would like to solve the problem $(\mathcal{P}_{\text{elast}})$ in dimension $N = 2$:

$$\boxed{\inf_{\Omega \in \Omega_{adm}} C(\Omega)} \qquad (\mathcal{P}_{\text{elast}})$$

where Ω_{adm} is the set of open bounded and connected domains Ω with Lipschitz boundary, such that $|\Omega| = V_0$, inradius $r(\Omega) \geqslant 1$ and mass density $\Delta(\Omega) \leqslant \alpha$. $C(\Omega)$ is the compliance defined by

$$C(\Omega) = \int_{\Gamma_{\text{ext}}} -p_0 u \cdot n \; ds.$$

where $u \in L^2(\Omega)$ solves

$$\begin{cases} -\operatorname{div}(Ae(u)) = 0 & \text{in } \Omega \\ Ae(u)n = -p_0 n & \text{on } \Gamma_{\text{ext}} \\ Ae(u)n = 0 & \text{on } \Gamma_T \end{cases}$$

Γ_T is the inner boundary and Γ_{ext} is the outer boundary.

This chapter is devoted to two works. The first work is devoted to the investigation of the existence of an optimal shape to a slightly modified problem. Indeed we consider a perimeter perturbation in order to facilitate the existence. Hence we consider the following problem:

$$\inf_{\Omega \in \bar{\Omega}_{adm}} C(\Omega) + \operatorname{Per}(\Omega) \qquad (7.1)$$

where in $\tilde{\Omega}_{adm}$ volume and mass density are prescribed with an equality, and we drop the connectedness constraint.

For this purpose we relied on a work of Antonin Chambolle and Blaise Bourdin and we use different notations as the one used previously in order to work in a three phase model approach.

In the second work we consider the original problem, for which we did not provide the existence of a solution, but still try to figure out what could be an optimal shape through the use of optimality conditions.

7.1 Existence of a solution

In order to study the existence question, we follow the work of Antonin Chambolle and Blaise Bourdin in [20]. They worked on the same kind of problem where their goal was to find the optimal shape of a structure that is subjected to pressure forces. It is well known that without further hypothesis there is no solution to the compliance minimisation problem. Indeed, due the lack of strong compactness in a minimising sequence, the solution tends to a mixture of phases, and we can observe homogenization phenomena. In order to avoid this kind of problem, the authors perturbed the compliance problem by adding a perimeter functional, preventing multitude of small holes from appearing. In this section we mainly adapt their work for our own problem. A first part is dedicated to the setting of the problem, and then we provide a sketch of the proof in which we give the main ideas. The proofs being the same as the aforementioned article, we do not provide those, and directly refer to the original paper.

7.1.1 A naïve formulation

We consider an open, convex, bounded and smooth domain $D \subset \mathbb{R}^2$ which contains the unit disk $D_0 = D(0,1)$. Then we consider a partition $\{S, L, V\}$ of D. S stands for solid, L for liquid, and V for void. The solid phase corresponds to the shell of the eggs, the liquid phase will be seen as the external environment, from where the pressure forces are applied, and the void stands for the holes in the shell.

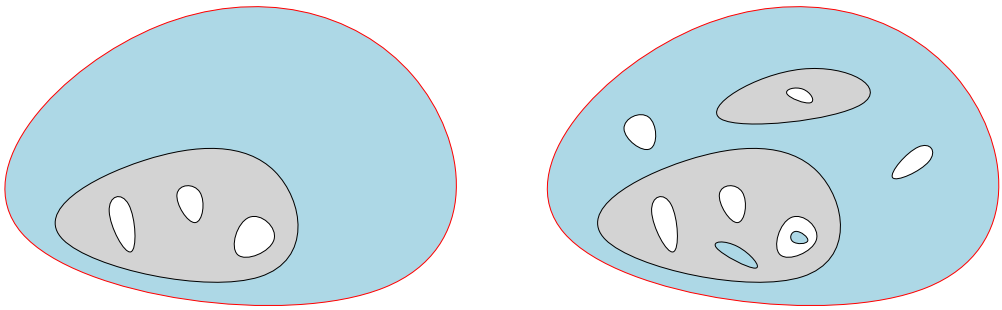

(a) An ideal setting where the egg is represented as a connected set, and liquid and void are isolated.

(b) A possible setting where the egg is not connected and where there are absurd interactions between void and liquid.

Figure 7.1: The set D and its three phases: The liquid phase is represented in blue, the solid phase in grey and void in white. The boundary of D is highlighted in red

Note that the partition has a priori no constraint: liquid and void may have a common boundary, S may not be connected etc (see Figure 7.1). The liquid phase exerts the pressure

force p_0 that we suppose constant here, whereas the void phase does not apply kind of force. Similarly, if the sets S,L,V are regular enough we can define an elastic energy. With a slight abuse of notation let us denote by $H^1_0(D)$ the set of functions $u \in H^1(D, \mathbb{R}^2)$ such that $u_{/\partial D} = 0$. For every $u \in H^1_0(D)$ define:

$$\mathcal{E}_{S,L,V}(u) = \frac{1}{2}\int_S Ae(u) : e(u)\ dx - \int_{\partial L \cap D} p_0 u \cdot n_L\ ds \tag{7.2}$$

where n_L is the outer normal to L and $\mathcal{H}^1$ is the 1-dimensional Hausdorff measure. Note that $n_L = -n_S$ on $\partial L \cap \partial S$, hence the minus sign compared to (6.6). The equilibrium displacement is given by the minimiser of this energy.

In the settings where there is no interface between void and liquid, then if we write the first optimality conditions for the minimiser $u^\star$, the Euler-Lagrange equation yields that $u^\star$ is solution of (6.4) where S stands for D. We finally get the definition for the compliance:

$$C(S, L, V) = -2 \inf_{u \in H^1_0(D)} \mathcal{E}_{S,L,V}(u) = -2\mathcal{E}_{S,L,V}(u^\star) \tag{7.3}$$

if $u^\star$ exists. Anyway the compliance is defined by the infinimum.

In this framework, the constraints are the following: let $\theta_S + \theta_L + \theta_V = 1$ and $D_0 = D(0, 1)$ and

$$\mathcal{P}_{adm} = \{(S, L, V) \text{ Lipschitz partition of } D, |S| = \theta_S,\ |L| = \theta_L,\ |V| = \theta_V, D_0 \subset S\ \}$$

Ideally we would like to solve the minimisation problem:

$$\inf_{\mathcal{P}_{adm}} C(S, L, V)$$

Due to the lack of strong compactness we cannot guarantee the existence of a maximiser, and it is well known that with no control on the number of holes, a minimising sequence tends to a mixture of phase (see [4, 3]). In order to deal with those problems we will add a perimeter penalization. Indeed, a perimeter constraint adds compactness properties (see e.g [5, 7]). We also work with functions of bounded variations because it allows more freedom in the formulation in the problem that now involves perimeter. For the basics we refer to 1.6.

7.1.2 The formulation in the settings of functions of bounded variations

In this context we consider that S, L, V are finite perimeter sets, i.e their characteristic functions are with bounded variations. Now the energy functional rewrites:

$$\mathcal{E}_{S,L,V}(u) = \frac{1}{2}\int_S Ae(u) : e(u)\ dx - \int_D p_0 u \cdot D\chi_L. \tag{7.4}$$

As said previously, we consider a perimeter penalization, written in the following way:

$$P(S, L, V) = \mathcal{H}^1(\partial_\star L) + \mathcal{H}^1(\partial_\star V) \tag{7.5}$$

where $\partial_\star L$ is the reduced boundary of L (see 1.6). Disregarding $\mathcal{H}^1(\partial_\star S)$ in the definition (7.5) comes from the fact that we can guess that at the optimum, L and V will share no boundary. Indeed the void opposes no resistance to pressure force, so if L and V share boundaries, the pressure force would push the void to infinity. In those conditions, adding the perimeter of S

is equivalent to count twice those of L and V. A technical proof of this fact is available in [20] Section 5.

We already stated a Dirichlet condition over the test functions u. Now let us specify a boundary condition for the sets S, L, V, illustrating the fact that the liquid phase represents the whole exterior environment:

$$\partial D \subset \overline{L}.$$

Note that this last condition is unfortunately unstable by L^1 convergence of the characteristic functions: a sequence of functions L_n with trace equal to 1 on ∂D may converge to a function whose trace is not 1. In order to avoid this kind of problem we can chose a space that would penalize such a phenomenon.

Let $BV(\overline{D})$ the space of functions with bounded variations in $\overline{D}$

$$BV(\overline{D}) = \left\{ f \in L^1(D), \sup \left\{ \int_D f \operatorname{div} \varphi \, dx, \varphi \in C^1(\overline{D}, \mathbb{R}^2), |\varphi(x)| \leqslant 1 \right\} < +\infty \right\} \tag{7.6}$$

If $f \in BV(\overline{D})$, it has an outer trace f^{ext} as a function that is also defined on ∂D and an inner trace f^{int} as the classical trace of a function in $BV(D)$. Its derivative is now a measure on D defined by:

$$Df = (f^{\text{ext}} - f^{\text{int}}) n_D \mathcal{H}^1 \llcorner \partial D + Df \llcorner D \tag{7.7}$$

The second term is only to be seen as the derivative of f as a function in $BV(D)$.

In the settings of finite perimeter sets in $\overline{D}$, those are sets E whose characteristic function are in $BV(D)$ together with an outer trace $\chi_E^{\text{ext}} \in \{0, 1\}$ on ∂D. The consequence is that the reduced boundary is now:

$$\overline{\partial}_\star E = \partial_\star E \cup \{x \in \partial D \mid \chi_E^{\text{ext}}(x) \neq \chi_E^{\text{int}}(x)\}$$

We have the derivative

$$D\chi_E = -n_E \mathcal{H}^1 \llcorner \overline{\partial}_\star E. \tag{7.8}$$

And the perimeter constraints becomes:

$$\overline{P}(S, L, V) = \mathcal{H}^1(\overline{\partial}_\star L) + \mathcal{H}^1(\overline{\partial}_\star V) \tag{7.9}$$

Now we see that this definition gives a penalization to sets that artificially fill the boundary constraint: parts of the boundary where the liquid phase is isolated will have 0 as interior trace and will be counted in the perimeter penalization (see Figure 7.2).

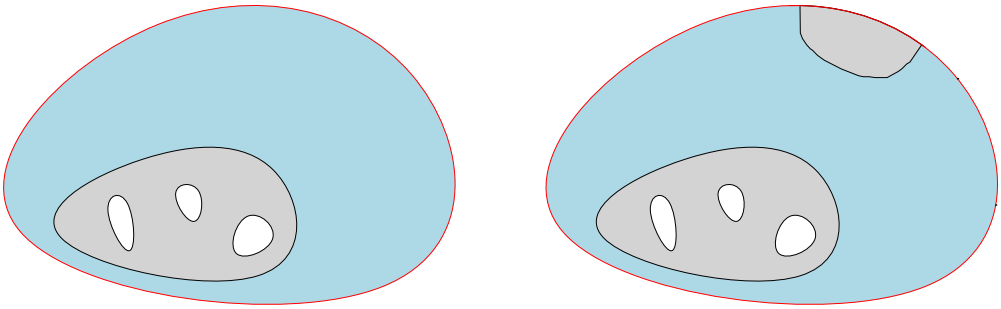

(a) A setting where the boundary constraint for the liquid phase is perfectly fulfilled: the inner trace is equal to the outer trace

(b) A setting where the boundary constraint is artificially fulfilled. The inner trace of the liquid is 0 where the solide phase touches the boundary.

Figure 7.2: The liquid phase is represented in blue, the solid phase in grey and the void phase in white. The outer boundary of the liquid phase is highlighted in red. On Figure 7.2b the perimeter functional will penalize the whole boundary of D where the solide phase is touching.

The correct formulation for the energy is finally:

$$\mathcal{E}_{S,L,V}(u) = \frac{1}{2}\int_S Ae(u) : e(u)\ dx - \int_{\overline{D}} p_0 u \cdot D\chi_L. \tag{7.10}$$

And the compliance:

$$C(S,L,V) = -2 \inf_{u \in H^1_0(D)} \mathcal{E}_{S,L,V}(u) \tag{7.11}$$

The shape optimisation is now written in its final form:

$$\boxed{\inf_{(S,L,V)\in\mathcal{P}_D} C(S,L,V) + \lambda \overline{P}(S,L,V)} \tag{$\mathcal{P}'_{\text{elast}}$}$$

where $\mathcal{P}_D$ is the set of finite perimeter partitions of D such that $\partial D \subset \overline{L}$, $|S| = \theta_S|D|$, $|L| = \theta_L|D|$, $|V| = \theta_V|D|$ and $\chi_S \geqslant \chi_{D_0}$. We do not require conectedness of S.

We now can give the existence theorem for this problem.

Theorem 13. *[[20]] Assume that there exists a finite-perimeter partition of D with finite compliance, then problem ($\mathcal{P}'_{\text{elast}}$) admits a solution.*

In order to prove Theorem 13, we need to study some relaxed problems that we describe in the next section.

7.1.3 Two relaxed problems

First step: the fictitious material method

The first step consists in filling the void and liquid with a material with very small elastic tensor δA, $\delta > 0$. In this context the energy rewrites:

$$\mathcal{E}^\delta_{S,L,V}(u) = \int_D (\delta + (1-\delta)\chi_S) Ae(u) : e(u)\ dx + \int_{\overline{D}} p_0 u \cdot D\chi_L, \tag{7.12}$$

and $C^\delta(S,L,V)$ defined as previously as the minimiser of the energy in $H^1_0(D)$.

And now consider for every δ the problem:

$$\boxed{\inf_{(S,L,V)\in\mathcal{P}_D} C^\delta(S,L,V) + \lambda\overline{P}(S,L,V)} \qquad ({\mathcal{P}^\delta}_{\text{elast}})$$

Theorem 14. *For every $\delta > 0$, $({\mathcal{P}^\delta}_{\text{elast}})$ has a solution $(S^\delta, L^\delta, V^\delta)$. Moreover, if there exists a finite perimeter partition of D with finite perimeter, then there exists a sequence $S^\delta, L^\delta, V^\delta$ and a finite perimeter partition S, L, V of D such that $\chi_{S^\delta} \to \chi_S$, $\chi_{L^\delta} \to \chi_L$, $\chi_{V^\delta} \to \chi_V$ in $L^1(D)$, and S, L, V is a solution of $({\mathcal{P}'}_{\text{elast}})$.*

The second step consists in proving Theorem 14 by using a phase-field approximation.

Second step: phase-field approximation

This method consists in replacing sets by their characteristic function, and give an approximation of them by more regular functions. So now we replace S, L, V by a function $\rho \in BV(\overline{D})$ ideally taking value in $\{-1, 0, 1\}$ and $S(\rho) = \{\rho = 0\}$, $L(\rho) = \{\rho = 1\}$, $V(\rho) = \{\rho = -1\}$. Let

$$\overline{X}_\rho = \{\rho \in BV(\overline{D}; \{-1, 0, 1\}) \mid \rho^{\text{ext}} = 1 \text{ on } \partial D, \rho = 0 \text{ in } \ D_0\}.$$

Again in the sense of measure, we have

$$D\rho = D\rho \llcorner D + (1 - \rho^{\text{int}}) n_D \mathcal{H}^1 \llcorner \partial D,$$

and we see that

$$|D\rho|(\overline{D}) = \overline{P}(\{\rho = 0\}, \{\rho = 1\}, \{\rho = -1\}).$$

For $\delta > 0$, $\rho \in \overline{X}_\rho$, $u \in H^1_0(D)$, formula (7.12) becomes:

$$\mathcal{E}^\delta_\rho(u) = \int_D (\delta + (1-\delta)\chi_{S(\rho)}) Ae(u) : e(u)\ dx - \int_{\overline{D}} p_0 u \cdot D\chi_{L(\rho)}\ dx, \tag{7.13}$$

and

$$C^\delta(\rho) = -2 \inf_{u \in H^1_0(D)} \mathcal{E}^\delta_\rho(u)$$

Problem $({\mathcal{P}^\delta}_{\text{elast}})$ now has an equivalent formulation in terms of $\rho \in \overline{X}_\rho$:

$$\boxed{\inf_{\rho \in \overline{\rho}_{\text{adm}}} C^\delta(\rho) + \lambda |D\rho|(\overline{D})} \qquad ({\mathcal{P}^{\delta,\overline{\rho}}}_{\text{elast}})$$

where $\overline{\rho}_{\text{adm}}$ is the set of $\rho \in \overline{X}_\rho$ such that$|L(\rho)| = \theta_L |D|$, aswell for S and V, and $\rho = 0$ in D_0.

In order to show that this problem has a solution, we proceed to a relaxation of the phase indicator function ρ, which means that we allow ρ to take other values than $-1, 0$ or 1. We define

$$X_\rho = \{\rho \in H^1(D) \mid \rho = 1 \text{ on } \partial D, \rho = 0 \text{ in } D_0\}.$$

Then we define three smooth functions $\tilde{S}, \tilde{L}, \tilde{V} : \mathbb{R} \mapsto [0, 1]$ such that:

- $\tilde{S}(0) = 1$, $\tilde{S}(1) = \tilde{S}(-1) = 0$ and $\tilde{S}$ is increasing on $[-1, 0]$ and decreasing on $[0, 1]$.
- $\tilde{L}(1) = 1$, $\tilde{L}$ is null on $[-1, 0]$ and increasing on $[0, 1]$

- $\tilde{V}(-1) = 1$, $\tilde{V}$ is null on $[0,1]$ and decreasing on $[-1,0]$
- $\tilde{S} + \tilde{L} + \tilde{V} = 1$

Combined with ρ, those functions represents the portion of each phase we have at point x. Note that if $\rho \in \overline{X}_\rho$ then we have for example $\tilde{L}(\rho) = \chi_{\{\rho=1\}}$, the indicator function of the liquid phase $L(\rho)$,

For $\rho \in X_\rho$ we extend the energy $\mathcal{E}^\delta_\rho$:

$$\mathcal{E}^\delta_\rho(u) = \int_D (\delta + (1-\delta)\tilde{S}(\rho))Ae(u) : e(u)\ dx - \int_D p_0 u \cdot \nabla \tilde{L}(\rho)\ dx. \tag{7.14}$$

Integrating by part we get:

$$\mathcal{E}^\delta_\rho(u) = \frac{1}{2}\int_D (\delta + (1-\delta)\tilde{S}(\rho))Ae(u) : e(u)\ dx + \int_D \tilde{L}(\rho)\,\mathrm{div}(p_0 u)\ dx - \int_{\partial D} p_0 u \cdot n_D\ ds. \tag{7.15}$$

This expression is valid for any $\rho \in X_\rho \cup \overline{X}_\rho$ and also makes sense for $\rho \in L^1(D)$.
Now we have a new definition for the compliance given in terms of $\rho \in L^1(D)$

$$C^\delta(\rho) = -2 \inf_{u \in H^1_0(D)} \mathcal{E}^\delta_\rho(u) \tag{7.16}$$

We also extend the perimeter penalization to any $\rho \in L^1(D)$ by the formula:

$$\overline{P}(\rho) = \begin{cases} |D\rho|(\overline{D}) & \text{if } \rho \in \overline{X}_\rho \\ +\infty & \text{otherwise} \end{cases} \tag{7.17}$$

We give a new formulation of problem $(\mathcal{P}^{\delta,\overline{\rho}}_{\text{elast}})$ which is equivalent:

$$\boxed{\inf_{\rho \in \rho_{\text{adm}}} C^\delta(\rho) + \lambda \overline{P}(\rho)} \tag{$\mathcal{P}^{\delta,\rho}_{\text{elast}}$}$$

Where ρ_{adm} is the set of functions $\rho \in L^1(D)$ such that $\int_D S(\rho) = \theta_S |D|$, aswell for L and S, and $\rho = 0$ in D_0. This formulation is equivalent to the one of the problem $(\mathcal{P}^\delta{}_{\text{elast}})$

For $\rho \in X_\rho$ the expression of the perimeter penalization is not relevant anymore. So we introduce an energy that takes account of the mixture of phases, inspired by the so called Cahn-Hilliard Energy. Take a function W that is positive except at -1,0,1 where it is equal to 0, and such that $\int_{-1}^0 \sqrt{2W} = \int_0^1 \sqrt{2W} = 1$. For instance take $W(t) = 8t^2(1-t^2)^2$. For $\rho \in L^1(D)$, and $\varepsilon > 0$,

$$P_\varepsilon(\rho) = \begin{cases} \frac{\varepsilon}{2}\int_D |\nabla \rho|^2\ dx + \frac{1}{\varepsilon}\int_D W(\rho)\ dx & \text{if } \rho \in X_\rho \\ +\infty & \text{otherwise} \end{cases} \tag{7.18}$$

The first term stands for the perimeter penalization while the second term punishes the mixture of phase. This energy was studied as an interfacial energy for mixed phases e.g in [2, 74]. In fact instead of considering that the interface is a line splitting the phases, we say that there exists a thin film of thickness ε that is constituted of a mixture of phases.

We prove the following result.

Proposition 39. *P_ε is lower semi-continuous in $L^1(D)$.*

Proof. Let ρ_n a sequence of $L^1(D)$ that converges in L^1 to ρ, and such that $P_\varepsilon(\rho) < +\infty$. Then up to a subsequence, $\rho_n \to \rho$ a.e . Since W is continuous, $W(\rho_n) \to W(\rho)$ a.e and by Fatou Lemma, we obtain the lower semi continuity of the term $\int_D W(\rho)\, dx$. Now for the second term observe that in fact $\rho_n \in H^1(D)$ and is bounded, hence it converges up to a subsequence weakly in $H^1(D)$ and strongly in $L^2(D)$ to a function $\tilde{\rho} \in H^1(D)$ by the embedding $L^2(D) \subset L^1(D)$ we deduce that $\tilde{\rho} = \rho$ and by lower semi continuity of the first term for weak convergence, we deduce that the whole functional is l.s.c. □

The last problem we get is finally:

$$\boxed{\inf_{\rho \in \rho_{\text{adm}}} C^\delta(\rho) + \lambda P_\varepsilon(\rho)} \qquad (\mathcal{P}^{\delta,\rho,\varepsilon}_{\text{elast}})$$

Now we state the theorem:

Theorem 15. *Let $\delta > 0$. For every $\varepsilon > 0$, problem $(\mathcal{P}^{\delta,\rho,\varepsilon}_{\text{elast}})$ has a solution $\rho_\varepsilon \in X_\rho$, and there exists a sequence $\varepsilon_j \to 0$ and $\rho \in \overline{X}_\rho$ such that $\rho_{\varepsilon_j} \to \rho \in L^1(D)$. Furthermore, ρ is a solution of $(\mathcal{P}^{\delta,\rho}_{\text{elast}})$. If one writes $L = \{\rho = 1\}$ aswell for S and V, then (S,L,V) is a solution of $(\mathcal{P}^{\delta}{}_{\text{elast}})$*

This is a long and technical proof. In the following section we give some some ideas of the proof, but we refer to [20] for more details.

7.1.4 Sketch of the proof

The main ingredient of the proof is the Γ-convergence for which we give the definition and the main properties.

Definition 20. *Let (X, d) a metric space and for $\varepsilon > 0$ define: $F_\varepsilon : X \mapsto [-\infty, +\infty]$. We say that F_ε Γ-converges to F as ε goes to 0 if for every $x \in X$*

1. *for every sequence $(x_\varepsilon)_{\varepsilon>0}$ converging to x, $F(x) \leqslant \liminf_{\varepsilon\to 0} F_\varepsilon(x_\varepsilon)$*
2. *there exists a sequence (x_ε) converging to x such that $\limsup_{\varepsilon\to 0} F_\varepsilon(x_\varepsilon) \leqslant F(x)$*

Proposition 40. 1. *The Γ-limit is always l.s.c*

2. *If G is a continuous function over X and F_ε Γ-converges to F, then $F_\varepsilon + G$ Γ-converges to $F + G$.*
3. *Assume F_ε Γ-converges to F and let x_ε be a minimiser of F_ε over X. Then every limit point of x_ε is a minimiser of F.*

It is very useful then to show Γ−convergences of a suitable sequence of functionals together with compactness properties of the minimising sequences. More details can be found e.g in [27]

Proof of theorem 15 We study problem $(\mathcal{P}^{\delta,\rho,\varepsilon}_{\text{elast}})$ by showing that it Γ- converges to problem $(\mathcal{P}^{\delta,\rho}_{\text{elast}})$ as ε goes to 0 together with a compactness result, and we prove that problem $(\mathcal{P}^{\delta,\rho,\varepsilon}_{\text{elast}})$ always admits a solution. For that purpose we need to slightly modify the perimeter penalization in order to insert the volume constraints.

for $\rho \in L^1(D)$, let

$$P_\varepsilon^\theta(\rho) = \begin{cases} P_\varepsilon(\rho) & \text{if } \int_D \tilde{L}(\rho)\, dx = \theta_1|D| \text{ etc...} \\ +\infty & \text{otherwise} \end{cases}$$

Similarly define for $\rho \in L^1(D)$, $\overline{P}^\theta(\rho) = \overline{P}(\rho)$ if $|\{\rho = \alpha\}| = \theta_\alpha|D|$ for $\alpha = -1, 0, 1$ and $\overline{P}^\theta(\rho) = +\infty$ otherwise.

Note that the inradius constraint does not cause problem because if $(\rho_n)_{n\in\mathbb{N}}$ is a sequence of functions in $L^1(D)$ with $\rho_n = 0$ a.e in D_0 for all n, with $\rho_n \to \rho$ in $L^1(D)$, then $\rho = 0$ a.e. in D_0. As a consequence, the condition that the solide phase contains a disk is stable. So we insert it in the spaces $\overline{X}_\rho$ and X_ρ and do not pay attention to it anymore.

The authors then provide two results. The first one is the continuity of the compliance:

Lemma 18 ([20], Lemma 3.2)**.** *For all $\delta > 0$, the functional $\rho \in L^1(D) \mapsto C^\delta(\rho)$ is continuous in $L^1(D)$.*

This result is shown by proving that the infinimum in the definition of the compliance is actually a minimum. Then they prove the Γ- convergence of the perimeter penalization together with a compactness result:

Proposition 41 ([20], Theorem 3.1)**.** *As ε goes to 0, P_ε Γ-converges to $\overline{P}$ and P_ε^θ Γ-converges to $\overline{P}^\theta$. Moreover if ρ_ε is a sequence in $L^1(D)$ such that $\sup_{\varepsilon>0} P_\varepsilon(\rho_\varepsilon) < +\infty$, then there exists a sequence $\varepsilon_j \to 0$ and $\rho \in \overline{X}_\rho$ such that $\rho_{\varepsilon_j} \to \rho$ in $L^1(D)$.*

This result is an adaptation of the Modica-Mortola theorem about the Γ-convergence of the Cahn-Hiliard energy to the perimeter functional. The original theorem was stated in a two phases model and the authors adapted it for three phases.

From this we deduce that the functional $C^\delta + P_\varepsilon^\theta$ Γ- converges to $C^\delta + \overline{P}^\theta$.

It remains to prove that $C^\delta + P_\varepsilon^\theta$ admits a minimiser ρ_ε.

Proposition 42. *The functional $C^\delta + P_\varepsilon^\theta$ admits a minimiser $\rho_\varepsilon \in X_\rho$ which satisfies the volume constraints.*

Proof. If ρ_n is a minimising sequence, then it is bounded in $H^1(D)$, hence converges up to a subsequence to $\rho \in H^1(D)$ strongly in $L^2(D)$ weakly in $H^1(D)$. Since D is bounded, ρ_n converges in $L^1(D)$. By lower semicontinuity of P_ε and continuity of C^δ in $L^1(D)$ we deduce that ρ is a minimiser of $C^\delta + P_\varepsilon^\theta$. By definition of P_ε^θ we have $\rho \in X_\rho$ and satisfies the volume constraint. □

Now we apply Proposition 41 to a sequence ρ_ε of minimisers of $C^\delta + P_\varepsilon^\theta$ together with Proposition 40, we deduce that the limit function ρ is a minimiser of $C^\delta + \overline{P}^\theta$, hence is a solution of the problem $(\mathcal{P}^{\delta,\rho,\varepsilon}_{\text{elast}})$. Hence the result is proved for any $\delta > 0$. At this stage it remains to prove the convergence of the fictitious material formulation, as δ goes to 0.

Convergence of the fictitious material formulation: proof of theorem (14) The analysis of this problem is performed by a dual formulation of a perturbed problem. For that purpose we proceed as in the book of I. Ekeland and R. Teman [35]. Recall that

$$C^\delta(\rho) = -2 \inf_{u \in H^1_0(D)} \mathcal{E}^\delta_\rho(u) \tag{7.19}$$

with

$$\mathcal{E}_\rho^\delta(u) = \frac{1}{2}\int_D (\delta + (1-\delta)\tilde{S}(\rho))Ae(u) : e(u)\ dx + \int_D \tilde{L}(\rho)\,\mathrm{div}(p_0 u)\ dx - \int_{\partial D} p_0 u \cdot n_D\ ds.$$

Hence we introduce for $\rho \in L^1(D)$ and $\delta > 0$ fixed a perturbed energy:

$$\Phi_{\delta,\rho}(u,q) = \frac{1}{2}\int_D (\delta+(1-\delta)\tilde{S}(\rho))(Ae(u)+q) : (e(u)+q)\ dx + \int_D \tilde{L}(\rho)\,\mathrm{div}(p_0 u)\ dx - \int_{\partial D} p_0 u\cdot n_D\ ds,$$

defined for $u \in H_0^1(D)$ and $q \in L^2(D, \mathbb{S}_2(\mathbb{R}))$. Since A is a positive operator, and $\delta + (1-\delta)S(\rho) > 0$, $\Phi_{\delta,\rho}$ is convex. Note that $\Phi_{\delta,\rho}(u,0) = \mathcal{E}_\rho^\delta(u)$, hence the notion of perturbed energy: the original energy is perturbed by adding a term. Now we define the function h by:

$$h(q) = \inf_{u\in H_0^1(D)} \phi_{\delta,\rho}(u,q) \tag{7.20}$$

Note that $h(0) = C^\delta(\rho)$.

Following the theory developed in [35], we consider the dual problem of (7.19):

$$\sup_{\sigma\in L^2(D,\mathbb{S}_2(\mathbb{R}))} -\Phi^\star_{\delta,\rho}(0,\sigma), \tag{7.21}$$

where $\Phi^\star_{\delta,\rho}$ is the Fenchel conjugate of $\Phi_{\delta,\rho}$. Recall that the Fenchel conjugate of a functional F defined on a vector space V and its dual space $V^\star$ is a function defined on $V^\star$ by:

$$F^\star(u^\star) = \sup_{u\in V}(\langle u^\star, u\rangle - F(u)),$$

for all $u^\star \in V^\star$. The quantity may be equal to $+\infty$. So by definition:

$$\Phi^\star_{\delta,\rho}(0,\sigma) = \sup_{u\in H_0^1(D), q\in L^2(D,\mathbb{S}_2(\mathbb{R}))} \int_D q : \sigma\ dx - \Phi_{\delta,\rho}(u,q).$$

After computations (see [20])it comes:

$$\Phi^\star_{\delta,\rho}(0,\sigma) = \frac{1}{2}\int_D \frac{1}{\delta+(1-\delta)\tilde{S}(\rho)} A^{-1}\sigma : \sigma\ dx + \sup_{u\in H_0^1(D)} \int_D -e(u) : \sigma + S(\rho)f\cdot u + \tilde{L}(\rho)\,\mathrm{div}(pu)dx - \int_{\partial D} p_0 u\cdot n_D ds. \tag{7.22}$$

Finally we have:

$$\Phi^\star_{\delta,\rho}(0,\sigma) = \frac{1}{2}\int_D \frac{1}{\delta+(1-\delta)\tilde{S}(\rho)} A^{-1}\sigma : \sigma\ dx$$

if for all $u \in H_0^1(D)$

$$\int_D -e(u) : \sigma + \tilde{S}(\rho)f\cdot u + \tilde{L}(\rho)\,\mathrm{div}(pu)dx - \int_{\partial D} p_0 u\cdot n_D ds = 0,$$

and $\Phi^\star_{\delta,\rho}(0,\sigma) = +\infty$ else.

Now define $F_\delta(\rho,\sigma) = \Phi^\star_{\delta,\rho}(0,\sigma)$.

Proposition 43. *For all $\rho \in L^1(D)$.*

$$C^\delta(\rho) = 2 \inf_{\sigma \in L^2(D,\mathbb{S}_2(\mathbb{R}))} F_\delta(\rho,\sigma),$$

and there exists $\sigma_\rho \in L^2(D,\mathbb{S}_2(\mathbb{R}))$ such that $C^\delta(\rho) = 2F_\delta(\rho,\sigma_\rho)$

This result is a direct consequence of paragraph III,4 of [35], and more precisely Theorem 4.1.

Now consider $\mathcal{F}_\delta(\rho,\sigma) = 2F_\delta(\rho,\sigma) + \lambda\overline{P}(\rho)$ for $\delta > 0$, $\rho \in L^1(D)$ and $\sigma \in L^2(D,\mathbb{S}_2(\mathbb{R}))$, and $\mathcal{F}^\theta_\delta(\rho,\sigma) = 2F_\delta(\rho,\sigma) + \lambda\overline{P}^\theta(\rho)$.

We define what will be the limit functional as δ goes to 0. For $\rho \in \overline{X}_\rho$, $\sigma \in L^2(D,\mathbb{S}_2(\mathbb{R}))$,

$$F_0(\rho,\sigma) = \frac{1}{2}\int_{S(\rho)} A^{-1}\sigma : \sigma \; dx,$$

if $\sigma = 0$ a.e in $V(\rho) \cup L(\rho)$ and for all $u \in H^1_0(D)$:

$$\int_D -e(u) : \sigma + \tilde{S}(\rho) f \cdot u + \tilde{L}(\rho)\,\mathrm{div}(pu)dx - \int_{\partial D} p_0 u \cdot n_D ds = 0,$$

and $F_0(\rho,\sigma) = +\infty$ otherwise.

We define

$$C_0(\rho) = 2 \inf_{\sigma \in L^2(D,\mathbb{S}_2(\mathbb{R}))} F_0(\rho,\sigma).$$

the authors show in Section 4.3 that for $\rho \in \overline{X}_\rho$,

$$C_0(\rho) = C(S,L,V). \tag{7.23}$$

where $S = \{\rho = 0\}$, $V = \{\rho = -1\}$, $L = \{\rho = 1\}$.

Again define $\mathcal{F}_0(\rho,\sigma) = 2F_0(\rho,\sigma) + \lambda\overline{P}(\rho)$ and $\mathcal{F}^\theta_0(\rho,\sigma) = 2F_0(\rho,\sigma) + \lambda\overline{P}^\theta(\rho)$.

Proposition 44. *[20][Theorem 4.1] As δ goes to 0, $\mathcal{F}_\delta$ Γ-converges to $\mathcal{F}_0$ in $L^1(D)\times(L^2(D,\mathbb{S}_2(\mathbb{R}))-$ weak) and $\mathcal{F}^\theta_\delta$ Γ-converges to $\mathcal{F}^\theta_0$. Moreover if for $\delta > 0$ $\rho_\delta, \sigma_\delta$, $\mathcal{F}_\delta(\rho_\delta,\sigma_\delta) < +\infty$, there exists ρ,σ and a sequence $\delta_j \to 0$ such that $\rho_{\delta_j} \to \rho$ in $L^1(D)$ and $\sigma_{\delta_j} \rightharpoonup \sigma$ weak in $L^2(D,\mathbb{S}_2(\mathbb{R}))$.*

They finally show the last result by considering a sequence σ_ρ of minimiser of $F_\delta(\rho,\bullet)$ to define C^δ.

Proposition 45. *[20][Corolary 4.2] $C^\delta + \lambda\overline{P}$ Γ- converges to $C_0 + \lambda\overline{P}$ in $L^1(D)$ and $C^\delta + \lambda\overline{P}^\theta$ Γ- converges to $C_0 + \lambda\overline{P}^\theta$ in $L^1(D)$.*

In the end we deduce that there exists a sequence $\delta_j \to 0$ such that the sequence ρ_{δ_j} of solutions of $(\mathcal{P}^{\delta,\rho}_{\text{elast}})$ converges in L^1 to $\rho \in \overline{X}_\rho$ a minimiser of $C^0 + \lambda\overline{P}^\theta$,since by (7.23), $C_0(\rho) = C(S,L,V)$, where $S = \{\rho = 0\}$, $V = \{\rho = -1\}$, $L = \{\rho = 1\}$, we deduce that the triplet (S,L,V) solves $(\mathcal{P}'_{\text{elast}})$.

7.2 Optimality conditions

In this section we go back to the initial problem $(\mathcal{P}_{\text{elast}})$ with the initial notations. For this problem we have no existence results. Let us assume that $(\mathcal{P}_{\text{elast}})$ admits a solution, and try to describe the optimal shape with the help of optimality conditions. We assume that the optimal set $\Omega^\star$ has enough regularity. Let us first show that the inradius constraint is saturated.

Proposition 46. *If $\Omega^\star$ solves the problem $(\mathcal{P}_{\text{elast}})$ then $r(\Omega^\star) = 1$.*

Proof. To prove this, we first show that if Ω is an admissible set and $t > 0$, then $C(t\Omega) = t^3 C(\Omega)$. Indeed, let u be the solution of (6.4) on Ω. Then it is easy to check that $u_t(x) = t \times u(x/t)$ for $x \in t\Omega$ solves the problem on $t\Omega$. Then using a change of variable in the expression on the compliance leads to the desired identity. It follows that if $r(\Omega) = r > 1$ then taking $t = 1/r < 1$ and $\Omega_t = t\Omega$, then Ω_t is still admissible with regard to the constraints and verifies $C(\Omega_t) = tC(\Omega) < C(\Omega)$. This concludes the proof. □

To go further in the analysis we need to compute the shape derivative of the compliance.

Proposition 47 ([6])**.** *Let V be a deformation field on $\mathbb{R}^2$, i.e $V \in W^{1,\infty}(\mathbb{R}^2, \mathbb{R}^2)$. Then the shape derivative of C with respect to the vector field V is given by:*

$$\langle DC(\Omega), V\rangle = -\int_{\Gamma_T} (Ae(u) : e(u))\, V \cdot n - \int_{\Gamma_{\text{ext}}} (Ae(u) : e(u) + 2p_0 \operatorname{div}(u))\, V \cdot n \tag{7.24}$$

where u is the solution of the linear elasticity system (6.4)*.*

The first order optimality condition states that for each admissible deformation field,

$$\langle DC(\Omega), V\rangle \geqslant 0 \tag{7.25}$$

Now let us make some observations about the admissible deformations:

1. Notice that taking $V \cdot n \geqslant 0$ on Γ_T is the same as both increasing the size of Ω and decreasing the size of T.
2. Taking $V \cdot n \geqslant 0$ on Γ_{ext} only implies that we increase the size of Ω.
3. If none of the constraints are saturated then any transformation is admissible.
4. If the volume constraint is saturated, then if we take $V \cdot n \geqslant 0$ somewhere on Γ_T or Γ_{ext} we need to have $V \cdot n \neq 0$ somewhere else so that the volume deformation is 0.
5. If the mass density constraint is saturated, then if we take $V \cdot n \geqslant 0$ on Γ_T we have to take $V \cdot n \leqslant 0$ on Γ_{ext} to compensate the loss of volumes in holes.
6. The inradius is modified only if we deform the boundary at the contact points. Recall that the inradius constraint is saturated. then at those points only a deformation $V \cdot n \geqslant 0$ is admissible.

Let $f_{\text{ext}}(x) = Ae(u) : e(u)(x) + 2p\operatorname{div}(u)(x)$ and $f_T(x) = Ae(u) : e(u)(x)$ so that the derivative of the compliance writes:

$$\langle DC(\Omega), V\rangle = \int_{\Gamma_T} -f_T V \cdot n + \int_{\Gamma_{\text{ext}}} -f_{\text{ext}} V \cdot n \tag{7.26}$$

From the previous observations we see that a deformation field V such that $V \cdot n \leqslant 0$ on Γ_{ext} (resp. Γ_T) is always possible.

Writing the condition (7.25) immediately states that $f_{\text{ext}} \geqslant 0$ on Γ_{ext} (resp. $f_T \geqslant 0$ on Γ_T). We are also able to prove the following:

Proposition 48. *Let $\Omega^\star$ be a solution of $(\mathcal{P}_{\text{elast}})$ and $D_{\Omega^\star}$ the incircle of $\Omega^\star$. then there exists $c_{\text{ext}}, c_T \in \mathbb{R}$ such that for all.*

$$\begin{array}{ll} f_{\text{ext}} = c_{\text{ext}} & \text{on } \Gamma_{\text{ext}} \backslash \overline{D_{\Omega^\star}} \\ f_T = c_T & \text{on } \Gamma_T \backslash \overline{D_{\Omega^\star}} \end{array} \tag{7.27}$$

Proof. For each $x_1, x_2 \in \Gamma_{\text{ext}} \backslash \overline{D_{D^\star}}$ and $\varepsilon > 0$ consider V_1^ε (resp V_2^ε) a deformation field such that $x_1 \in \text{Supp}(V_1^\varepsilon)$ (resp. $x_2 \in \text{Supp}(V_2^\varepsilon)$) and $\text{Supp}(V_1^\varepsilon \cap \text{Supp} V_2^\varepsilon) = \emptyset$ with:

$$\int_{\Gamma_{\text{ext}}} V_1^\varepsilon \cdot n = -\int_{\Gamma_{\text{ext}}} V_2^\varepsilon \cdot n = 1.$$

And consider $V^\varepsilon = V_1^\varepsilon + V_2^\varepsilon$.

Then V^ε is admissible since it does not change the volume, and by the first order optimality condition we get:

$$\int_{\Gamma_{\text{ext}}} \left(-Ae(u) : e(u) - 2p \operatorname{div}(u)\right) V_1^\varepsilon \cdot n + \int_{\Gamma_{\text{ext}}} \left(-Ae(u) : e(u) - 2p_0 \operatorname{div}(u)\right) V_2^\varepsilon \cdot n \geqslant 0. \tag{7.28}$$

If we let V_1^ε (resp. V_2^ε) converge to $\delta_{x_1} n(x_1)$ (resp. $-\delta_{x_2} n(x_2)$) in the sense of distributions we deduce that:

$$-f_{\text{ext}}(x_1) + f_{\text{ext}}(x_2) \geqslant 0 \tag{7.29}$$

since inequality (7.29) holds for any $x_1, x_2 \in \Gamma_{\text{ext}} \backslash \overline{D_{\Omega^\star}}$ we deduce that the function is constant on $\Gamma_{\text{ext}} \backslash \overline{D_{\Omega^\star}}$.

We can do the exact same on Γ_T holes to obtain the second equality. □

In what follows, we assume that the incircle is unique and that contact regions between the incircle and the boundary of Ω has 0 length. Let V be a deformation field and $\Omega_t = (\text{Id} + tV)(\Omega)$ the deformed domain with respect to V. We recall that the area has the following asymptotic development:

$$|\Omega_t| = |\Omega| + t \int_{\partial\Omega} V \cdot n + o(t) \tag{7.30}$$

Now denote

$$\begin{array}{l} v_{\text{ext}} = \int_{\Gamma_{\text{ext}}} V \cdot n \\ v_T = -\int_{\Gamma_T} V \cdot n \end{array} \tag{7.31}$$

v_{ext} corresponds to an increase of the volume of Ω through the inflation of the outer boundary whereas v_T stands for an increase of the volume of the holes through an inflation of those latter. If v_T is positive, then the holes inflates, and the volume of Ω decreases. To sum up, we obtain the following formulas:

$$\begin{array}{l} |\Omega_t| = |\Omega| + t(v_{\text{ext}} - v_T) + o(t) \\ |T_t| = |T| + t v_T + o(t) \end{array} \tag{7.32}$$

Let us also give the derivative of the compliance in terms of v_{ext} and v_T

$$\langle DC(\Omega), V\rangle = -c_{\text{ext}} v_{\text{ext}} + c_T v_T \tag{7.33}$$

Now we can compute the derivative of the mass density $\Delta(\Omega)$.

Lemma 19. *Let V be a deformation field and $\Omega_t = (Id + tV)(\Omega)$. Then the derivative of $\Delta(\Omega)$ with respect to V is given by:*

$$\langle D\Delta(\Omega), V\rangle = \frac{1}{|\Omega \cup T|^2}\left(|T| v_{ext} - |\Omega \cup T| v_T\right) \tag{7.34}$$

Proof. The density of Ω_t is the following:

$$\begin{aligned}
\Delta(\Omega_t) &= \frac{|\Omega| + t(v_{\text{ext}} - v_T)}{|\Omega \cup T| + t v_{\text{ext}}} \\
&= \frac{|\Omega|}{|\Omega \cup T|} \frac{1 + t\frac{v_{\text{ext}} - v_T}{|\Omega|}}{1 + t\frac{v_{\text{ext}}}{|\Omega \cup T|}} \\
&= \frac{|\Omega|}{|\Omega \cup T|}\left(1 + t\left(\frac{v_{\text{ext}} - v_T}{|\Omega|} - \frac{v_{\text{ext}}}{|\Omega \cup T|}\right) + o(t)\right) \\
&= \Delta(\Omega) + t\frac{1}{|\Omega \cup T|^2}\left(|T| v_{\text{ext}} - |\Omega \cup T| v_T\right) + o(t)
\end{aligned}$$

Hence the result.

□

We deduce that a deformation V such that

$$\frac{v_T}{v_{\text{ext}}} = 1 - \Delta(\Omega) \in (0, 1)$$

does not change the mass density of Ω at the first order

Proposition 49. *Let $\Omega^\star$ be a solution of $(\mathcal{P}_{\text{elast}})$. Then either $|\Omega^\star| = V_0$ or $\Delta(\Omega^\star) = \alpha$.*

Proof. Suppose that neither of those conditions are saturated, then the deformation V such that $V \cdot n > 0$ on Γ_{ext}, and $V = 0$ in a neighborhood of Γ_T is admissible, and decreases the compliance. We deduce that at least one of those constraints is saturated. □

Now let us distinguish three possible cases:

1. Only the volume constraint is saturated.
2. Only the mass density constraint is saturated.
3. Both the mass density and volume constraint are saturated.

Before we investigate each case, let us analyse the behavior of the functional under a homothetic transformation.

If one takes $V = \text{Id}$, then

$$\Omega_t = (1 + t)\Omega.$$

We have previously shown that

$$C(\Omega_t) = (1+t)^3(\Omega),$$

leading to the following derivative:

$$\langle DC(\Omega), \mathrm{Id}\rangle = 3C(\Omega). \tag{7.35}$$

On the other hand, formula (7.24) provides another way of computing the derivative:

$$\langle DC(\Omega), \mathrm{Id}\rangle = \int_{\Gamma_T} -c_T x\cdot n + \int_{\Gamma_{\mathrm{ext}}} -f_{\mathrm{ext}} x\cdot n, \tag{7.36}$$

then applying Green theorem, with $\mathrm{div}(x) = 2$,

$$\langle DC(\Omega), \mathrm{Id}\rangle = 2(c_T|T| - c_{\mathrm{ext}}|\Omega\cup T|), \tag{7.37}$$

Combining (7.37) and (7.35) implies:

$$c_T|T| - c_{\mathrm{ext}}|\Omega\cup T| = \frac{3}{2}C(\Omega). \tag{7.38}$$

Now let us take a look at the first case. If the volume is saturated and the mass density is not, then take a deformation V such that $v_{\mathrm{ext}} = v_T > 0$. It is admissible since the volume is not changed, and the mass density is not saturated. Applying formula (7.33) yields

$$c_T \geqslant c_{\mathrm{ext}}. \tag{7.39}$$

Now observe that a deformation V with $v_{\mathrm{ext}} = v_T < 0$ is also admissible and gives the reverse inequality. We finally obtain, in this case:

$$c_T = c_{\mathrm{ext}} \tag{7.40}$$

But this equality is not compatible with equation (7.38) because the left-hand side is negative whereas the right-hand side is positive. We deduce that this case is not possible.

If the mass density constraint is saturated and the volume constraint is not, then take a deformation field V such that $\frac{v_T}{v_{\mathrm{ext}}} = 1 - \Delta(\Omega)$. Then by the same method we obtain:

$$(1-\alpha)c_T = c_{\mathrm{ext}} \tag{7.41}$$

where $\alpha = \Delta(\Omega)$. Now injecting (7.41) in the left-hand side of (7.38) gives:

$$c_T|T| - c_{\mathrm{ext}}|\Omega\cup T| = c_T\left(|T| - \frac{|T|}{|\Omega\cup T|}|\Omega\cup T|\right) = 0$$

which is also incompatible with the right-hand side of (7.38). This case is also not possible.

Remark 24. We actually should have taken $v_{\mathrm{ext}} < v_T$ in order to be certain that the transformation is admissible. But taking a sequence V_n such that $v_{\mathrm{ext}}^n \nearrow v_T^n$ leads to the same conclusion.

We deduce the following result:

Theorem 16. *Let $\Omega^\star$ be an optimal shape for problem $(\mathcal{P}_{\mathrm{elast}})$. Suppose that the incircle is unique, and that the intersection between the boundary of the incircle and the boundary of $\Omega^\star$ has 0 length. Then $r(\Omega^\star) = 1$, $|\Omega^\star| = V_0$, and $\Delta(\Omega^\star) = \alpha$.*

The end of this part is devoted to the study of the creation of holes. Although very useful, the Hadamard derivative does not allow to treat the creation of holes. Fortunately there is a specific tool that studies the evolution of a functional shape when creating a hole: the topological derivative.

Definition 21. *Let $D \subset \mathbb{R}^2$ an reference set and $x_0 \in \Omega$. for $\rho > 0$ consider $D_\rho = x_0 + \rho D$ and $\Omega_\rho = \Omega \backslash D_\rho$. The functional J is said to have a topological derivative at Ω with respect to D and x_0 if J admits an asymptotic expansion at Ω:*

$$J(\Omega_\rho) = J(\Omega) + h(\rho)G(x_0) + o(h(\rho)) \tag{7.42}$$

where $h(\rho) > 0$ and $\lim_{\rho \to 0} h(\rho) = 0$. $G(x_0)$ is the topological derivative of Ω.

There already exists a formula for the topological derivative for the compliance when we create a small circular hole at location x_0

Proposition 50 ([44])**.** *Let Ω a bounded Lipschitz domain in $\mathbb{R}^2$, $x_0 \in \Omega$ and $D = D(0,1)$. Then J has the following asymptotic expansion:*

$$C(\Omega_\rho) = C(\Omega) + \rho^2 G(x_0) + o(\rho^2). \tag{7.43}$$

where

$$G(x_0) = \frac{\pi(\lambda + 2\mu)}{2\mu(\lambda + \mu)} \left[(4\mu Ae(u) : e(u) + (\lambda - \mu) \operatorname{Tr}(Ae(u)) \operatorname{Tr}(e(u)))(x_0) \right].$$

If we replace A by its expression: $AX = 2\mu X + \lambda \operatorname{Tr}(X) I_2$, we obtain:

$$G(x_0) = \frac{\pi(\lambda + 2\mu)}{2\mu(\lambda + \mu)} \left[(8\mu^2 |e(u)|^2 + 2(\lambda^2 - \mu^2 + 2\mu\lambda) \operatorname{div}(u)^2)(x_0) \right].$$

If $A \in \mathbb{S}_2(\mathbb{R})$ is a symmetric matrix, consider the decomposition

$$A = A^d + A^h,$$

where $A^d = A - \frac{1}{2} \operatorname{Tr}(A) I_2$ and $A^h = \frac{1}{2} \operatorname{Tr}(A) I_2$, then $A^d : A^h = 0$ and $|A|^2 = |A^d|^2 + |A^h|^2$. We obtain that:

$$4\mu^2 |A|^2 + (\lambda^2 - \mu^2 + 2\mu\lambda) \operatorname{Tr}(A)^2 = 4\mu^2 |A^d|^2 + 2(\lambda + \mu)^2 |A^h|^2 > 0,$$

From which we deduce that $G(x_0) > 0$ for all $x \in \Omega$ because $\operatorname{Tr}(e(u)) = \operatorname{div}(u)$. That means that creating a hole increase the compliance, which is not a surprise.

Remark 25. This result could have been proven by using the definition of compliance as a minimum of an energy functional and by choosing suitable test functions.

The real question here is whether it is worth to create a small hole while reducing the size of another one. Indeed, if it is always the case, then there is no solution to our problem since whatever the shape we have, it is possible to improve it indefinitely by repeating this operation.

Let $\Omega^\star$ be the solution of $(\mathcal{P}_{\text{elast}})$ and consider the creation of a hole of radius ε at location $x_0 \in \Omega^\star$. That hole has area $\pi\varepsilon^2$, and In order to satisfy the constraints we need to diminish the size of another hole. For that purpose consider a deformation field V such that $v_{\text{ext}} = 0$ and $v_T = -\pi$. Let $\Omega_\varepsilon = \Omega + \varepsilon^2 V(\Omega^\star) + D(x_0, \varepsilon)$, then

$$J(\Omega_\varepsilon) = J(\Omega) - \pi\varepsilon^2 c_T + G(x_0)\varepsilon^2 + o(\varepsilon^2) \tag{7.44}$$

The question is now phrased in this way: is there $x_0 \in \Omega$ such that $G(x_0) < \pi c_T$?
That problem remains to be investigated.

Conclusion

In this thesis we studied a problem of biology where the aim is to explain the shape of *Eulimnadia* eggs. For this purpose we used the inverse modeling method. We proposed biological hypotheses that we modeled in a mathematical manner, more precisely as a shape optimization problem. We have proposed two models.

First model based on a packing approach The first model is based on the general idea that to ensure the survival of a species it is advantageous to have many offspring. For *Eulimnadia* this implies the capacity to store a large number of eggs in its brood chamber, leading to packing problem. For the mathematical modeling that we obtained, we were able to provide the solution: depending on the value of certain parameters the solution is a shape varying from the 2 cap body to its tiling closure. Although this particular shape is observed in a specific species of *Eulimnadia*, *Australimnadia giganta*, in general the shape of eggs of *Eulimnadia* does not quite resemble the theoretical solution. However, by studying a close shape optimization problem in Part II, we have identified more similar shapes. This gives an idea of how to improve the model.

Second model based on an elasticity approach In the second model we studied the resistance of the shell to external pressures, taking into account the fact that the shell must be light enough to float on the surface. In the second model we studied the resistance of the shell to external pressures, taking into account the fact that the shell must be light enough to float on the surface. It is still an ongoing work: for the moment we obtained the existence of a solution, but we cannot ensure that the solution is connected, i.e it is made of a single piece. We are working on adding constraints that ensure that the solution is connected. However there is little hope that the we can theoretically compute the solution and we are working on programming an algorithm to compute it numerically.

Perspectives

Mathematical perspective As underlined throughout the manuscript we worked in two dimensions. A natural prospect is to extend the work to the higher dimensions. We could also carry out the same study as the one carried out in the first part, but this time considering a minimization of the diameter rather than a maximization, which seems to give shapes closer to the real shape of the eggs.

As said previously, in the problem of elasticity it remains to adapt the work already done by adding a functional penalizing the non-connectedness, and to carry out numerical experiments using a geometric shape optimization approach, as well as the algorithm described in the proof of existence of an optimal shape.

Biological perspective Work is in progress with Nicolas Rabet to compute the real values of the functional described in the first part and compare it to more conventional shapes such as the sphere. it requires to compute the packing density of a given shape. We are working on an algorithm that is capable to compute the smallest p-hexagon circumscribed about a given convex set.

In this thesis we focused more on the main shape of the egg, as opposed to the folds observed on the surface of the shell. Now let us discuss a little bit about the folds. We propose two leads for that problem. Some biologists suggest that ornaments provide defenses against predators (see [34]) and resistance to erosion (see [42]). These explanations seem satisfactory when the ornamentation is in the shape of spikes. Let us highlight another point of view. There are works in mechanical science studying the surface-pattern selection in curved bilayer systems consisting of a stiff film on a soft substrate (see e.g [91]). In other words, we consider a rigid outer layer connected to a flexible inner layer. When the inner layer contracts, this causes a deformation of the rigid layer and we observe shapes as described in Figure 3. The different shapes are obtained by considering different rigidity parameters:

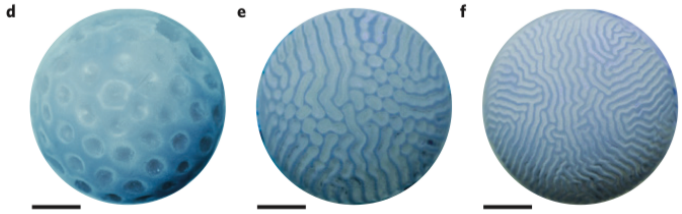

Figure 3: Ornementation obtained by a bi-phase modeling. Source [91]

The shapes obtained are rather convincing and it would be interesting to see if this modeling can be applied to the eggs of Eulimnadia. However, this study goes beyond the field of mathematics.

Bibliography

[1] What is a random packing? *Nature*, pages 488–489, 1972.

[2] G. Alberti. Variational models for phase transitions, an approach via Γ-convergence. In *Calculus of variations and partial differential equations (Pisa, 1996)*, pages 95–114. Springer, Berlin, 2000.

[3] G. Allaire. *Shape optimization by the homogenization method*, volume 146 of *Applied Mathematical Sciences*. Springer-Verlag, New York, 2002.

[4] G. Allaire. *Conception optimale de structures*, volume 58 of *Mathématiques & Applications (Berlin) [Mathematics & Applications]*. Springer-Verlag, Berlin, 2007. With the collaboration of Marc Schoenauer (INRIA) in the writing of Chapter 8.

[5] G. Allaire and A. Henrot. On some recent advances in shape optimization. *Comptes rendus de l'Académie des Sciences de Paris*, 329(5):383–396, 2001.

[6] G. Allaire, F. Jouve, and A.-M. Toader. Structural optimization using sensitivity analysis and a level-set method. *J. Comput. Phys.*, 194(1):363–393, 2004.

[7] L. Ambrosio and G. Buttazzo. An optimal design problem with perimeter penalization. *Calc. Var. Partial Differential Equations*, 1(1):55–69, 1993.

[8] L. Ambrosio, N. Fusco, and D. Pallara. *Functions of bounded variation and free discontinuity problems*. Oxford Mathematical Monographs. The Clarendon Press, Oxford University Press, New York, 2000.

[9] P. Antunes and B. Bogosel. Parametric shape optimization using the support function. *Preprint*, 2018.

[10] P. R. S. Antunes and A. Henrot. On the range of the first two Dirichlet and Neumann eigenvalues of the Laplacian. *Proc. R. Soc. Lond. Ser. A Math. Phys. Eng. Sci.*, 467(2130):1577–1603, 2011.

[11] T. Bayen. *"Shape optimization in the class of constant width bodies and of rotors"*. Theses, Université Pierre et Marie Curie - Paris VI, June 2007.

[12] T. Bayen and J.-B. Hiriart-Urruty. Objets convexes de largeur constante (en 2D) ou d'épaisseur constante (en 3D): du neuf avec du vieux. *Ann. Sci. Math. Québec*, 36(1):17–42 (2013), 2012.

[13] L. Bellec and N. Rabet. Dating of the limnadiidae family suggests an american origin of eulimnadia. *Hydrobiologia*, 773:149–161, 2016.

[14] M. Belloni and E. Oudet. The minimal gap between $\Lambda_2(\Omega)$ and $\Lambda_\infty(\Omega)$ in a class of convex domains. *J. Convex Anal.*, 15(3):507–521, 2008.

[15] M. Berger. *Geometry revealed*. Springer, Heidelberg, 2010. A Jacob's ladder to modern higher geometry, Translated from the French by Lester Senechal.

[16] W. Blaschke. Konvexe Bereiche gegebener konstanter Breite und kleinsten Inhalts. *Math. Ann.*, 76:504–513, 1915.

[17] W. Blaschke. Eine Frage über konvexe Körper. *Jahresber. Dtsch. Math.-Ver.*, 25:121–125, 1916.

[18] T. Bonnesen and W. Fenchel. *Theory of convex bodies*. BCS Associates, Moscow, ID, 1987. Translated from the German and edited by L. Boron, C. Christenson and B. Smith.

[19] K. Böröczky, Jr., M. A. Hernández Cifre, and G. Salinas. Optimizing area and perimeter of convex sets for fixed circumradius and inradius. *Monatsh. Math.*, 138(2):95–110, 2003.

[20] B. Bourdin and A. Chambolle. Design-dependent loads in topology optimization. *ESAIM Control Optim. Calc. Var.*, 9:19–48, 2003.

[21] H. Brezis. *Functional analysis, Sobolev spaces and partial differential equations*. Universitext. Springer, New York, 2011.

[22] D. Bucur, G. Buttazzo, and I. Figueiredo. On the attainable eigenvalues of the Laplace operator. *SIAM J. Math. Anal.*, 30(3):527–536, 1999.

[23] G. Buttazzo and G. Dal Maso. An existence result for a class of shape optimization problems. *Arch. Rational Mech. Anal.*, 122(2):183–195, 1993.

[24] P. G. Ciarlet. *Mathematical elasticity. Vol. I*, volume 20 of *Studies in Mathematics and its Applications*. North-Holland Publishing Co., Amsterdam, 1988. Three-dimensional elasticity.

[25] P. G. Ciarlet. On Korn's inequality. *Chin. Ann. Math. Ser. B*, 31(5):607–618, 2010.

[26] R. Courant. The least dense lattice packing of two-dimensional convex bodies. *Comm. Pure Appl. Math.*, 18:339–343, 1965.

[27] G. Dal Maso. *An introduction to* Γ*-convergence*, volume 8 of *Progress in Nonlinear Differential Equations and their Applications*. Birkhäuser Boston, Inc., Boston, MA, 1993.

[28] F. Dayrens, S. Masnou, M. Novaga, and M. Pozzetta. Connected perimeter of planar sets, 2019.

[29] A. Delyon, A. Henrot, and Y. Privat. Nondispersal and density properties of infinite packings. *SIAM J. Control Optim.*, 57(2):1467–1492, 2019.

[30] A. Delyon, A. Henrot, and Y. Privat. The missing (A, D, r) diagram. preprint, https://hal.archives-ouvertes.fr/hal-02559553v1, May 2020.

[31] K. R. Doheny. On the lower bound of packing density for convex bodies in the plane. *Beiträge Algebra Geom.*, 36(1):109–117, 1995.

[32] P. W. Dondl, M. Novaga, B. Wirth, and S. Wojtowytsch. Approximation of the relaxed perimeter functional under a connectedness constraint by phase-fields. *SIAM J. Math. Anal.*, 51(5):3902–3920, 2019.

[33] R.-J. Duff, S.-K. Reed, and S. Weeks. A systematic study of the genus eulimnadia. *Journal of Crustacean Biology*, 35:379–391, 2015.

[34] H. J. Dumont, S. Nandini, and S. S. S. Sarma. Cyst ornamentation in aquatic invertebrates: a defence against egg-predation). *Hydrobiologia*, 486(1):161–167, 2002.

[35] I. Ekeland and R. Témam. *Convex analysis and variational problems*, volume 28 of *Classics in Applied Mathematics*. Society for Industrial and Applied Mathematics (SIAM), Philadelphia, PA, english edition, 1999. Translated from the French.

[36] L. C. Evans and R. F. Gariepy. *Measure theory and fine properties of functions*. Textbooks in Mathematics. CRC Press, Boca Raton, FL, revised edition, 2015.

[37] I. Fáry. Sur la densité des réseaux de domaines convexes. *Bull. Soc. Math. France*, 78:152–161, 1950.

[38] L. Fejes. über die dichteste Kugellagerung. *Math. Z.*, 48:676–684, 1943.

[39] G. Fejes Tóth. Densest packings of typical convex sets are not lattice-like. *Discrete Comput. Geom.*, 14(1):1–8, 1995.

[40] L. Fejes Tóth. Some packing and covering theorems. *Acta Sci. Math. (Szeged)*, 12:62–67, 1950.

[41] I. Ftouhi and J. Lamboley. Blaschke-Santaló diagram for volume, perimeter and first Dirichlet eigenvalue. Preprint, https://hal.archives-ouvertes.fr/hal-02850711, June 2020.

[42] E. Garcia-Roger, M. Carmora, and S. M. Deterioration patterns in diapausing egg banks of brachionus. *J. Exp. Mar. Biol. Ecol.*, pages 149–161, 2005.

[43] M. Gardner. *Time travel and other mathematical bewilderments*. W. H. Freeman and Company, New York, 1988.

[44] S. Garreau, P. Guillaume, and M. Masmoudi. The topological asymptotic for PDE systems: the elasticity case. *SIAM J. Control Optim.*, 39(6):1756–1778, 2001.

[45] B. Gilchrist. Tscanning electron microscope studies of the egg shell in some anostraca (crustacea: Branchiopoda). *Cell Tissue Res*, pages 337–351, 1978.

[46] H. Groemer. Some basic properties of packing and covering constants. *Discrete Comput. Geom.*, 1(2):183–193, 1986.

[47] P. M. Gruber. *Convex and discrete geometry*, volume 336 of *Grundlehren der Mathematischen Wissenschaften [Fundamental Principles of Mathematical Sciences]*. Springer, Berlin, 2007.

[48] P. M. Gruber and J. M. Wills, editors. *Handbook of convex geometry. Vol. A, B*. North-Holland Publishing Co., Amsterdam, 1993.

[49] B. Grünbaum and G. C. Shephard. *Tilings and patterns*. W. H. Freeman and Company, New York, 1987.

[50] T. Hales and W. Kusner. Packings of regular pentagons in the plane, 2016.

[51] T. C. Hales. The honeycomb conjecture. *Discrete Comput. Geom.*, 25(1):1–22, 2001.

[52] T. C. Hales. A proof of the Kepler conjecture. *Ann. of Math. (2)*, 162(3):1065–1185, 2005.

[53] E. M. Harrell, A. Henrot, and J. Lamboley. On the local minimizers of the Mahler volume. *J. Convex Anal.*, 22(3):809–825, 2015.

[54] E. M. Harrell, II. A direct proof of a theorem of Blaschke and Lebesgue. *J. Geom. Anal.*, 12(1):81–88, 2002.

[55] S. Hathaway, D. Sheehan, and M. Simovich. Vulnerability of branchiopod cysts to crushingt. *J. Crustacean Biol.*, pages 448–452, 1996.

[56] M. Henk and G. A. Tsintsifas. Some inequalities for planar convex figures. *Elem. Math.*, 49(3):120–125, 1994.

[57] M. Henk and G. A. Tsintsifas. Some inequalities for planar convex figures. *Elem. Math.*, 49(3):120–125, 1994.

[58] A. Henrot and M. Pierre. *Shape Variation and Optimization*, volume 28 of *Tracts in Mathematics*. European Mathematical Society, Zürich, 2018.

[59] M. A. Hernández Cifre. Is there a planar convex set with given width, diameter, and inradius? *Amer. Math. Monthly*, 107(10):893–900, 2000.

[60] M. A. Hernández Cifre. Optimizing the perimeter and the area of convex sets with fixed diameter and circumradius. *Arch. Math. (Basel)*, 79(2):147–157, 2002.

[61] M. A. Hernández Cifre and S. Segura Gomis. The missing boundaries of the Santaló diagrams for the cases (d, ω, R) and (ω, R, r). *Discrete Comput. Geom.*, 23(3):381–388, 2000.

[62] M. a. A. Hernández Cifre and G. Salinas. Some optimization problems for planar convex figures. *Rend. Circ. Mat. Palermo (2) Suppl.*, (70, part I):395–405, 2002. IV International Conference in "Stochastic Geometry, Convex Bodies, Empirical Measures & Applications to Engineering Science", Vol. I (Tropea, 2001).

[63] I. M. Jaglom and V. G. Boltjanskiĭ. *Convex figures*. Translated by Paul J. Kelly and Lewis F. Walton. Holt, Rinehart and Winston, New York, 1960.

[64] Y. Kallus. Pessimal packing shapes. *Geom. Topol.*, 19(1):343–363, 2015.

[65] R. B. Kershner. On paving the plane. *Amer. Math. Monthly*, 75:839–844, 1968.

[66] V. Klee and M. C. Laskowski. Finding the smallest triangles containing a given convex polygon. *J. Algorithms*, 6(3):359–375, 1985.

[67] G. Kuperberg and W. Kuperberg. Double-lattice packings of convex bodies in the plane. *Discrete Comput. Geom.*, 5(4):389–397, 1990.

[68] W. Kuperberg. Packing convex bodies in the plane with density greater than $\frac{3}{4}$. *Geom. Dedicata*, 13(2):149–155, 1982.

[69] J. Lamboley and A. Novruzi. Polygons as optimal shapes with convexity constraint. *SIAM J. Control Optim.*, 48(5):3003–3025, 2009/10.

[70] G. Letac. Mesures sur le cercle et convexes du plan. *Ann. Sci. Univ. Clermont-Ferrand II Probab. Appl.*, (1):35–65, 1983.

[71] I. Lucardesi and D. Zucco. On blaschke-santaló diagrams for the torsional rigidity and the first dirichlet eigenvalue. preprint, https://arxiv.org/abs/1910.04454, October 2019.

[72] F. Maggi. *Sets of finite perimeter and geometric variational problems*, volume 135 of *Cambridge Studies in Advanced Mathematics*. Cambridge University Press, Cambridge, 2012. An introduction to geometric measure theory.

[73] C. Mann, J. McLoud-Mann, and D. Von Derau. Convex pentagons that admit i-block transitive tilings. *Geom. Dedicata*, 194:141–167, 2018.

[74] L. Modica. The gradient theory of phase transitions and the minimal interface criterion. *Arch. Rational Mech. Anal.*, 98(2):123–142, 1987.

[75] J. Morris and A. BA. The structure of the shell and outer membranes in encysted artemia salina embryos during cryptobiosis and development. *J. Ultra. Mol. Struct. R*, pages 244–259, 1967.

[76] F. Murat and J. Simon. Sur le contrôle par un domaine géométrique. *Technical support*, 1976.

[77] J. A. Nitsche. On Korn's second inequality. *RAIRO Anal. Numér.*, 15(3):237–248, 1981.

[78] J. O'Rourke, A. Aggarwal, S. Maddila, and M. Baldwin. An optimal algorithm for finding minimal enclosing triangles. *J. Algorithms*, 7(2):258–269, 1986.

[79] O. Pârvu and D. Gilbert. Implementation of linear minimum area enclosing triangle algorithm. *Comput. Appl. Math.*, 35(2):423–438, 2016.

[80] N. Rabet. Revision of the egg morphology of eulimnadia (crustacea, branchiopoda, spinicaudata). *Zoosystema*, pages 373–391, 2010.

[81] M. Rao. Exhaustive search of convex pentagons which tile the plane. *Arxiv.org, arXiv:1708.00274*.

[82] J. W. S. Rayleigh, Baron. *The Theory of Sound*. Dover Publications, New York, N. Y., 1945. 2d ed.

[83] K. Reinhardt. *"Über die Zerlegung der Ebene in Polygone"*. Theses, Hohe Naturwissenschaften Fakultät der Königlichen Universität zu Frankfurt a.M, 1918.

[84] K. Reinhardt. Über die dichteste gitterf örmige lagerung kongruenter bereiche in der ebene und eine besondere art konvexer kurven. *Abh. Math. Sem. Univ. Hamburg*, 10(1):216–230, 1934.

[85] A. Rodriguez-Navarro, O. Kalin, Y. Nys, and J. Garcia-Ruiz. Influence of the microstructure on the shell strength of eggs laid by hens of different ages. *British Poultry Science*, 43(3):395–403, 2002. PMID: 12195799.

[86] C. A. Rogers. The closest packing of convex two-dimensional domains. *Acta Math.*, 86:309–321, 1951.

[87] C. A. Rogers. *Packing and covering*. Cambridge Tracts in Mathematics and Mathematical Physics, No. 54. Cambridge University Press, New York, 1964.

[88] L. A. Santaló. On complete systems of inequalities between elements of a plane convex figure. *Math. Notae*, 17:82–104, 1959/61.

[89] R. Schneider. *Convex bodies: the Brunn-Minkowski theory*, volume 151 of *Encyclopedia of Mathematics and its Applications*. Cambridge University Press, Cambridge, expanded edition, 2014.

[90] P. R. Scott and P. W. Awyong. Inequalities for convex sets. *JIPAM. J. Inequal. Pure Appl. Math.*, 1(1):Article 6, 6, 2000.

[91] N. Stoop, R. Lagrange, D. Terwagne, P. M. Reis, and J. Dunkel. Curvature-induced symmetry breaking determines elastic surface patterns. *Nature Materials*, 14:337–342, 2014.

[92] A. D. Vaĭnsteĭn. Construction of the minimal enclosing parallelogram. *Diskret. Mat.*, 2(4):72–81, 1990.

[93] Y. Yang and D. Zhang. Two optimisation problems for convex bodies. *Bull. Aust. Math. Soc.*, 93(1):137–145, 2016.

[94] C. Zong. Packing, covering and tiling in two-dimensional spaces. *Expo. Math.*, 32(4):297–364, 2014.

Résumé

Dans cette thèse nous nous intéressons à un problème de mathématiques appliquées à la biologie. Le but est d'expliquer la forme des oeufs d'*Eulimnadia*, un petit animal appartenant à la classe des *Branchiopodes*, et plus précisément les *Limnadiides*. En effet, d'après la théorie de l'évolution il est raisonnable de penser que la forme des êtres vivants où des objets issus d'êtres vivants est optimisée pour garantir la survie et l'expansion de l'espèce en question.

Pour ce faire nous avons opté pour la méthode de modélisation inverse. Cette dernière consiste à proposer une explication biologique à la forme des œufs, puis de la modéliser sous forme d'un problème de mathématique, et plus précisément d'optimisation de forme, que l'on cherche à résoudre pour enfin comparer la forme obtenue à la forme réelle des oeufs. Nous avons étudié deux modélisations, l'une amenant à des problèmes de géométrie et de packing, l'autre à des problèmes d'optimisation de forme en élasticité linéaire.

Durant la résolution du premier problème issue de la modélisation, une autre question mathématique s'est naturellement posée à nous, et nous sommes parvenus à la résoudre, donnant lieu à l'obtention du diagramme de Blaschke Santalo (A,D,r) complet. En d'autre mots nous pouvons répondre à la question suivante: étant donné trois nombres A,D, et r positifs, est il possible de trouver un ensemble convexe du plan dont l'aire est égale à A, le diamètre égal à D, et le rayon du cercle inscrit égal à r?

Mots-clés: Biologie, Eulimnadia, Optimisation de forme, Géométrie convexe, Analyse convexe, Analyse fonctionnelle, Calcul des Variations, Elasticité Linéaire

Abstract

In this thesis we are interested in a problem of mathematics applied to biology. The aim is to explain the shape of the eggs of *Eulimnadia*, a small animal belonging to the class *Branchiopods*, and more precisely the *Limnadiidae*. Indeed, according to the theory of evolution it is reasonable to think that the shape of living beings or objects derived from living beings is optimized to ensure the survival and expansion of the species in question.

To do this we have opted for the inverse modeling method. The latter consists in proposing a biological explanation for the shape of the eggs, then modeling it in the form of a mathematical problem, and more precisely a shape optimisation problem which we try to solve and finally compare the shape obtained to the real one. We have studied two models, one leading to geometry and packing problems, the other to shape optimisation problems in linear elasticity.

After the resolution of the first modeling problem, another mathematical question naturally arose to us, and we managed to solve it, resulting in the complete Blaschke-Santaló (A,D,r) diagram. In other words we can answer the following question: given three positive numbers A,D, and r, and it is possible to find a convex set of the plane whose area is equal to A, diameter equal to D, and radius of the inscribed circle equal to r.

Keywords: Biology, Eulimnadia, Shape optimisation, Convex geometry, Convex analysis, Functional analysis, Calculus of variations, Linear Elasticity